Determinants of Endoplasmic Reticulum Structure and Dynamics

MERJA JOENSUU

Institute of Biotechnology and
Department of Biosciences
Division of Biochemistry
Faculty of Biological and Environmental Sciences
Integrative Life Science doctoral program
Doctoral School in Health Sciences
University of Helsinki

ACADEMIC DISSERTATION

To be presented for public examination with permission of the Faculty of Biological and Environmental Sciences of the University of Helsinki in the C-building, lecture hall C1, Latokartanonkaari 5, Helsinki, on May 9th 2014 at 12 o'clock noon.

Supervisor
Adjunct professor Eija Jokitalo
Institute of Biotechnology
Electron Microscopy unit
University of Helsinki, Finland

Custodian
Professor Kari Keinänen
Department of Biosciences
Division of Biochemistry
University of Helsinki, Finland

Reviewers
Adjunct Professor Varpu Marjomäki
Department of Biological and
Environmental Science
University of Jyväskylä, Finland

Adjunct Professor Jussi Jäntti
VTT Technical Research Centre of Finland
Espoo, Finland

Follow-up group
Adjunct Professor Eeva-Liisa Eskelinen
Department of Biosciences
Division of Biochemistry
University of Helsinki, Finland

Ph.D. Maria K. Vartiainen
Institute of Biotechnology
University of Helsinki, Finland

Opponent
Adjunct Professor Marko Kaksonen
Cell Biology and Biophysics Unit
European Molecular Biology Laboratory
Heidelberg, Germany

Cover image Electron tomographic model from high-pressure frozen and freeze substituted Huh-7 cell (upper left; endoplasmic reticulum in yellow, microtubules in blue and actin filaments in red), live cell confocal optical section (upper right) and transmission electron microscopic image (bottom) of Huh-7 cells expressing endoplasmic reticulum (green signal and dark precipitate in upper right and bottom, respectively) and actin (magenta in upper right) markers.

ISBN 978-952-10-9876-5 (Paperback)
ISBN 978-952-10-9877-2 (E-Thesis, PDF)
ISSN 1799-7372

http://ethesis-helsinki.fi
Unigrafia, Helsinki 2014

Dear past,

Thank you for all the lessons.

Dear future,

I’m now ready.

TABLE OF CONTENTS

I LIST OF ORIGINAL PUBLICATIONS

This thesis is based on the following publications, which are referred to in the text by their roman numbers. Unpublished data is also presented. Contribution to publications is indicated in the table.

I **Joensuu, M.**, Belevich, I., Rämö, O., Nevzorov, I., Vihinen, H., Puhka, M., Witkos, T.M., Lowe, M., Vartiainen, M.K. and Jokitalo, E. (2014): ER sheet persistence is coupled to myosin 1c – regulated dynamic actin filament arrays. *Mol. Biol. Cell* 7: 1111-26.

II Puhka, M., **Joensuu, M.**, Vihinen, H., Belevich, I. and Jokitalo, E. (2012): Progressive sheet-to-tubule transformation is a general mechanism for endoplasmic reticulum partitioning in dividing mammalian cells. *Mol. Biol. Cell* 13: 2424-32.

III Puhka, M., Vihinen, H., **Joensuu, M.** and Jokitalo, E. (2007): Endoplasmic reticulum remains continuous and undergoes sheet-to-tubule transformation during cell division in mammalian cells. *J. Cell Biol*. 5: 895-909.

	Publication
Experimental design	I, II
Experimental performance	I, II, III
Image acquisition	I, II, III
Image processing	I, II
Data collection	I, II, III
Data quantitation	I, II
Method development	I
Manuscript preparation	I, II, III

II ABBREVIATIONS AND ACRONYMS

ΔABL	deleted actin binding loop
ADP	adenosine diphosphate
ATP	adenosine triphosphate
$[Ca^{2+}]$	Ca^{2+}-concentration
CHO-K1	Chinese hamster ovary K1
Climp-63	cytoskeleton-linking membrane proteins of 63 kDa
CMVTag1	pCytomegalovirus-Tag 1
COPI/II	coat protein I/II
DP1	dorsal protein 1
EM	electron microscopy
ER	endoplasmic reticulum
ERES	endoplasmic reticulum exit sites
ERGIC	endoplasmic reticulum Golgi intermediate compartment
ET	electron tomography
FLAG	FLAG-tag
GFP	green fluorescent protein
GTP	guanosine-5'-triphosphate
HeLa	cervical cancer cells of Henrietta Lachs
HPF/FS	high pressure freezing and freeze substitution
HRP	horse radish peroxidase
Hsp47	heat shock protein 47 kDa
Huh-7	human hepatocellular carcinoma 7
INM	inner nuclear membrane
K892A	myo1c tail domain amino acid 892 substitution of Lysine (K) to Alanine (A)
KASH	klarsicht, ANC-1, and syne homology
kDa	kilodalton
KDEL	ER retention signal (Lysine (K), Aspartic acid (D), Glutamic acid (E), Leucine (L))
latA	latrunculin A
LBR	lamin beta receptor
LINC	linker of nucleoskeleton and cytoskeleton
LM	light microscopy
mCherry	monomeric cherry
MT	microtubule
myo	myosin
NE	nuclear envelope
NEBD	nuclear envelope breakdown
NRK-52E	normal rat kidney 52E
ONM	outer nuclear membrane
p180	protein of 180 kDa
PAC	paclitaxel

PH	pleckstrin homology
PIP_2	phosphatidylinositol 4,5-bisphosphate
PM	plasma membrane
REEP1	receptor expression enhancing protein 1
RER	rough endoplasmic reticulum
RFP	red fluorescent protein
Rtn	reticulon
SB-EM	serial block face scanning electron microscopy
SD	standard deviation
sem	standard error of mean
SER	smooth endoplasmic reticulum
shRNA	small hairpin ribonucleic acid
siRNA	small interfering ribonucleic acid
ss	signal sequence
STIM1	stromal interaction molecule 1
SUN	Sad1p/UNC-84
TAC	tip-attachment complex
TEM	transmission electron microscopy
TSA	trichostatin A
Vero	kidney cells of African green monkey, Verda Reno (Esperanto)
wt	wild-type
Yop1	yeast homolog of the polyposis locus protein 1

III SUMMARY

The cell boundaries and the intracellular organelles are defined by a diversity of biological membranes consisting of lipids, proteins and sugars, which create hydrophobic barriers limiting the distribution of aqueous molecules. Cells use membranes for a number of purposes, of which, probably the most important one is the compartmentalization of the cell's functions into separate organelles. The characteristic shapes of the different organelles are conserved across species, suggesting that the structural features are connected to the specific functions assigned to them. Understanding the morphogenesis of the organelles, and identifying the players involved, allows us to connect the organelle structures to their functions or dynamics and, importantly, to the disorders associated with malfunctioning organelles. How these processes in endoplasmic reticulum (ER) are coupled has remained unclear.

In this thesis, the structure and dynamics of ER and their connections to some of the ER's functions were analysed. By using live cell imaging and 3D-electron microscopy, biochemical approaches, and novel quantitative image analysis, we revealed the great variation in the interphase ER network structure and organization among several cultured mammalian cell lines. Our work described, for the first time, the interphase ER sheet dynamics and showed that sheets were static and persistent. We discovered that a specific subset of actin filaments, localizing to polygons defined by ER sheets and tubules, have a role in ER sheet persistence and the subsequent network organization. Furthermore, we discovered a novel role for molecular motor myosin 1c in regulating these actin structures. Based on our results we propose that ER–associated actin filament arrays have a role in sheet persistence in interphase cells, supporting the sheets as a stationary subdomain of the otherwise highly dynamic network. In addition, our results showed that ER undergoes a progressive spatial reorganization and a structural transformation towards more fenestrated sheets and tubular forms in mitosis. Moreover, mitotic ER did not fragment and the partition of nuclear envelope was subordinate to ER, which, in addition to structural transformations of ER into smaller subunits, favours the stochastic model of inheritance. Importantly, we showed that the natural increase of ER fenestrations and tubulation in mitosis correlated with the reduced number of membrane-bound ribosomes, and that the structural transformation could be mimicked by dissociating the membrane-bound ribosomes from the interphase ER by a drug treatment. We propose that the structural changes in mitotic ER are linked to the dissociation of membrane-bound ribosomes and the subsequent disengagement of the associated luminal protein machinery.

Collectively, this work describes the significant plasticity of ER morphology and organization in different commonly used cell culture cells at interphase and upon inheritance of ER. Importantly, this work also demonstrates the dynamic rearrangements of ER in mitosis and interphase cells and provides novel information about the role of ribosomes and actin on ER sheets and the role of myosin 1c on ER–associated actin arrays, which will serve as an opening for further studies on variety of regulatory possibilities of the interplay between ER subdomains and the identified player involved.

IV INTRODUCTION

"It is the pervading law
of all things organic and inorganic,
Of all things physical and metaphysical,
Of all things human and all things super-human,
Of all true manifestations of the head,
Of the heart, of the soul,
That the life is recognizable in its expression,
That form ever follows function. This is the law."
L.H. Sullivan, 1896: The tall office building artistically considered. Lippincott's Magazine, 57:403–409.

1. Endoplasmic reticulum structure and function

Living organisms are made up of distinct units called cells. In multicellular animals, such as humans, a variety of specialized cells work in conjunction to form the body's organs that perform the bodily functions. Cells that contain nucleus and other membrane-confined compartments are called eukaryotic cells. Mammalian cells and yeast are examples of such cells. Cells that do not have nucleus, like bacteria, are prokaryotic cells. Eukaryotic cells are structurally complex, and by definition contain nucleus and are otherwise organized in specialized membrane enclosed compartments, called organelles. Biological membranes are composed of lipids and proteins that form hydrophobic barriers limiting the distribution of aqueous molecules. Cells use membranes for a number of different purposes, of which, probably the most important one is the compartmentalization of the cell's functions. The diverse organelles have characteristic shapes that are conserved across species, suggesting that the structural features are connected to the specific functions assigned to them.

The endoplasmic reticulum (ER) is a large singular organelle in all eukaryotic cells, with its lipid bilayer membranes comprising about half of the total cellular membrane and its lumen enclosing roughly 10% of the volume of a typical cell. ER hosts a multitude of crucial functions and forms a dynamic and complex network spreading throughout the cytoplasm. ER is the first step in the secretory pathway that comprises of a series of vesicular and membrane trafficking steps cells use to secrete proteins out of the cell (Figure 1), reviewed in Baumann and Walz, (2001). Protein synthesis starts at the numerous cytosolic ribosomes which are responsible for the translation of the messenger RNA (ribonucleic acid) information, that convey the genetic information of the DNA (deoxyribonucleic acid), to produce a specific amino acid chain, or polypeptide, that will later fold into an active protein. The newly synthetized polypeptides emerging from the ribosome, and destined either for the lumen of an organelle or for secretion, are first directed to the ER by a short signal sequence (ss) that interacts with cytoplasmic targeting factors and the ER-resident translocation machinery and are co-translationally translocated to the ER. Molecular chaperones are a functionally related group of proteins in the cytosol and ER lumen, *e.g.,* heat shock proteins (Hsp) and calreticulin, which facilitate the protein translocation and folding. Protein folding is the process by which a protein structure assumes its functional shape or conformation. The conventional pathway of protein secretion has its origins in the ribosome-studded rough ER (RER) when properly folded and glycosylated (*i.e.,* addition of carbohydrates) newly synthesized proteins are selectively packed into COPII-

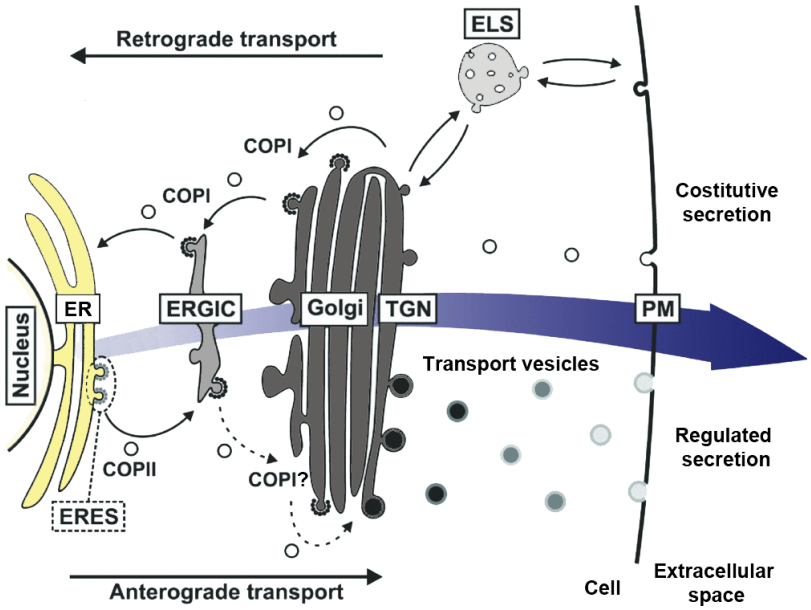

Figure 1. ER is the entry point to the conventional secretory pathway. Proteins are packed into vesicles at ERES and, after budding, they fuse with ERGIC or form a new compartment, and travel then to the *cis*-Golgi and through the Golgi stacks to the *trans*-cisterna and finally exit at the TGN. Proteins are then sorted into vesicles targeted either to the endosomal/lysosomal system (ELS), PM or the extracellular space via constitutive or regulated secretion. Direction of the anterograde and retrograde transport is indicated. Image modified from Strating and Martens (2009).

coated (coat protein II) transport vesicles at ER exit sites (ERES). After budding, these vesicles shed their coat and fuse with ERGIC (ER Golgi intermediate compartment) or form a new compartment (Saraste and Kuismanen, 1984; Saraste and Kuismanen, 1992). Secreted cargo travels then to the Golgi complex, which is the second major site for glycosylation and sorting. From *cis*-Golgi the cargo travels through the Golgi stacks to the *trans*-cisterna and finally exits at the *trans*-Golgi network (TGN). The transport occurs either via COPI vesicles, via membrane tubules or through a process called cisternal maturation (Marsh *et al.*, 2001b; Rizzo *et al.*, 2013). At TGN, cargo proteins are sorted into vesicles targeted to the endosomal/ lysosomal system, plasma membrane (PM) or the extracellular space (Goda and Pfeffer, 1989). The secretion to PM/extra cellular space occurs through two routes: the constitutive secretory pathway continuously delivering cargo is found in all secretory cells, and the regulated secretory pathway releasing cargo only upon stimulus is found in highly specialized secretory cells (such as neurons). Anterograde transport occurs from ER to ERGIC and through Golgi complex to endosomal/ lysosomal system, PM or extracellular space, and retrograde transport occurs to the opposite direction (reviewed in Brandizzi and Barlowe (2013); Hong (1998); and, Vazquez-Martinez *et al.* (2012)) (Figure 1). In contrast, proteins that are secreted without entering the classical ER–Golgi complex pathway use the unconventional protein secretion route. It is not clear whether these proteins, which lack a ss for entering ER, follow a common pathway of export from the cytoplasm across the PM (Rabouille *et al.*, 2012) or if these proteins are secreted at certain basal rate (Malhotra, 2013).

1.1 Endoplasmic reticulum structure

How the characteristic shape of a membrane-bound organelle is created and maintained and how the different shapes are related to the organelle functions are fundamental questions in cell biology. Membrane-bound organelles in eukaryotic cells have characteristic shapes. Some organelles, such

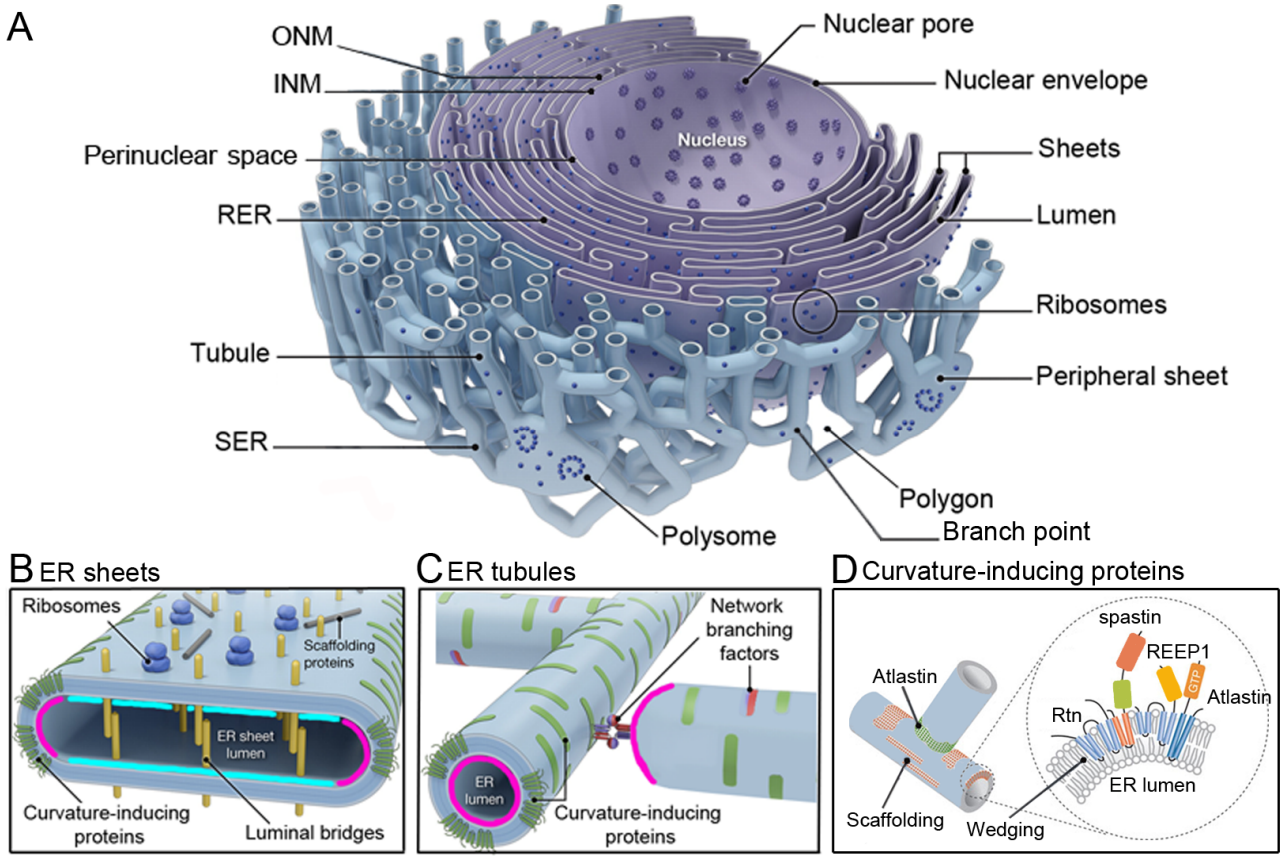

Figure 2. Schematic view of the NE and ER morphology and some of the determinants of the peripheral ER. (A) An illustration of the NE and the peripheral ER network of sheets and tubules. Perinuclear space, ER lumen, network polygons and branch points, SER, RER, ribosomes, polysomes and nuclear pores are indicated. (B) Localization of the ribosomes, curvature-inducing and scaffolding proteins, and luminal bridges, on the peripheral sheets. (C) Curvature inducing proteins and the network branching factors on the ER tubules. The high curvature (magenta) and low curvature (cyan) areas in the ER sheets and tubules are indicated. (D) Proposed membrane topology and localization of reticulons (Rtn), spastin, REEP1 and atlastin. Scaffolding and wedging mechanism are indicated. Images modified from Goyal and Blackstone (2013) and Park and Blackstone (2010).

as lysosomes and peroxisomes, are relatively spherical. Mitochondria consist of a double-membrane system from which the outermost membrane is relatively flat while the inner membrane folds into structures called cristae. Golgi complex, on the other hand, consists of a stack of perforated flat membranes. Structurally, ER has been classically divided into the nuclear envelope (NE), the RER and the smooth ER (SER) (Figure 2A), which lacks the membrane-bound ribosomes, and hence, has a smooth appearance (Palade, 1956).

The different morphologies of the ER result from variations in the membrane curvature in a continuous membrane system. Sheets are relatively flat membrane structures (Figure 2B), often extending over several micrometres with little membrane curvature. NE, whose curvature is negligible owing to the large size of the nucleus it surrounds, forms the largest sheet. In contrast, ER tubules are cylindrical structures with high membrane curvature in their cross-section (Figure 2C). This is, however, an over simplification of ER structure as, in addition, the network contains specialized regions that form contacts with

other organelles in the cell, areas that are specialized in transport, i.e. ERES, or in ER quality control, as well as areas that are highly dynamic or static. NE comprises of two large, flat membrane bilayers, the inner and outer nuclear membrane (INM and ONM, respectively) that enclose the nucleoplasm, which together create the nucleus that contains most of the cell's genetic material. The INM and ONM are separated by the perinuclear space that is continuous with the peripheral ER lumen, and connect to each other at nuclear pores (reviewed in Hetzer *et al.* (2005)). The peripheral ER extends from the ONM to the PM generating an extensive network of interconnected tubules, sheets and branch points (Baumann and Walz, 2001; Shibata *et al.*, 2006; Voeltz *et al.*, 2002) (Figure 2A).

In thin-section transmission electron microscopic (TEM) images, RER appears as long ribosome-covered profiles, and SER as ribosome-free vesicular-tubular structures (Palade and Siekevitz, 1956). These morphological observations indicated that RER resembles sheet morphology and SER tubular morphology, which lead, accordingly, to proposal that RER corresponds to ER sheets and SER to tubules (Shibata *et al.*, 2006). How the morphologically distinct domains are generated is still poorly understood, and the main focus of the studies has been in elucidating the mechanism by which the tubular ER is generated and maintained. The following chapters summarize what is known about the formation and maintenance of the tubules, sheets, ERES and contact sites with other organelles, and, how the structural defects of ER are connected to disease phenotypes.

1.1.1 High curvature membranes

Cellular membranes are generally dynamic, changing under steady state conditions, but also during processes such as cell migration, growth and division. For example, membrane-bound compartments communicate with one another by small vesicles that can bud and fuse from and to membranes. Membrane shaping relates to the generation of membrane curvature (McMahon and Gallop, 2005; Zimmerberg and Kozlov, 2006) (Figure 2B and C). High membrane curvature in the ER is seen in the cross-sections of tubules, at sheet edges, at small perforations passing the flat sheets that are known as the fenestrations, and in the small vesicles budding from the ER. The membrane topology changes in the ER network remodelling processes which most often mean fusion of two membranes (*e.g.,* ER tubules can fuse with an existing tubule or sheet to create a branch point) or fission, where continuous membrane is split into two. Alternatively, ER can change its shape without altering the basic membrane topology, *e.g.,* flat membranes can bend and tubules can be pulled out from flat membranes.

1.1.1.1 Smooth endoplasmic reticulum and tubular morphology

SER is composed of a network of short tubules and can be found in great abundance in hepatocytes and as a specialized form of SER (called sarcoplasmic reticulum) in muscle cells, but also in varying degree in common cell culture cells (Palade, 1956) (Figure 2A). ER tubules across most species have diameter of about 60 to 100 nm, suggesting that common structural elements underlie these morphologically distinct domains (Shibata *et al.*, 2006). In contrast, the tubular diameter of

~30 nm in yeast *Saccharomyces cerevisiae* (*S. cerevisiae,* i.e baking yeast) (Bernales *et al.*, 2006; Hu *et al.*, 2008) is considerably narrower than in mammalian cells.

Curvature-inducing proteins involved in the ER tubule formation (Figure 2C-D) were first discovered from *in vitro* experiments done with ER-enriched vesicles derived from *Xenopus laevis* eggs (Dreier and Rapoport, 2000): The authors identified reticulon (Rtn) 4a whose modification inhibited the reticular ER network formation. These findings were further supported by the inhibitory effect of Rtn4a antibodies on the ER network formation (Voeltz *et al.*, 2006). Further studies in mammalian cells and *S. cerevisiae* revealed that Rnt4a and other reticulons can homo-oligomerize (Shibata *et al.*, 2008) and, furthermore, hetero-oligomerize with the ubiquitously expressed DP1 (dorsal protein 1 which is also known as receptor expression enhancing protein 1, REEP1) (Park *et al.*, 2010) or its yeast homolog, Yop1p (Shibata *et al.*, 2008) (Figure 2D).

There are four reticulons (each with different splice variants) and six DP1 isoforms in mammals (Oertle and Schwab, 2003; Park *et al.*, 2010), and two reticulons in *S. cerevisiae* (Rtn1p and Rtn2p) (Shibata *et al.*, 2008). The deletion of yeast reticulons, Rtn1, Rtn2, and Yop1, leads to a drastic loss of tubular ER and conversion of peripheral ER into sheets in *S. cerevisiae*, while the deletion of Rtn1 and Rtn2 alone does not result in morphological defects (Voeltz *et al.*, 2006). Furthermore, the triple-depletion of Rtn1, 3 and 4 in mammalian cells (Anderson and Hetzer, 2008), or truncation of REEP1 (Park *et al.*, 2010), results in similar ER phenotype. In contrast, the over-expression of yeast Rtn1p or Yop1p, or some of the mammalian reticulon isoforms, leads to long unbranched tubules and to the disappearance of peripheral ER sheets (Voeltz *et al.*, 2006). In addition to being necessary for tubule formation, reticulons and DP1/Yop1p are sufficient to form tubules, as the purified yeast Yop1p or Rtn1p, reconstituted with pure lipids into proteoliposomes, deform the lipid bilayer into narrow (15–17 nm) tubules, and, when over-expressed *in vivo*, lead to decreased tubular diameter (Hu *et al.*, 2008).

The conserved C-terminal reticulon homology domain of approximately 200 amino acids contains two long hydrophobic segments. While the DP1/Yop1p proteins do not share any primary sequence homology with the reticulons, they also contain two hydrophobic segments of similar length. The ability of the reticulons and DP1/Yop1p proteins to induce tubules owes at least partly to the embedding of the hydrophobic hairpins -of unknown structure- to the outer leaflet of the lipid bilayer, and only shallowly to the inner leaflet, causing membrane curving in an analogous way to the insertion of amphipathic helices (Hu *et al.*, 2009; Voeltz *et al.*, 2006). This is called the hydrophobic insertion mechanism (wedging) (Figure 2D). In addition, it has been proposed that the reticulons and DP1/Yop1p might shape ER tubules by another cooperating mechanism: the scaffolding (Figure 2D). The ability to form homo- and hetero-oligomers immobilizes the proteins in scaffolds, which are thought to shape the tubular ER. Mutant forms defective in oligomerization cannot form scaffolds and are unable to induce tubules (Hu *et al.*, 2008; Shibata *et al.*, 2008; Voeltz *et al.*, 2006). Consistent with their proposed role in creating membrane curvature, the reticulons

and DP1/Yop1p localize almost exclusively to the tubular ER; they avoid the low-curvature areas of the NE and the peripheral sheets even when highly overexpressed (Voeltz *et al.*, 2006). In addition, the overexpression of the reticulons or DP1 prevents the ER collapse that normally follows the depolymerization of the microtubules (MT), which are one of the cytoskeletal filament types, indicating that these proteins can also stabilize ER tubules (Shibata *et al.*, 2008).

In addition, the varying shapes and quantities of membrane lipids in the two lipid leaflets may contribute to creation of asymmetric lipid bilayer and generation of membrane curvature (Zimmerberg and Kozlov, 2006). However, it is generally believed that reticulons and DP1/Yop1p are the major components forming the tubular ER, while the main functions for membrane lipids are the participation to signalling cascades, affecting the local membrane protein structure, organization and function, as well as giving biological membranes identity and certain physiological properties (van Meer and de Kroon, 2011; van Meer *et al.*, 2008).

1.1.1.2 Network branching and homotypic fusion

The formation of reticular ER network of tubules requires interplay between several proteins. Tubular fusion with other tubules or sheets defines the network areas that are called the polygons (Figure 2A). The atlastin (1-3) proteins (and their yeast homolog Sey1p) belong to a large protein family that interact with the reticulons and DP1/Yop1p and stimulate homotypic fusion, *e.g.,* membrane fusion between ER tubules and other tubules or sheets, to produce branched reticular ER network (Hu *et al.*, 2008; Orso *et al.*, 2009; Rismanchi *et al.*, 2008). Although atlastins and Sey1p do not share sequence homology, they belong to the same family of dynamin-like GTPases (enzymes capable of binding and hydrolyzing guanosine-5'-triphosphate) and have the same domain structure and membrane topology; that is, they possess two C-terminal hydrophobic segments (Figure 2D). Mutations in or depletion of atlastins in mammalian cells leads to long unbranched ER tubules, and to network fragmentation in fruit fly *Drosophila melanogaster* neurons, while the over-expression leads to ER membrane expansion (Hu *et al.*, 2009; Orso *et al.*, 2009). Antibodies against atlastins inhibit ER network formation *in vitro*, and yeast cells lacking Sey1p and either Rtn1p or Yop1p exhibit tubular ER defects. Given that Sey1p is much less abundant than Rtn1p or Yop1p in yeast, it seems likely that the reticulons and DP1/Yop1p are liable for tubule formation, whereas the atlastins and Sey1p associate with the tubule-forming proteins at discrete points, generating network branching and inducing polygon formation (Hu *et al.*, 2009). Atlastin has been shown to bind to ATPase spastin (an enzyme that can dephosphorylate adenosine triphosphate, ATP, to adenosine diphosphate, ADP, and a phosphate ion; Figure 2D) (Sanderson *et al.*, 2006) that interacts with Rnt1 (Mannan *et al.*, 2006). The over-expression of ATPase defective spastin in cultured mammalian cells leads to tubular network, but the precise role of spastin at the ER remains unclear (Sanderson *et al.*, 2006).

Another protein that participates in the ER branch point formation is p22. The microinjection of the protein increases the number of branch points (Andrade *et al.*, 2004). In addition to proteins mentioned

above, Rab (Ras-related proteins in brain) GTPases, which belong to the Rab family of proteins that regulate membrane trafficking, have also been implemented in reticular ER morphogenesis (Audhya *et al.*, 2007; English and Voeltz, 2013; Turner *et al.*, 1997). The position of new ER tubule growth is marked by Rab10 which localizes to ER and ER-associated structures that track along MTs. Rab10 depletion or expression of Rab10 GDP-locked mutant reduce the ability of the ER tubules to grow out and successfully fuse with adjacent ER, altering the ER morphology and resulting in fever tubules (English and Voeltz, 2013). Furthermore, depletion of Rab5 in nematode *Caenorhabditis elegans* (*C. elegans*) inhibits the formation of reticular network and results in ER morphology defect similar to Yop1p/Rtn1 depletion (Audhya *et al.*, 2007). In contrast, Lnp1p, a member of conserved Lunapark protein family, is antagonistic to Sey1p, but works in synergy with the reticulons and Yop1p. Lnp1p localizes to the ER branch points in both yeast and mammalian cells and it has been proposed that Lnp1p counterbalances Sey1p-directed polygon formation by promoting polygon loss through ring closure (Chen *et al.*, 2012). Most recently identified player of the ER network formation is the spastic gait (SPG) protein 33, also known as protruding, which was shown to interact with REEPs, spastin and atlastins, and suggested to act antagonistically to the atlastin GTPases (Chang *et al.*, 2013).

The formation and maintenance of a continuous membrane system requires constant fusion and fission of the membranes (Chernomordik and Kozlov, 2005; Chernomordik and Kozlov, 2008). During fusion, two lipid bilayers come in close contact with one another, leading initially to the fusion of the approaching lipid monolayer followed by the fusion of the inner monolayers. Similarly, the membrane fission proceeds through two-step division of the two lipid bilayer (Kozlov and Chernomordik, 2002). Both fusion and fission require substantial membrane shaping and are tightly connected to the ER network remodelling. It has been estimated that the energy requirements for lipid bilayer shaping correlate with the induced degree of curvature, i.e. tubule creation requires less energy than vesicle formation but more than the creation of flat membranes (Shibata *et al.*, 2009). *In vitro* fusion of ER-derived microsomes (Dreier and Rapoport, 2000; Lavoie *et al.*, 1996) and the subsequent formation of reticular ER is powered by GTP and ATP (Anderson and Hetzer, 2007; Hetzer *et al.*, 2001), although it is unclear if sheet were present in the formed network. Further shaping and remodelling of the membranes employ proteins that generate high membrane curvature (Voeltz *et al.*, 2006). While the heterotypic fusion, *e.g.,* fusion of transport vesicles with target membranes of different origins, has been studied extensively, the homotypic fusion between membranes of same origins is poorly understood. Some of the heterotypic fusion steps can, however, be applied to homotypic fusion events: Fusion is facilitated by both soluble and membrane bound tether proteins which augment the t-SNARE (target- soluble NSF attachment protein receptor) and v-SNARE (vesicle-) binding, bringing the adjacent membranes close to each other leading to membrane fusion. Based on SNARE-theory, ATP energy is required for the separation of the paired SNAREs rather than for the fusion itself (Sollner *et al.*, 1993). Although the ER

network formation has been shown to require energy, there are indications that the maintenance of the tubular network is not dependent on ATP energy: *in vivo* ATP depletion does not abolish ER tubules in COS-7 (monkey kidney fibroblasts) cells (Shibata *et al.*, 2008). However, a prolonged ATP depletion was shown to lead to ER tubulation in HeLa (Cervical cancer cells of Henrietta Lachs) cells (Lingwood *et al.*, 2009), which might indicate that energy is required for the maintenance of the ER sheets.

1.1.2 Low curvature membranes

In contrast to highly curved areas of the ER network, flat sheets only curve prominently at the sheets edges (Voeltz and Prinz, 2007) and/or at fenestrations. The low curvature membranes in the ER network are the peripheral sheets, which show great variation in their abundance, structure and organization, and the NE, which is the largest ER sheets and presents a unique subdomain of the ER network. Morphogenesis and maintenance of the peripheral sheets and NE is summarized in the next two chapters.

1.1.2.1 Rough endoplasmic reticulum and peripheral sheets

While sheets, tubules and branch points are the basic building blocks of the ER, their structure and the network organization shows great variation across species. RER is commonly found in all cell types containing ER, but it is especially prominent in highly secreting cells such as liver hepatocytes. RER is mainly composed of flat sheets that are typically thought to reside at the perinuclear area (Palade, 1956) (Figure 2). However, the location, abundance, size, morphology and organization of the sheets show great variation in-between different cell types. The diameter of ER sheets in mammalian cells (50–100 nm) is slightly larger than in *S. cerevisiae* (30 nm), and in contrast to the even network spreading throughout the cytoplasm in mammalian cells, the bulk of ER in yeast cells resides in the cell cortex and is connected to NE via few sheets and tubules (Bernales *et al.*, 2006; Shibata *et al.*, 2006; Voeltz and Prinz, 2007). In addition to intact sheets, sheets with fenestration of different quantities or sizes can be found in across species. Fenestrations are quite often found in metabolically active cell types and there seems to be some correlation between the ribosome density on the membranes and sheet morphology (Brown, 1978; Hepler, 1981; Lieberman, 1971; Palade, 1956; Rambourg *et al.*, 2001). The creation of fenestration is connected to curvature-inducing proteins: the depletion of reticulons and Yop1 abolishes most of the fenestrations from the PM-associated cortical ER sheets in yeast cells. These results indicate that reticulons stabilize curvature at the edges of sheets fenestrations (West *et al.*, 2011) - which is in contrast to previous localization studies showing that reticulons are not found in flat ER membranes, i.e. peripheral sheets or NE (Voeltz *et al.*, 2006). Creation of the fenestrations and their functional significance remains elusive.

While ER sheets in cultured mammalian cells are usually found separately, in some cell types, *e.g.,* cerebellar Pukinje neurons and B lymphocytes, ER sheets can be organized in stacks (Benyamini *et al.*, 2009; Takei *et al.*, 1994; Wiest *et al.*, 1990). Over-expression of the full-length inositol 1,4,5-trisphosphate receptor (IP3R), responsible for Ca^{2+} release

from the ER, induces ER sheet stacks in COS cells, reminiscent of those observed in Purkinje neurons (Takei *et al.*, 1994). In addition, over-expression of an ER transmembrane protein involved in the cholesterol metabolism also induces sheet stack formation in yeast (Wright *et al.*, 1988).

It has been suggested that sheets can be formed spontaneously and do not require stabilization (Goyal and Blackstone, 2013). Consistently, lipid bilayers tend to remain flat because the generation of curvature requires energy (Helfrich and Jakobsson, 1990; Lingwood *et al.*, 2009). While the precise mechanism for creating intact/ fenestrated sheets or stacked organization remains unclear, several determinants affecting the sheet morphology have been identified. Climp-63 (Cytoskeleton-linking membrane protein 63kDa) is an integral membrane protein of ER that binds to MTs (Klopfenstein *et al.*, 1998). The α-helical coiled-coil segments of Climp-63 form luminal structures that bridge the two opposing ER membranes and control the width of peripheral ER sheets (Klopfenstein *et al.*, 2001) (Figure 2B). The formation of intraluminal bridges and the subsequent immobilization of Climp-63 restricts its distribution to ribosome studded peripheral ER and excludes it from the NE, and therefore, the width of the NE, is controlled by other means (Klopfenstein *et al.*, 2001). Over-expression of Climp-63 rearranges the MT cytoskeleton extensively, and redistributes the ER parallel to MTs (Klopfenstein *et al.*, 1998). By contrast, over-expression of a Climp-63 mutant protein, which lacks the MT binding domain, causes the mutant protein to accumulate in perinuclear sheets and results in retraction of the peripheral network towards the nucleus (Klopfenstein *et al.*, 1998). Recently, based on FRAP *(*fluorescence recovery after photobleaching) experiments, it was shown that the depletion of Climp-63 or MT depolymerization increase the lateral mobility of the ER translocation complex in mammalian cells (Nikonov *et al.*, 2007). These data collectively suggest that Climp-63 and MTs may contribute to the generation of rough ER domains, probably peripheral ER sheets, where translocation complexes are mostly partitioned. However, while Climp-63 has been shown to localize to peripheral sheets (Shibata *et al.*, 2009; Shibata *et al.*, 2010; Shibata *et al.*, 2006), it does not localize to organized smooth ER (OSER) that appears as stacked SER sheets (Korkhov and Zuber, 2009). This might indicate that stacked organization of sheets serves other functions than usually assigned for sheets and, further, that the sheet morphology might depend on additional factors. Interestingly, Climp-63 over-expression leads to altered tubular morphology (Klopfenstein *et al.*, 1998), which is unexpected, as Climp-63 is located preferably to ER sheets (Klopfenstein *et al.*, 2001; Shibata *et al.*, 2010). One explanation for this could be that Climp-63 mediates the interaction between MTs and the tubules that are drawn straight out from the ER sheets (Lee and Chen, 1988) and that the over-expression of the protein disturbs the structural transformations of the ER.

p180 is a mammalian ER protein that binds to ribosomes. p180 over-expression in mammalian cells leads to aberrant patterns of both ER and MTs (Ogawa-Goto *et al.*, 2007), and to generation of ribosome studded tubules and sheets (Benyamini *et al.*, 2009), suggesting that p180 mediates interaction between MTs and ER. In accordance, the

p180 upregulation by ascorbate treatment leads to creation of RER (Ueno *et al.*, 2010). p180 depletion, on the other hand, results in lower ribosome density on the ER membranes, a shift towards tubular network morphology, ER network retraction from the cell periphery and a severe decrease in total ER (Benyamini *et al.*, 2009; Ogawa-Goto *et al.*, 2007). A homolog for p180 does not exist in yeast, however, the over-expression of mammalian p180 in yeast leads to extensive proliferation of RER (Becker *et al.*, 1999). Interestingly, p180 over-expression results in a coordinated upregulation of genes transcribing RER–specific proteins: *KAR2* (Vogel *et al.*, 1990)*, SEC61,* and *SEC72* (Silberstein *et al.*, 1995)*,* which all encode proteins required for protein translocation; and *OST1,* which encodes a protein mediating *N*-glycosylation (Silberstein *et al.*, 1995). Upregulation of the gene transcription was shown to lead to increased levels of the proteins they encode (Wanker *et al.*, 1995) and the proper localization of these proteins was demonstrated by immunofluorescence (Becker *et al.*, 1999). Increased protein levels were shown to be accompanied by a several fold increase in the secretion of an ectopically expressed protein by colorimetric assay (Becker *et al.*, 1999). Another protein enriched in peripheral ER sheets but largely missing from the ER tubules and NE is kinectin (Shibata *et al.*, 2010). In contrast to Climp-63, the coiled-coil domains of p180 and kinectin are cytoplasmic and have been suggested to form scaffolds that stabilize the flatness of the sheets (Shibata *et al.*, 2010) (Figure 2B). While overexpression of Climp-63, p180 and kinectin induce sheet proliferation, the depletion of the proteins leads to decrease in luminal width but does not abolish the sheets (Shibata *et al.*, 2010).

These results suggest an involvement of additional sheet stabilizing mechanisms, which might include the protein synthesis and folding machinery consisting of a translocon, which is a protein complex associated with the translocation of polypeptide across ER membrane, with bound polysomes (i.e. clustering of multiple ribosomes reading one mRNA simultaneously to synthesize the same protein; Figure 2A) and luminal chaperones. In accordance, a recent study on cultured fibroblast cells showed that p180 depletion results in dramatically reduced density of polysomes on ER and to almost complete blockade of protein synthesis in the polysome membrane fractions. In contrast, p180 upregulation by ascorbate stimulation leads to high protein synthesis activity in the polysome membrane fractions (Ueno *et al.*, 2012). These results indicate that p180 most likely accelerates the membrane association of polysomes and thereby leads to high density of ribosomes on the ER followed by activation of protein synthesis (Ueno *et al.*, 2012). Although the effects of p180 depletion on ER were, according to the authors interpretation, minimal, based on their TEM images, the resulting ER profiles appear smaller and shorter than the extensive sheets in the control human erythroleukemia cells, indicating that the polysome association with ER membranes is required for the sheet maintenance. It has also been shown that the disassembly of translating ribosomes leads to redistribution of some sheet-preferring proteins, such as Climp-63 and kinectin, into the tubular region (Shibata *et al.*, 2010), implicating a coordination between these components.

A growing body of work suggest that the curvature inducing proteins are involved in

sheet stabilization at sheet edges and fenestrations (Shibata *et al.*, 2010; West *et al.*, 2011; Voeltz *et al.*, 2006). The results are, however, conflicting: The depletion of Rnt1, Rnt3 and Rtn4 in mammalian cells (Anderson and Hetzer, 2008), or Rnt1, Rtn2 and Yop1p in yeast (Voeltz *et al.*, 2006), has been shown to lead to ER sheet proliferation, which is not logical if their proposed role is to create and/or maintain sheet edges and fenestrations. Moreover, overexpression of Rtn4a leads to long tubules and Climp-63 to abundant sheets, and when both proteins are simultaneously over-expressed, a normal ER network prevails (Shibata *et al.*, 2010), clearly indicating that there is a tug-of-war between Rtn4a and Climp-63 regulating the sheet-tubule balance. It has also been proposed that reticulons solely would be responsible for the basic mechanism of creating both tubules and sheets; consistent with this idea is that Climp-63, p180 and kinectin are not expressed in lower organisms, such as *Drosophila* S2 cells (Shibata *et al.*, 2010), silkworm (Senda and Yoshinaga-Hirabayashi, 1998), and *S. cerevisiae* (Bernales *et al.*, 2006), whereas reticulons and DP1/Yop1p are (Shibata *et al.*, 2010), and despite the lack of these proteins, ER sheets are present in these organisms.

1.1.2.2 Nuclear envelope

The NE appears spherical in cells, but due to its large diameter (6–10 µm in mammalian cells), it actually consist of both low- and high-curvature membranes, which are, to some extent, created by the same morphological determinants as the peripheral ER. The ONM is directly continuous with the peripheral ER and contains same features as peripheral network, such as ERES and ribosomes. Most RER membrane proteins are also present in the ONM because of the protein diffusion in the continuous membranes, although it has also been suggested that there are special constriction sites between peripheral ER and NE, called the NE-ER gates, that may control the diffusion between these subdomains as shown in plant cells (Staehelin, 1997). In agreement, these connective sites between NE and ER appear narrower than the reticular network diameter also in mammalian cells. However, despite the lipid continuity between the NE and the peripheral ER, NE presents a unique ER subdomain, as ONM and INM also contain a diversity of proteins not enriched in the ER (see reviews Bastos *et al.* (1995); Hetzer *et al.* (2005)). These proteins either associated with nuclear pores or nuclear lamins (Stuurman *et al.*, 1998); are involved in bidirectional traffic between cytoplasm and nucleoplasm (Mattaj and Englmeier, 1998; Talcott and Moore, 1999); or, in the maintenance of the nucleoplasm (Mancini *et al.*, 1996). NE shields the genome from cytoplasmic components, but also represents a highly specialized membrane that provides anchoring sites for chromatin and the cytoskeleton (D'Angelo and Hetzer, 2006). The four classes of proteins involved in the creation and maintenance of the NE are discussed below.

SUN proteins (Sad1p/UNC-84) in the INM and KASH proteins (Klarsicht, ANC-1, and Syne Homology) in the ONM (Starr and Fridolfsson, 2010; Starr and Han, 2002; Wilhelmsen *et al.*, 2006) form a bridge spanning the perinuclear space (diameter of ∼28–50 nm) creating the LINC complex (Linker of Nucleoskeleton and Cytoskeleton) (Padmakumar *et al.*, 2005). Depletion of these proteins causes expansion of perinuclear space (Crisp *et al.*, 2006),

indicating that LINC has a role in NE shaping. As the SUN proteins are connected to the nuclear lamins and the KASH-proteins to the cytoplasmic MTs, actin and intermediate filaments (Starr and Fridolfsson, 2010), LINC complex might also be involved in the nuclear positioning and migration (Lombardi *et al.*, 2011), as well as in the signal transduction from the extracellular space to the chromatin (Jaalouk and Lammerding, 2009; Starr and Fridolfsson, 2010).

INM contains over 60 integral membrane proteins not present in the peripheral ER or ONM (Schirmer and Foisner, 2007). Although most of these proteins are uncharacterized, interaction with nuclear lamins and chromatin, and the subsequent immobilization of the proteins, have been shown for lamin beta receptor (LBR), lamina-associated polypeptide (LAP) 1 and 2, emerin, and MAN1 (for reviews, see: Akhtar and Gasser (2007); Dorner *et al.* (2007); Schirmer and Foisner (2007)). Of these, the role of LBR in the creation and maintenance of the NE morphology has been well characterized (Ellenberg *et al.*, 1997; Gruenbaum *et al.*, 2005; Hoffmann *et al.*, 2007; Ye and Worman, 1994). The third class of proteins dictating the NE structure are the approximately 30 nucleoporin proteins that are known to be involved in formation of nuclear pore complexes (NPCs) at nuclear pores (Figure 2A) (D'Angelo and Hetzer, 2008; Tran and Wente, 2006). NPCs are aqueous channels through which proteins, RNA and ribonucleoprotein complexes are exchanged between the nucleoplasm and cytoplasm (Beck *et al.*, 2004; Terry *et al.*, 2007). Except for three transmembrane proteins that are believed to anchor the NPC to the NE, form the NPC core (Mansfeld *et al.*, 2006; Stavru *et al.*, 2006) and stabilize the highly curved and energetically unfavorable pore membrane (Alber *et al.*, 2007), all other nucleoporin proteins are soluble (D'Angelo *et al.*, 2006; Rabut *et al.*, 2004). In addition, the nuclear pore formation has been shown to require the reticulons and DP1/Yop1p (Dawson *et al.*, 2009), although, as these proteins were first reported to be absent from the NE some discrepancy on the matter remains (Voeltz *et al.*, 2006). The last group of proteins involved in NE morphology constitutes from A- and B-type lamin intermediate filaments forming the nuclear lamina in the nucleoplasm (Gruenbaum *et al.*, 2000). The lamina has been shown to be critical for nuclear stability, particularly in muscle cells that are exposed to mechanical forces (Cohen *et al.*, 2008), and to have a major role in chromatin function and gene expression (Gruenbaum *et al.*, 2005).

1.1.3 Endoplasmic reticulum exit sites

ERES are often located near Golgi complex (Rossanese *et al.*, 1999) but also at cell periphery and at NE (Bannykh *et al.*, 1996) in mammalian cells (Figure 3). In yeast *Pichia pastoris*, the connection between ERES and Golgi is so profound that for each ERES an adjacent Golgi stack exists (Bevis *et al.*, 2002). This level of organization, however, has not been described in mammalian cells. ERES can form *de novo* in mammalian cell and yeast (Bevis *et al.*, 2002; Stephens, 2003) and there are multiple ERES present in cells and majority of them are static (Gupta *et al.*, 2008). ERES have an asymmetric ribosome distribution: ribosomes are absent from the areas of budding profiles, but are present on the opposing membrane (Sesso *et al.*, 1994).

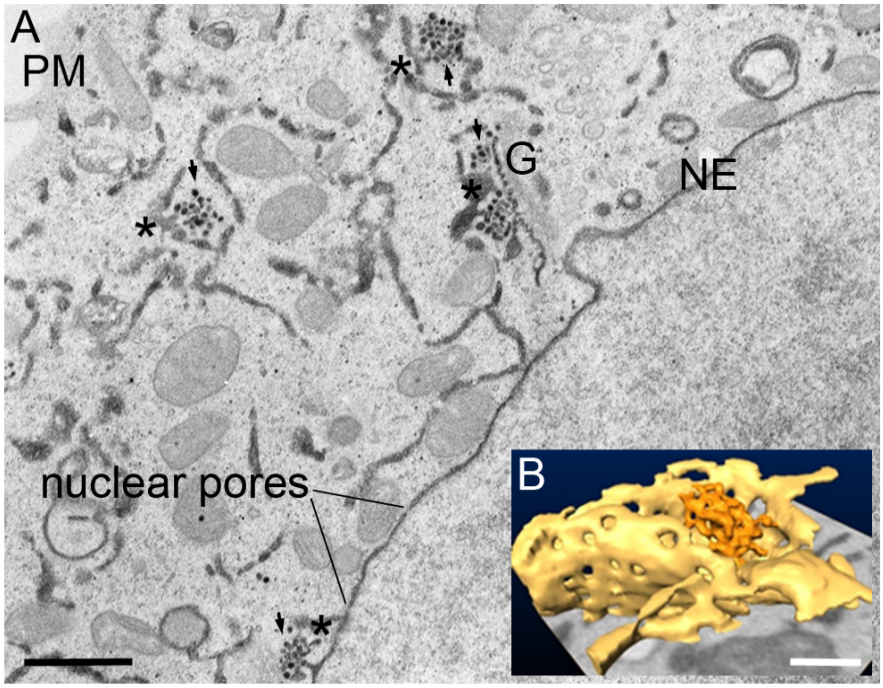

Figure 3. The first membrane trafficking step in the secretory pathway occurs at ERES. Huh-7 (human hepatocyte derived carcinoma) cells transiently expressing ssHRP-KDEL (HRP coupled to the ER-targeting ss and ER retention signal KDEL [Lysine, Aspartic acid, Glutamic acid, Leucine]) were cytochemically stained and processed for (A) TEM or (B) serial block face scanning electron microscope (SB-EM) and 3D-modelling. Fusion protein is packed into vesicles (seen as dark precipitate after cytochemical staining) at ERES (asterisks in A; orange structures in B) in the peripheral ER (yellow in B) and NE. After budding, the cargo travels to the *cis*-Golgi (dark signal in at the Golgi complex marked by G). From there, the cargo carrying the KDEL can be returned back to the ER (Yamamoto *et al.*, 2001). Secreted proteins travel through the Golgi stacks to the *trans*-cisterna and finally exit at TGN (not shown). Nuclear pores are indicted. Bar 1 µm in A and 0.5 µm in B. SB-EM model courtesy of Ilya Belevich.

The morphology of ERES range from discrete buds to networks of tubules and vesicles (Bannykh *et al.*, 1996; Bednarek *et al.*, 1995; Orci *et al.*, 1991) (Figure 3). The mechanisms used for creating high curvature in the forming vesicles at ERES and flattening of the membrane when vesicles fuses to the target membrane differ from the curvature inducing mechanisms of the peripheral ER tubules, branch points and sheet edges. The generated high curvature at the ERES is transient and local, and the mechanisms creating high membrane curvature in network scale must therefore differ from generating curvature in vesicles. The highly curved vesicles and/or transport carriers are formed from relatively flat membranes and the vesicles generally dispatch their high membrane curvature quickly by fusing with the target membrane. By contrast, ER tubules, though highly dynamic, maintain their curvature over long time periods. Furthermore, all curvature-inducing proteins involved in vesicle formation are soluble proteins that associate transiently with the ER membranes, whereas at least reticulons and DP1/Yop1p are integral membrane proteins.

Interestingly, while the ERES are considered a specialized subdomain of ER and crucial part of the secretory pathway, virtually nothing is known about the sites where retrograde (Figure 1) vesicles fuse back to ER in mammalian cells. Whereas ER export appears to be constant, the retrograde transport back to ER import sites (ERIS) was recently shown to occur temporally and to depend on Golgi dynamics (Lerich *et al.*, 2012). The identified ERIS markers, however, are plant-specific, and no yeast or animal orthologs (*i.e.,* genes in different species that evolved from a common ancestral gene and have retained the same function in the course of evolution) exist (Sanderfoot *et al.*, 2000), indicating that these features, however, are

unique to plants. If these sites form specific sites in the ER or if the fusion can occur uniformly anywhere in the ER in mammalian cells, remains to be solved.

1.1.4 Contact sites with other cellular organelles

Membrane-bound organelles of the eukaryotic cell allow the segregation of sometimes incompatible biochemical reactions into specific compartments with specific biochemical environments (Vance, 2003). This however, restrains the diffusion of metabolites and information from one part of the cell to the other. To ensure cooperation of cellular functions, cells use a network of contact sites between different organelles. Contact sites are transient or stable areas where membranes of different origins, usually ER and either Golgi complex, mitochondria, endosomes, peroxisomes, lipid droplets, autophagosomes or PM, are tethered into close proximity (<30 nm). It is believed that ER spreads throughout the cytoplasm to form contacts with other organelles. While the functional importance of these interactions is still poorly understood and only few components have been identified, it is likely that these contact sites are specialized for exchange of compounds or information between two organelles most often involving Ca^{2+} and/or direct, *i.e.,* non-vesicular, lipid exchange (Friedman *et al.*, 2010). Trafficking must be controlled, firstly, because Ca^{2+} can be toxic when unregulated, and secondly, because the variety of membrane lipids contributes to the identity of all membrane-bound organelles (English *et al.*, 2009; Levine and Loewen, 2006). The extent and roles of these interactions are discussed below.

In addition to the active retrograde and anterograde vesicular transport between ER and Golgi (Figure 1), there are also direct interactions between the compartments, most likely enabling the transport of lipids, such as ceramide, between the compartments (Funato and Riezman, 2001; Kawano *et al.*, 2006; Levine and Loewen, 2006; Mogelsvang *et al.*, 2004). ER-Golgi membrane contact sites are coordinated by integral membrane proteins VAP-A and VAP-B (vesicle-associated membrane protein-associated protein A and B) in the ER (Peretti *et al.*, 2008) and the lipid transfer binding protein Nir2 (Amarilio *et al.*, 2005), oxysterol-binding protein (Wyles *et al.*, 2002) and ceramide-transfer protein (Kawano *et al.*, 2006) in the Golgi, dictating the lipid composition of the membranes.

The proper spacing between ER and mitochondria are important for phospholipid exchange (Vance, 1990), Ca^{2+} signalling and regulation of apoptosis (Csordas *et al.*, 2006; Hajnoczky *et al.*, 2006; Iwasawa *et al.*, 2011), and synthesis of cytochrome *c* oxidase and glycosphingolipids (de Brito and Scorrano, 2010). Based on electron microscopy (EM) and electron tomography (ET) studies, the mitochondria-associated membranes (MAM) consists of SER, or both SER and RER membranes (Csordas *et al.*, 2006; Marsh *et al.*, 2001a; Wang *et al.*, 2000) that cover roughly 20% of the mitochondrial surface (Rizzuto *et al.*, 1998). The ER-mitochondria tethers include mitofusin 2 (de Brito and Scorrano, 2008), VDAC1-porin (voltage-dependent anion-selective channel protein 1), IP3R (Szabadkai *et al.*, 2006) and ERMES complex (endoplasmic reticulum -mitochondria encounter structure) (Kornmann *et al.*, 2009) in yeast. However, orthologs of ERMES

components have, to date, only been identified in fungi (Kornmann and Walter, 2010). Interestingly, physiological [Ca^{2+}] in the cytosol stimulates ER-mitochondria dissociation, indicating that the free cytosolic [Ca^{2+}] regulates the ER-mitochondria associations (Wang *et al.*, 2000). A recent pioneering study showed that these contact sites are coordinated by acetylated MTs and despite the constant rearrangements of the organelles, MAMs are persistent (Friedman *et al.*, 2010).

The contact sites between ER and early endosomes are persistent, and their dynamics coordinated (Friedman *et al.*, 2010; Rocha *et al.*, 2009; West *et al.*, 2011). Recently, it was shown that ER tubules wrap round endosomes and rearrange their structure according to endosome trafficking, and that both organelles form contacts with MTs at or near membrane contact sites (Friedman *et al.*, 2013). The major implication of these results is that endosomes mature and traffic while coupled to the ER membrane rather than in isolation. VAPs have been shown to tether the late endosome cholesterol sensor ORP1L in hypo-cholesterol conditions and regulate the intracellular distribution of late endosomes in mammalian cells (Rocha *et al.*, 2009). These interactions might provide potential sites for lipid exchange and protein–protein interactions between the organelles, although even in the light of the latest results, the functional importance of the ER-endosome interactions remains unclear.

One organizational feature of ER network is its extensive relationship with PM. In yeast, 20–45% of the cytoplasmic surface of the PM is in contact with a mixture of ER tubules and fenestrated sheets (Schuck *et al.*, 2009; West *et al.*, 2011). The spacing between ER and PM is approximately 30 nm, excluding the ribosomes from the contact sites (West *et al.*, 2011). Three ER-PM tethering protein families in yeast have been identified: Ist2 (Wolf *et al.*, 2012), tricalbins 1-3 and Scs2/22 (Loewen *et al.*, 2007; Manford *et al.*, 2012). Depletion of all six tethering proteins results in loss of ER-PM contacts and accumulation of ER to the perinuclear area (Caputo *et al.*, 2008; Giordano *et al.*, 2013; Manford *et al.*, 2012). This leads to alterations in phosphoinositide signalling and to the constitutive activation of the unfolded protein response (*i.e.,* conserved system activated in response to an accumulation of unfolded or misfolded proteins in ER that aims to restore normal function of the cell by halting protein translation and by activating the signalling pathways increasing chaperone production). The importance of ER-PM interactions lies in lipid transport and Ca^{2+} signalling. Based on a biochemical study, the ER subdomain adherent to the PM in yeast has high capacity for synthetizing phospholipids (Pichler *et al.*, 2001), which, in addition to cholesterol (Urbani and Simoni, 1990), are transported to PM by non-vesicular transport (Sleight and Pagano, 1983). While the cholesterol transport depends on the Osh family proteins (Canagarajah *et al.*, 2008; Schulz and Prinz, 2007; Sullivan *et al.*, 2006), proteins involved in the phospholipids transport have not been identified. In mammalian cells, the ER–PM contact sites are also essential for store-operated Ca^{2+} entry, a process of extracellular Ca^{2+} influx in response to the depletion of Ca^{2+} stores in the ER. Stromal interaction molecule 1 (STIM1) is a transmembrane protein that localized predominantly to the ER and upon Ca^{2+} depletion of ER (Orci *et al.*, 2009)

undergoes a structural reorganization and relocalization under the PM (Liou *et al.*, 2007), where it interacts with Orai1 to form a channel that allows Ca^{2+} influx into the ER (Park *et al.*, 2009). In a recent study, Rtn4b was shown to be required for STIM-Ora1 coupling (Jozsef *et al.*, 2014), indicating that ER tubules are the preferred subdomain for store-operated Ca^{2+} entry and ER-PM contacts sites.

Growing body of evidence indicates that ER is the source of lipids for multiple other membrane-bound compartments in the cells. In yeast and mammalian cells, peroxisome membranes originate, at least partly, from the ER (Hoepfner *et al.*, 2005; Kim *et al.*, 2006) and, furthermore, remain in close contact with the ER over time (Kim *et al.*, 2006). Peroxisomes are the site for fatty acid break-down in the cells, and the lipid transfer between ER and peroxisomes in yeast occurs by non-vesicular trafficking (Raychaudhuri and Prinz, 2008). However, factors regulating this lipid transfer have not been identified. Lipid droplets are also derived in part from factors synthesized in ER and mature lipid droplets remain tethered to the ER in yeast (Jacquier *et al.*, 2011). These interactions have been shown to be important for lipid metabolism (Ye *et al.*, 2009) and ER protein quality control (Klemm *et al.*, 2011). And lastly, a consensus is emerging that the autophagosome membrane originates from ER in mammalian cells, although Golgi (Geng *et al.*, 2010; Yamamoto *et al.*, 1990), PM (Ravikumar *et al.*, 2010) and mitochondria (Hailey *et al.*, 2010) contribute to the expansion of the nascent autophagosome. Autophagy is an intracellular degradation process essential for cell development, homeostasis and survival (for review, see Lamb *et al.* (2013)). Autophagy is initiated by the formation of the isolation membrane that is directly connected to the ER, which is then expanded to form the autophagosome (Hayashi-Nishino *et al.*, 2009; Yla-Anttila *et al.*, 2009).

1.2 Endoplasmic reticulum functions

ER is particularly striking for its heterogeneity of form and function. Relative position of the organelles in the cytoplasm and in respect to other organelles is often crucial for proper organelle function (Marsh *et al.*, 2001a) and it is, therefore, believed that reflecting the multiple functions it hosts, ER has a large surface area, a cell-wide distribution and is continuous. This begs the question of why the ER must maintain its continuity. The most logical explanation is that it allows a cross-talk between ER domains that are located in distal regions of the cytoplasm, *e.g.,* it might be that ER Ca^{2+} signals or stress responses cannot be handled locally, but require the global ER. The reason why ER has a continuous lumen, on the other hand, might be to help ensure that the entire ER responds rapidly and appropriately to signals such as Ca^{2+} or stress responses (Friedman and Voeltz, 2011). Another explanation might be the regulation of the constant pH throughout the ER network (Casey *et al.*, 2010), as well as, to maintain lumen's oxidizing environment (Sevier *et al.*, 2007). The diffusion of GFP-tagged proteins in the ER lumen has been shown to be slower than in the cytosol (Dayel *et al.*, 1999) and, therefore, the continuous lumen could also serve as a confined space for diffusion of soluble proteins enabling protein targeting to certain areas of the cell with adjusted speed, compared to less confined diffusion in the cytosol. Furthermore,

it has been proposed that ER lumen in plant cells is continuous with that of their neighbors, allowing cell-to-cell communication and movement of small ER-luminal molecules between cells (Barton *et al.*, 2011). Such connections, however, have not been shown in mammalian cells.

To accommodate its many functions, the ER has perhaps the most complicated structure of any organelle. Despite the continuity of the ER network, some of the ER-resident proteins are non-uniformly enriched in specific subdomains of different morphologies, implying an existence of functional segregation according to their specific requirements. As the functional importance of ERES and contact sites with other organelles were discussed earlier, here I will discuss what is known about the functions assigned for ER tubules and sheets.

1.2.1 Functional segregation into structural subdomains

How the ER functions are distributed to the ER subdomains is a critical question in the field. As both tubules and sheets are the main building blocks of the ER across species and cell types, these structures must serve separate, and specific, purposes/ funcitions. It is therefore interesting that the Rtn1, Rtn2 and Yop1p deletion in yeast, and the subsequent loss of ER tubules, exhibits only a moderate growth defect, indicating that in yeast much of the tubular ER is dispensable (Voeltz *et al.*, 2006). However, the simultaneous depletion of Rtn1 and Yop1 in *C. elegans* causes a 60% decrease in embryonic viability (Audhya *et al.*, 2007). These results suggest that either the functional segregation into ER subdomains can be modulated or that an intact tubular ER is more important in higher eukaryotes.

Indications that the ER form and organization follows its functions came from the observations of ER in secretory cells. The secretion activity and the amount of RER in the cells seem to correlate (Benyamini *et al.*, 2009; Rajasekaran *et al.*, 1993; Ueno *et al.*, 2010; Wiest *et al.*, 1990); The secretory cells in liver and pancreas translocate and secrete a large number of proteins and the ER is organized into parallel arrays of RER (Baumann and Walz, 2001; Rajasekaran *et al.*, 1993). In contrast, in muscle cells that are specialized in contraction and must be able to rapidly regulate cell's Ca^{2+} levels, ER is organized into specialized sheets void of ribosomes, called the sarcoplasmic reticulum (Baumann and Walz, 2001; Rossi *et al.*, 2008). Consistent with the hypothesis that ribosome-studded ER is accountable for protein production, there is an active sorting of protein production machinery, *i.e.,* proteins responsible for protein translocation (Blobel and Dobberstein, 1975a; Blobel and Dobberstein, 1975b; Jamieson and Palade, 1968; Walter and Lingappa, 1986) and glycosylation (Czichi and Lennarz, 1977), into RER (Shibata *et al.*, 2010). These results are consistent with previous cell fractionation experiments, which demonstrated that general ER proteins distribute throughout the ER, whereas translocon-associated proteins are enriched in RER microsomes (Hinman and Phillips, 1970; Kreibich *et al.*, 1978). The ER lumen provides an optimal environment for protein folding and modification. The protein folding in the ER and therefore the proper functionality of the proteins include covalent modifications of the proteins: removal of ss, *N*-linked glycosylation and disulphide bond

formation. The redox-potential in the ER lumen promotes disulphide bond formation (Marquardt *et al.*, 1993) and the glycosylation is used to monitor the status of protein folding, acting as a quality control mechanism to ensure that only properly folded proteins are trafficked to the Golgi. Together these observations indicate that the protein synthesis, folding and quality control are specific functions assigned for RER. However, RER might also host other functions since, as discussed earlier, recent studies have shown that autophagosome formation involves RER membranes (Hayashi-Nishino *et al.*, 2009; Yla-Anttila *et al.*, 2009).

Biochemical studies of SER have shown that SER is rich in enzymes involved in drug detoxification in the cells (Galteau *et al.*, 1985; Orrenius *et al.*, 1965) and it is, thus, believed that detoxification processes occur in SER. Furthermore, SER is thought to be the major Ca^{2+} storage site in the cells (Hales *et al.*, 1974; McGraw *et al.*, 1980). While luminal Ca^{2+} binding protein calreticulin (Pezzati *et al.*, 1997) and SERCA (sarco/endoplasmic reticulum Ca^{2+}-ATPase) pumps are homogenously distributed throughout the ER, the IP3R and ryanodine receptor localize specifically to SER (Satoh *et al.*, 1990; Takei *et al.*, 1992), suggesting that specific ER areas, with different Ca^{2+} uptake and release abilities, might exist.

Based on morphological observations of actively secreting cells, the RER was proposed to corresponds to ER sheets and, accordingly, SER to ER tubules (Shibata *et al.*, 2006). The segregation of RER/SER into sheets/tubules is, however, obscure for a few reasons: Firstly, although polysomes localize preferentially to ER sheets, ribosomes localize also to tubules, although in lower density, and secondly, the overexpression of certain ER-membrane proteins leads to a proliferation of OSER which has a sheet morphology but lacks the membrane-bound ribosomes (Baumann and Walz, 2001). Despite the precise evidence to support that ER sheets resemble RER and ER tubules SER, the proposal have been quite widely and generally accepted. Therefore, based on the current knowledge, specific functions assigned for ER sheets and NE are the RER-associated ER functions *i.e.,* protein synthesis, folding and quality control, as well as recently described function in the unfolded protein response (Schuck *et al.*, 2009). This study demonstrated that in yeast, ER stress-induced unfolded protein response leads to sheet expansion. However, the stress response does not depend on the sheet shape because sheets-to-tubules conversion does not inhibit stress alleviation. NE, in addition, regulates the movement of macromolecules between the nucleoplasm and the cytoplasm (Hetzer *et al.*, 2005; Prunuske and Ullman, 2006) and while the role of ER sheet fenestrations is not known, they might serve a similar function -a passage of cytoplasmic molecules. How is the sheet morphology connected to its functions? The answer may lie in the membrane topology: The low curvature of the sheets (Figure 2B) may better accommodate large arrays of actively translating and translocating polysomes (Shibata *et al.*, 2006). Supporting this idea, over-expression of p180 promotes ER sheet proliferation in mammalian cells (Benyamini *et al.*, 2009; Ogawa-Goto *et al.*, 2007) and artificially in yeast (Becker *et al.*, 1999). The expression level of p180 varies from high expression level in actively secreting cells to negligible in other cell types

(Langley *et al.*, 1998). How does the high membrane curvature of tubules serve tubular functions? The greater surface-to-volume ratio of the highly curved tubules, compared to sheets, may facilitate rapid transport of lipids and be involved in Ca^{2+} -related functions (Shibata *et al.*, 2006). Tubules might also be the preferred site for lipid synthesis and forming contact sites with other organelles (Baumann and Walz, 2001). Furthermore, high membrane curvature at tubules might serve for COPII-vesicle formation and budding. In agreement, ERES-markers are found at ER tubules (Hammond and Glick, 2000), although it is not known if these markers are excluded from ER sheets. Based on 3D-EM, however, the vesicles at ERES bud out from ER sheets (Bannykh *et al.*, 1996). To conclude, the functional assignment of ER tubules remains elusive and it is possible that tubular ER might simply provide a useful architecture to allow a cell wide distribution without disrupting general diffusion and trafficking in the cytosol (Friedman and Voeltz, 2011). In addition to specific subdomains listed above, additional sites for ER quality control associated protein degradation (Lederkremer, 2009) might exist. However, the morphological description of these sites is lacking.

It is noteworthy that our current understanding of SER/RER-specific protein localization, and the functional segregation into these subdomains, are largely based on the biochemical studies done in *in vitro* assays few decades ago, and have not been reproduced with modern cell biological techniques.

1.2.2 Form and function: Adaptation of endoplasmic reticulum structure and organization to cell's needs

Further evidence for the structure-function relationship of ER came from the differentiating B lymphocytes where the ER expansion was observation to be accompanied by an induction of ER chaperones (van Anken *et al.*, 2003), and increased level of synthesis and secretion of antibodies (Wiest *et al.*, 1990). Furthermore, in the presence of high amounts of toxins such as ethanol, SER size increases (Iseri *et al.*, 1966; Lieber, 2004) in conjunction with an increased level of SER-associated detoxifying enzymes (Takahashi *et al.*, 1993).

Physiological conditions can also induce large-scale reorganization of ER network. ER can adapt to cell's needs, and it has been reported to reorganize into packed wave-like sinusoidal ER (Anderson *et al.*, 1983), or ordered arrays of membrane tubules/sheets with hexagonal or cubic symmetry (Chin *et al.*, 1982), in response to changes in cholesterol levels; to concentric membrane whorls (Koning *et al.*, 1996), that are in straight continuity with the rest of the network and have been observed in a large number of normal tissues, including testicular, adrenocortical, melanoma cells and neuronal cells (Chin *et al.*, 1982); to tightly packed whorls following the upregulation of the detoxification processes in hepatocytes (Feldman *et al.*, 1981); and, to stacked membranes that have ribosomes attached only to the outermost membranes of the stack, which are directly continuous with non-stacked ER membranes, in apoptotic Purkinje neurons (Wolf *et al.*, 2012). OSER can also be induced by drug treatments or by upregulation of a variety of membrane-

anchored ER proteins (Chin *et al.*, 1982). The structures may represent different stages of SER differentiation and are all therefore referred to as OSER (Korkhov and Zuber, 2009; Snapp *et al.*, 2003). Interestingly the depletion of ERES-localizing Yip1A, that is involved in the biogenesis of COPII vesicles (Heidtman *et al.*, 2003), induced ER network reorganization into concentrically stacked membrane whorls (Dykstra *et al.*, 2010). These morphological changes, in turn, were sufficient to delay COPII-mediated secretion. Based on these observations it was suggested that the ER reorganization into whorls may provide means for transient down-regulation of cargo exit without directly modifying components of the COPII machinery (Dykstra *et al.*, 2010). However, this hypothesis remains to be proven.

Such large-scale ER reorganizations suggest that ER form follows its function and, furthermore, that the ER structure can be adapted to cell's needs. However, the functional importance of the different reorganizations remains unclear.

1.2.3 Endoplasmic reticulum malfunction and diseases

Given the essential functions of the ER, the number of disorders associated with malfunctioning ER, and also ER-derived organelles such as the Golgi complex, lipid droplets and peroxisomes, are increasingly characterized. Historically, ER-associated diseases were summarized as ER storage diseases where various stresses, which impair ER function, lead to an accumulation of unfolded or misfolded proteins, *e.g.,* cystic fibrosis, LDL receptor defects and coagulation factor V and VIII deficiencies (Rutishauser and Spiess, 2002). Increasing evidence suggests that ER stress is involved in variety of neurodegenerative diseases such as Alzheimer's disease, Parkinson's disease and cerebral ischaemic insults, as well as cancer, obesity and diabetes (for a review see Hosoi and Ozawa (2010)). Nowadays, the center of the attention lies strongly on the MAMs (de Brito and Scorrano, 2010): Numerous disease-associated proteins, for instance, presenilins associated with Alzheimer's disease (Area-Gomez *et al.*, 2009) and mitofusin 2 involved in Charcot-Marie-Tooth disease type 2A neuropathy (Zuchner *et al.*, 2004), are found from MAM. Silencing of mitofusin 2 in mouse embryonic fibroblasts and HeLa cells disrupts ER morphology and loosens ER-mitochondria interactions (de Brito and Scorrano, 2008). The common cause for these diseases is likely connected to dysfunctional ER-mitochondria Ca^{2+} signalling that misregulate the apoptotic onset.

Curvature-inducing proteins of ER have also been implemented in human diseases. Mutations in atlastin, REEP1 and spastin have been linked to hereditary spastic paraplegia (Park *et al.*, 2010), a disease affecting the long axons of corticospinal motor neurons (Salinas *et al.*, 2008). Given the role of the atlastins in ER network formation, the disease may be caused by ER morphology defects (Hu *et al.*, 2009). Indeed, atlastin mutants are defective in ER fusion (Bian *et al.*, 2011), indicating that ER continuity and shape is crucial for cell functions. Atlastin, REEP1 and spastin collectively account for well over 50% of all hereditary spastic paraplegia cases, suggesting that morphological defects, that also affect ER functions, may be a predominant mechanism underlying these neuropathogenic disorders (Park *et al.*, 2010).

The improper localization and function of INM proteins have been linked to numerous human diseases, for example, but not restricted to: Pelger-Huët anomaly caused by *LBR*-mutations which lead to an abnormal nuclear shape and chromatin organization in blood neutrophils; Osteopoikilosis, Buschke-Ollendorff syndrome, and nonsporadic melorheostosis, which are caused by loss-of-function mutations in *LEMD3* encoding MAN1; and, autosomal recessive cerebellar ataxia that is caused by mutations in *SYNE1* (for review, see Worman *et al.* (2010)). Similar to INM proteins, mutations in lamins are linked to a large number of laminopathies, *e.g.,* Emery-Dreifuss muscular dystrophy and related myopathies, Dunnigan-type familial partial lipodystrophy, Charcot-Marie-Tooth disease type 2B1 and developmental and premature ageing syndromes (reviewed in Worman and Bonne (2007); Vlcek and Foisner (2007)), highlighting the crucial role of the NE for normal cell function.

2. Endoplasmic reticulum dynamics

ER is a structure in flux and constantly rearranging. However, ER does not move *en masse*, but the network movement is achieved through remodelling and as movement of individual structures. While the reason for the dynamics and rearrangements is not known, it has been suggested that the dynamics might allow the ER to adapt to changes in cell morphology during cell migration, differentiation, and polarization (Friedman and Voeltz, 2011). While integral membrane proteins are indispensable for the maintenance of ER, the dynamics and the network remodelling are accomplished through interactions with the cytoskeleton. ER sheets and tubules might interact with different cytoskeletal elements (Baumann and Lautenschlager, 1994).

2.1 Dynamic network remodelling in interphase

What is 'movement through remodelling'? Tubules and sheets create a polygonal network, which can be altered by changing branching patterns or network nodes (*i.e.,* small punctate that may resemble small sheets) rather than moving by a global shift of sheets or tubules. Based on live cell imaging of plant cells, tubules can form sheets and *vice versa* (Knebel *et al.*, 1990; Quader *et al.*, 1989). Sheets transform into tubules by producing tubules at their edges or by extensive fenestration (Griffing, 2010). All of these events are called remodelling or transformations. While ER in plants is more dynamic than in animal cells, perhaps due to being driven by different cytoskeletal systems (Sparkes *et al.*, 2009), their structural resemblance is remarkable and may share similar rules for remodelling. The ground work for ER dynamics in animal cells was done by Lee and Chen (1988) who identified three basic events that remodel the ER network. Firstly, tubules fuse to form new branch points and polygons; secondly, junctions at the branch points slide; and, thirdly, junctional sliding may result polygonal closing. In addition to these basic events, several additional events are common in both plant and animal cells: Tubules shrink, kink and deform; Network nodes at kinks and branch points participate in the network dynamics; Polygon filling with membrane generate new sheets; And finally, polygon opening within sheets creates smaller sheets or alters the sheet structure (Sparkes *et al.*, 2009; Waterman-Storer and Salmon, 1998).

While the purpose of movement through remodelling is unclear, it is thought that ER network structure, and perhaps, ultimately, the functions of the subdomains, are consequence of the balance between tubule growth and shrinkage, tubule and sheet persistence and tubule–to-sheet and sheet-to-tubule transitions (Griffing, 2010). As ER contacts almost every other organelle in the cell, performs a variety of functions at these contact sites, and even appears to share coordinated movements with some of these organelles, it is possible that the ER dynamics serve to establish and maintain these specialized subdomains throughout the cell, linking ER dynamics and morphology to its functions.

2.2 Endoplasmic reticulum and cytoskeleton

While tubular ER network can be generated *in vitro* from *Xenopus laevis* eggs membrane vesicles independent of MTs and actin filaments in the presence of cytosol (Dreier and Rapoport, 2000), it is unclear if sheets can be formed in this way. According to *in vitro* experiments done in rat hepatocyte microsomes, sheets can be generated in the presence of GTP, and tubules in the presence of both GTP and ATP, in cell-free systems (Lavoie *et al.*, 1996). However, to my view, the formed sheets appear uncharacteristic: the luminal diameter varies from practically non-existing to swollen protrusions. Furthermore, the ribosome distribution on the formed sheets seems and the formed network of RER and SER does not appear characteristic, and it is therefore plausible that the formation of typical ER phenotype requires interplay of several factors - including the different cytoskeletal filaments.

2.2.1 Tubular dynamics, microtubules and molecular motors

Treatment with nocodazole, a MT disassembly reagent, or by a cold-shock, which is also known to disrupt the MTs, results in conversion of ER network towards sheets and a slow retraction of ER from the cell periphery towards the NE (Bannai *et al.*, 2004; Terasaki *et al.*, 1986; Waterman-Storer and Salmon, 1998), indicating that MTs play a major role in tubular ER dynamics in animal cells. There are two mechanisms how ER tubules move along MTs: In TAC (Tip Attachment Complex) mechanism, the tip of the ER tubule binds to the tip of a dynamic MT, and the ER tubule grows and shrinks in concert with the dynamics of the plus-end of the MT. TAC rearrangements are nocodazole sensitive (Waterman-Storer and Salmon, 1998) and dependent on the STIM1 and EB1 (end binding protein 1) binding to MTs, and motor protein independent (Grigoriev *et al.*, 2008). The second mechanism of ER tubule dynamics is referred to as sliding, whereby ER tubule tip binds to the shaft of an existing MT and as the ER tubule grows it slides along the stable MT (Lee and Chen, 1988; Waterman-Storer and Salmon, 1998). In contrast to TAC-mechanism, sliding does not correlate with MT growth or shrinkage. In addition, sliding is less sensitive to nocodazole treatment (Waterman-Storer and Salmon, 1998) or to depletion of STIM1 or EB1 (Grigoriev *et al.*, 2008). Another differing aspect is the frequency and velocity of the tubule movement: ER tubule sliding events are much more frequent and faster than TAC dynamics (Grigoriev *et al.*, 2008; Waterman-Storer and Salmon, 1998) and are therefore the predominant mechanisms for ER dynamics in interphase cells.

Motor proteins are a class of molecular motors that are able to move along the surface of a suitable substrate. They are powered by the hydrolysis of ATP and convert chemical energy into mechanical work. Kinesin and dynein are motor proteins that move along MTs. ER sliding occurs in both directions along MTs (Waterman-Storer and Salmon, 1998) and is thought to be driven by both dynein and kinesin-1 (Wozniak *et al.*, 2009). Kinesin-1 drives the ER tubular movement towards the MT plus end via ER membrane protein adaptor, kinectin, whereas dynein-dynactin-complex drives the tubular movement towards the MT minus end (Kumar *et al.*, 1995; Wozniak *et al.*, 2009). However, reduced frequency of ER sliding in the absence of kinectin has not been shown. Antisense oligonucleotides to kinesin-1 reduced ER extension to the cell periphery in the brain and spinal cord glial cells (Feiguin *et al.*, 1994) and inhibited ER motility in dendrites (Bannai *et al.*, 2004). The outward ER tubule movement in Vero (Kidney cells of African green monkey) cells is inhibited by dominant-negative mutants of kinesin-1 (Wozniak *et al.*, 2009). While kinectin depletion results in ER retraction to perinuclear area (Santama *et al.*, 2004), and the over-expression of the inhibitory domain of either kinectin or kinesin-1 induces ER clustering and disrupts the lamellar localization of the ER (Santama *et al.*, 2004; Zhang *et al.*, 2010), surprisingly, the kinesin-1 heavy chain knockout had no effect on ER position in mouse embryo fibroblasts (Tanaka *et al.*, 1998).

While the major role assigned for kinesin-1 is to accomplish ER tubular movement, kinectin localize to ER sheets and, when over-expressed, causes sheet proliferation (Santama *et al.*, 2004), indicating that kinesin-1 and kinectin interaction might have an additional roles on ER sheets. There is also further evidence on MTs interacting with ER sheets: Climp-63 and p180 have been shown to bind directly to MTs (Klopfenstein *et al.*, 1998; Ogawa-Goto *et al.*, 2007). Over-expression of these proteins leads to MT bundling, but the physiological significance of the MT interaction with ER sheets remains to be solved as the role of Climp-63 as a luminal ER bridge does not rely on its MT-binding ability (Klopfenstein *et al.*, 1998; Klopfenstein *et al.*, 2001; Vedrenne *et al.*, 2005). Furthermore, as Climp-63 depletion has not been shown to abolish ER sheets, the role of Climp-63 MT-attachment, rather than accomplish ER sheet movements or work as a determinant of ER sheet formation, could be to reduce the mobility of the translocon complex and facilitate protein translocation (Nikonov *et al.*, 2007).

The differences between TAC and ER sliding mechanisms suggest that they might contribute to very different ER functions. The TAC protein STIM1 also functions in store-operated Ca^{2+} entry at the PM, and TAC might have a specific role on this, although this has not been proven (Friedman *et al.*, 2010). The significance of ER sliding dynamics is not known, even though the cell likely consumes a great deal of energy to constantly reorganize ER on MTs by using motor proteins. Interestingly, a recent study showed that ER tubule sliding occur on stable acetylated MTs and that the TAC-based tubular dynamics occur only on dynamic, non-acetylated, MTs (Friedman *et al.*, 2010), indicating that different tubular ER dynamics occurs on defined paths of the MT cytoskeleton. The authors also demonstrated that mitochondria,

but not endosomes, preferentially localize alongside acetylated MTs, which suggests that ER might use different means of dynamics to establish or maintain contacts with other membrane-bound organelles (Friedman *et al.*, 2010).

The association sites between tubular ER and Rab10 GTPase (*i.e.,* able to hydrolyse GTP) are enriched with enzymes involved in phospholipid biosynthesis (English and Voeltz, 2013), indicating that Rab10 complex could mediate tubular ER extension and fusion along MTs, and the phospholipid biosynthesis enzymes could synthetize the phospholipids necessary for ER growth and/or fusion. These results suggest that ER growth, fusion and lipid synthesis might be coupled. Another possibility could be that ER tubule growth is not driven by the lipid synthesis, but rather that the synthesis of specific phospholipids at the tip of dynamic ER tubules facilitates transfer of these lipids to other membrane-bound compartments during ER dynamics.

2.2.2 Interactions with the actin cytoskeleton

While actin cytoskeleton is the major track for ER remodelling in yeast (Prinz *et al.*, 2000; Pruyne *et al.*, 2004), plants (Gupton *et al.*, 2006; Sparkes *et al.*, 2009) and cell cycle dependently in *C. elegans* (Poteryaev *et al.*, 2005), its interaction with mammalian ER are considered less important. However, although MTs and the associated protein machinery are the main mechanism to accomplish ER remodelling in interphase animal cells (Grigoriev *et al.*, 2008; Nikonov *et al.*, 2007; Wozniak *et al.*, 2009), MTs and ER tubules do not have identical distribution in cells and there is a body of work indicating that ER can also interact with actin cytoskeleton in animal cells or during different stages of differentiation or cell cycle.

ER has been shown to align along stress fibers in kidney epithelial cells (Sanger *et al.*, 1989); move along actin filaments in locust photoreceptor cells (Sturmer *et al.*, 1995) and squid axons (Kuznetsov *et al.*, 1994); have a structural interaction with actin cytoskeleton in honeybee photoreceptor cells (Baumann and Lautenschlager, 1994); and, enable ER spreading in mouse embryonic fibroblasts (Lynch *et al.*, 2011). Furthermore, retraction of ER to perinuclear area upon MT depolymerisation has been shown to be actin dependent and it has been suggested that the ER structure at cell periphery is determined by a balance of MT and actin filament forces and their motor proteins (Terasaki and Reese, 1994). In accordance, by using an actin depolymerizing drug, Cytochalasin B, the retrograde movement of ER was halted in frog kidney cells (Terasaki and Reese, 1994). Furthermore, actin cytoskeleton has been linked to one of the most important ER functions, the regulation of Ca^{2+} homeostasis, by showing that the store-operated Ca^{2+} release from ER is modulated by actin polymerization in rat hepatocytes (Wang *et al.*, 2002).

Inverted formin 2 (INF2) was the first protein shown to be directly associated with ER and actin filaments in cultured fibroblasts (Chhabra *et al.*, 2009). INF2 is peripherally bound to the cytoplasmic face of the ER and it possesses a unique ability to both nucleate and depolymerize actin filaments. Dominant-negative expression of mutated INF2 with abolished depolymerization activity causes the ER to collapse at perinuclear area, with accumulation of actin filaments around the

collapsed ER. While the authors claim that INF2 knockdown did not cause apparent changes in the ER morphology, the study was done at in light microscopy (LM) level and the ER ultrastructure was not studied. Recently it was shown that INF2 actin polymerization activity is required for efficient mitochondrial fission in mammalian cells (Korobova *et al.*, 2013).

Studies done in mammalian, frog and nematode cells indicate that cells might switch their preferred cytoskeletal filament system cell-cycle dependently or during differentiation. In mitotic HeLa cells, RER is located at the cell periphery and it associates closely with the cortical actin (McCullough and Lucocq, 2005). Upon actin depolymerization, RER was observed to relocate to the cell cortex and shift towards tubular morphology. While it is believed that MT- and actin-based organelle movements are down-regulated in mitosis, in *in vitro* experiments on *Xenopus laevis* egg extracts the movement of ER, and the subsequent ER network formation, occurred along actin filaments in metaphase extracts (Wollert *et al.*, 2002), suggesting that the cells might switch to actin-mediated movement during mitosis. Furthermore, there are indications that dynamics and morphological transitions of the ER in *C. elegans* can switch between MTs and actin cell-cycle dependently and based on developmental stage (Poteryaev *et al.*, 2005). Together, these results indicate an existence of variety of possibilities for controlling the ER dynamics and morphology in different organisms and that this plasticity in even more profound when taking into account the events during cell cycle and differentiation.

While ER tubules are generated along actin filaments by using actin-binding molecular motor myosin 4p in *S. cerevisiae* (Estrada *et al.*, 2003), the alignment of ER tubules with the actin filaments is not perfect. Furthermore, actin depolymerization does not collapse ER network in yeast (Prinz *et al.*, 2000), and even in mammalian cells ER retracts only with some delay upon MT depolymerization (Terasaki *et al.*, 1986). Thus, mechanisms other than those based on either MT and/or actin cytoskeleton most likely stabilizes and maintains the ER network. These players might include the ER fusion machinery and reticulons, which have been suggested to stabilize the overall ER structure during these dynamic events (Friedman and Voeltz, 2011). While the results summarized here clearly indicate that ER-actin interaction exist, the reports on ER-actin interactions in mammalian cells are mainly descriptive, and the mechanisms by which actin contributes to ER dynamics and/or morphology is unclear.

2.2.2.1 Unconventional myosin motor proteins

Myosins constitute a large superfamily of ATP- and actin-dependent molecular motors that are best known for their role in muscle contraction, but also for actin-based motility. Myosins are single or double-headed motor proteins that can bind to and move along actin filaments, and are commonly categorized as un-conventional or conventional molecular motors, respectively. Interestingly, a growing body of work indicates a crosstalk between unconventional myosins and MTs, in addition to the more conventional interaction of myosins with actin filaments. Although there is no evidence that myosins can use MTs as motor substrate, several unconventional myosins, *e.g.,* myosin

Va (Cao *et al.*, 2004), myosin-X (Weber *et al.*, 2004), myosin VI (Lantz and Miller, 1998), myosin VIIA (Todorov *et al.*, 2001) and myosin-XV (Liu *et al.*, 2008), have been shown to associate with MTs in other ways, and mechanically couple actin cytoskeleton to MTs. The functional importance of the link between these cytoskeletal elements is unknown, but the connection could provide means for coordination of the cell's tasks or dynamics.

The only identified myosin so far involved in ER-actin interactions in mammalian cells is the myosin Va. ER transport from the dendritic shaft to dendritic spine in Purkinje neurons is dependent on the myosin Va, and nocodazole insensitive (Bridgman, 1999; Takagishi *et al.*, 1996; Wagner *et al.*, 2011). The absence of ER in the dendritic spines of myosin Va knockout neurons was rescued by re-introduction of the wild-type (wt) myosin Va, but not by its mutant. In accordance, myosins have been shown to enable short-range ER mobility *in vitro* (Tabb *et al.*, 1998; Wollert *et al.*, 2002). Myosin Va, in addition to many other unconventional motor proteins, including myosin I family members, have been shown to associate directly with membrane lipids (McConnell and Tyska, 2010) instead of binding to adaptors, and to link cellular membranes directly to actin filaments.

2.2.2.2 Myosin 1 as a membrane–cytoskeleton crosslinker

The class I myosin motors are single-headed unconventional motor proteins. Eight myosin I isoforms, myosin 1a-1h (myo1a-1f) (Figure 4), are present in humans (Gillespie *et al.*, 2001) and although many of them are expressed in nearly all cell types, some of them are tissue specific (Berg *et al.*, 2001). The first myosin to be isolated from the mammalian cells, myosin 1c (myo1c) (Barylko *et al.*, 1992), also known as myosin I (Barylko *et al.*, 1992), myosin 1β (Reizes *et al.*, 1994), and myr 2 (rat ortholog) (Ruppert *et al.*, 1995), is widely expressed in tissues and cell culture types (Wagner *et al.*, 1992). Regardless of the expression profile, a defining feature of all class I myosins is their ability to interact directly with cell membranes and actin. Membrane interactions are mediated by a C-terminal tail homology 1 (TH1) domain that contains a putative pleckstrin homology (PH) lipid-binding motif, while actin binding is localized to the N-terminal motor domain (Figure 4). The motor domain, also known as the catalytic core, binds to and hydrolyses nucleotide ATP to ADP. The N- and C-terminal domains are connected by the neck region that is a single alpha-helix which is supported by calmodulin light chains and acts as a mechanical lever arm, coupling conformational changes in the motor domain to a physical displacement of the membrane-binding domain. The neck region is the most variable domain among myosin I motor proteins displaying different numbers of IQ motifs (refers to the first two amino acids, isoleucine and glutamine, of the motif), which bind variable number of calmodulins that, in-turn, sensor [Ca^{2+}] and regulate the motor function (De La Cruz and Ostap, 2004; Hokanson *et al.*, 2006; Reizes *et al.*, 1994) (Figure 4). Conformational changes associated with nucleotide binding, hydrolysis and product release result in the ability of the motor proteins to sense strain and move. Myo1e has a high duty rate catalytic core and extended tail domain, which are well suited for rapid contractile events such as

pseudopod extension that are temporary projections of eukaryotic cells membranes (De La Cruz and Ostap, 2004; El Mezgueldi *et al.*, 2002), whereas myo1c has a low duty rate catalytic core and a short tail and is therefore better suited for structural roles or for tension generation and maintenance (Coluccio and Geeves, 1999; Conibear, 1999) (Figure 4B). The highly divergent tale regions of the myosin I motors bind to specific lipids at particular membranes enabling individual functions (Akhmanova and Hammer, 2010).

Myo1a, 1b and 1c associate with endosomal/ lysosomal membranes (Bose *et al.*, 2002; Raposo *et al.*, 1999; Salas-Cortes *et al.*, 2005; Sokac *et al.*, 2006), PM (McConnell and Tyska, 2007) and Golgi membranes (Almeida *et al.*, 2011). Myo1e is implemented in exocytosis and endocytosis (Krendel *et al.*, 2007; Schietroma *et al.*, 2007) and myo1g have been shown to localize to PM lipid rafts in B-lymphocytes (Nebl *et al.*, 2002). Myo1c has also been shown to localize to these lipid raft membrane micro-domains (Zhu *et al.*, 1996), which are characterized by sphingolipids, cholesterol and phosphatidylinositol 4,5-bisphosphate (PtdIns(4,5)P_2 or PIP_2) (Owen *et al.*, 2012; Simons and Ikonen, 1997). One of the three myo1c isoforms, the nuclear myo1c, (Nowak *et al.*, 1997) has been shown to be involved in transcription (Dzijak *et al.*, 2012; Philimonenko *et al.*, 2004) and chromatin reorganization (Chuang *et al.*, 2006), while the other two isoforms localize to distinct punctate under PM and in the cytoplasm, as well as, diffusely throughout the cytoplasm (Wagner *et al.*, 1992). Myr2 immunoreactivity from isolated sucrose gradient membrane fractions have showed that Myr2 associates

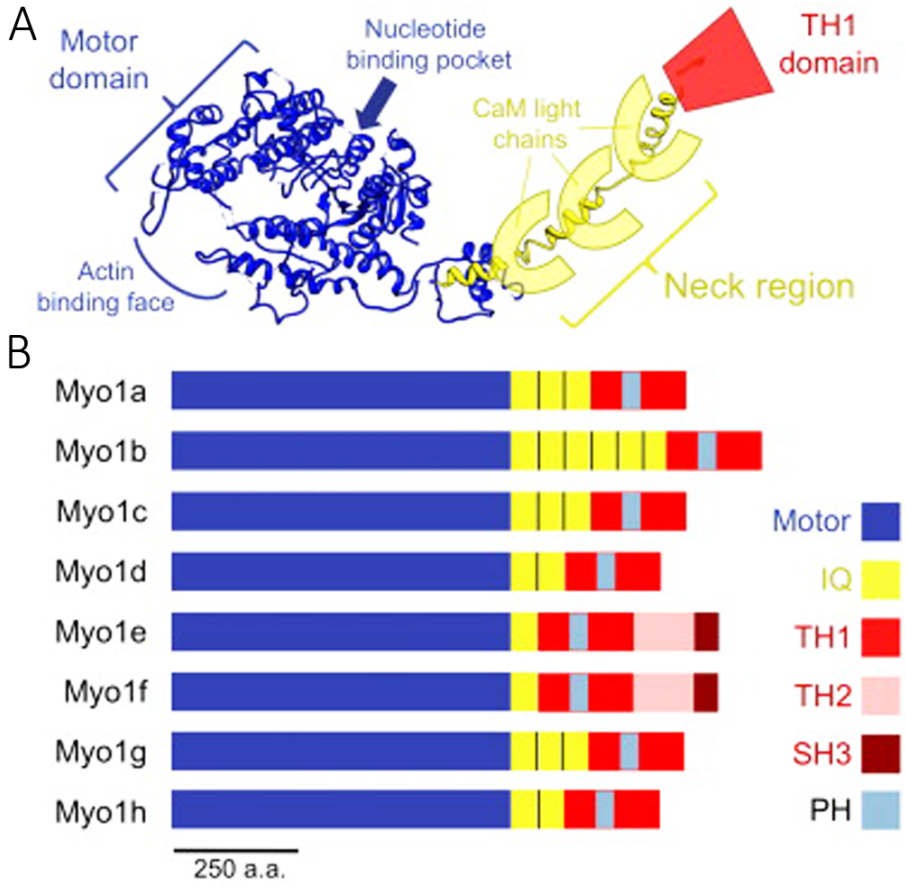

Figure 4. An introduction to class I myosins. All class I myosins share a common structural arrangement, with a globular N-terminal motor domain (blue) that is connected to a membrane-binding tail (TH1 and TH2; red) by an α-helical neck region (IQ; yellow) which binds 1–6 calmodulin light chains. (A) Predicted structure of myo1a. (B) Domain structures of myo1a-1h. The long-tailed myo1e-1f have an extended C-terminal tail possibly mediating ATP-independent interactions with actin and direct binding to other proteins (via SH3 domain). The PH-domain at the tail and the approximate size in amino acids (a.a.) are indicated. Image modified from McConnell and Tyska (2010).

with fractions enriched with ER and PM, but not with Golgi, intermediate compartment, lysosomes, peroxisomes or mitochondria (Ruppert *et al.*, 1995).

Myo1c has been shown to bind specifically and with high affinity to PIP_2 via its PH-domain, and to lesser extent to other lipids (Hirono *et al.*, 2004; Hokanson *et al.*, 2006), and based on live cell imaging experiments, the myo1c localization in the cells is dependent on its binding to PIP_2 (Hokanson *et al.*, 2006; Hokanson and Ostap, 2006), and therefore myo1c relies on PIP_2 on its intracellular localization. In support, Myr2 has been shown to localize to lipid rafts enriched with PIP_2 (Barylko *et al.*, 2005). PIP_2 is commonly referred to as a PM localizing lipid (Levental *et al.*, 2009; Ozato-Sakurai *et al.*, 2011; Simone *et al.*, 2013) and indeed, based on LM, PIP_2 was shown to predominantly reside at the PM in CHO (Chinese hamster ovary) cells (Di Paolo and De Camilli, 2006). To my view, however, distinct punctate-like signal of PIP_2 in the cytoplasmic area can also be observed, although this was not disclosed in the study. Interestingly, PIP_2 has also been shown to localize to ER based on an immuno-EM study done in mammalian glial and epithelial cells (Watt *et al.*, 2002), and a cell permeabilization and *in vitro* assays done in NRK cells (normal rat kidney) (Baughman *et al.*, 2008). PIP_2 has also been shown to be synthetized in ER in CHO cells (Helms *et al.*, 1991) and proposed to play a role in ER-Golgi transport (Godi *et al.*, 1998). Furthermore, PIP_2 has been shown to localize to NE based on *in vivo* studies in HeLa (Domart *et al.*, 2012) and *in vitro* studies on hepatocyte cell fractions (Slomiany *et al.*, 2006). The conflicting results may result from few reasons: Firstly, based on chosen methods (*e.g.,* LM level localization of the molecule); secondly, PIP_2 might be present at ER only transiently; and thirdly, the distinct localization of PIP_2 at cytoplasm, *i.e.,* the punctate patterning, does not resemble typical ER staining and might be easily overlooked.

In addition to cellular functions mentioned above, there are implications that myo1c functions in the maintenance and organization of actin filaments: The cortical actin rearrangements require myo1c in adipocytes (Bose *et al.*, 2004; Hagan *et al.*, 2008); Lamellar dynamics is accomplished through myo1c in neurons (Diefenbach *et al.*, 2002); Transport of actin monomers to cell's leading edge is myo1c dependent in migrating cells (Fan *et al.*, 2012); Specific organization of actin cytoskeleton at visceral epithelial cells requires myo1c for down-stream activation of Arp2/3 and subsequent actin polymerization and branching (Arif *et al.*, 2011; Garg *et al.*, 2007); And, actin rearrangements are regulated by myo1c in cell lamella and filopodia in spreading B lymphocytes (Maravillas-Montero *et al.*, 2011).

2.2.3 Nuclear envelope migration and anchorage via intermediate filaments

While there are no clear indications that peripheral ER and intermediate filaments interact, the A- and B-type lamins are involved in the NE morphogenesis (Gruenbaum *et al.*, 2000) and critical for the nuclear stability when cells are exposed to mechanical forces (Cohen *et al.*, 2008). Indeed, lamins impede cell migration through solid tissue but also promote survival against migration-induced stress (Harada *et al.*, 2014). Mechanisms for nuclear migration and anchorage differ cell type and organism

dependently but rely on the communication with the cytoskeleton (Starr, 2007). All three components of the cytoskeleton, MTs, actin filaments, and intermediate filaments, function together to position nucleus, although the role of each filament type varies in different cell types. Positioning of nucleus within the cell occur through two steps: nuclear migration to appropriate location and subsequent anchorage to prevent drift. While migration and anchorage are predicted to be coordinated, the precise molecular mechanism is yet lacking.

In humans, there are at least 67 genes that encode functional intermediate-filament proteins, which makes this gene family one of the largest in the human genome (Herrmann *et al.*, 2003). Desmin is a major intermediate filament-type in mammalian muscle fibers and in desmin knockout mice the NE anchorage is disrupted (Ralston *et al.*, 2006). Furthermore, mutant forms of another intermediate filament-type, vimentin, has been shown to induce nuclear morphology defects (Toivola *et al.*, 2005). Owing to its linkage to the cytoskeleton, LINC complex has been suggested to be involved in the nuclear positioning and migration (Lombardi *et al.*, 2011). A newly identified member of the LINC-complex is the KASH- protein, nesprin-3, that likely connects the ONM to cytoplasmic intermediate filaments (Wilhelmsen *et al.*, 2005). Based on yeast two-hybrid assay, nesprin-3 interacts with plectin, that has an intermediate filament-binding domain (Fuchs and Karakesisoglou, 2001; Wilhelmsen *et al.*, 2005) and could mediate the interaction with NE. Since there are no known motors that move along intermediate filaments and because they do not have the polar dynamic growth properties of MTs or actin filaments, intermediate filaments are thought to form a more static scaffold for nuclear anchoring or to recruit components that can interact with other members of the cytoskeleton.

2.3 Dynamic membrane shaping of endoplasmic reticulum during mitosis

2.3.1 Nuclear envelope breakdown and assembly

Animal cells undergo an open mitosis, and NE is disassembled in prophase to allow interaction of the spindle MTs with chromosomes. NE breakdown (NEBD) is at least in part driven by the phosphorylation of nuclear lamins, nucleoporin and NE transmembrane proteins (Foisner, 2003; Goss *et al.*, 1994), leading to the disruption of protein-protein interactions necessary for the integrity of NE structures. After the disassembly of nucleoporins and nuclear pores, the nuclear membrane detaches from the chromatin and the NEBD proceeds by rapid fenestration and expansion of membrane holes (Ellenberg *et al.*, 1997). Depletion of Yop1p and Rtn1 in *C. elegans* delays NEBD, indicating that NEBD proceeds through membrane bending/ fenestration (Audhya *et al.*, 2007). NEBD is facilitated by the cytoskeleton: MT-based dynein-dynactin motor complex generates tension to rupture the NE (Beaudouin *et al.*, 2002). Based on *in vitro* and *in vivo* studies, the disassembled NE components have different faiths: nuclear pore complexes disassemble into stable subcomplexes, which are released into the cytoplasm, and the NE transmembrane nucleoporin proteins POM121 and gp210, as well as all most of the NE transmembrane proteins (LBR, LAP2β, emerin, Sun1-2 and

nurim) are absorbed into the mitotic ER (Anderson and Hetzer, 2007; Beaudouin *et al.*, 2002; Ellenberg *et al.*, 1997; Yang *et al.*, 1997b), which at the end of mitosis, serves as the precursor membrane for NE formation (Burke and Ellenberg, 2002). In contrast, the INM protein p58 localizes to vesicles that are essentially depleted of ER membrane proteins (Maison *et al.*, 1993), indicating that not all NE components are inherited in similar manner. The specific location of the NE proteins within mitotic peripheral ER is not known. However, it's been suggested that NE proteins that are redistributed into the mitotic ER might preferentially localize to ER subdomains based on preference on membrane curvature: nuclear pore complexes POM121 (Daigle *et al.*, 2001) and Ndc1 (Mansfeld *et al.*, 2006), which in interphase localize to the curved membranes at the nuclear pores, might be present at higher concentrations in tubules, whereas INM proteins such as Sun1 and Sun2 might translocate to ER sheets (Shibata *et al.*, 2006). Interestingly, based on FRAP-experiments, the redistributed LBR in the mitotic ER membranes is highly mobile, compare to rather immobilized appearance in interphase cells (Ellenberg *et al.*, 1997).

In late anaphase / telophase, the NE starts to reassemble around the segregated chromosomes by targeting of ER tubule ends to the chromatin, shown both *in vitro* and *in vivo* (Anderson and Hetzer, 2007; Anderson and Hetzer, 2008). Importin-β recruits LBR, which targets the precursor membranes to chromatin (Ellenberg *et al.*, 1997; Lu *et al.*, 2010), which occurs simultaneously to the assembly of nuclear pores (Hetzer, 2010). LBR depletion blocks membrane binding to chromatin (Pyrpasopoulou *et al.*, 1996). Moreover, *in vivo* depletion of Sun1, that targets the initial ER-chromatin contact, delays the nuclear reassembly (Chi *et al.*, 2007). Based on cell-free studies, the NE assembles on chromatin surface through intermediate structure composed of tubules and small sheets (Anderson and Hetzer, 2007; Dreier and Rapoport, 2000), which fuse NSF- and p97/p47-dependently, forming larger sheets that eventually seal the nucleus (Baur *et al.*, 2007; Hetzer *et al.*, 2001). The formation of NE has been shown to depend on curvature-inducing proteins both in mammalian cells *in vivo* (Anderson and Hetzer, 2007) and in *Xenopus* egg extracts *in vitro* (Kiseleva *et al.*, 2007), however, the precise mechanism how the reticulons contribute to the event is unclear.

At the end of cell division, NE reassembles in the forming daughter cells, and NE regains its identity that was lost during the cell division. In interphase, the NE and the number of nuclear pores in the newly formed daughter cells grows in size and number, respectively, and the required membrane for NE expansion most likely originates from the peripheral ER (Anderson and Hetzer, 2007; Kiseleva *et al.*, 2007).

2.3.2 Mitotic morphology of the peripheral endoplasmic reticulum

In addition to steady state dynamics in interphase cells, ER shows remarkable dynamic organizational changes throughout the cell cycle across species (Friedman *et al.*, 2010). The morphogenesis of the ER during mitosis, the partitioning of the NE or other functional subdomains in relation to, or within, the reticular ER in animal cells have remained unclear (Lowe and Barr, 2007). Two models of

ER partitioning has been presented: First, a complete fragmentation of the NE and fragmentation of the rest of the ER to a variable extent, yielding a heterogeneous population of fragments was suggested mainly based on EM studies (Du *et al.*, 2004; Tamaki and Yamashina, 1991; Warren and Wickner, 1996; Zeligs and Wollman, 1979) and studies done on cell free systems (Collas and Courvalin, 2000; Dreier and Rapoport, 2000). Second, based on FRAP experiments on mammalian cells (Ellenberg *et al.*, 1997) and sea urchin embryos (Terasaki, 2000), the NE proteins disperse into the ER after NEBD and ER remains continuous during cell division. In addition there are reports on HeLa (Mullins, 1984) and plant cells (Hawes *et al.*, 1981; Hepler, 1980) showing that ER is highly fenestrated during mitosis. In addition, mitotic HeLa cells have been reported to remain interconnected and transform into sheet-like organization (McCullough and Lucocq, 2005).

The mitotic ER in *C. elegans* forms clusters composed of tubules (Audhya *et al.*, 2007). Upon depletion of YOP-1 and RET-1, homologues of DP1 and Rtn4a, the formation of the mitotic tubular clusters was disabled, indicating that curvature-inducing proteins are involved in mitotic re-arrangement of ER. In agreement, upon depletion of Epsin (endocytic adapter protein during interphase), that is a curvature inducing protein, the ER in mitotic HeLa cells was composed of long, stacked and clustered ER membranes, suggesting that the membrane-bending ability of Epsin was responsible for mitotic conversion of ER. The morphology of mitotic ER varies considerably between cells of different species, cell types and developmental stage. Despite the discrepancy on mitotic ER morphology, most of the studies agree on the reorganization of the ER; it is excluded from the mitotic spindle area (Ellenberg *et al.*, 1997; McCullough and Lucocq, 2005; Parry *et al.*, 2005).

Mechanisms behind the ER's structural changes in mitotic are not known. One possible mechanism could raise from the cell cycle dependent changes in the cytoskeleton. Motor protein driven movement on MTs has been shown to rupture the NE at the beginning of mitosis (Beaudouin *et al.*, 2002) - although NEBD has also been shown to occur without MTs *in vitro* (Lenart *et al.*, 2003)- after which the MTs form the mitotic spindle, and most of the MT-based cellular movements are down-regulated (Niclas *et al.*, 1996; Warren and Wickner, 1996). There are few studies showing that ER loses its interaction with MTs during mitosis through phosphorylation of proteins mediating the MT-ER interactions or by down-regulation of protein expression. Climp-63-mediated stable anchoring of the ER to MTs is required for maintenance of the spatial distribution of the ER during interphase, this interaction is abolished by phosphorylation during mitosis (Vedrenne *et al.*, 2005). The level of p180 is reduced prior cell division leading to a reduced ribosome density on ER membranes (Benyamini *et al.*, 2009) and, subsequently, leading to lesser ER-MT interaction. Furthermore, STIM1 is phosphorylated, losing its interaction with MTs and PM (Smyth *et al.*, 2009). Furthermore, there are few indications of a switch to actin-based movement during mitosis; Studies done on *Xenopus laevis* egg extracts show that mitotic movements of ER occur on actin and are myosin Va-dependent (Wollert *et al.*, 2002) and the mitotic ER in HeLa cells have been shown to associate

closely with cortical actin (McCullough and Lucocq, 2005). Another possible mechanism regulating the mitotic structural changes of ER is the recent suggestion that the creation and/or maintenance of ER sheets could be linked to the membrane-bound polysomes, and the associated protein machinery (Shibata *et al.*, 2006). In accordance, it has been shown that the translation is down-regulated during mitosis (Le Breton *et al.*, 2005), and, based on sucrose-gradient analysis and EM, the polysomes are broken down during metaphase in both wt HeLa cells and those arrested in metaphase by treatment with colchicine (Le Breton *et al.*, 2005; Scharff and Robbins, 1966; Sivan *et al.*, 2007; Steward *et al.*, 1968). However, systematic and quantitative studies are needed to test this hypothesis.

In principle, there are a few ways an organelle can be inherited: The simplest way is the *de novo* synthesis, which means that provided with the information encoded in the genetic material and the machinery needed to interpret the code, the daughter cell could create a new organelle without a template of the original organelle. An alternative way is either to inherit a template that can be used to expand the organelle, or the organelle can be inherited as a whole. In theory, multi-copy organelles, such as mitochondria, can simply be shared out and do not need to be dismantled. If there are sufficient copies of the organelle or fragments derived from the original intact organelle, then a stochastic partitioning mechanism can explain efficient inheritance, which is most likely the case of inheriting ER (reviewed in Warren (1993); Lowe and Barr (2007)). Although it appears that ER is not actually broken down into fragments or vesicles, there are indications that its structure is transformed into smaller subunits, which would improve the stochastic inheritance. As ER is essential for the viability of every cell, it is crucial that both daughters inherit a sufficient fraction of the organelle. It has been demonstrated that in response to acute stress, yeast cells exhibit asymmetric division and inhibit ER inheritance by the bud (Babour *et al.*, 2010), and the daughter cell produced without ER is unviable, as predicted. However, even in normal divisions, the organelle fragments that are inherited by each daughter can be non-equivalent, as shown in yeast (Darzacq *et al.*, 2003), and the cells are still viable. Compared with chromosome segregation, which needs to be very precise to ensure that each cell inherits only one copy of each chromosome, organelle inheritance appears to be less controlled. In this context, it seems that it is only necessary that each daughter inherits sufficient amount of material for seeding the further expansion of the organelle.

V AIMS OF THE STUDY

This study aimed at revealing the structural and dynamic features of the endoplasmic reticulum and the nuclear envelope and the significance of interplay with the actin cytoskeleton. The specific aims were to study the

1. progression of morphological changes of ER and NE during mitosis
2. interphase ER sheets dynamics and transformations
3. interaction between ER and actin cytoskeleton in interphase
4. mechanism between ER-actin interactions by identifying the participating actin-binding proteins

VI MATERIALS AND METHODS

Methods I personally applied in this study are listed in the table below. Roman numerals refer to the publication in question. Asterisk indicates minor contribution. Methods used for unpublished results are listed below.

METHODS	PUBLICATION
Cell culturing	
CHO-K1	II, III
CHO-K1/LBR-GFP	III
CHO-K1/LBR-HRP	III
HeLa	I, II
Huh-7	I, II
NRK-52E	II
Cell biology	
Single or triple plasmid transfections	I, II, III
Over-expression experiments	I
siRNA silencing experiments	I
shRNA silencing experiments	I
Dominant-negative expression studies	I
Rescue experiments	I
Endocytic assays (Transferrin, Dextran)	I
Metabolic labelling to analyse protein synthesis and secretion rates	I
Latrunculin A, Nocodazole and Trichostatin A treatment	I
shRNA screen for actin binding proteins	I
BCH knockdown validation	I
Fluorescence labeling	I, II, III
Sample preparation for microcopy	
Immunofluorescence	I, II, III
Flat embedding for EM	I, III
Cytochemical staining	I, III
OTO-staining for serial block face SEM	I
Microtome thin sectioning	I
Microscopy and modelling	
Wide-field microcopy of live cells (TILL)	I
Wide-field microcopy of fixed cells (IX-71 inverted microscope)	I, II
Laser scanning confocal microscopy (fixed cells)	I, II
Laser scanning confocal microscopy (live cells)	I, II
Transmission electron microcopy	I, II
Serial block face Scanning Electron Microscopy	I
Electron tomography	I, III
Image acquisition and processing	
TILL VisION (TILL Photonics)	I
Las-AF	I, II
AxioImager M2	I, II
Leica Confocal software for SP2 AOBS	I
AX70 Provis microscope	II, III
Amira	II, III
Imaris Bitplane	II
ImagePro	I, II
Photoshop CS5.1	I, II, III*
Image J	I, II
MatLab Image browser	I
AutoQuant AutoDeblur 3D Blind deconvolution	I, II
VideoMacher	I, II
AIDA image analysis software	I

Phosphor imaging for radiolabelled proteins	I
Image quantitation	
Intersection method	I
Mean grey intensity measurements	I
Western blot band density measurements	I
Sheet persistency	I
Center-of-mass	I
Structural quantitation	I
Time-lapse	II
Statistical analysis	
PASW Statistics 18 software, SPSS, IBM	I
PASW Statistics 17 software, SPSS, IBM	I
Excel	I, II
Statistica software (Statsoft)	I*
Protein methods	
SDS-PAGE and Western blotting	I, II
BCA protein assay	I
Instant Blue staining	I

Cell culturing, transfections, immunofluorescence staining, immunoblotting and drug treatments

Huh-7, HeLa and NRK-52E were cultured as described in (II). Transfections were done as described in (I). Construction of ssHRP-KDEL was described in Connolly *et al.* (1994) and provided by the respective laboratory. The depletion of myo1b, myo1d and myo1e were done with three pooled shRNAs (1:1:1 ratio, weight/weight), obtained from the shRNA-based knockdown library provided by Genome Biology Unit (GBU; Biocenter Finland). Myo1c-K892A-EGFP (provided by Ilya Nevzorov and Maria K. Vartiainen, Institute of Biotechnology, University of Helsinki) was obtained from myo1c-EGFP by means of overlap-extension PCR. Plasmid was mutagenized based on results from the Ostap lab showing that the putative PH-domain in the tail part of myo1c is responsible for myo1c binding to PIP_2 and that K892A substitution abolishes myo1c binding to PIP_2 (Hokanson *et al.*, 2006). Immunofluorescence sample preparation and immunoblotting were done as described in (I) with the following exceptions when appropriate: DNA was stained with 1 µg/ml DAPI (Roche) in phosphate buffered saline for 5 min before mounting, acetylated MTs were stained with anti-Acetylated Tubulin (Sigma-Aldrich, T7451), vimentin with anti-Vimentin (Sigma-Aldrich, V6630) and MTs with β-Tubulin (Cell Signaling, #2128). Actin stabilization was done with 0.5 µM jasplakinolide (Molecular Probes, J7473) for 60 min, the MT stabilization and bundling with 50 nM paclitaxel (Sigma Aldrich, T7191) in Huh-7 cells and 50 nM and 1 µM in NRK-52E cells for 4 h, and the hyperacetylation of MTs with 125 nM Trichostatin A (Sigma Aldrich, T8552) for 45 min.

Specimen preparation for EM, microscopy, image analysis and modelling

For ET of MTs passing ER fenestrations, Huh-7 cells expressing ssHRP-KDEL was cytochemically stained after chemical fixation and subjected to ET. ER and MTs within one region of a 250-nm EM section were modeled as described in (III) resulting in 4.4 x 4.4 x 4.4 nm voxel size.

Sample preparation protocol for yeast ET (Rambourg *et al.*, 2001) was adapted according to personal communication with Ricardo Nunes-Bastos (University of Helsinki), Monica Yabal

(University of Helsinki) and Heinz Schwarz (Max Planck Institute for Developmental Biology, Tübingen, Germany). *S. cerevisiae* was grown in YPD or SC at +24˚C (until OD_{600} = 0.5-1). Cell were fixed at +24˚C for 1 h, by adding equal volume -to that of the culture- of double strength fixative 8% Paraformaldehyde, 1% GA, 2 M Sorbitol in 0.2 M Citrate-phosphate buffer, pH 4.8. At every stage after this, cells were pelleted by 3000 rpm 3 min centrifugation. Cells were washed and treated 2 x 5 min 0.1 M KPO_4/ 1 M Sorbitol, pH 6.5, 3 x 5 min with 0.1 M Citrate/1 M Sorbitol buffer, pH 4.8 and 3 x 5 min with 0.1 M Citrate/1 M Sorbitol buffer, pH 4.8. Cell wall was permeabilized for 15 min at RT with 1% Sodium-metaperiodate/ 1 M Sorbitol in Milli-Q (*i.e.,* filtered and deionized ultrapure water) and washed 3 x 10 min with 0.5 M Sorbitol in Milli-Q. Samples were post-fixed with 2% $KMnO_4$/0.5 M Sorbitol in Milli-Q for 2 h on ice and washed 3 x 10 min with 0.2 M Sorbitol in Milli-Q. The following day, cells were dehydrated with 70% EtOH 3 x 30 min, 96% EtOH 3 x 30 min and 100% EtOH 3 x 30 min. Next day, cell were embedded as follows: 1 h 50% (v/v), 1 h 75%, quick rinse in 100% and o/n in fresh 100% Low Viscosity Embedding Resin. Next morning, the resin was refreshed with new 100% Low Viscosity Embedding Resin and cell were pelleted at 8000 rpm for 10 min and polymerized at 60˚C for at least 17 h. For 3D-modelling, 6 successive 250-nm thick sections were subjected to ET, 4 of which with dual axis. ET image acquisition, alignment and reconstruction was done as described in (III; II) with the exception of 9600x magnification, 4K-camera, binning of 2, resulting in 2.3 x 2.3 x 2.3 nm voxel size and 4.0 µm bounding box width at the front (Figure 6).

High-pressure freezing-freeze substitution (HPF-FS) of Huh7 cells to model actin, MTs and ER was done as described in (II). Two successive 250-nm sections were subjected to ET. ET image acquisition, alignment, reconstruction and modelling of ER, MTs and actin were done as described in (II; III) resulting in 2.3 x 2.3 x 2.3 nm voxel size with 2.0 x 1.9 x 0.3 µm bounding box (Figure 9).

SB-EM sample preparation, image acquisition and modelling were done as described in (I; II), resulting in 13.4 x 13.4 x 30.0 nm (Figure 11), 16.7 x 16.7 x 30.0 nm (Figure 13A-C), 9.4 x 9.4x 25.0 nm (Figure 15D-E) and 15.7 x 15.7 x 30.0 nm (Figure 20) voxel size.

Thin section TEM of Huh-7 transiently expressing ssHRP-KDEL (Figure 3), wt Huh-7 (Figure 15C, courtesy of Maija Puhka) and wt CHO (Figure 7, courtesy of Helena Vihinen) were all done as described in III and Jokitalo *et al.* (2001). Pre-embedding immunolabeling of myo1c in Huh-7 cells (Figure 16) was done as described previously (Salonen *et al.*, 2003) with the exception that cells were transiently transfected with myo1c-2FLAG and immunolabeled with anti-FLAG (I).

Actin-binding proteins screen

Protein depletion conditions were validated using the BCH Knockdown Setup Kit (http://www.biocenter.helsinki.fi/bi/gbu/kd/setupkit.html) with two GFP-tagged expression plasmids, CDK2-GFP (backbone pEGFP-C1) and PDK1-GFP (backbone pEGFP-C1), and four knockdown shRNA plasmids, pS-GFP (pSuper based), GFP_4 (as pS-GFP, in pENTR-H1-BgH), CDK2_8 (sequenced CDK2 target in pENTR-H1-BgH; target seq AAAGCACGTACGGAGTTGTGTA) and PDK1_4 (sequenced target in pENTR-H1-BgH;AAAGTTTGAACTGGACTTACAG). Depletion efficiency was 59-98% in different combinations of co-transfections and most efficient at 1:4 (weight/weight) ratio.

Quantitation was done from parallel samples by measuring the relative fluorescence intensity from equally exposed controls (co-transfection of one of the expression plasmids and CMVTag1) and depletions (co-transfection of one of the expression plasmids and shRNAs). The screen was carried out with shRNA plasmids that did not carry a marker, and therefore, the co-transfection efficiency was tested with two fluorescent markers, H2B-mRFP which was obtained from the respective laboratory (Keppler *et al.*, 2006) and Hsp47-GFP (1:4 ratio [weight/weight]). Quantitation in Huh-7 cells (n= 828 cells) showed that 95% of the cells positive for H2B-mRFP were also positive for Hsp47-GFP. Prior screening, the depletion efficiency of one of the targets of the screen, cofilin-1, was tested by immunofluorescence and -blotting. Huh-7 cells were transfected with sole Hsp47-GFP or additionally with CMVTag1 or 3 pooled or individual shRNAs against cofilin-1 for 48h, fixed and prepared for immunofluorescence (as described in I) by using cofilin-1 antibody (Hotulainen *et al.*, 2005). Wide-field images were collected in randomized manner and with equal exposure time. The mean fluorescence intensity of cofilin-1 was equal in cells transfected with Hsp47-GFP (n = 21 cells) or Hsp47-GFP and CMVTag1 (n = 15 cells). The relative fluorescence intensity of cofilin-1 decreased by 54% in cells transfected with the triple pooled cofilin-1 specific shRNAs (n = 40 cells), and by 53% (n = 42 cells), 26% (n = 31 cells) and 42% (n = 49 cells) in the samples transfected with individual shRNAs. The cofilin-1 depletion was also analysed by standard immunoblotting with the cofilin-1 antibody. The mean grey intensity of the cofilin-1 in the cells expressing Hsp47-GFP or Hsp47-GFP and CMVTag1 was equal. The intensity decreased by 37%, 31%, 27% and 10% in cells transfected with pooled shRNAs or by three individual shRNAs, respectively. Based on the setup experiments, the screen was done with pooled shRNAs. Transfections, imaging and sample preparation were done as described in (I).

Wound-healing assay

Wound-healing assays were done using continuous cell culturing platform with phase contrast imaging (Cell-IQ, ChipMan Technologies). Huh-7 cells grown on 24-well culture plates were co-transfected with pHsp47-GFP and CMVTag1 or pooled myo1c shRNAs and incubated for 24h. The wound was created on a confluent cell monolayer with a pipette tip and then imaged in 10 min intervals until the wounds had closed. Images were collected from 2 adjacent positions in 2x2 grids and from 2 independent samples. 2x2 grids were then patched up into 1 image by using Cell-IQ Analyzer program's batch process tool; the background of stitched movies was corrected and judder was removed to even out the brightness differences between the grids and to remove excess vibration in the movies. Analysis was performed with the Wound Healing assay of Cell-IQ Analyzer and the results present an average of four independent experiments and are shown as a function of wound area (mm^2) versus time (min).

VII RESULTS AND DISCUSSION

1. The structural organization of endoplasmic reticulum in cultured mammalian cell types and yeast

In order to describe the ER network in interphase and mitosis, few attributes of the network have to be disclosed. The part of ER network that spreads out from the NE has been commonly referred to as the peripheral ER network, which describes the portion of the organelle that consists of ER tubules and sheets (*i.e.,* peripheral tubules and sheets), and excludes the NE. This does not describe the distribution of the network. Parallel to this, the parts of the organelle localizing either to the central parts or to the edges of the cell have been described as perinuclear or peripheral ER, respectively, of which the latter describes any area in the cytoplasm out of the close vicinity of the NE. In other words, the perinuclear ER describes the ER network at perinuclear region and the peripheral ER, in this context, refers to the ER network outside the perinuclear area. In the following text, both the ER structure and the network distribution in the cytoplasm are discussed. While there is some overlap in the description of the ER network localization in cell context and the description of the ER network structure, in the following text I will use the these established nominators.

1.1 The structure and organization varies among different mammalian cell types (II; III; Unpublished)

The interphase ER in mammalian cells spreads from the NE to the cell periphery as a relatively even network of sheets and tubules. Different cell types, however, exhibit some variation to this, and to better understand the interphase ER structure, we studied the ER network organization in several cultured mammalian cell lines from different origins. In the perhaps most commonly used mammalian cell type, HeLa, the majority of peripheral sheets were located to the perinuclear area and a network of interconnected tubules prevailed at the cell periphery (II: Fig.S1B and S1D). We also found similar distribution of the sheets and tubules in Vero (II: Fig.S1A and S1C) and CHO-K1 cells (III: Fig.2, 6A and 6B). In contrast, the interphase ER in Huh-7 and NRK-52E cells showed a different organization from the typical pattern: abundant sheets were found both at perinuclear and peripheral area (II: Fig.2A and 2B). In addition to altering localization of the ER subdomains, the sheet-tubule ratio was observed to vary between the cell types: Sheets were more abundant in Huh-7 and NRK-52E cells than in HeLa, Vero or CHO-K1 cells, indicating that, at steady state, the balance between sheets and tubules varies in different cell types.

In addition variance in localization and abundance of ER subdomains, the morphology of the sheets and tubules varied between different cell types and, surprisingly, within a cell type. Based on live cell confocal imaging and ET of CHO-K1 cells, the tubules close to PM and especially at the leading edge of the cell were longer than at the central parts of the cell (III: Fig.1A and 2A), indicating that ER tubules might be controlled spatially, and, further, that specialized tubular subdomains might exist. We further discovered that the network at the cell periphery was less dense than at the central parts of the CHO-K1 cells (III: Fig.1A, 1B and 2A) and that the ER at the Golgi area (III:

boxed area B in Fig.2 illustration) was composed of tight network of small tubules and sheets which differ from the rest of the network (III: highlighted dark area in Fig.2B). Similar organization around Golgi area could also be observed in Huh-7 cells (data not shown). These findings support the hypothesis that ER might not be uniformly regulated throughout the network, *i.e.,* all the tubules or sheets might not be similar. TEM-analysis of the morphological details in Huh-7 (II: Fig.2C and 2E) and NRK-52E (II: Fig.2D and 2F) cells revealed that Huh-7 sheets were heavily fenestrated, while fenestrations of similar size or quantity were not found from NRK-52E sheets. In HeLa and Vero (II: Fig.S1C and S1D), the ER sheets were significantly less fenestrated than Huh-7 but showed more fenestrations than NRK-52E or CHO-K1 (III: Fig.1B). ET models of Huh-7 (II: Fig.2G) and NRK-52E (II: Fig.2H) cells, prepared by HPF/FS, verified that these results were not artefacts of chemical fixation as suggested by Lu *et al.* (2009).

While the role of the sheet fenestrations remains unknown, there are some conclusions to be drawn from different cell types analysed here. Based on the correlation between the secretion activity of the cells and the abundance of sheets (Benyamini *et al.*, 2009; Rajasekaran *et al.*, 1993; Ueno *et al.*, 2010; Wiest *et al.*, 1990), Huh-7 cells, containing the most abundant sheets among the cell types analysed here, and might, accordingly, have the highest secretion activity. Interestingly, Huh-7 sheets also contained the highest amount of sheet fenestrations. The simplest explanation would be that the fenestrations might, analogously to nuclear pores, simply present sites of passage for the cytoplasmic transport. It is quite challenging to imagine how an efficient transport and diffusion of cytosolic material could take place in the Huh-7 cells with such abundance of sheets if fenestrations would not be present.

How the fenestrations are created and maintained is unclear. The fenestrations in Huh-7 cells did not appear to have a specific pore structure and varied somewhat in shape and size (II: diameter of 75 ± 3 nm). Fenestrations were found irrespective of fixation method used and in both wt cells and cells expressing ER marker proteins. Moreover, the fenestrations were not abolished when cells were exposed to various ER stress inducing treatments (II): inhibiting Ca^{2+}-ATPase pump function by thapsigargin treatment, changing the pH-level of the culture medium from 5.0 to 9.0, or perturbing lipid metabolism by serum deprivation. This indicates that the fenestrations are rather stable structures. Moreover, depolymerizing the actin cytoskeleton by latrunculin A (latA) treatment or the dynamic MTs by nocodazole treatment (II) did not abolish sheet fenestrations, indicating that the creation/ maintenance of the fenestrations is not dependent on actin or MTs. This does not, however, mean that trafficking could not occur through fenestration. In accordance, based on our ET models of Huh-7 cells, MTs were often observed passing through the sheet fenestrations (Figure 5). Another explanation for the fenestrations could be that the observed fenestrated sheets would present an intermediate structure of sheets transforming into tubules. In accordance, the NEBD in prophase proceeds through rapid fenestration and expansion of membrane holes, resulting in smaller sheets and tubules (Ellenberg *et al.*, 1997).

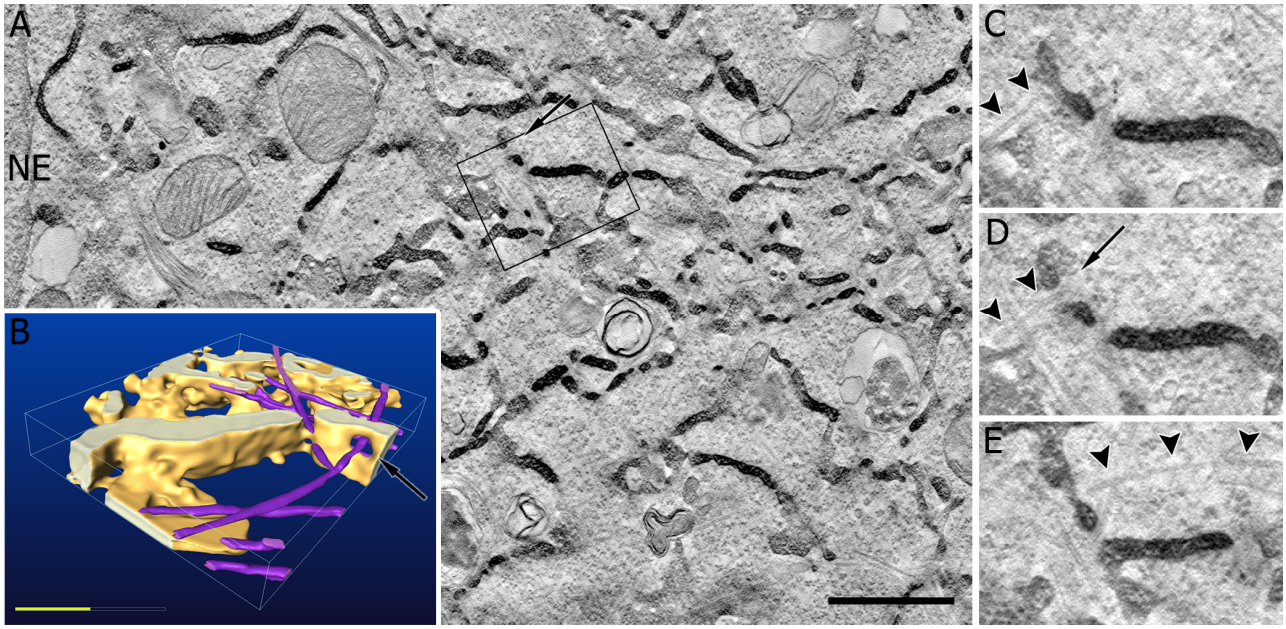

Figure 5. MTs may pass through ER sheet fenestrations in interphase Huh-7 cells. Huh-7 cell expressing ssHRP-KDEL was chemically fixed, cytochemically stained and subjected to ET and 3D-modelling. (A) A slice image of the tomogram shows a fenestration (arrow) in a transverse section of a sheet. (C-E) Twice-magnified slice images depict a MT (arrowheads) extending through the same fenestration (arrow). (B) Model (of the boxed area in A) of ER (yellow) showing the same fenestration (arrow) through which the MT (lilac) passes. Bars 1 µm in A and 0.5 µm in B. Picture courtesy of Helena Vihinen, Ilya Belvich and Maija Puhka (Institute of Biotechnology, University of Helsinki).

Together, these observations suggested that the regulation of the morphological determinants of the ER might not be homogeneously distributed throughout the network or that the observed variation among the subdomains is obtained by different means. This raises the possibility of an existence of tubular subgroups that might perform separate specific tasks. In agreement, ER tubules have been shown to slide on acetylated MTs to contact mitochondria, and by TAC-mechanism on non-acetylated MTs to contact endosomes, giving ER tubules identity and, further, indicating that specific subsets of tubules might exist (Friedman *et al.*, 2010). Despite of showing that the curving of acetylated MTs coincided with curving of the ER tubules along their horizontal axis, the morphological description of such tubular subdomains remains elusive. Furthermore, the purpose of the network distribution throughout the cytoplasm and the reason for organizational differences of the subdomains remains unknown. The reason for the large size of the organelle and the wide distribution of the network could be to have large enough surface area to host all ER's functions and to spatially be able to contact other cellular organelles throughout the cytoplasm. It could be envisioned that the reason why ER sheets resides close to the NE is because the next organelle in-line in the secretory pathway is the Golgi complex, which also locates to the cell center. Many cell types, however, differ from this typical ER organization and especially in the professionally secreting cells the sheets are distributed all the way to the cell periphery. These results clearly indicated that different cell types show large variations in the proportions of sheets and tubules, as well as in the morphology of the sheets themselves.

1.2 Network in *Saccharomyces cerevisiae* contains similar subdomains as in mammalian cells but differs in its organization (Unpublished)

The genome of *S. cerevisiae* was the first fully sequenced genome among eukaryotic cells, released in 1996 (Goffeau *et al.*, 1996). Yeasts are used widely to study the cell functions, as they have GRAS status (generally regarded as safe), they are less complicated than mammalian cells, they have secretory pathway which enables the production and secretion of proteins, they are easy to modify genetically and they grow rapidly to high cell densities in a simple media. There are, however, substantial differences between yeast and mammalian cells, for example -but not restricted to- the ellipsoidal/ round cell shape and the enclosing of the cell by a thick cell wall. Despite the differences, yeast has its functions compartmentalized into membrane bound organelles such as nucleus and ER, similarly to mammalian cells.

To study the ER structure and organization in *S. cerevisiae*, we prepared samples for ET. In accordance to previous results (West *et al.*, 2011), we identified four main ER domains (Figure 6): the NE, central sheet-like ER ($_{cec}$ER) extending from the NE to the cell periphery, tubular ER ($_{tub}$ER) and PM-associated ER ($_{pma}$ER) that was composed of sheets and tubules. The yeast ER, therefore, was composed of the same building blocks of sheets and tubules as the mammalian ER. In contrast to PM-ER contact sites in mammalian cells, $_{pma}$ER formed extensive connections with the PM (Pichler *et al.*, 2001) and the compartments sometimes resided so close to one another that they were hard to distinguish from each other. In agreement, these contact sites have been shown to be so tight that ribosomes are exclude from the membranes (West *et al.*, 2011). The most distinct difference between yeast and mammalian ER network, however, was the distribution/ organization of the network. Nucleus resided at the cell center, like in mammalian cells, but instead of a uniform distribution of the reticular ER network from the NE to the cell periphery, only few $_{cec}$ER and $_{tub}$ER profiles were observed to connect

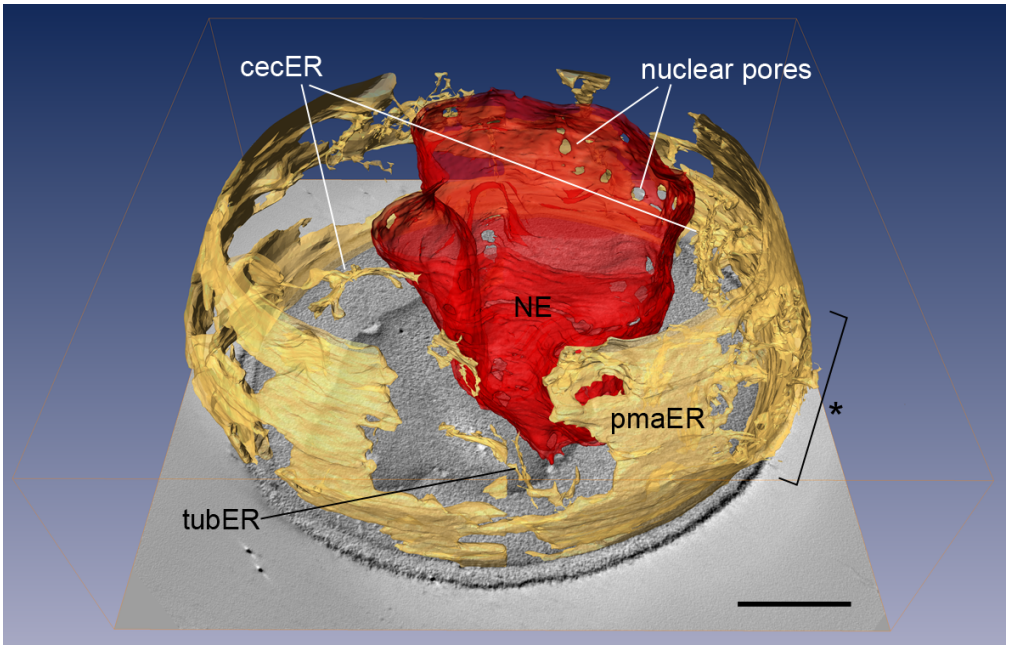

Figure 6. ET model of ER and NE in *S. cerevisiae*. NE (red) resides at the cell center and few $_{cec}$ER and $_{tub}$ER profiles connect the NE to the $_{pma}$ER (all yellow) residing at the cell periphery. The bud neck between the mother and the daughter cell (asterisk) and nuclear pores are indicated. Daughter cell was not modelled. Bar 0.5 µm.

the NE to the bulk of ER (*i.e.,* $_{pma}$ER) at the cell periphery. In contrast to the typical mammalian ER pattern, the majority of ER sheets were not located at perinuclear area, but at the cell periphery. This unique localization of sheets, and the previous observation that the $_{pma}$ER sheets are highly fenestrated (West *et al.*, 2011), provides further support for a passage-role for the fenestrations: If the sheets were intact, they would form a barrier at the cell periphery preventing trafficking and secretion at substantial portion of the yeast cell. The reason for the extensive contact with the PM, which to our knowledge, has not been reported for any interphase mammalian cell types, and the organizational differences, remains unknown. However, it could be envisioned that the cell shape might affect the overall organization of the ER, which is consistent with previous suggestion that ER might adapt to changes in cell morphology during cell migration, differentiation, and polarization (Friedman and Voeltz, 2011). The mammalian cell culture cells chosen for our studies grow as monolayers and, in interphase, exhibit a flat spread-out shape. In mitosis, most of them round up and the mitotic spindle pushes ER aside and network reorganizes to the cell periphery (McCullough and Lucocq, 2005). In contrast, in NRK-52E, a specialized cell type that does not round up during mitosis, similar reorganization of the network was not observed (II: Fig.6). The *S. cerevisiae*, on the other hand, are rather round cells that remain round even when the cell is dividing and a daughter cell is budding out from the mother cell, and the bulk of ER remains at the cell periphery throughout the cell cycle. These events, however, are most likely not connected to changes in cell volume, *i.e.,* that ER would be forced into peripheral configuration during mitosis, as our measurements of confocal sections of CHO-K1 cells showed that the ER takes up a similar volume of the cell in interphase and in mitosis despite the changes in cell shape (III).

Another interesting aspect is the connection to actin cytoskeleton. The yeast ER inheritance is actin dependent (Fehrenbacher *et al.*, 2002). In mitotic mammalian cells, the actin cytoskeleton is reorganized extensively (Field and Lenart, 2011), most likely to enable the changes in the cell shape, *i.e.,* rounding up (III: Fig.3 and Fig.4). This reorganization has been shown to be accompanied by a relocation of ER to the cell periphery in the mitotic HeLa cells (McCullough and Lucocq, 2005). The mechanism of relocation is not known, but it is tempting to speculate if these events are connected. Considering that both ER and actin reside at the cell periphery, and that MTs are mainly involved in the chromosomal movements, could the role of actin cytoskeleton on mammalian ER become more profound during mitosis (McCullough and Lucocq, 2005), similarly to the cell cycle dependent switch to actin-mediated reorganization in *C. elegans* (Poteryaev *et al.*, 2005)? In agreement, actin depolymerisation in mitotic HeLa cell affects the peripheral ER network organization (McCullough and Lucocq, 2005).

2. Characteristics of endoplasmic reticulum sheet transformations and dynamics

The ER dynamics occur on multiple levels. Firstly, there are indications that the ER structure changes substantially when the cells enter mitosis —most likely to ensure an equal inheritance of the ER. While the yeast cell

undergoes a closed mitosis and the NE remains intact in cell division, mammalian cells undergo an open mitosis and the most profound chance of the ER is the NEBD at the beginning of mitosis.

Multiple efforts have been made to study the dynamic events and the fate of ER and NE in mitosis. However, the outcome of these studies have created some discrepancy in the field: Based on EM-studies mainly, either complete fragmentation of the NE and fragmentation of the peripheral ER to a variable extent has been suggested (Dreier and Rapoport, 2000; Du *et al.*, 2004; Warren and Wickner, 1996; Zeligs and Wollman, 1979). In contrast, based on FRAP experiments, the ER has been shown not to vesiculate and, therefore, ER was proposed to remain continuous during cell division (Ellenberg *et al.*, 1997).

Secondly, in addition to the dynamic mitotic events, the interphase ER is highly dynamic and constantly rearranging. The studies of ER dynamics so far have been mostly concentrating on ER tubular dynamics (Lee and Chen, 1988; Terasaki *et al.*, 1986; Waterman-Storer and Salmon, 1998), while the description of ER sheet dynamics and transformations has remained obscure.

2.1 Nuclear envelope is transformed into a part of the endoplasmic reticulum in prophase and regains its identity at the end of mitosis (II; III; Unpublished)

Mitotic mammalian cells are challenging to study for a few reasons. Firstly, the portion of mitotic cells in the cell culture at any given time was only roughly 6%[1]. Synchronizing the cells with drug treatments, usually by manipulating MTs or by starvation, increased the proportion of mitotic cells, but also affected the cell behavior[1], and we therefore chose to use naturally occurring mitotic cells throughout our studies despite the scarceness of the natural mitotic cells. Secondly, the dividing cells appear to be loosely attached to the substratum and more fragile, and, therefore, the live cell imaging of mitotic cells had to be done carefully with low laser-power, moderate imaging intervals and short total duration of the imaging.

To address the fate of the NE during mitosis, two stable CHO-K1 cell lines with moderate expression level of LBR coupled to EGFP (Ellenberg *et al.*, 1997) or HRP (Connolly *et al.*, 1994), *i.e.,* CHO-K1/LBR-GFP or CHO-K1/LBR-HRP, respectively, were created. It is noteworthy, that the LBR-fusion-proteins did not contain the full LBR protein, but only the nucleoplasmic domain for lamin- and chromatin-binding and the first trans-membrane segment, which was attached to the luminal EGFP or HRP-marker. LM analysis has revealed that NE components, including LBR, diffuse into peripheral mitotic ER, and concentrate in the reforming NE after the chromosome segregation (Ellenberg *et al.*, 1997; Yang *et al.*, 1997a). In accordance, based on our confocal live cell imaging, in interphase, the LBR-GFP was retained at NE (III: Video 4) and although NE is in straight continuity with peripheral ER, the marker has been shown to leak to the reticular ER only when highly over-expressed, inducing simultaneous changes in the NE morphology

[1]Giuseppa Piras, Institute of Biotechnology, University of Helsinki, personal communication of unpublished results. The proportion of mitotic cells was calculated based on the number of mitotic cells related to total number of Huh-7 cells (n = 800 cells), grown on continuous cell culturing platform, Cell-IQ, for 48 h.

(Ellenberg *et al.*, 1997). Consistent with previous results in COS-7 cells (Ellenberg *et al.*, 1997), live cell confocal imaging of mitotic CHO-K1/LBR-GFP showed that upon NEBD the LBR-GFP-marker redistributed to the peripheral ER network until the anaphase/ telophase when GFP-positive profiles started to accumulate near the chromosomes, which, at the end of mitosis, formed the NE in both daughter cells (III: Fig.S1 and Video 4).

To study the morphological changes of the NE and the distribution of LBR fusion-protein in detail, we continued the analysis using EM and peroxidase cytochemistry using the CHO-K1/LBR-HRP (III: Fig.7). In interphase, NE was darkly stained, whereas the rest of the ER remained unstained (III: Fig.7a). During prophase, the LBR-HRP still appeared in the seemingly intact NE, although the number of stained profiles outside the NE increased and conversely, the NE staining became weaker (III: Fig.7b-c). The NEBD occurred at prophase/ pro-metaphase (III: Fig.7d-e). The NE remnants retained their identity even after the NE had been perforated at several points as some nuclear pores were still observed in the membranes (III: Fig.7d-e). In metaphase, NE had lost its identity as a separate subdomain of ER and became a part of the reticular ER (III: Fig.7f). After the NEBD and until late anaphase, LBR staining was observed distributed throughout the network (III: Fig.7e–g), however, in majority of the cells both unstained and stained ER profiles were found (III: Fig.7f-g), indicating that the redistribution of LBR was not homogeneous in the network. At anaphase, HRP-positive membrane stretches started to surround the chromosomes (III: Fig.7g) and eventually formed the NE at the late anaphase/ telophase (III: Fig.7h). LBR-HRP signal could no longer be observed in the reticular ER. However, to obtain more in-depth knowledge about the mitotic localization of the LBR in respect to the ER network, detection of endogenous LBR would be required.

Our results demonstrated that LBR-HRP redistributed unevenly into the mitotic ER. Studies concerning the partitioning of the NE at LM level have shown the spreading of the NE membrane proteins homogenously into the mitotic ER (Ellenberg *et al.*, 1997; Yang *et al.*, 1997a). In contrast, we frequently found unstained tubules that were connected to stained profiles, indicating that LBR-HRP might be redistributed into distinct subdomains within the mitotic ER. This finding supports the idea that NE building units might be kept as assembly-ready subdomains during mitosis (Mattaj, 2004). However, the extent of HRP-induced cytochemical staining depends heavily on the expression level of the LBR fusion protein, which was, based on Western blotting, approximately one third of the amount of ssHRP-KDEL fusion protein (data not shown), which is distributed evenly throughout the mitotic ER network. Whether this amount of LBR fusion protein could disperse and occupy the entire ER remains unanswered. However, if the protein was evenly distributed throughout the mitotic ER, and the protein expression level was low, we would not be able to observe the HRP-staining. Therefore, our results of uneven distribution of the fusion-protein could mean that the marker locates to distinct subdomains in the network, or, that the marker is distributed throughout the network, but the concentration exceeds the threshold only at certain locations, where the HRP-staining can be seen.

2.2 Mitotic endoplasmic reticulum undergoes a structural transformation and reorganization

Based on a few studies where structural changes of ER during cell division and differentiation have been systematically characterized, it has become evident that the ER structures and distribution within the cell varies among different species and according to the developmental stage or differentiation (Bobinnec *et al.*, 2003; McCullough and Lucocq, 2005; Poteryaev *et al.*, 2005; Terasaki, 2000; Terasaki *et al.*, 2001; Wollert *et al.*, 2002). The description of the dynamic events of ER in mitotic mammalian cells, however, and systematic studies combining LM, EM and quantitation have not been reported (Lowe and Barr, 2007).

2.2.1 Sheets are progressively transformed into highly fenestrated sheets and tubules in mitosis (II; III; Unpublished)

In order to study the changes in the ER network during mitosis, we started by developing a novel method to quantify the ER profile lengths and the number of branch points (III: Fig.2C, three types of branch points), which are regarded as direct determinants of the ER network formation (Dreier and Rapoport, 2000; Lee and Chen, 1988; Uchiyama *et al.*, 2002; Waterman-Storer and Salmon, 1998), from live CHO-K1/Hsp47-GFP cells. The confocal stacks of spanning the cells were deconvoluted to subtract the background noise, and the ER network was converted into skeleton model with branch- and endpoint filter (ImagePro) (III: Fig.5A, a-c, one optical section shown). The ER profiles forming three-way (or higher) junctions were scored as branch points and the tubular lengths were measure from branch point to branch point and from branch point to ending point of a profile. The created skeleton is a one-pixel-thick 2D model of the ER network, of which the ER tubule and sheets could not be reliably identified, and therefore, the ER profile lengths include both tubules and sheets. The ER profile lengths and the number of branch points were related to the manually traced cytoplasmic area containing ER (ER area, μm^2), excluding areas void of ER, and quantified with ImagePro software. To obtain reliable average value for each cell, we selected three to five optical sections at regular intervals to cover the whole cell depth. The minimum length of ER profiles was set to 0.200 µm, which is the theoretical resolution limit of the diffraction limited LM. This morphometric analysis of confocal stacks of live CHO-K1/Hsp47-GFP cells revealed that towards metaphase, the network became more branched and the proportion of short profiles increased (III: Table I). The average number of branch points increased by 23-36% ($p < 0.05$) when cells progressed from interphase to mitosis, peaking at metaphase (III: Fig.5B and Table I). Also, the total number of ER profiles (*i.e.,* the summarized value of ER profile lengths from 0.200 µm to ≥ 1.500 µm) was significantly ($p < 0.05$) higher in mitotic cells than in interphase cells (III: Table I). The observed change was mainly due to an increase in number of short ER profiles (0.200-0.400 µm) in mitotic cells (III: Fig.5C and Table I): 26% increase in prophase, 31% in metaphase, 20% in anaphase, and 14% in telophase cells. In addition, there was 13-30% induction in profile numbers in 0.400 to 1.500 µm length groups, while there were no significant changes observed in the longest profile category (>1.500 µm). Morphometric analysis of CHO-K1/ssGFP-KDEL ((EGFP coupled to the

ss and KDEL, described in Kuokkanen *et al.* (2007)) TEM images confirmed the confocal microscopy results: the number of branch points per area occupied by the ER increased 39% from interphase to metaphase and dropped back to the interphase level upon mitotic exit (III: Fig.5D and Table II), and the total ER profile number per area occupied by the ER increased by ~70%. Again, the biggest increase in profile numbers was seen at the shortest length groups, which was balanced by a decrease in number of long ER profiles whose proportion reduced by more than 90% during metaphase and anaphase. In accordance to earlier LM and EM observations of NEBD, the longest profiles starting from 2.500 µm and consisting almost entirely of the NE profiles were absent during meta- and anaphase and increased back to the interphase level during telo-/prophase coinciding with the NE reassembly. These results were further supported by morphometric analysis done on thin section TEM images of pelleted wt interphase and mitotic Huh-7 and NRK-52E cells (II: Fig.7). The analysis revealed that the fraction of short ER profiles (0-0.249 µm and 0.250-0.499 µm) increased by >70% during mitosis in both cell types ($p < 0.01$). In addition, the longest profiles were over 0.200 µm during interphase but less than 0.150 µm in mitotic cells. For profiles over 0.100 µm, the reduction of number of profiles between interphase and mitotic cells was over 75% in both cell types (75% in NRK-52E and 79% in Huh-7; $p < 0.05$) (II: Fig.7). These results indicated that NE and peripheral ER membranes are converted from long membrane structures into a large number of shorter, highly branched, structures in CHO-K1, Huh-7 and NRK-52E cells.

To correlate the observed increase of short profiles and branch points with the structural changes in mitosis, we studied the ER structure in multiple cell lines by using LM and EM. Based on LM, ER in mitotic CHO-K1 cells appeared reticular and was predominantly composed of tubules (III: Fig.3b-f), while in Huh-7 (II: Fig.3, 4C and 4D), Vero (II: Fig.S3A), HeLa (II: Fig.S3B) and NRK-52E (II: Fig.6A) the mitotic ER network was cell type dependently composed of tubules and/or small sheets. To analyse the structures in more detail, cells were subjected to TEM and 3D-EM: ET analysis of mitotic CHO-K1 cells revealed almost complete loss of sheets and that the ER network was composed of tubules in metaphase (III: Fig.6C and Video 3). Correspondingly, in thin section TEM, the mitotic ER profiles appeared short and fairly evenly distributed, although mainly excluded from the spindle area (III: Fig.4a-d). SB-EM analysis of mitotic Huh-7 cell revealed numerous fenestrated sheets and short tubules in planar layers in the cell cortex (II: Fig.5A-D). Sheets were smaller and more fenestrated compared to interphase ER. In addition, modelling the middle parts of the cell revealed the existence of numerous long tubules originating from the cortical ER and extending toward the mitotic spindle and the center of the cell (II: Fig.5D and 5E). TEM analysis of NRK-52E cells showed profiles of heavily fenestrated sheets in addition to tubular profiles (II: Fig.6B). ET modelling of HPF/FS samples verified the results obtained by chemical fixation (II: Fig.6C and Video S7) showing fenestrated sheets intermixed with short tubules. TEM analysis of mitotic Vero and HeLa cells were reminiscent of Huh-7 and NRK-52E cells and showed extensively fenestrated ER sheets along with tubular

profiles (II: Fig.S3C and S3D). Furthermore, in all analysed cell types, mitotic ER remained continuous and no fragmentation was observed. While the mechanism by which the ER network is divided between the daughter cells remains unclear, our TEM studies revealed some interesting aspects of the ER at cleavage furrow (unpublished). Cleavage furrow is an indentation of the cell's surface that is formed by a contractile ring of actin filaments that begins the progression towards the cytokinesis splitting the PM between the daughter cells. Based on our observations, as the cytokinesis progressed, the ER profiles became gradually scarcer at the cleavage furrow site. Interestingly, few ER profiles were observed passing through the cleavage furrow, parallel to thick actin filament bundles, until the very last stages before cytokinesis, while other organelles were mainly excluded from the area (data not shown). These observations indicate that the ER network is dynamically rearranged so that the network is increasingly bipolar between the forming daughter cells, and the connective ER in-between the daughter cells is gradually diminished. The mechanism of the transformation remains to be solved but could be accomplished by either increased fission of ER tubules, which must occur at least at cytokinesis, or by controlling the other aspects of the ER transformations dynamics *e.g.,* rate of tubular fusion or the directionality of the dynamics. The observation that the ER network in daughter cells remains connected until the cytokinesis could indicate a uniform controlling and/or signalling throughout the forming daughter cells.

Thus, the combination of live and fixed cell LM, thin section EM and 3D-EM (ET and SB-EM) with both chemical fixation and HPF/FS, demonstrated that ER remained continuous and that ER sheets were transformed towards tubules and fenestrated sheets during mitosis in all mammalian cell culture cells analysed here. Along with tubules, the highly fenestrated sheets account for the indicated increased number of branch points and short profiles in the mitotic ER observed by morphometric analysis. However, our results are contradictory to some of the earlier published work; In sea urchin embryos and *Xenopus laevis* oocytes the ER accumulates at the mitotic poles, and while ER remains continuous during mitosis, structural transformations were not reported (Terasaki, 2000; Terasaki *et al.*, 2001); In the early *C. elegans* embryo and *Drosophila melanogaster* syncytial embryos the ER forms sheets during mitosis and cycles between dispersed and accumulated states (Bobinnec *et al.*, 2003; Poteryaev *et al.*, 2005); Most recently, mainly based on LM data, mitotic ER was proposed to undergo a tubule-to-sheet transformation in five cultured mammalian cells lines (Lu *et al.*, 2009). Only few tomograms were presented and, in our view, those tomograms contained fenestrated sheets (slice images showed lines of ER profiles separated by small gaps) and tubules, although this point was not disclosed in the article, indicating that the structural reorganization of the mitotic ER into concentric layers may have been misinterpreted as a structural conversions towards sheets and as the ultra-structural studies were inadequate, these results remain unclear. The resolution of conventional LM is not sufficient to resolve subtle morphological changes such as fenestrations on ER sheets or differences between planar tight tubular networks and fenestrated sheets.

Interpretation of images becomes even more challenging in those mitotic cells in which ER is packed into tight layers. In addition, the layers mostly align along the *z*-axis of imaging, which has the poorest resolution. Therefore a systematic EM-level analysis with sufficient statistics and volumes is needed to support LM data. Together, our results indicate that ER structures and distribution within the mitotic cells shows variation among different cell types, however, all of the cell types observed follow the common line and direction of change towards more fenestrated sheets and tubular networks.

2.2.2 Mitotic endoplasmic reticulum is reorganized towards planar layers in some mammalian cell types (II; Unpublished)

To address the discrepancy raised by Kirchhausen laboratory (Harvard medical school) of planar mitotic ER profiles corresponding to sheets (Lu *et al.*, 2009; Lu *et al.*, 2011) rather than a network of highly fenestrated sheets and tubules (I), we first imaged Huh-7 (II: Fig.3), Vero (II: Fig.S4A) and HeLa (II: Fig.S4B) cells live by confocal LM. In agreement to Lu *et al.*, 2009, mitotic ER was occasionally found to align along the PM as concentric layers, a feature that was not found in CHO-K1 cells (III: Fig.3). However, this was not the exclusive organization in any of the cell lines we analysed, and it was common to find cells or regions of cells where the mitotic ER was non-planar. Metaphase is a relatively long mitotic phase[1], during which the chromosomes are aligned to the equatorial plane and it is possible that during that time, ER shows a variety of organizations. In accordance, reorganization of the ER into planar layers seemed to be occurring more often towards the end of metaphase (II: Fig.3), simultaneously to cell rounding. Accordingly, SB-EM model of early metaphase Huh-7 cell, that was still in the process of rounding up (II: Fig.S2 and Video S4), showed that the appearance of ER layers seemed to coincide with the rounding of the cells during mitosis; On the adherent side of the cell, the ER had a non-planar organization, whereas on the more rounded side the ER was packed into concentric layers (II: Fig.S2C and S2D). Furthermore, SB-EM analysis of several entire pro-metaphase/ metaphase Huh-7 cells revealed numerous fenestrated sheets and short tubules forming concentric ER layers in the cell cortex (II: Fig.5A-D, Video 6A and 6B). Sheets were smaller or more fenestrated compared with interphase ER. The side-view image revealed that many of the sheets were so heavily fenestrated that they resembled more of a tubular network (II: Fig.5C). Instead of forming an extensive 3D-network, however, these tubules remained organized in planar layers together with the fenestrated sheets. ET modelling of HPF/FS samples verified the results obtained with chemical fixation (II: Fig.6C and Video S7) showing fenestrated sheets intermixed with short tubules in planar layers. However, some regions had greater dimensionality and appeared more reticular rather than being restricted to a planar form. In Huh-7 cells, non-planar ER networks were prevalent in 13% of the cells, concentric planar ER layers in 57%, and in the remaining 30% of cells the ER was composed of a combination of both features (II) (n = 23 detached and pelleted pro-metaphase to anaphase cells).

To directly compare mitotic ER structures acquired by LM and EM, we performed correlative-light EM, including ET analysis, of Huh-7 cells co-expressing ssGFP-KDEL and

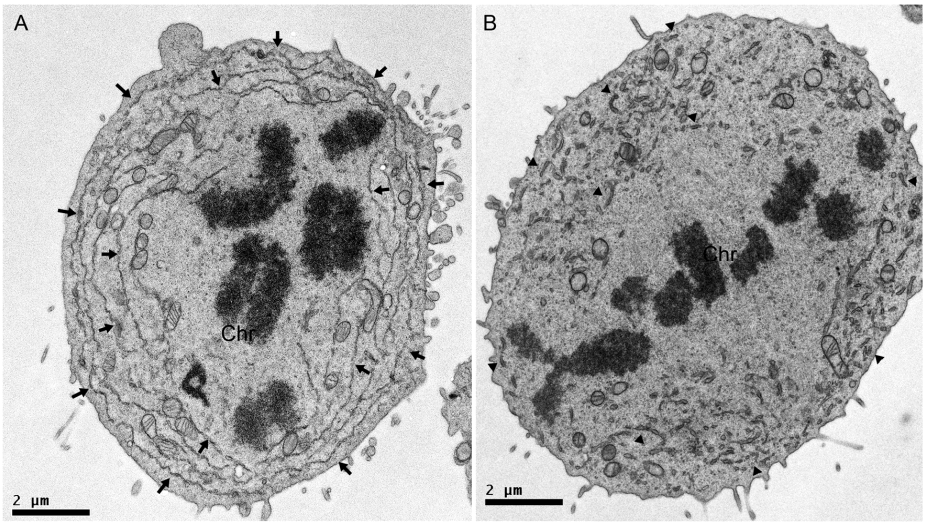

Figure 7. Thin section EM of CHO metaphase cells. Mitotic CHO cells showed both (A) planar reorganization (arrows) and (B) non-planar reticular arrangement (arrowheads) at the peripheral areas excluded from the mitotic spindle. Chromosomes (Chr) are indicated. Images are courtesy of Helena Vihinen (Institute of Biotechnology, University of Helsinki).

ssHRP-KDEL (II: Fig.4 and Video S5). The concentric layers of long ER profiles observed at the LM level (II: Fig.4C and 4D) could be resolved by EM, revealing largely fenestrated sheets (II: Fig.4E and 4F) aligned parallel to the PM as observed in the sections obtained from the middle of the cell (II: Fig.4D and 4F). Sections from the adhering side of the cell, where ER was mostly parallel to the sectioning plane, showed large profiles of sheets with extensive fenestrations (II: Fig.4E), which were, at times, very difficult to distinguish from tight planar tubular networks. ER sheet fenestrations are not, therefore, resolvable with diffraction-limited LM.

It is noteworthy that while Lu *et al*. (2009) claim they had used the same CHO cell line in their studies as we in (III), we, in fact, used CHO-K1 cells. CHO-K1 presents a special sub-clone that has been derived from an ancestral Chinese hamster ovary cell line and have a different DNA content and requirements for growth (Kao and Puck, 1968; Lewis *et al.*, 2013), and, thus, should be regarded as a separate cell line. The origin and clone number of the CHO cells was not stated, and we were not able to replicate our studies with the definite cell line. However, our analysis of a CHO cell line showed that there were many cells with abundant short ER profiles with no particular orientation, but also some cells with a tendency to arrange the ER in layers along the PM (Figure 7).

The tendency for this reorganization during mitosis is likely a consequence of many factors. McCullough and Lucocq (2005) suggested that the cortical association and layering of ER sheets are dependent on the actin cytoskeleton and ER abundance, respectively. Lu *et al.* (2009) used Lipofectamine for transfections, and from their images it is apparent that the transfected genes were highly expressed. In addition, they mainly used membrane marker proteins, and it has been documented that over-expression of membrane proteins can yield expansion and deformation of membrane structures (Ellenberg *et al.*, 1997; Ma *et al.*, 2007; Snapp *et al.*, 2003). Our data imply that the layering correlates with cell rounding, the abundance of ER in cells, and the expression level of the fusion proteins. To

minimize the risk of artefacts, we used FuGENE HD and FuGENE 6 to transfect cells and soluble luminal ER markers that, when over-expressed, leak to the *cis*-Golgi. However, we were able to induce the formation of planar ER layers already in prophase Huh-7 cells when over-expressing soluble Hsp47-GFP-marker (luminal collage-specific chaperone Hsp47 (Nagata, 1998) coupled to EGFP (Kano *et al.*, 2005)), underlining the importance of moderate expression levels of the marker when studying cell morphology (data not shown).

Together these data suggests that although the spatial organization of the ER and the extent of mitotic sheet-to-tubule transformation vary among different cells, the tendency towards smaller and more fenestrated ER sheets and tubular network clearly exist. From our data it is evident that the ER has several morphological features that are beyond the resolution of conventional LM and, thus, diffraction-limited LM should not solely be used to resolve ER morphology but rather to assess the ER distribution within the cell. Reorganization of ER into concentric layers and structural changes of ER sheets during mitosis are two separate events that occur in parallel in certain cell types since our morphometric analysis indicated that ER profiles get shorter even in cells in which ER is packed into concentric layers.

2.3 Interphase sheets are persistent and undergo characteristic transformations (I; Unpublished)

The big question in the field is how the functional subdomains are created and maintained, and why the network is constantly rearranging. So far we had shown that the ER sheets are transformed towards more fenestrated sheets and tubular forms during mitosis indicating that ER sheets underwent extensive remodelling cell cycle dependently. Since previous studies of ER dynamics have concentrated almost entirely on tubules we were interested in studying the ER sheet dynamics in interphase. We acquired 60 s (1 frame/s) wide-field videos of the ER from the thin lamella at the leading edge of the Huh-7 and NRK-52E (NRK-52E results present unpublished data) expressing Hsp47-GFP and HeLa expressing ssGFP-KDEL. The ER in these plate-like extensions resides mostly in one plane, allowing simultaneous imaging and identification of tubules and individual sheets. Based on the observations of separate sheets, we identified three characteristic ER sheet transformation events in addition to sheets that remained persistent: 1) transformation into tubules, 2) fusion with other sheets, or 3) fission into smaller sheets (I: Fig.8A). These characteristics were also observed in HeLa and NRK-52E cells. To quantify the occurrence of sheet remodelling events versus persistent sheets, separate sheets with clear boundaries were randomly selected from the first acquired frame and observed for the acquisition time, or until any sheet transformation events (1-3) were observed (I: Fig.8A), and then scored accordingly. The highly fenestrated Huh-7 sheets were remarkably stable: 75.0% persisted for the analysis duration (I: Fig.8B).

Interestingly, the sheet persistency seemed to correlate with the degree of fenestrations: the moderately fenestrated HeLa sheets were less persistent (I: 49.4%) than Huh-7 sheets, and in agreement, only 31.4% of the non-fenestrated, *i.e.,* intact, NRK-52E sheets (n =

58 sheets in 17 cells) remained persistent. Huh-7 (I: Fig.8B) sheets underwent fewer transformations (I: 25%) than HeLa (I: 51%) or NRK-52E (68.4%) sheets and the sheet lifetime was longer in Huh-7 (I: 53.7 s ± 1.5 sem) than in HeLa (I: 42.6 s ± 2.4 sem) or NRK-52E (38.0 s ± 3.4 sem). Interestingly, the most common transformation event observed in Huh-7 was the sheet transformation into tubules (I: 12.5%), which attracts to speculate if the relatively higher portion of curvature, gained from the sheet fenestrations, somehow assists the formation of the high-curvature tubules. In contrast, the most commonly observed transformations in HeLa (I: 28.4%) and NRK-52E (58.8%) cells were the sheet fusion and fission events.

2.4 The dynamics of interphase sheets differ from the tubular dynamics (I; Unpublished)

To quantify the lateral sheet movement and velocity of the sheets in Huh-7, HeLa and NRK-52E, we adapted a method that calculates the sheet's center point of mass and follows its movement over time. The outlines of individual sheets were traced manually throughout the 60-s wide-field acquisition (1 frame/s) and based on the calculated center-of-mass of sheet (*i.e.,* the centroid), the centroid's movement and velocity were quantified (I: Fig.8C-E). The analysis was done only to the persistent sheets to ensure that events that significantly increased or reduced sheet mass would not artificially shift the centroid. The observation duration was set to 60-s so that the cell motility would not affect the centroid movement, and to ensure a representative balance between persistent and transforming sheets. The analysis showed that the average sheet size in HeLa was slightly larger than in Huh-7 or NRK-52E (3.82 μm^2 ± 0.5 SD, 2.73 μm^2 ± 0.37 SD, or 2.85 μm^2 ± 0.34 SD, respectively), and that in all cell types the average sheet size showed similar ±30% fluctuation, indicating a control over the general sheet size. In smaller sheets, the portion of highly curved membranes at sheet edges related to the total area of the sheet is larger. These results provide further support to the hypothesis that the relatively higher portion of curvature of Huh-7 sheets, gained from the sheet fenestrations and small sheet area, somehow assists the formation of the high-curvature tubules, which was observed to be the most common transformation event in Huh-7. It is noteworthy, however, that the membrane curves in two directions at the fenestrations and exhibit negative curvature along the perpendicular axis and positive curvature along the horizontal axis and, therefore, the increase of curvature at fenestrations is counterbalanced by the decrease of curvature along the perpendicular axis.

Based on center-of-mass analysis, the sheet movements did not exhibit any clear directionality in any of the cell types analysed, as the sheets mainly fluctuated in small area (I: Fig.8D; Data not shown for HeLa or NRK-52E). In accordance, the average distance to initial centroid position was roughly the same in all cell types: 0.27 µm ± 0.32 (SD) in Huh-7 (I), 0.29 µm ± 0.01 (SD) in HeLa and 0.33 µm ± 0.01 (SD) in NRK-52E, indicating that sheets remain rather stationary. The average sheet velocity was roughly the same in all cell types (I: 0.15 µm/s ± 0.04 sem in Huh7 and 0.11 µm/s ± 0.01 sem in HeLa; 0.15 µm/s ± 0.05 sem in NRK-52E). According to previously published results, the average velocity of tubular sliding (0.485 µm/s ± 0.264) in COS-7

cells is roughly 10-fold faster than TAC-based movement of tubules (0.044 µm/s ± 0.018) (Friedman *et al.*, 2010), which are in accordance to previous reports in HeLa cells (Grigoriev *et al.*, 2008). Thus, ER tubule movement exhibit differing speeds, and based on our results, the sheet movement is over twice as fast as the TAC-based movement of tubules but significantly slower than the tubular sliding. Moreover, the measured sheet velocities were not constant and temporarily sheets showed higher and lower speeds (V_{max} 1.09 µm/s and V_{min} 0.09 µm/s in Huh-7, V_{max} 0.24 µm/s and V_{min} 0.07 µm/s in HeLa and V_{max} 1.21 µm/s and V_{min} 0.06 µm/s in NRK-52E) indicating that, like with tubules, there might be subgroups of sheets present in the cells that have differing dynamic properties.

Together the analysis of ER sheet dynamics showed that the dynamics of ER sheets differs from tubular dynamics, which usually shows directionality and greater velocity. These results provide support to the idea that ER tubules might present means for transportation. ER sheets undergo characteristic transformations, of which the event of sheet splitting (fission) into smaller sheets seems be a unique feature for the sheets: ER tubular fission is routinely mentioned in papers reviewing ER dynamics in mammalian cells (*e.g.,* see reviews McMahon and Gallop (2005); Pendin *et al.* (2011)) and is mainly based on the observations and characterization done by Lee and Chen (1988) and Waterman-Storer and Salmon (1998). However, live-cell imaging has not furnished compelling evidence for the occurrence of tubular ER fission and these results have not been replicated other than on studies done on neuronal cells (Kucharz *et al.*, 2013), where ER was shown to be capable of rapid fragmentation - a feature not described for non-neuronal cell culture cells. Based on our live cell observations, if an extending ER tubule fused with another membrane, it was not observed to detaching and retracting back. The disappearance of a tubule occurred only when tubular sliding reached another tubule or sheets and, subsequently, as the tubule fused with the target membrane the polygon was closed. Retraction could, however, take place before tubular fusion to target membrane.

Why do ER sheets undergo transformations? What is the purposed for their stationary positioning and the reason behind the variance of persistence between fenestrated and intact sheets? One explanation could be that the persistent sheets might provide a stationary and persistent subdomain, in otherwise dynamic network, for the synthesis and quality control of membrane and secretory proteins, which are the specific functions assigned especially for sheets. The reason behind remodelling is, however, harder to explain, and currently, we are mainly able to exclude possibilities that are the least likely explanations. The constant and active remodelling must require high amounts of energy, and accordingly, they must serve a purpose. From biochemical point of view, as ER lumen is continuous, sheet fission most likely does not serve to create luminal microenvironments. However, it could, in principle, segregate certain lipids or lipid rafts and membrane proteins into distinct micro-domains (Simons and Sampaio, 2011). Structure-wise, sheet fission creates smaller confinements, increases the relative surface area compared to volume and, furthermore, increases the relative proportion of high

membrane curvature on sheets. This might augment tubular formations, as tubules are drawn straight out from the sheets. Furthermore, smaller sheets would decrease the hindrance for the cytosolic trafficking. Sheet fusion, on the other hand, creates larger sheets that could, in principle, accommodate higher density of polysomes to increase the level of protein production. This could also work *vice versa*: smaller sheets have smaller density of ribosomes and produce fewer proteins, and could potentially provide a post-transcriptional regulatory step for the level of protein production. The sheet transformations into tubules are especially difficult to comprehend. There are specific functions assigned for both sheet and tubules, and the conversion of sheets into tubules, or *vice versa*, would also require adaptation of the functions. Why the cells do not simply create new tubules, instead of converting sheets into one, remains to be solved. One explanation could be that if the protein translation halts in a particular sheet, and it no longer produces proteins, that particular sheet is no longer needed and it its converted into a dynamic structure that can be relocated to another position. Based on our live cell observations, new ER structures are constantly being made and dismantled -a notion that is especially evident for the tubules. The reason for a tubule to grow out and immediately fuse to the target membrane and via sliding of the tubule eventually disappear, might be the confined trafficking of molecules: whereas diffusion is an efficient way to deliver molecules without ER bulk movement, the tubular dynamics could provide targeted system for delivering molecules. Finally, there is the question of the differing dynamics of fenestrated and intact ER sheets. Again, maybe the answer lies on the membrane curvature. ER sheets with fenestrations have relatively higher proportion of highly curved areas than the intact sheets and it might be possible that this increased curvature augments tubular formation. As mentioned earlier, the most common transformation event in Huh-7 cells was the transformation into tubules.

3. Structural determinants of the endoplasmic reticulum sheets

3.1 Endoplasmic reticulum membrane bound ribosomes

What is the mechanism behind the progressive sheet-to-tubule transformation during mitosis? It was recently suggested that polysomes and the associated protein machinery would stabilize the sheet structures (Shibata *et al.*, 2006). Accordingly, the translation is down-regulated during mitosis (Le Breton *et al.*, 2005), and, based on sucrose-gradient analysis and EM, the polysomes are broken down during metaphase in wt mitotic HeLa cells and in those arrested in metaphase by treatment with colchicine (Scharff and Robbins, 1966). In agreement, we noticed that the ERES, that mark the site of ongoing transport, quickly reduced in number after early pro-metaphase and emerged again during telophase (III: Fig.4a-d). Interestingly, based on time-lapse imaging of COPII-coated structures in live mammalian cells, the number of ERES continues increasing during interphase by *de novo* formation (Stephens, 2003), indicating that the level of protein production shows plasticity throughout the cell cycle. The role of membrane-bound ribosomes on the

structural conversion of the mitotic ER, and the emerging model of the mitotic ER inheritance, are discussed in the next five chapters.

3.1.1 The mitotic sheet-to-tubule transformation is accompanied by a decrease in ribosomal density on the membranes (II; III)

To test if the density of membrane-bound ribosomes correlated with the observed mitotic structural changes, we first quantified ER-bound ribosomes from interphase and mitotic CHO-K1 cells that undergo a complete sheet-to-tubule transformation during mitosis. Thin-section EM images were obtained from the perinuclear area of interphase cells, where most sheets are located and from corresponding areas of pro-metaphase to early anaphase cells (III: illustration in Fig.6, Fig.9Aa and 9Ab). The ribosome density on mitotic ER membranes (3.7 ribosomes/µm) was approximately 70% smaller than the density in interphase cells (12.5 ribosomes/µm). In Huh-7 cells, where the mitotic ER transformation is slightly more moderate, the ribosome density decreased by 45% in mitotic cells (II: 8.3 ± 0.4 ribosomes/µm) compared to interphase cells (II: 15.1 ± 0.7 ribosomes/µm) and, accordingly, by 43% in NRK-52E (II: 17.3 ± 1.2 and 9.8 ± 0.5 ribosomes/µm, respectively) (in both $p < 0.001$).

This data is in agreement with previous results showing that polysomes break down during mitosis. Our results indicate that the ribosome density on ER membranes decrease in mitosis. Ribosomes, and especially polysomes, are thought to predominantly bind the flat ER sheets that correspond to RER (Figure 2). However, based on our observations, 30% to 57% of the ribosomes are still present in curved mitotic membranes and, therefore, few questions arises from these observations: Firstly, is the remaining portion of ribosomes translationally active or merely present ribosome storage when translation is inhibited? Second interesting aspect of ribosome binding on mitotic membranes is the increased curvature of ER network in mitosis, caused by the transition towards more fenestrated sheet and tubules: Are the mitotic ribosome assemblies at ER membranes individual or small clusters of ribosomes instead of polysomes, which would require a larger membrane surface area to bind to? And, furthermore, does the ribosome density on the ER membranes correlate with the membrane curvature? And thirdly, is it the ER morphology that follows the ribosome binding or the other way around, *i.e.,* does the ribosome binding flatten out the ER membrane or ribosomes simply bind to readymade flat membrane areas? If ribosomes have, as suggested by our results, a structural role on ER sheets, additional factors, such as the translocon machinery with luminal chaperones, are most likely required for controlling the ER structure, as ribosomes are also found from the curved membrane areas and cannot, therefore, solely be responsible for stabilizing ER sheets. In accordance, OSER lack the membrane-bound ribosomes and yet exhibit predominantly sheet-like morphology (Baumann and Walz, 2001).

3.1.2 Ribosomal density on membranes correlates inversely with the membrane curvature (II)

To address the question of ribosome binding on membranes with different curvature, we prepared Huh-7 and NRK-52E samples using HPF/FS and quantified ribosomes on intact sheets, fenestrated sheets, and tubules from thin-section TEM images. The intact NRK-52E sheets contained the highest ribosome density (II: 24.6 ± 0.9 ribosomes/µm) and the fenestrated sheets of Huh-7 cells had 20% ($p < 0.01$) smaller ribosome density (II: 19.8 ± 1.1 ribosomes/µm) on the transverse membrane sections. The ribosome density on sheet edges and fenestrations was >30% lower compared with transverse sections of intact sheets ($p < 0.001$): 16.9 ± 1.1 ribosomes/µm in NRK-52E and 15.4 ± 1.0 ribosomes/µm in Huh-7 (II). Round profiles and tubular side views (*i.e.,* tubular membranes) clearly contained the lowest ribosome density in both cell types, 4.9 ± 0.6 ribosomes/µm in NRK-52E and 8.2 ± 0.8 ribosomes/µm in Huh-7. These values were >60% lower compared with transverse sections of intact sheets ($p < 0.001$) (II).

For definite structural identification, we also quantified ribosomes per membrane surface area in tomograms from HPF/FS specimens (II: Fig.8). Intact sheets from an NRK-52E tomogram had 824 ± 57 ribosomes/µm^2, whereas a slightly lower value of 786 ± 69 ribosomes/µm^2 was obtained for fenestrated sheets of Huh-7 cells. Tubules clearly had fewer ribosomes in both cell types: 203 ± 26 ribosomes/µm^2 in NRK-52E and 137 ± 20 ribosomes/µm^2 in Huh-7. The lower density of ribosomes on fenestrations, edges of sheets, and tubules was visible in the ET models (II: Fig.8C-F).

In conclusion, ribosome density correlates inversely with the amount of tubules and sheet fenestrations. Together the findings support the idea that high-curvature surfaces tend to have a low density of ribosomes and perhaps polysomes indicating that ribosomes, in conjunction with the associated protein machinery might be a general mechanism determining the structure of ER sheets. These results are interesting in the light of secretion activity of the cells: As discussed earlier, Huh-7 had the more abundant sheets compared to *e.g.,* NRK-52E, indicating that Huh-7 cells might be more actively secreting cell type. However, NRK-52E has a higher density of membrane-bound ribosomes compared to Huh-7. The net effect of these attributes on the secretion activity of the cells comprises an interesting question for future studies.

3.1.3 Translation inhibition does not affect the sheet structures (III)

To study the role of membrane-bound ribosomes on ER morphology further, we first tested the effects of translation inhibition on ER structures. Cycloheximide is a drug that binds to ribosomes and stabilizes the ribosomal association with translocon while inhibiting protein translation (Roy and Wonderlin, 2003; Seiser and Nicchitta, 2000). Quantitation of ER-bound ribosomes in CHO-K1 (11.4 ± 1.5 ribosomes/µm) showed that treatment did not significantly alter the ribosome density (8.8% decrease) on ER membranes (III: Fig.9Ac and Fig.9B). Based on ET, a 15-min cycloheximide treatment of interphase CHO-K1 cells did not induce changes in the ER morphology or network fragmentation (III: Fig.10A). Interestingly, a prolonged incubation with cycloheximide for 2 hours caused tubulation and perforation of

ER sheets that was not seen after the shorter incubation time. This might be explained by previous findings that higher concentration or prolonged incubation time of cycloheximide causes ribosomes stripping from the membranes (Van Coppenolle *et al.*, 2004). Indeed, we calculated a 32% decrease (8.5 ± 1.8 ribosomes/µm) in ribosome density (III: Fig.9Ad and Fig.9B) after prolonged treatment, suggesting that ribosome detachment might results in observed changes in the ER.

In TEM images, a certain level of uncertainty of observing the presence or the absence of the small ribosomal subunit is present. Therefore, the quantification of the membrane-bound ribosomes was confirmed and further investigated at LM level by staining the permeabilized and salt-washed CHO-K1 cells expressing Hsp47-GFP with an antibody against the small ribosomal subunit protein S6. The colocalization of S6-staining and Hsp47-GFP did not change after cycloheximide. In agreement with the EM-data, the comparison of the total intensities between control cells and the 15-min and 2-h cycloheximide treatments, indicated a 12% and 32% decrease (III: Fig.9C), respectively, in the ribosome attachment on ER.

While the extended cycloheximide incubation stripped a significant part of ribosomes from the ER membranes and induced ER tubulation, the effect on ER morphology can also be explained by other means than stripping of the membrane-bound ribosomes. The 2-h translation blockage, but not the short 15-min inhibition, might deprive ER from other proteins involved in sheet stabilization, and therefore the role of other players involved cannot be excluded. Furthermore, these results indicate that the previously reported protein translation down-regulation during mitosis (Le Breton *et al.*, 2005) most likely does not solely count for the observed structural changes in the ER. As discussed earlier, the protein translation/ secretion activity and the amount of ribosome covered ER sheets in the cells seems to correlate. Our results, however, indicate that the structural balance of ER sheet is stabilized by other factors than a mere level of protein production, and that while these events most probably are connected, the link between ER sheet structure and level of protein production is not direct.

3.1.4 Ribosomal association with translocon complex is required for sheet maintenance (III)

To study the effect of membrane-association of ribosomes on ER structure, we next treated CHO-K1/Hsp47-GFP cells with puromycin that, in addition to inhibiting translation, dissociate polysomes from ER membranes (Azzam and Algranati, 1973). A 15-min treatment of cells with puromycin led to a marked tubulation and perforation of ER sheets as is seen clearly in 3D-reconstruction (III: Fig.10B). The puromycin-treated interphase ER resembled mitotic ER; number of tubular profiles increased and any remaining sheets were either very small or extensively perforated. However, tubules outside the perforated sheets seemed longer than average mitotic tubules. TEM thin section quantitation revealed smooth ER membranes (III: Fig.9Ae and 9B) with markedly decreased (44.8 %) density of ribosomes (6.9 ± 1.2 ribosomes/µm). A prolonged 2-h puromycin treatment of interphase cells resulted in a similar outcome, although the number of ribosomes on ER membranes (5.5 ± 1.2

ribosomes/µm) was reduced by 56 % (III: Fig.9Af and 9B).

As discussed earlier, in EM images, the presence or the absence of the small ribosomal subunit cannot be reliably discerned. Puromycin has been shown to break down the ribosome, that is, dissociating the 40S subunit and leaving the 60S subunit bound to the translocon (Seiser and Nicchitta, 2000). The quantification of ribosomal detachment was confirmed at LM level by staining the permeabilized and salt-washed CHO-K1/Hsp47-GFP with an antibody against the small ribosomal subunit protein S6. In contrast to cycloheximide treatment, the 15-min and 2-h puromycin treatments led to 83% and 82% decrease in S6 intensity, respectively (III: Fig.9C).

Dissociation of ER-bound ribosomes with puromycin treatment, mimic the mitotic sheet-to-tubule transformation and suggest that ribosomes play a role in sheet stabilization in interphase because sheets were lost when ER-bound ribosomes decreased in number, analogously to mitotic events. Therefore, these results provide a mechanistic insight into the inheritance of the ER by showing that similar changes in the ER structure are obtained by stripping of ribosomes with puromycin from the interphase ER, but not by a mere translation inhibition by cycloheximide. Importantly, these results provide evidence that is it the ER morphology that follows the ribosome binding and not the other way around, *i.e.,* sheets are not created first, to which the ribosomes bind to, but that the ribosomes are essential for creating the flat sheets. The observed structural changes, both in naturally occurring mitotic cells as well as drug-induced cells, might be explained by Ca^{2+} signalling. The mitotic progression has been shown to depend on Ca^{2+} -signals originating from ER (Parry *et al.*, 2005), suggesting that Ca^{2+} might control mitotic transformations of ER. Puromycin treatment has been shown to lead to Ca^{2+} leakage to the cytosol through the translocon (Roy and Wonderlin, 2003; Van Coppenolle *et al.*, 2004) and the structural resemblance of the puromycin treated interphase ER to mitotic ER might be explained by the changes in the cytosolic Ca^{2+} levels. In accordance, Ca^{2+} efflux from the ER has been shown to accompany the ER network formation *in vitro* in *Xenopus laevis* vesicles and, furthermore, in high concentrations to lead to ER fragmentation (Dreier and Rapoport, 2000; Voeltz *et al.*, 2006). Since cycloheximide stabilizes the ribosome binding to the translocon channels it does not result in Ca^{2+} leakage or store depletion (Roy and Wonderlin, 2003). The exact role Ca^{2+} plays in ER transformations is unclear. Our observations support the structural stabilizing role of ribosomes, and it is possible that ribosomes and Ca^{2+} play cooperational roles. Ca^{2+} might control some aspects of ER morphogenesis, such as network branching via p22 (Andrade *et al.*, 2004). However, it is unclear if translocon channels leak Ca^{2+} under normal physiological conditions (Roy and Wonderlin, 2003; Van Coppenolle *et al.*, 2004). Another, and not necessarily mutually exclusive, mechanism could be the natural reduction of p180 at ER sheets prior cell division: p180 knockdown leads to a reduced ribosome density on ER membranes (Benyamini *et al.*, 2009) and, in our view, to profiles of fenestrated sheets on thin sections.

3.1.5 The proposed model for mitotic conversion of endoplasmic reticulum (II)

Based on our observations, the structural transformations of ER in mitosis and upon drug-induction, and the correlation of the membrane-bound ribosomes with the ER morphology, a trend of structural transformation became evident and we, thereby, present a general model for the mitotic conversion of ER in mammalian cells (Figure 8). The mitotic transformation of intact sheets to a tubular network (Figure 8:

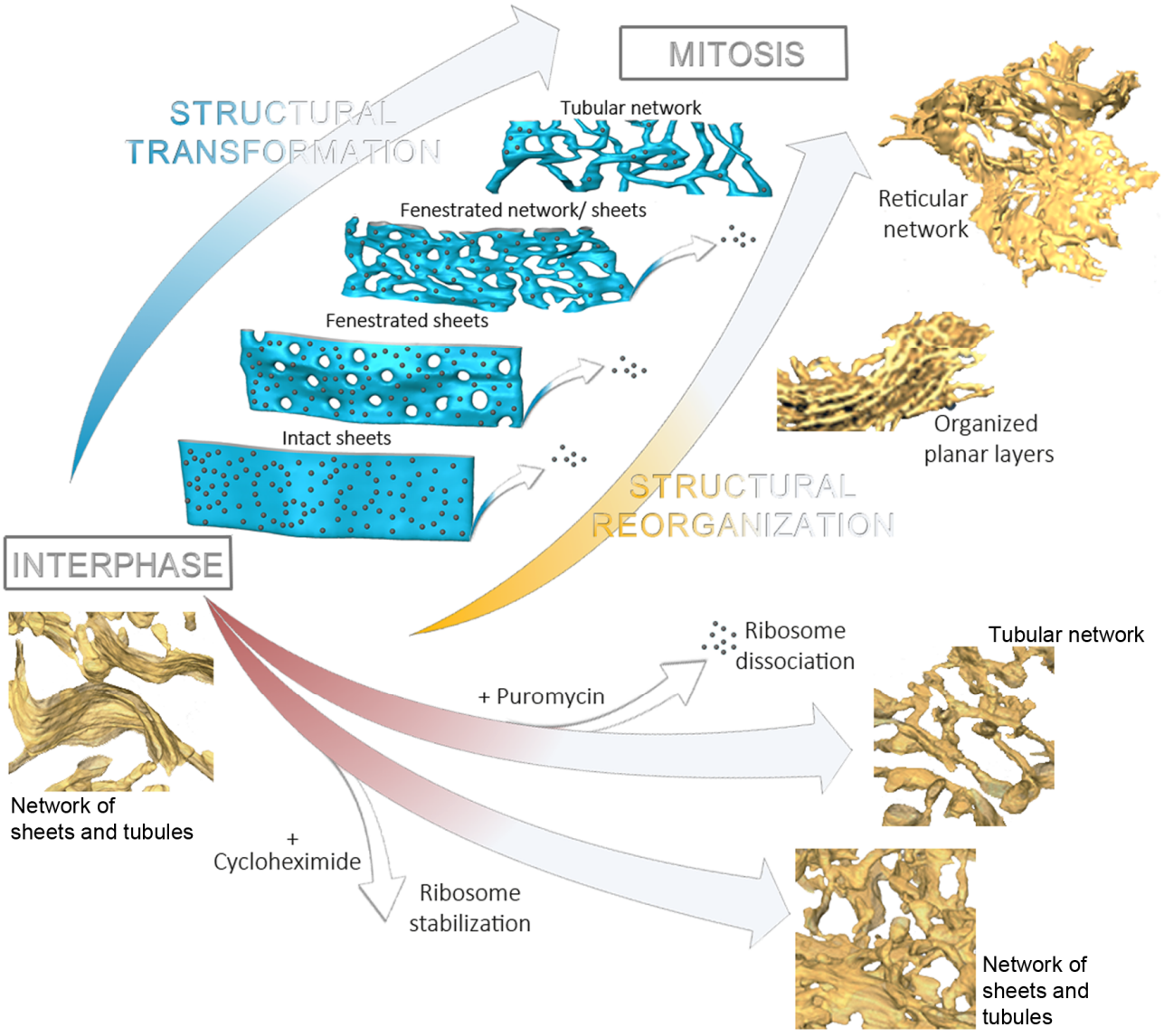

Figure 8. A model of mitotic ER structural transformation and reorganization. The structural transformation (blue arrow and structures) of interphase RER starts from intact/ fenestrated sheets and proceeds towards more fenestrated sheets and tubular network during mitosis. The transformation magnitude correlates with the dissociation of the membrane-bound ribosomes (red circles). The starting and ending points along of the mitotic conversion are cell type dependent (CHO-K1, NRK-52E, HeLa, Vero and Huh-7), but the direction of the conversion is the same. The structural reorganization from interphase to mitosis (yellow arrow) results in either a reticular or an organized planar network of highly fenestrated sheets and tubules. The mitotic sheet-to-tubule structural transformation of CHO-K1 cells can be mimicked in interphase cells by stripping of the ER-bound ribosomes with puromycin treatment. Ribosome stabilization by cycloheximide treatment does not induce sheet-to-tubule transformation. Image modified from II: Fig.9 and Fig.S2; III: Fig.10.

Structural transformation) occurred through an increase of number and enlargement of fenestrations until the structure resembled reticular network or an organized planar network of highly fenestrated sheets and tubules (Figure 8: Structural reorganization). The starting point (intact vs. fenestrated sheets) and ending point (smaller intact or fenestrated sheets vs. tubules) may vary cell type dependently and according to ribosome density, but the direction of transformation was the same in CHO-K1, NRK-52E, HeLa, Vero and Huh-7 cells. The structural transformation might be caused -directly or indirectly- by the ongoing detachment of the membrane-bound ribosomes. The mitotic sheet-to-tubule transformation could be mimicked in interphase cells with detachment of ribosomes by puromycin, but not by cycloheximide treatment, which does not detach the membrane-bound ribosomes (Figure 8: Red arrows). The model presented here favours the stochastic model of inheritance that serves for equal inheritance of the ER network (Lowe and Barr, 2007; Warren, 1993).

3.2 Endoplasmic reticulum and the cytoskeleton

Based on our results, the tubular ER network is highly dynamic and the persistent ER sheets undergo characteristic transformation events. While the movements of tubular ER are accomplished through interactions with the MTs and associated protein machinery (Terasaki *et al.*, 1986; Waterman-Storer and Salmon, 1998), the mechanisms employed to maintain ER sheets, or accomplish sheet movements or transformations, are largely unknown.

3.2.1 Endoplasmic reticulum resides in close proximity with microtubules and actin filaments (I; II; III; Unpublished)

To best visualize the ER and the surrounding cytoskeleton, Huh-7 cells were subjected to HPF/FS, followed by high-resolution ET. Although actin filaments could be observed in chemically fixed EM samples, HPF/FS enabled near native preservation of cytoskeletal filaments, thus enabling the segmentation of ER, MT, and actin filaments from the tomogram. There are indications that actin filaments are, at least partially, destroyed during TEM sample preparation (Svitkina, 2009). The acquired 3D-model revealed that MTs and ER tubules do not have identical distribution in cells, and that ER resides in close proximity with both actin filaments and MTs (Figure 9), indicating that interaction with both filament systems, in theory, could be possible. Dynamic interactions among the three cytoskeletal systems -microtubules, actin and intermediate filaments- regulate to a great extent the structural organization of the cytoplasm of mammalian cells. Where there are no indications that peripheral ER interacts with intermediate filaments, we were interested to see if these interactions, along actin filaments and MTs, could be possible. Intermediate filaments are composed of a family of proteins sharing common structural and sequence features. To study the interactions of the whole intermediate filament family of proteins, encoded by over 60 genes, with ER would be very laborious, and therefore, we chose to study the localization of the most widely distributed intermediate filament protein, vimentin, which is commonly expressed in fibroblasts.

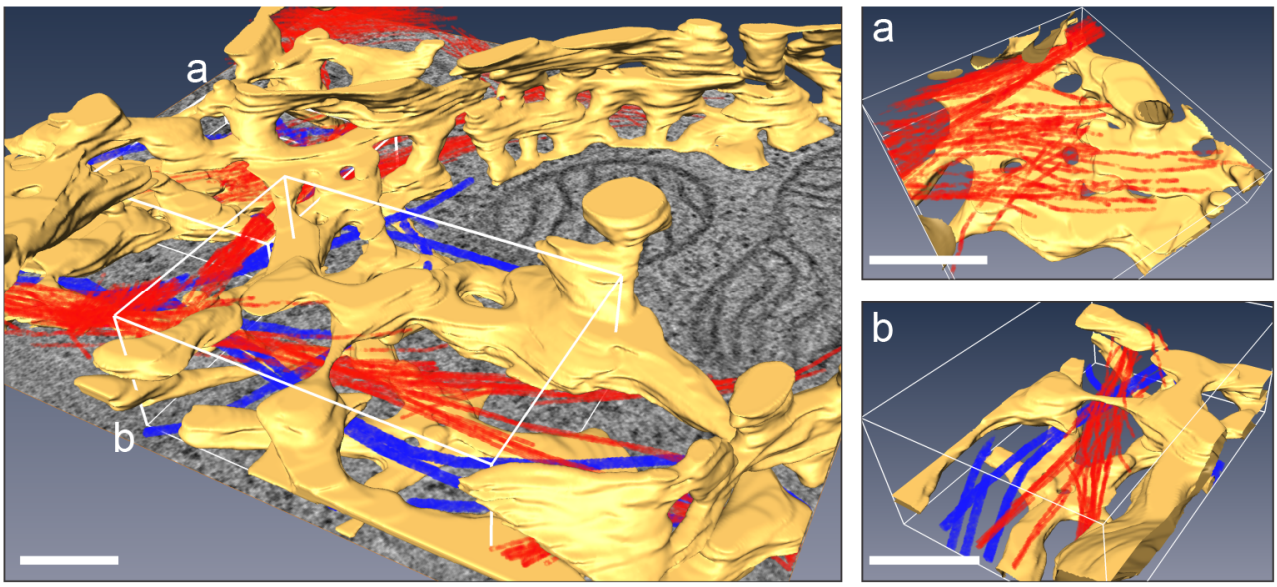

Figure 9. ER resides in close proximity with both microtubules and actin filaments. Two successive 250-nm sections from wt Huh-7 cells were prepared using HPF/FS, and subjected to ET. From the resulting tomogram, MTs (blue), actin filaments (red), and ER (yellow) were modelled. A detailed view of ER, actin filament meshwork and actin bundles and MTs from the boxed areas (a and b) are shown with higher magnification on right. Bars 0.25 µm.

Vimentin has been shown to support cellular membranes and to have a role in nuclear positioning (Chang and Goldman, 2004) making it a good candidate to study the possible roles on ER dynamics and/or structure. Wide-field LM imaging of Huh-7 cells immunolabeled for vimentin and β-tubulin and stained with phalloidin to visualize intermediate filaments, MTs and actin filaments, respectively, showed that the distribution of the three filament types differed from one another (Figure 10A). While actin filaments were found throughout the cytoplasm, the bulk of MTs concentrated near the nucleus, most likely to MT organizing center. In addition, the distribution of MTs at the cell periphery was more confined compared with actin filaments, possibly indicating towards the roles that actin cytoskeleton has on maintenance of cell shape and on cell migration. In agreement with previous studies (Lee *et al.*, 1989; Terasaki *et al.*, 1986), vimentin was located exclusively to the perinuclear area and could not be found at the cell periphery. While we cannot exclude the possibility of ER interacting with other types of intermediate filaments, the different distribution of vimentin in relation to ER (Figure 10B) makes it clear that this intermediate filament type cannot provide the means for a cell scale regulation/maintenance of the peripheral ER. However, in accordance to earlier findings (Chang and Goldman, 2004), vimentin could provide means for NE positioning.

As the MT connection to ER tubules has been well described, the close proximity of ER and actin in our ET model raised a question of possible interplay between the actin filaments and ER. For this, we studied the dynamics of ER and actin by confocal microscopy in Huh-7 cells co-expressing Hsp47-GFP and mCherry-Actin, which is a fusion protein for live cell actin filament dynamics monitoring (Vartiainen *et al.*, 2007). To overcome the challenges of visualizing a complex and highly dynamic 3D-structure that has subdomains

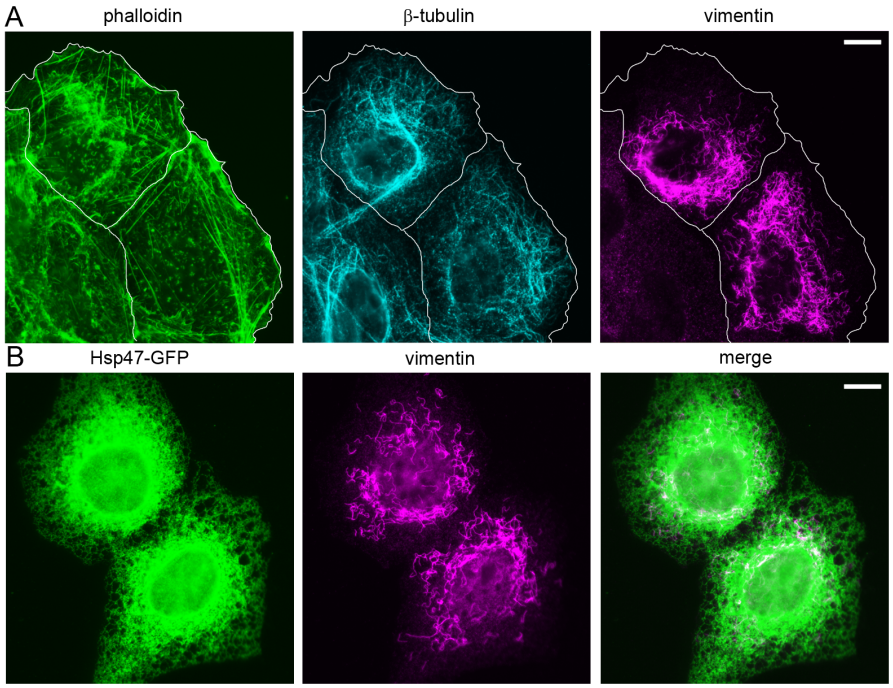

Figure 10. The three cytoskeletal filament types of mammalian cells. (A) Wide-field LM images of Huh-7 cells (outlines for clarity) immunolabeled for vimentin (magenta) and β-tubulin (cyan) and stained with phalloidin (green) show that the distribution of the three filament types differ from one another. (B) Wide-filed images of fixed Huh-7 expressing Hsp47-GFP (green) immunolabeled for vimentin (magenta) highlight the differential distribution of vimentin in relation to ER. Bars 10 µm.

large enough to occupy more than one imaging plane we, again, acquired live videos from the thin lamella at the leading edge of the cells allowing simultaneous imaging and identification of tubules and individual sheets. Live-cell confocal imaging of ER and actin revealed the close proximity and coinciding movement of ER and short actin filament arrays and foci (I: Fig.3A). These actin structures resembled the actin filament arrays and foci observed after phalloidin staining (I: Fig.1C) and were found throughout the cell volume (I: Fig.S3), diverging from relatively longer actin filaments *i.e.,* stress fibers or cortical actin which mostly localized to the cell bottom and cell periphery and had no clear interactions, nor simultaneous movement, with the ER (I: Fig.3A). Similar results could be observed using another construct for filamentous actin in living cells, LifeAct-RFP (I: Fig.3A), which has been shown not to interfere with actin dynamics *in vitro* and *in vivo* (Riedl *et al.*, 2008). The actin filament arrays and foci localized to the

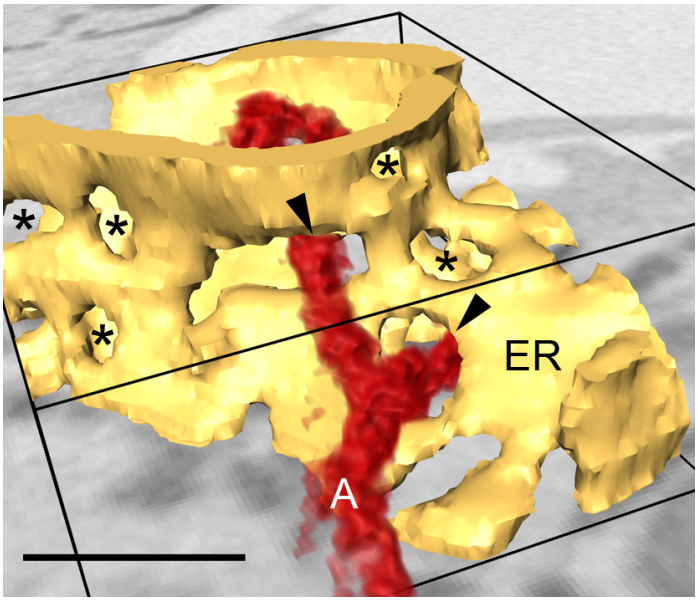

Figure 11. Model of actin filaments traversing the polygons of ER network. Actin filaments (red, marked with (A) traverse the polygons (arrowheads) defined by the surrounding ER (yellow) structures. The 3D-model was obtained from chemically fixed and cytochemically stained Huh-7/ssHRP-KDEL cell, and imaged with SB-EM. Sheet fenestrations, considerably smaller in size than polygons, are indicated with asterisks. Image is presented in orthogonal view and the 0.5 µm bar applies to the center of image.

polygons defined by the surrounding ER structures. Based on our ET-analysis of CHO-K1 cells, the non-uniform space between the ER structures, *i.e.,* the network polygons, were defined by three types of branch points formed either by tubules, tubules and sheets, or, sheets (III: Fig.2C). It is noteworthy that the polygons (Figure 2A) differ from ER sheet fenestrations (II: Fig.2C and E; Figure 5), that are considerably smaller openings and beyond the resolution limit of conventional LM. In agreement to our LM analysis of ER and actin, SB-EM imaging and 3D-modelling of ER and actin in Huh-7 showed that actin filaments were often observed to transverse the network polygons (Figure 11) and more seldom, the fenestrations. If MTs show preference to ER fenestrations (Figure 5) and actin to network polygons (Figure 11) and, furthermore, what is the functional importance of such interactions, create an interesting question for suture studies.

3.2.2 Sheet-tubule ratio is counterbalanced by microtubules and actin filaments (I)

In contrast to typical view of ER organization (Terasaki *et al.*, 1986), where sheets are found close to nucleus and tubular network prevails at cell periphery (II: Fig.2A and III: Fig.1A), the interphase ER at cell lamella in Huh-7 cells consists of a network of abundant sheets and tubules (I: Fig.1A and S1A; II: Fig.2A, 2C, 2E and 2G). Intersection quantification of LM images of Huh-7 cells, immunolabeled for endogenous calreticulin, revealed a 67%/ 33% ratio of sheet and tubules (I: Fig.1B) indicating that majority of ER in these cells is composed of sheets.

To study the effects of actin or MT cytoskeleton depolymerization on ER, Huh-7 cells were treated with latA or nocodazole, respectively. Consistent with previous studies (Lee *et al.*, 1989; Terasaki *et al.*, 1986), wide-field imaging of cell lamella revealed that the depolymerization of non-acetylated MTs (Friedman *et al.*, 2010) with 30-min nocodazole treatment shifted the ER structural balance towards sheets, resulting in 82%/ 18% sheet-tubule ratio and a retraction of the ER network towards NE. In contrast, after 15-min latA treatment, the amount of sheets at the cell periphery decreased substantially (22%/ 78% sheet-tubule ratio) and the ER network appeared more reticular (I: Fig.1A and 1B). Similar effects were observed in Huh-7 cells over-expressing luminal ER marker (I: Fig.S1A), in HeLa cells immunolabeled for calreticulin (I: Fig.S2A) and in fixed NRK-52E cells expressing Hsp47-GFP and imaged with wide-field LM (data not shown), indicating that the effects observed are not specific for Huh-7 cells. The results obtained from actin manipulation are in conflict with a previous study showing that ER organization is not dependent on actin filaments in Vero cells (Lee *et al.*, 1989). The study concentrated on the rebuilding of the ER after nocodazole washout, showing that actin depolymerization had no effect on the formation of the reticular network. However, the formation of ER sheets was not disclosed in the study and, furthermore, the results concerned only the ER network formation, the possible role of actin cytoskeleton on the maintenance of ER cannot be excluded. The conflicting results may rise from the use of different cell types or drugs. For example, the latA-effects could easily be overlooked in cell types where ER is mostly tubular and sheets are preferentially located close to NE, such as CHO-K1. However, in agreement to our

results, the retrograde movement of ER in newt lung epithelial cells has been shown to be inhibited by cytochalasin D (Waterman-Storer and Salmon, 1998), a drug that depolymerizes actin filaments, implying that actin cytoskeleton might interact specifically with a subset of ER instead of the whole network.

To study if the changes observed in the sheet-tubule balance resulted from a structural conversion of sheets and tubules or from changes in the total amount of ER, we measured the relative fluorescence intensity of calreticulin in control, latA- and nocodazole-treated HeLa cells. Based on the measurements, the labelling intensity of calreticulin remained unaltered after the nocodazole or latA treatments compared to control cells (I: Fig.S2B), indicating that the actin cytoskeleton and MTs counterbalance the sheet-tubule ratio of ER and that the changes observed did not arise from consumption of the ER but from a true conversion of structures.

To analyse more carefully the effects of two commonly used actin depolymerizing drugs on actin cytoskeleton, and consequently, to the cell shape, we tested Cytochalasin B and latA with number of concentrations and incubation times and stained the actin cytoskeleton with phalloidin. In untreated cells, the phalloidin staining revealed long actin filaments, *i.e.,* cortical actin and stress fibers, and in addition, shorter, less than 5 µm long, actin filament arrays and punctate-like foci (I: Fig.1C and Fig.S2C). The thickness or length of any of the structures was not constant, indicating that the observed actin arrays were composed of varying number of actin filaments. LatA and Cytochalasin B both depolymerized the filamentous actin, but cells seemed to tolerate the latA treatment slightly better: after 15-min treatment with 1 µM concentration, longer actin filaments remained unaffected while most of the shorter actin filament arrays collapsed into actin foci (I: Fig.1C and Fig.S2C). The cells remained spread and their flat shape was not altered (I: Fig.1C; Figure 12) -effect that were induced with using higher concentrations or longer incubation times (data not shown). We chose to use the mild (1 µM) and short (15 min) latA treatment for our further studies in order to not stress the cells excessively. LatA treatment revealed the direct dynamic relation between actin arrays and foci, and further suggested that foci might be the initial polymerization sites. The effect of latA treatment on actin filaments and to free monomeric actin can be monitored by phalloidin (I: Fig.1C) and DNaseI staining (I: Fig.S1B) (Mannherz *et al.*, 1980), respectively. The quantitation of the relative fluorescence intensity revealed a 34% decrease in filamentous actin and, correspondingly, 55% increase in monomeric actin upon latA treatment in Huh-7 cells (I: Fig.1D and Fig.S1C). Quantification of the actin depolymerization effects in HeLa (I: Fig.S2D; Figure 12C) and NRK-52 (Figure 12A, 12B and 12D), showed similar trends than in Huh-7, however in a milder manner: The corresponding numbers in HeLa and NRK-52E were 34% and 9% decrease in filamentous actin and 31% and 31% increase in monomeric actin, respectively (NRK-52E presents unpublished data). The more moderate effect of latA on actin cytoskeleton in these cells might be the extensive stress fibers present in HeLa and NRK-52E cells, which seem to endure the latA treatment as

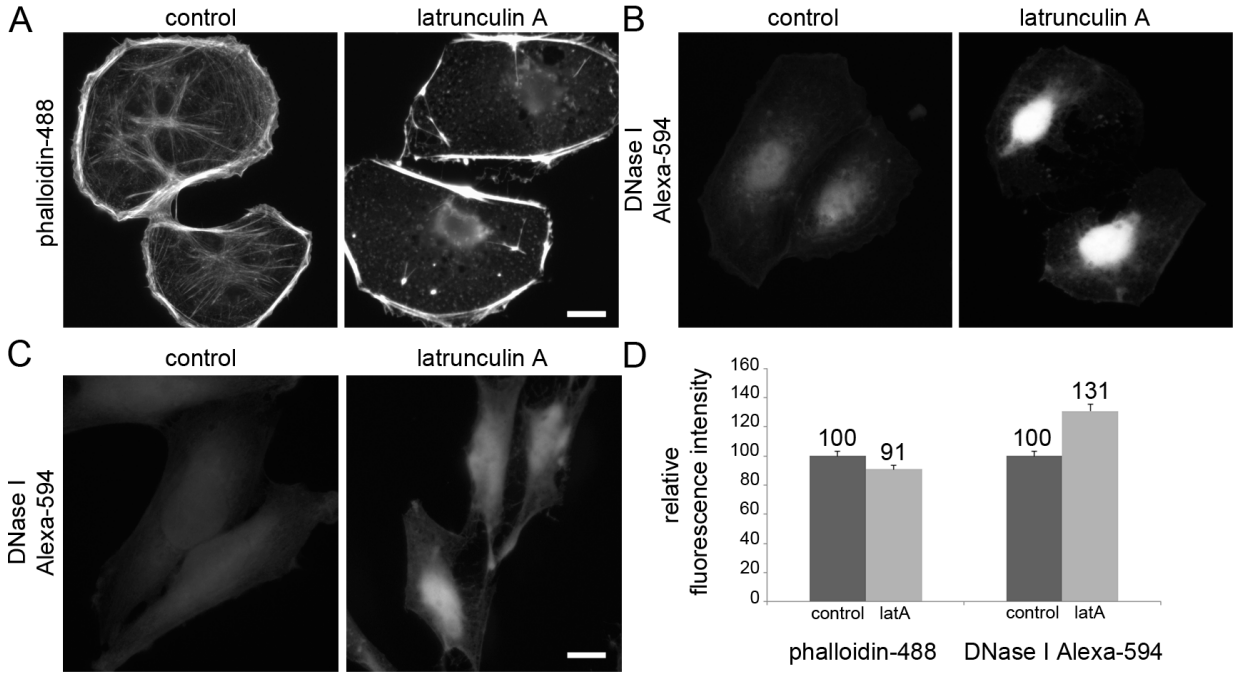

Figure 12. Effect of latrunculin A treatment on actin cytoskeleton in HeLa and NRK-52E cells. Wide-field images of fixed (A-B) NRK-52E or (C) HeLa cells stained with phalloidin or DNaseI in control and latA treatment. Bars 10 µm. (D) The relative fluorescence intensity of phalloidin and DNaseI in control and latA-treated NRK-52E (n = 100 cells) cells. Error bars shown as sem.

they remain abundantly present after the treatment (I: S2C; Figure 12A). However, most of the shorter actin filament arrays collapsed into actin foci similarly than in Huh-7 cells after latA treatment. The sample preparation and relative fluorescence measurements of phalloidin and DNaseI in HeLa and NRK-52E were done as described in I.

In conclusion, ER sheet-tubule ratio is counterbalanced by MTs and actin filaments and the observed changes in the ER morphology upon actin depolymerization are most likely due to collapse of actin filament arrays into foci. These results suggest that actin filament arrays and foci might present similar structures, only in different stages of polymerization, *i.e.,* actin foci could be the polymerization initiations sites forming the actin filament arrays. Furthermore, these results indicate an involvement of a specific pool of actin filaments in maintaining ER sheet-tubule balance.

3.2.3 Dynamic actin filament arrays are essential for sheet morphology and the network distribution

3.2.3.1 Actin depolymerization results in reduced sheets and unevenly distributed network (I)

In order to study the actin depolymerization effects on ER morphology in detail, we used high-resolution EM analysis to reveal specific details of the ER phenotype. The 3D-EM models covered area extending from cell periphery to the NE and therefore enabled detailed structure identification within the whole 3D-volume of the cell and thus provide a more reliable visualization of the effects of the treatment compared to LM analysis. We prepared Huh-7 cells transiently expressing ssHRP-KDEL for SB-EM imaging. The cells were cytochemically stained to improve the contrast for semi-automated segmentation and to reliably identify ER. ER models of latA-

treated (I: Fig.2B) cells revealed that the sheets became smaller (I: Fig.2Bc) and less abundant (I: Fig.2Ba) compared to highly fenestrated and large control sheets (I: Fig.2Ac and 2Aa), and, while the ER network remained continuous, its distribution was uneven and areas void of ER were frequently found (I: asterisk in Fig.2Bb). Accordingly, actin cytoskeleton has been shown to have a role in controlling the sheet-tubule transformations in living embryos in *C. elegance* (Poteryaev *et al.*, 2005). Due to better resolution and reliable identification of the structures, we concluded that some profiles categorized as tubules in LM images after latA treatment (I: Fig.1A and B) may actually originate from diminished sheets and, therefore, indicating that the portion of tubules was lower than LM image quantitation had earlier suggested. Importantly, these results highlight the importance of complementing the resolution-limited LM studies with other methods, such as EM.

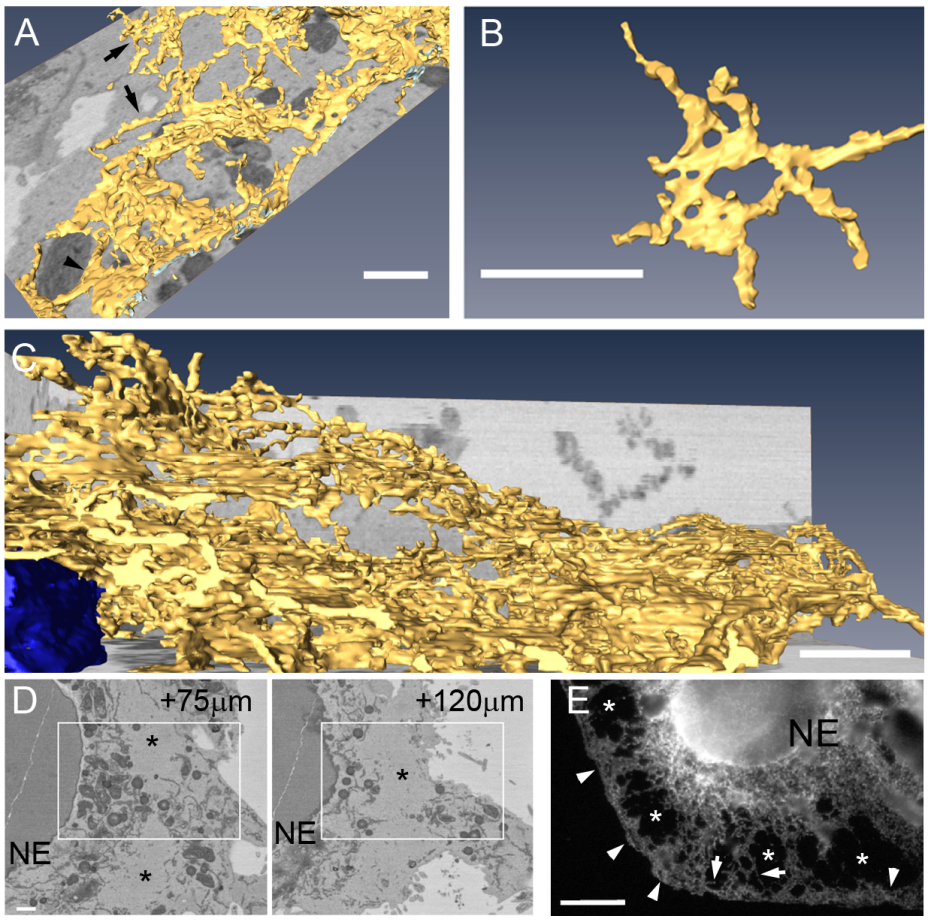

Figure 13. Actin stabilization affects the ER network distribution and sheet morphology. Jasplakinolide-treated Huh-7 cell transiently expressing ssHRP-KDEL was cytochemically stained and imaged with SB-EM for 3D-modelling. (A) Model of ER network (yellow) and NE (blue), (B) a representative sheet, (C) side view of the ER network, and (D) two block-face images taken at indicated heights from the beginning of the dataset are shown. Boxed area in (D) indicate the region modelled for (A and C). (E) A wide-field image of jasplakinolide-treated and fixed Huh-7 cell immunolabeled against calreticulin. NE, areas void of ER (asterisks), tubules (arrows) and sheets (arrowheads) are indicated. Bars 1 µm (A-D) and 10 µm (E).

3.2.3.2 Actin filament stabilization leads to endoplasmic reticulum phenotype (Unpublished)

As the actin filament depolymerization led to clear changes in the ER network distribution and alteration in the ER sheet morphology, we were interested in studying how the induced actin polymerization and stabilization would affect the ER. Jasplakinolide is a drug that is commonly used to polymerize and stabilize actin filaments (Holzinger, 2009). Jasplakinolide and phalloidin binding on actin filaments is competitive (Bubb *et al.*, 1994) and, thus, we monitored the jasplakinolide treatment indirectly by phalloidin

staining, which was observed to be defective upon actin stabilization, verifying the jasplakinolide effect on actin filaments (data not shown).

Huh-7 cells expressing ssHRP-KDEL were treated with jasplakinolide, cytochemically stained and prepared for SB-EM. A model of ER and NE revealed a striking ER network distribution defect with areas void of ER in the cell periphery (Figure 13A, 13C, 13D and 13E), and, furthermore, a degenerated sheet morphology (Figure 13B). Morphologically, the ER phenotype resembled latA treatment phenotype (I: Fig.2B), while distribution-wise the two phenotypes differed substantially. In both treatments the ER network was unevenly distributed and areas void of ER were found. However, actin filament polymerization and stabilization led to a strong accumulation of ER sheets at the cell periphery (Figure 13E), which was not evident upon latA treatment. Together these results indicate that actin cytoskeleton manipulations either by depolymerization or increased polymerization/stabilization affected ER sheet morphology and network distribution, suggesting that the dynamic actin filaments are required for interaction with the ER.

3.2.3.3 Dynamics of actin filament arrays and sheet transformations occur interdependently (I)

Previous studies have shown that, at steady state, the polygonal ER network is balanced by ring, *i.e.,* polygonal, closure (Lee and Chen, 1988) and that the filling of a polygon within an ER sheet leads to larger sheets (Griffing, 2010). Based on our analysis, the movement of actin filament arrays and foci in respect to ER revealed that the naturally occurring relocation, disappearance or formation of the actin arrays frequently preceded the closure or opening, respectively, of an adjacent polygon, leading to the subsequent ER sheet transformations (I: Fig.3B and C). One characteristic transformation event that we frequently observed was the membrane fusion leading to larger sheets (*i.e.,* ring closure) that followed closely the loss of associated actin filament (I: Fig.3B). We also observed that the local actin polymerization in confined area preceded the formation of an ER sheet to the polymerization area (Figure 14) and that the formation of an actin filament array was connected to the creation of polygons in the ER sheets (I: Fig.3C; Figure 14). In accordance to our previous wide-field imaging results of live cells, sheet fission events (*i.e.,* sheets splitting into smaller sheets) were regularly observed, whereas tubular fission was not.

While the precise mechanism by which the certain subset of actin filaments contribute to the ER structure and dynamics remains unclear, our results indicate that the dynamics of actin arrays and the ER sheets are interdependent. The mechanism by which actin could contribute to the formation of ER sheets could be the formation of a scaffold supporting the spreading of the sheet. Despite the lack of the definite mechanism, one thing becomes clear after observing the ER and actin dynamic in live cells: ER sheet dynamics does not occur on actin filaments as ER tubules grow or slide on MTs, indicating that the lateral movement of ER sheets is not driven by actin polymerization, but rather that it occurs on existing actin filaments, or that the dynamics of actin filament arrays modulate the existing ER sheets. In

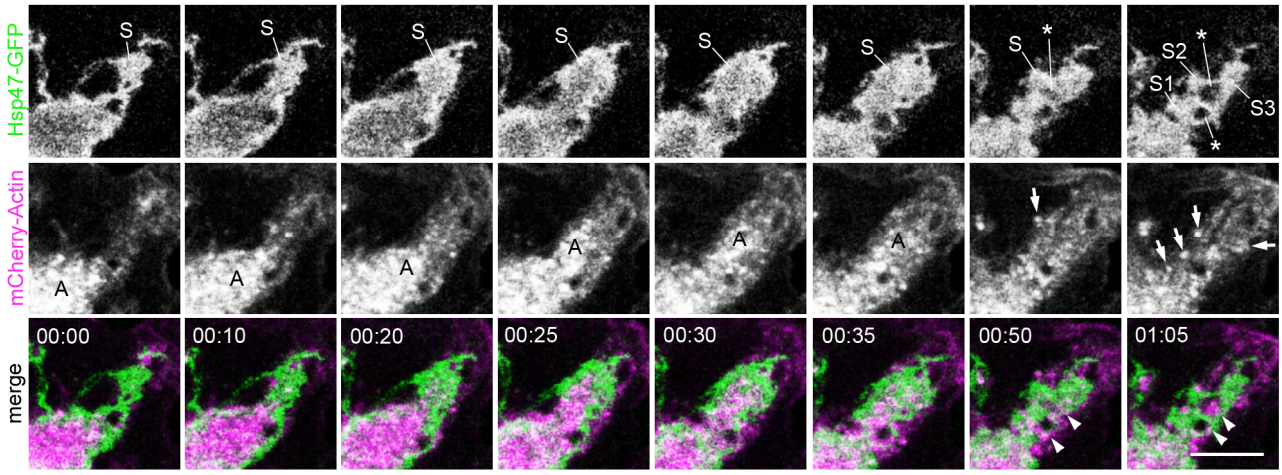

Figure 14. Dynamics of actin cytoskeleton and ER sheets are interdependent. Time-lapse confocal frames of Huh-7 cell co-expressing Hsp47-GFP (green) and mCherry-Actin (magenta) demonstrate the coincidence of actin polymerization and formation of actin filament arrays with ER sheet spreading and polygon creation. Actin polymerization (A) is observed from the bottom left corner towards the top right corner of the image, followed by the subsequent spreading and growth of the ER sheet (S) to the polymerization area. The formation of actin filament arrays (arrowheads) leads to polygon openings (asterisk) within the ER sheet, splitting the sheet into smaller sheets (S1, S2 and S3). Actin arrays localizing to the sheet edges are indicated with arrows. Time scale, min:sec. Bar 5 µm.

agreement, our earlier results demonstrated that ER sheets do not show clear directionality in their movement. Moreover, based on our center-of-mass analysis of live cell confocal imaging of Huh-7 transiently expressing mCherry-Actin, the mean velocity of the actin foci was 0.081 µm/s ± 0.04 SD (n = 25 foci in 10 cells), which is almost equal to the earlier FRAP-experiment report on polymerizing rates of F-actin in *Xenopus laevis* (0.07 µm/s) (Semenova *et al.*, 2008), and approximately half slower than the average sheet velocity.

3.2.3.4 Depolymerization of actin filament arrays increase the sheet movements and the rate of transformations (I; Unpublished)

Our earlier studies had shown that the disruption of the actin filaments affected the ER sheet-tubule balance and that the naturally occurring relocation and/or disappearance of the actin filament arrays frequently preceded ER sheet transformations. These results suggested an active interplay between actin filament arrays and ER sheet transformations. To mimic the naturally occurring relocation or loss of actin filament arrays from ER polygons (I: Fig.3B and 3C), we disrupted the actin filament arrays with latA, which allowed us to study the ER sheet dynamics in conjunction with real time depolymerization of actin filament arrays located in the ER network polygons.

For center-of-mass analysis, we chose to use trichostatin A (TSA) as a control, as it increases the proportion of acetylated MTs (I: Fig.S8A and S8B) that form the tracks for ER tubule sliding (Friedman *et al.*, 2010). The latA or TSA treatments did not induce changes in the directionality of the sheet movements in Huh-7 cells (I: Fig.8D), HeLa or NRK-52E cells (data not shown), nor the average sheet velocity in any of the cell types (I: 0.11 µm/s ± 0.01 sem or 0.11 µm/s ± 0.01 sem in Huh-7

and 0.12 µm/s ± 0.01 sem or 0.10 µm/s ± 0.01 sem in HeLa; 0.08 µm/s ± 0.01 or 0.10 µm/s ± 0.01 sem in NRK-52E, respectively). Remarkably, after latA treatment in Huh-7 cells, the average sheet centroid distance to the initial centroid position increased significantly ($p<0.05$) (I: from 0.27 µm ± 0.32 SD in controls to 0.43 µm ± 0.34 SD in latA treatment), indicating that the actin depolymerization allowed a greater lateral movement of the sheets, while the MT hyper-acetylation had no effect (I: Fig.8E) on the lateral movement (I: 0.30 µm ± 0.30 SD). The latA treatment did not induce significant changes in the cell migration, which could have potentially affected the sheet centroid movements. When the centroid's distance measurements to the initial centroid position were sub-grouped into categories against the occurrence, the histogram revealed an increased frequency of events in further distances in latA-treated cells compared to controls or TSA-treated cells (I: the graph in Fig.8E).

As a result of actin depolymerization, ER sheets started to fluctuate more, *i.e.,* move in a larger area. We therefore wanted to study if the larger movements were accompanied by greater occurrence of sheet transformations. The actin depolymerization increased the sheet transformations >3-fold as only 14% of the sheets persisted in Huh-7 cells (I). In accordance, the average sheet life time, counted from the first acquired frame, decreased from 53.7 s ± 1.5 sem (control) to 18.4 s ± 2.8 sem in latA-treated cells (I). Similarly, the proportion of persistent sheets decreased after latA treatment (I: 38.0% and; 26.0%, respectively) in HeLa and NRK-52E cells, respectively, increasing the occurrence of sheet transformations in slightly milder manner, by >2-fold. The average sheet lifetime decreased accordingly (I: 35.6 s ± 3.1 sem in HeLa; 32.0 s ± 3.1 sem in NRK-52E). Depolymerization of MTs by nocodazole did not have any effect on sheet persistence (I: Fig.8B). The persistency analysis for HeLa ($n_{control}$ = 81 sheets in 28 cells and n_{latA} = 50 sheets in 24 cells) and NRK-52E ($n_{control}$ = 50 sheets in 17 cells and n_{latA} = 50 sheets in 13 cells) was done as described in I.

This data provides further evidence on the live cell observations that sheets do not move along the actin cytoskeleton as tubules move in conjunction with growing MTs, but rather that sheet repositioning to another area of the cell is likely to occur through new sheet formation, and furthermore, that MTs are mainly involved in ER tubular dynamics but do not have a role in sheet dynamics or persistence. As a conclusion of the dynamics analysis, sheet persistence and the static localization are dependent on the interplay with the actin filament arrays. Together our results provide a mechanistic view on interplay between ER and actin, suggesting that the loss of actin filament arrays from the polygons allow ER sheets to move in a larger area and that the lateral movement is subsequently accompanied by increased sheet transformations. The fenestrated sheets in Huh-7 cells were more susceptible to latA treatment than the less fenestrated or intact sheets in HeLa and NRK-52E, indicating that the relative importance of actin filaments may vary between cell types. Moreover, as the dynamics study was done by using drugs that affect not only the small subset of filaments but more globally the whole cell - and surely cause secondary effects (Hoshikawa *et al.*, 1994) - more precise and focused methods to study the coupling of

actin filament arrays to ER sheets could be beneficial to reveal the mechanism by which actin-ER interplay occurs.

3.2.4 Fenestrated sheets respond to microtubule stabilization and bundling more readily that intact sheets (Unpublished)

As discussed earlier, MTs form the main tracks for tubular sliding. According to our studies, the nocodazole or TSA manipulations of MTs did not affect the lateral movement of the ER sheets, nor the sheet transformations. This does not mean, however, that MTs and ER sheets could not interact in another manner. As shown earlier, we often observed MTs passing through the highly curved membrane areas of sheets, *i.e.,* fenestrations (Figure 5). Interestingly, stabilization and bundling of MTs (Yvon *et al.*, 1999) with 25 nM paclitaxel (PAC) treatment resulted in a striking ER phenotype in Huh-7 cells: extremely long and unbranched ER sheets at the central parts of the cells were observed in LM (Figure 15A and 15B), TEM thin sections (Figure 15C) and SB-EM images (Figure 15D and 15E). This shift of the structural balance towards sheets was, however, restricted to a portion of the ER sheets located at the central parts of the cell and the appearance of peripheral sheets remained unaltered (Figure 15A). The resulting sheet morphology at perinuclear area differed considerably from the control sheets: The long sheets lacked fenestrations in the immediate vicinity of bundled MTs (Figure 15C), although they were directly continuous with sheets that were not in vicinity of the MTs and had typical fenestrated outlook (Figure 15C). In contrast, the MT depolymerization with nocodazole did not affect the fenestrations (data not shown). Based on LM and TEM-analysis in NRK-52E and HeLa cells, similar MT bundling was achieved with 1 µM PAC concentration, which induced straight, albeit shorter, ER profiles reminiscent to those of Huh-7 sheets that were, however, significantly rarer and milder than in Huh-7 cells (data not shown).

Many questions arise from these results. Firstly, why do not all ER sheets respond similarly to the manipulations that affect the whole cell? One possible explanation is the existence of subsets of ER sheets, which would be controlled by specific mechanisms. It is noteworthy that our dynamics analysis was done at the cell lamella and on peripheral sheets, which seem to be resistant to MT-manipulations, and we cannot exclude the possibility of existence of specific ER sheet subdomains. However, based on 3D-EM, actin manipulations had a uniform effect on all ER sheets it the cells. In accordance with the hypothesis of existence of specific sheet and tubule subgroups, it has been shown that tubular ER dynamics occur on distinct MT populations giving specific identity to a portion of ER tubules, and to establish or maintain membrane contacts with different organelles (Friedman *et al.*, 2010). It is therefore possible that similar subgrouping of sheets might exist. Another interesting aspect is the observation that the sheets in different cell types respond at varying levels to MT manipulations. Our results show that stabilization and/or bundling of MTs resulted in strongest phenotype in Huh-7 cells: The most striking effect of MT bundling on ER was the formation of non-fenestrated sheets at the central areas of the cells. This effect was also observed in HeLa and NRK-52E but in milder manner. As MTs interact with tubules that have high membrane curvature, and we often observe MTs passing through sheet

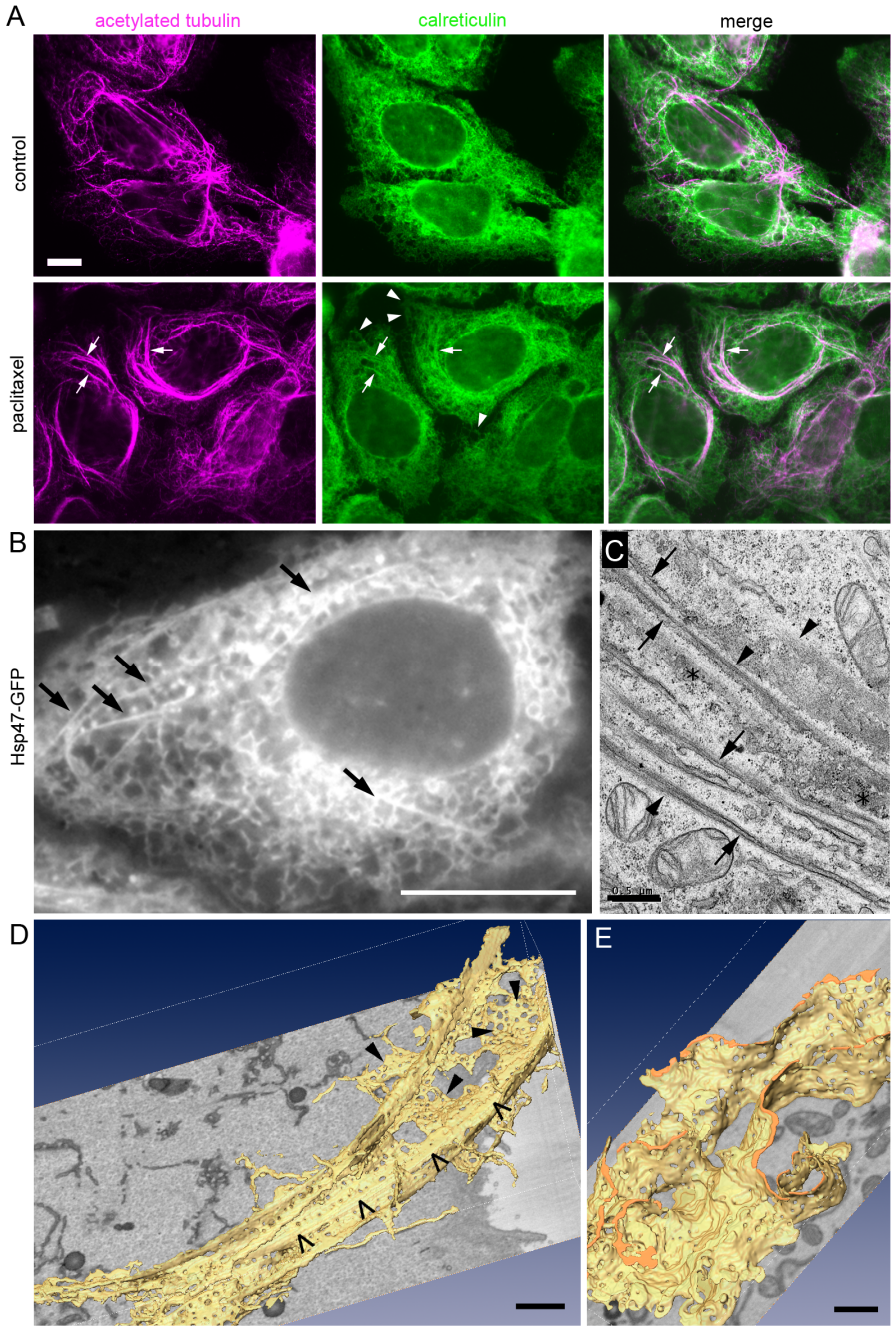

Figure 15. MT stabilization and bundling effects on ER. Wide-field images of fixed (A) control and PAC-treated Huh-7 cells immunolabelled for calreticulin (green) and acetylated tubulin (magenta). PAC-treatment induced MT bundling and long ER sheets (arrows) and the unaltered peripheral ER sheets (arrowheads) are indicated. (B) Wide-field image of live PAC-treated Huh-7/Hsp47-GFP and (C) Huh-7. Long ER profiles (arrows) are mainly observed at central parts of the cell. (C) PAC-induced long, non-perforated, ER sheets (arrows) reside in vicinity of MT bundles (arrowheads) and are directly continuous with fenestrated ER profiles (asterisk). (D) PAC-treated and (E) control Huh-7/ssHPR-KDEL were cytochemically stained and processed for SB-EM modelling. (D) Planar and long ER sheets lack fenestrations from regions in close proximity of MTs (open arrow heads), but are directly connected to the typical fenestrated sheets (arrowheads). Bars are 10 µm (A and B), 0.5 µm (C) and 1.0 µm (D and E). A and C-D in courtesy of Ilya Belevich and Maija Puhka.

fenestrations (Figure 5), it is tempting to speculate that the MTs are somehow connected to the highly curved areas of the Huh-7 sheets, namely the fenestrations or sheet edges. This could explain why Huh-7 sheet respond more readily to PAC treatment than HeLa and NRK-52E. The high membrane curvature could augment the formation of ER tubules that can be pulled out straight from the ER sheets by MT-action. Moreover, this would explain why ER sheets do not respond significantly to nocodazole treatment in any cell types analysed here: MT role on ER sheets would not be to create or maintain the sheet structures. MTs are, however, indirectly connected to ER sheet as they pull out the ER tubules from the sheets. Nocodazole treatment, therefore, leads to loss of ER tubules as they are not able to form without the MT tracks, leaving ER sheets unaffected.

ER tubular sliding have been show to occur on stable MTs (Friedman *et al.*, 2010) and it is possible that PAC-induced stabilization and bundling of MTs could increase the MT-action on ER fenestrations and lead to formation of uncharacteristic straight and non-fenestrated ER profiles. This hypothesis, however, remains to be solved. And finally, although actin cytoskeleton and MTs fulfil many functions independently, they often act in a coordinated manner that is, at least partly, based on direct physical interactions between the filaments (Goode *et al.*, 2000; Hoshikawa *et al.*, 1994). Therefore, we cannot exclude the possibility that by affecting one cytoskeletal system, we would not affect the others.

3.3 Endoplasmic reticulum and actin binding proteins

Eukaryotic cells generate diverse actin filament networks in a common cytoplasm to perform functions such as cell motility and adhesion, endocytosis and cytokinesis. Each of these networks is autonomously controlled by its interacting proteins and the spatial organization which maintain the precise mechanical and dynamic properties of the actin filaments. Actin filaments in cells are not disorganized meshworks, but rather organized assemblies localized in precise areas in the cytoplasm where they can perform their functions in response to different stimuli. Numerous studies have indicate that the properties of the actin networks are specifically adapted for each cellular function, and that these properties are tightly controlled by specific sets of actin-binding proteins (reviewed in Kaksonen *et al.* (2006); Pollard *et al.* (2000); Moseley and Goode (2006); Saarikangas *et al.* (2010)).

3.3.1 Actin-binding protein screen identified several proteins potentially involved in the endoplasmic reticulum - actin cytoskeleton interplay (I; Unpublished)

To gain better understanding of the ER-actin interplay, we performed shRNA-based screen against functional human actin-binding proteins to identify those that would have morphological, temporal, and/or spatial effects on the ER. Huh-7 cells were co-transfected with the Hsp47-GFP plasmid and either pooled shRNAs or empty vector (I). 208 targets in the library were depleted one by one and imaged live using a wide-field microscope to visualize morphological, temporal, and/or spatial changes in the ER. Afterwards, the cells were fixed, stained with phalloidin, and screened for morphological ER and actin cytoskeleton phenotypes. Phenotypes that affected severely the cell shape were omitted. The clones that showed alterations in the ER were ranked in three categories (strong, moderate and mild phenotype) according to depletion effect magnitude, depletion lethality and changes in the ER or NE morphology, or, ER dynamics. In total, 26 targets were scored to the strong phenotype category, including 5 members of the unconventional motor protein myosin I family, whose depletion induced clear changes in ER morphology and/or dynamics (Table 1).

The 26 hits did not present uniform phenotypes and could not be further sub-grouped, indicating that each of these targets would be required to be verified separately. As the depletion of individual myosin I family members induced changes in the ER, we concluded that as a strong indication to focus our studies on myosin I family. As mentioned earlier, in total, eight myosin I genes have

Ensemble	Gene	Description	Lethality % apoptotic	ER dynamics	ER morhology	Structural balance	ER network	NE
ENSG00000082438	*COBLL1*	cordon-bleu WH2 repeat protein-like 1		+		a-	sd	
ENSG00000065618	*COL17A1*	collagen, type XVII, alpha 1		-	cs	s-	nr, p	pn
ENSG00000106328	*FSCN3*	fascin homolog 3	>30%	-				
ENSG00000132139	*GAS2L2*	growth arrest-specific 2 like 2	< 30%		t	t+	p	
ENSG00000130787	*HIP1R*	huntingtin interacting protein 1 related			uc		d	
ENSG00000145012	*LPP*	LIM domain containing preferred translocation partner in lipoma	>30%	-	st		nr	
ENSG00000130224	*LRCH2*	leucine-rich repeats and calponin homology domain containing 2			t			
ENSG00000164877	*MICALL2*	MICAL-like 2			uc		nr	x
ENSG00000105357	*MYH14*	myosin, heavy chain 14, non-muscle				s+	rn	
ENSG00000128641	*MYO1B*	myosin 1B		-	r			
ENSG00000197879	*MYO1C*	myosin 1C	>30%		s, r, ps		nr	x
ENSG00000176658	*MYO1D*	myosin 1D		-	uc	a-	d, p	
ENSG00000157483	*MYO1E*	myosin 1E			cs	t+		
ENSG00000142347	*MYO1F*	myosin 1F	lethal	-	ps	s-	nr, d	x
ENSG00000128833	*MYO5C*	myosin VC	< 30%	-	uc	t+	sd	
ENSG00000133454	*MYO18B*	myosin XVIIIB		-			nr	
ENSG00000183091	*NEB*	nebulin		-			nr	
ENSG00000133789	*SWAP70*	SWAP switching B-cell complex 70kDa subunit		-	ps+, 3-w-	a-	nr	x
ENSG00000130241	*INF2*	inverted formin-2 isoform 1			3-w	3-w	nr	
ENSG00000132613	*MTSS1L*	metastasis suppressor 1-like		-	td+	s+	p	
ENSG00000197893	*NRAP*	nebulin-related anchoring protein		-	td+	t+		
ENSG00000163110	*PDLIM5*	PDZ and LIM domain 5	>30%	uc	r, t			x
ENSG00000156232	*WHAMM*	WAS protein homolog associated with actin, golgi and MTs	>30%	-	s+	s+	d, rn	x
ENSG00000072501	*SMC1A*	structural maintenance of chromosomes 1A	>30%		uc			
ENSG00000125834	*STK35*	serine/threonine kinase 35	>30%	uc	uc		nr	
ENSG00000188459	*WASF4P*	WAS protein family, member 4, pseudogene	< 30%		uc		nr, rn	x

Table 1. The screen for actin-binding proteins involved in ER-actin interplay produced 26 hits. Ensemble codes refer to each target's database identifier. Gene names and the descriptions are retained from Ensemble genome database. The 26 hits were screen based on alteration in ER dynamics, morphology, sheet-tubule balance, network appearance, changes in NE and overall lethality of the depletion. Table key: + increase (+), decrease (-), tubules (t), sheets (s), 3-way junctions (3-w), polygon size (ps), structural diameter (d), reticularity (r), spreading deficiency (sd), retracted network (r), protrusions (p), abundance (a), poly-nucleic cells (pn), network remnants (nr), circular structures (cs), undefined change (uc), changes in the NE (x).

been identified (Berg *et al.*, 2001); however, the used shRNA library contained plasmids for myo1a-1f. While myo1h has been reported to be widely expressed in human tissues, including the liver (according to Human protein atlas; http:// www.proteinatlas. org/ ENSG00000174527/tissue), myo1g expression has been shown to be restricted to hematopoietic tissues and cells (Olety *et al.*, 2010). Myo1a depletion did not cause an ER phenotype, and we focused our further analyses on myo1b-1f. While other hits of the screen have not been further verified, and may contain false positive hits, they present interesting targets for future studies.

3.3.2 Unconventional myosin 1b-1f may have redundant roles (I; Unpublished)

To analyse which of the myosin I genes were expressed in Huh-7 cells, an amplified complementary DNA from total isolated mRNAs of three cell cultures were prepared and pair-end sequenced on the SOLiD (Sequencing by oligonucleotide ligation and detection) platform[2]. The sequencing reads were mapped to human transcriptome, and based on the Cufflinks estimation (Trapnell *et al.*, 2012) of the expression levels, revealed that *myo1a–e* were all expressed in Huh-7 cells, while *myo1f-1h* were not[2]. *Myo1b* expression was >10-fold higher than *myo1a, c,*

[2]Olli Rämö, Institute of Biotechnology, University of Helsinki. Personal communication of unpublished data. Expression profiling of Huh-7 cells was done as collaboration with the Kui Qian and Petri Auvinen, DNA Sequencing and Genomics Laboratory, University of Helsinki.

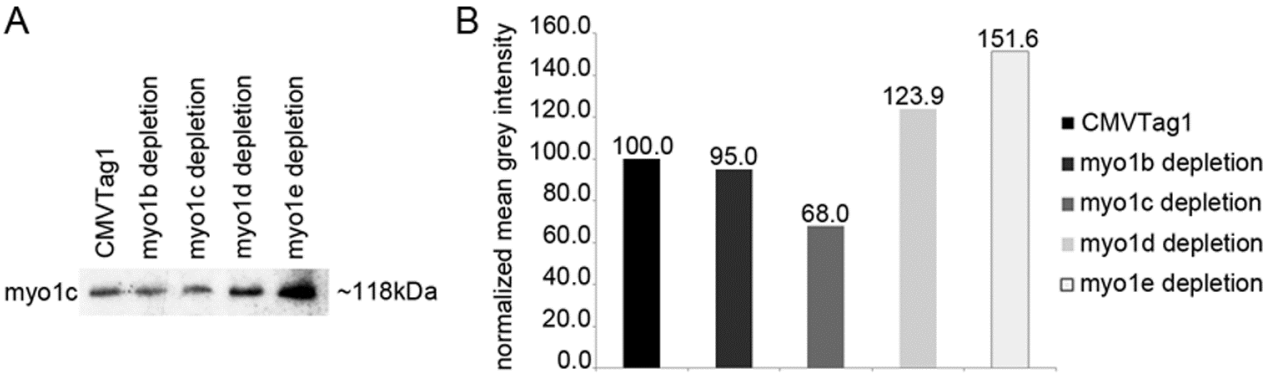

Figure 16. Myo1c depletion. Huh-7 cells were transfected with CMVTag1 or three pooled myo1b, myo1c, myo1d or myo1e shRNAs (myo1b-1e depletion). (A) An equal number of cells were lysed and analysed by Western blotting with an antibody against myo1c. (B) The mean grey intensity of the myo1c of the bands were measured and normalized to CMVTag1.

d or *e*[2]. The expression level of *myo1c*, *1d* and *1e* were roughly equal[2]. A previously published RT-PCR analysis have shown that *myo1b*, in conjunction with *myo1c* and *myo1e*, were prominently expressed in rodent auditory and vestibular epithelia, while *myo1a*, *myo1d* and *myo1f-1h* were less readily amplified (Dumont *et al.*, 2002). The observed myo1f depletion phenotype in the screen must have resulted from off-target effects of the used shRNAs. Indeed, BLAST (The Basic Local Alignment Search Tool) sequence analysis revealed that the used myo1f shRNAs did not uniquely target myo1f (data not shown). Together these results indicated that myo1b might have a more general role in the cells, and in accordance, myo1b have been shown to be involved in cellular movement (Novak and Titus, 1997). Based on the expression profiling, and the observations that myo1f depletion was to some extent lethal to the cells, we focused our further studies on myo1b-1e, omitting myo1f.

The myo1b-1e depletion induced ER-phenotypes were studied further and in more detail in Huh-7 and HeLa cells, by using wide-field LM for live and fixed cells, live cell confocal imaging, and EM: Analysis showed varying effects on the ER and NE morphology, and ER network distribution and dynamics, upon individual depletions (LM results summarized in Table 1; EM data not shown). Myo1b depletion decreased ER tubular dynamics and caused changes in the reticular appearance of the ER network. Myo1c depletion was, to some extent, lethal (>30% of the cells apoptotic) and induced changes in the reticular appearance of the ER network, in the size of the polygons, and in the morphology of the sheets and NE. Myo1d depletion decreased ER dynamics and the abundance of the network. It also affected the diameter of ER structures and induced formation of ER protrusions. Myo1e depletion induced circular ER structures and shifted the structural balance towards tubules, *i.e.,* led to loss of ER sheets. Comparison of the myo1b-1e depletion phenotypes in the Huh-7 and HeLa cells indicated that the myo1c depletion induced most consistent and clear ER-phenotype, whereas the myo1b, 1d and 1e depletion exhibited some variance and incoherent ER-phenotypes in HeLa compared to Huh-7. Interestingly, based on phalloidin staining, the depletion of myo1c induced

changes in the actin filament arrays, while similar and simultaneous changes in the ER and actin were not observed upon myo1b, 1d or 1e depletion. Importantly, while the shRNA library contained most of the known myosins, clear changes in the ER in conjunction with the actin filament arrays were only observed upon myo1c depletion.

Based on the comparison of the myo1b-1e depletions between the two cell types, detailed morphological analysis and the effects on the actin cytoskeleton, we chose to concentrate our studies on myo1c, as its depletion gave the most consistent and clear ER and actin filament array phenotype. However, we cannot exclude the possible cooperational roles of myo1b-1e. Interestingly, the depletion of myo1d and 1e led to an increase in the amount of myo1c, indicating an existence of functional redundancy between the family members (Figure 16A and 16B). Myo1c has been previously reported to be involved in the actin cytoskeleton dynamics and membrane protein anchoring in B lymphocytes (Maravillas-Montero *et al.*, 2011) and to have a role in multiple signalling pathways (Bond *et al.*, 2013). In addition, it has been shown that myo1 and actin filaments provide mechanical stability to microvillar ER, however, it is unclear which of the myosin I family members was studied (Pollard *et al.*, 1991). Myo1c has been suggested to link the actin cytoskeleton to cellular membranes (Novak *et al.*, 1995) and to localize to actin-rich sites of membrane ruffling and retraction at the cell periphery and to discrete punctate within the cytoplasm (Hokanson *et al.*, 2006; Ruppert *et al.*, 1995; Wagner *et al.*, 1992; Wagner and Molitoris, 1997), and therefore, myo1c was a good candidate for our further studies.

3.3.3 Subcellular localization of myosin 1c at endoplasmic reticulum and plasma membrane is revealed by immuno-EM (Unpublished)

To study the myo1c localization in relation to ER and the whole cell, we next prepared pre-embedding immuno-EM samples of Huh-7. Due to lack of specific antibodies against myosin 1c, the studies on endogenous myo1c were not possible. We, therefore, studied the localization of myo1c in Huh-7 cells transiently expressing myo1c-2FLAG that were pre-embedding immunolabeled against FLAG-tag. As the fusion protein over-expression can yield expansion and deformation of membranes (Ellenberg *et al.*, 1997; Ma *et al.*, 2007; Snapp *et al.*, 2003), we chose the cells carefully and omitted cells with very high gold-labelling or cross changes in the membranes.

Gold-labelling in the TEM images revealed that myo1c fusion protein localized under the PM and to a lesser extent to the ER membranes, but not to the Golgi complex, mitochondria or nucleus. Some labelling was also detected at lipid body membranes (data not shown) and as a diffuse staining in the cytosol (Figure 17A-D). These results are in accordance with previous immunoreactivity studies which have demonstrated that Myr2, the myo1c in rats, associates with fractions enriched with PM and ER, but not with Golgi or mitochondrial fractions (Ruppert *et al.*, 1995). Cells that had not been transfected with the construct had only little or no gold signal, verifying the antibody specificity. The labelling on the ER resided often at the edges of the sheets, but also on the flat parts of the ER sheets on perpendicularly cut membranes. Based on the immunolabelling, myo1c might localize to the polygonal membrane areas of the ER. In agreement, based on live cell

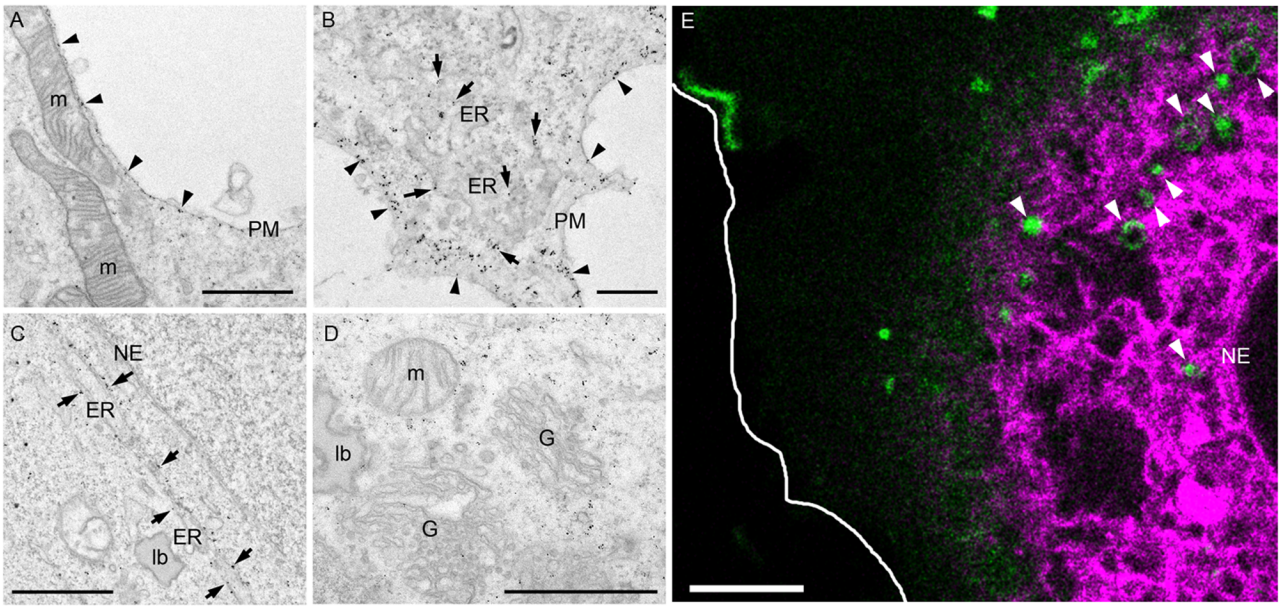

Figure 17. Myo1c localization in Huh-7 cells. (A-D) Thin section TEM images of cells transiently expressing myo1c-2FLAG and pre-embedding immunolabeled against FLAG-tag with nano-gold secondary antibody that was silver enhanced. Silver enhanced nano-gold-labelling of myo1c was observed (A) localizing under the PM (arrowheads) and (B and C) in the ER (arrows), but not in (C) the NE or nucleus, (D) Golgi complex (G) or mitochondria (m). Lipid bodies (lb) are indicated. Diffuse staining in the cytosol is evident in (D). (E) Live cell confocal optical section of Huh-7 cell co-expressing Hsp47-mCherry (magenta) and myo1c-EGFP (green) taken from the middle part of the cell. Outline of the cell and NE are indicated for clarity. The localization of the myo1c-EGFP signal at the ER-polygons are indicated by arrowheads. Bars 1 µm (in A-D) and 5 µm (in E).

confocal imaging of Huh-7 cell co-expressing Hsp47-mCherry and myo1c-EGFP, myo1c fusion protein localized to the ER polygons (Figure 17E). We cannot, however, draw strong conclusions from these studies based on not being able to detect the endogenous myo1c, because of the free cytosolic pool of myo1c that can be challenging to distinguish from background labelling, and, finally, because the interpretation of 2D TEM-images always present a level of uncertainty when studying 3D-structures.

3.3.3.1 Mutation in the myosin 1c pleckstrin-homology domain results in mislocalization of the protein (Unpublished)

Myo1c and Myr2 have been shown to bind with high affinity to PIP_2 (Barylko *et al.*, 2005; Hokanson *et al.*, 2006) and localization of the motor protein has been suggested to be solely dependent on its specific binding to PIP_2 via its PH-domain (Hirono *et al.*, 2004; Hokanson *et al.*, 2006; Hokanson and Ostap, 2006). To test if myo1c lipid-binding contributes to the localization of the motor protein, we created a myo1c construct that has a defective lipid-binding ability. It was previously shown that a bacterially expressed myo1c tail domain residues 820–1025 are liable for the myo1c lipid-binding (Hokanson *et al.*, 2006; Reizes *et al.*, 1994) and, therefore, the 892 Lysine (K) residue was replaced by Alanine (A) by mutagenesis to create myo1c-K892A-EGFP construct[3]. Based on wide-field LM of fixed Huh-7 cells, the localization of the myo1c-K892A-EGFP differed from the localization of the FLAG-tagged myo1c construct (I: Fig.4A for myo1c-2FLAG; Figure 18A): myo1c-K892A-EGFP accumulated to the

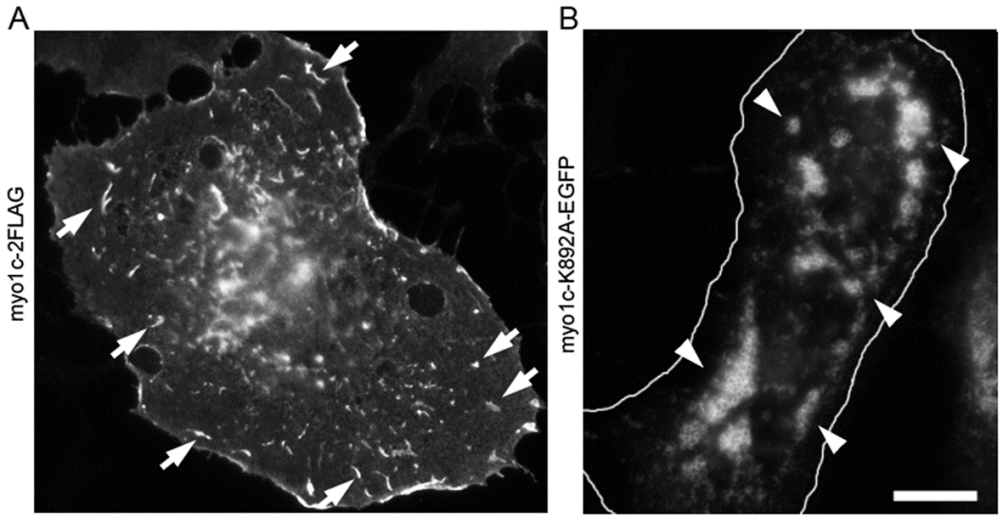

Figure 18. K892A substitution in the myo1c PH-domain resulted in mislocalization of the protein. Wide-field images of fixed Huh-7 cells that were transfected with (A) myo1c-2FLAG and immunostained for FLAG (punctate localization indicated with arrows), or with (B) myo1c-K892A-EGFP (arrowheads; cell outlined for clarity). Bar 10 µm apply to both images.

perinuclear area and to punctate structures throughout the cytosol, which most likely present protein aggregates (Figure 18B). Similar results were acquired with live cell confocal imaging (data not shown). These results agree with the previous findings that the 820–1025 tail domain is liable for the lipid binding and the correct localization of the protein. In addition, our results were in agreement with previous results suggesting that myo1c localization in the cells depends on its binding to PIP_2 via the PH-domain, (Hokanson *et al.*, 2006), and as the PIP_2 has been shown to localize also to ER (Watt *et al.*, 2002), in conjunction to PM, this binding may localize myo1c to the ER-actin filament array interphase.

3.3.4 Myosin 1c shows preference to dynamic actin filament arrays (I; Unpublished)

Based on the genetic screen, the depletion of myo1c induced changes in the actin filament arrays, indicating that myo1c might have a role on regulating the ER-polygon localizing actin filament arrays. We therefore set forth to study the role of myo1c on the actin arrays by first studying the localization of myo1c in respect to actin. Based on LM imaging, myo1c localized to the short actin filament arrays and foci throughout the cytoplasm (I: Fig.4). In addition, a diffuse staining throughout the cytoplasm was observed. Quantification of the actin filament arrays and foci revealed that 97% ± 6.4 (SD) of the short actin filament arrays were positive for myo1c (I).

Our LM-studies and immuno-EM results indicated that myo1c localize to the interphase between ER and the actin filament arrays at the network polygons throughout the cell volume (I: Fig.S3 and Fig.3A). These results are in accordance with previous studies showing that Myr2 and myo1c localize to punctate structures throughout the cell, to regions with elevated f-actin at cell periphery, and as diffuse staining at cytoplasm (Bose *et al.*, 2004; Ruppert *et al.*, 1995). The most likely reason why myo1c labelling on actin filaments was not observed in immuno-EM is the poor preservation of actin filaments during EM-sample preparation. Therefore, actin filaments cannot be reliably studied with

[3]A gift from Ilya Nevzorov and Maria K. Vartiainen, Institute of Biotechnology, University of Helsinki.

conventional EM. However, myo1c fusion protein localized to the ER-polygons, where actin filament arrays would be expected to reside. As myo1c has been shown to be able to bind simultaneously lipid membranes and actin filaments (Barylko *et al.*, 2005; Berg *et al.*, 2001), our observations suggested that myo1c either mediates the interaction between ER and actin, it recruits the actin to the ER-membranes, and/or it has a role on the creation and/or maintenance of the actin filament arrays.

3.3.5 Myosin 1c creates and/or maintains the short actin filament arrays (I; Unpublished)

To characterize the myo1c-positive actin arrays further, we co-transfected Huh-7 cells with myo1c-EGFP and mCherry-Actin and imaged the cells live focusing to the cell lamella. Confocal imaging demonstrated that myo1c-positive actin filament arrays were alternating between dynamic and static stages and that myo1c moved in conjunction with both dynamic and static actin foci (I: Fig.4B and Video S6). The appearance of myo1c-actin filaments changed substantially over time: the actin foci were observed to transform into actin filament arrays and *vice versa*, and to form plate-like actin structures, and to undergo fusion and fission with other actin filaments and foci (I: Video S6). While the actin filament arrays and foci appearances were dynamic (*i.e.,* their structure was constantly changing), the structures seemed only to fluctuate in small area rather than having a directional movement.

We next studied the functional role of myo1c on actin filament arrays. Based on wide-field LM, over-expression of myo1c in Huh-7 cells led to curved, bundled and unorganized actin filament arrays compared to punctate or rather straight actin filament arrays in control cells (I: Fig.5A and 5B). Moreover, there was a clear decrease in the number of actin foci and an induction in the number of actin filament arrays, suggesting that myo1c has a role in inducing the formation of actin filament arrays from the actin foci. The over-expression of myo1c seemed to induce formation of actin filament arrays in the expense of disappearance of actin foci (I: Fig.5B). The depletion of myo1c, on the other hand, abolished actin filament arrays and only actin foci were observed (I: Fig.5C and 6C). Together, these results provide further evidence that actin arrays and foci present same structures in different stages of polymerization and indicate that myo1c is required for formation of the actin filament arrays. In agreement, myo1c has been previously reported to be involved in the actin cytoskeleton dynamics (Maravillas-Montero *et al.*, 2011) and, moreover, some of the fission yeast *Schizosaccharomyces pombe* class I myosins have also been shown to stimulate actin filament nucleation via binding to Arp2/3 complex (Lee *et al.*, 2000), which plays a major role in the regulation of actin filament by stimulating actin polymerization and branching.

To study the myo1c role on actin filament arrays in more detail, we created a GFP-tagged mutant myo1c construct with abolished actin binding (EGFP-myo1cΔABL) (see *e.g.,* Sasaki *et al.* (1999) aiming to saturate the supposed myo1c binding sites in ER with dominant-negative expression of the fusion protein, and thus disrupting the proposed ER-actin link. While wt myo1c localized under the PM and to distinct foci at

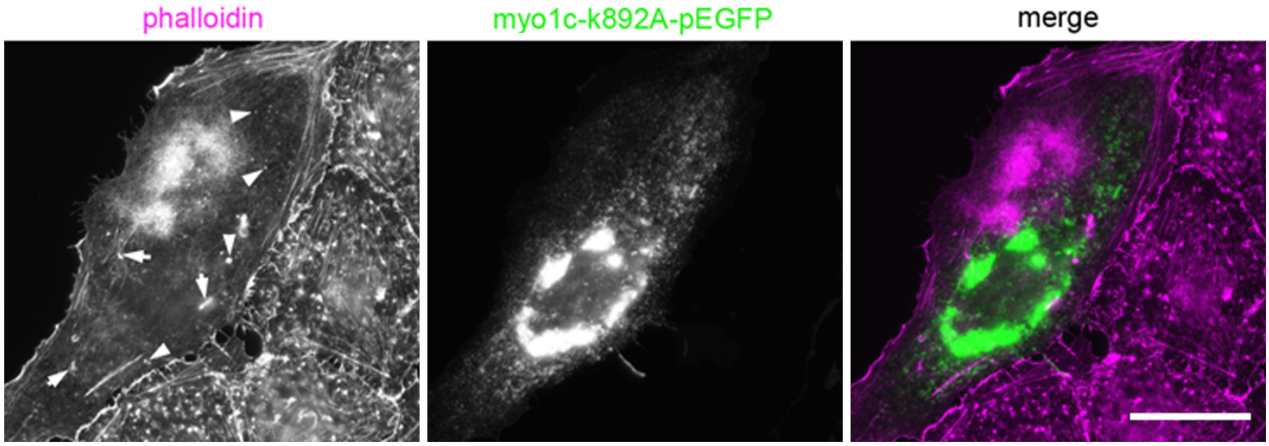

Figure 19. Dominant-negative expression of myo1c-K892A-EGFP led to loss of actin filament arrays. Wide-field image of fixed Huh-7 expressing myo1c-K892A-EGFP (green) and stained with phalloidin-568 (magenta). The expression of the fusion protein results in actin foci (arrowheads) and to loss of actin filament arrays (arrows) that can be seen in the phalloidin-staining in cells negative for the construct (right corner). An atypical accumulation of actin in the central part of the cell can also be seen in the cell expressing the fusion protein. Bar 10 µm.

the cytoplasm (I: Fig.4A), the EGFP-myo1cΔABL was observed as bright spots, likely protein aggregates, mostly at the perinuclear area and as a diffuse signal throughout the cytoplasm (I: inset a in Fig.5D). These results were in contrast to previous studies by us and others (Hokanson *et al.*, 2006), showing that myo1c localization is solely dependent on its PH-domain: Based on our observations, mutations in either lipid- or actin-binding domain of myo1c led to mislocalization of the protein. The two mutant fusion proteins showed slightly different localization patterns, and furthermore, based on confocal live cell imaging, the cytoplasmic aggregates of lipid-binding mutant were highly motile compared to the actin-binding mutant (Figure 18A, Video not shown), indicating that the mutation in myo1c-K892A-EGFP did not affect the motor function of the myo1c or high affinity binding to preferably PIP_2 immobilizes the wt myo1c to the ER (or PM) restricting its movement. We next studied the effects of dominant-negative expression of these mutant fusion proteins in relation to actin. Remarkably, both EGFP-myo1cΔABL (I: Fig.5D and Fig.S2I for expression in HeLa) and myo1c-K892A-EGFP expression resulted in the loss of actin filament arrays (Figure 19): only bright actin foci could be observed instead of arrays of actin filaments (I: Fig.5D), resembling latA-treated (I: Fig.1C) and myo1c-depleted (I: Fig.5C) cells. Together these data indicated that both actin- and lipid-binding of myo1c were essential for the correct localization of myo1c and, moreover, required for the creation/maintenance of the ER-associated actin filament arrays.

3.3.6 The effects of myosin 1c manipulations on actin filament arrays leads to endoplasmic reticulum phenotype (I; Unpublished)

Based on our results, the effects of both latA treatment and myo1c manipulations were targeted on the same specific subset of actin structures, the actin filament arrays. Furthermore, abolishing the actin filament arrays with latA led to ER network distribution

defect, ER sheet-to-tubule transformation and to smaller ER sheet remnants. These results suggested that ER sheet maintenance is coupled to the polygonal actin filament arrays, which are regulated by myo1c. In accordance, having the potential to serve as covalent linkers by physically connecting and generating force between the cellular membranes and actin filaments, the class I myosins have been implicated in the cellular membrane movements, deformation and bending (McConnell and Tyska, 2010; Novak *et al.*, 1995). To test if the myo1c manipulation induced changes in the actin filament arrays resulted in a subsequent ER phenotype, we next studied ER morphology after myo1c manipulations with LM and 3D-EM.

First we studied the effects of myo1c over-expression on ER in fixed Huh-7 and HeLa cells with wide-field microscopy. The over-expression of myo1c-2FLAG saturated the natural binding sites of myo1c and led to a strong accumulation of myo1c signal to the cell periphery and to distinct mass in the cytosol. In contrast, the over-expression of an empty control FLAG-construct (2FLAG-C1) was observed as diffuse staining throughout the cytosol (I: Fig.6A). The myo1c over-expression shifted the ER sheet-tubule ratio towards sheets, with few tubules remaining and, instead of individual sheets, an interlinked sheet mass extending to the cell periphery was observed in both Huh-7 (I: Fig.6A) and HeLa (I: Fig.S2F). In contrast, the expression of 2FLAG-C1 construct alone did not induce changes in the ER (I: Fig.6A and Fig.S2F).

We next examined what happens to ER when myo1c is depleted. Wide-field imaging revealed that myo1c depletion in live Huh-7 cells (I: Fig.6B and 6C) and fixed HeLa cells (I: Fig.S2G) led to a shift towards tubular network with only few degenerated sheets found at the cell periphery. In addition, the peripheral ER network appeared uneven and consisted of uncharacteristically long tubules extending to the periphery. Myo1c depletion with target-specific pooled siRNAs led to a similar morphological ER phenotype (I: Fig.S6A and S6B). The morphological changes induced by myo1c-depletion were even more evident in 3D models obtained from SB-EM datasets: Control Huh-7 sheets were large and heavily fenestrated (I: Fig.2A and Video S1), whereas in myo1c-depleted cells the sheets were smaller, unequally fenestrated and less abundant (I: Fig.6D and Video S7), resembling the actin depolymerization phenotype (I: Fig.2B). The ER network remained continuous. Similar phenotype was observed from SB-EM datasets obtained from myo1c depletion by using pooled siRNAs (I: Fig.S6C). Similarly to the latA results, the 3D-EM results here demonstrated that part of the reticular ER network appearance observed under the wide-field LM resulted from interconnected consumed sheet remnants and tubules, rather than tubules alone.

Morphologically, the myo1c depletion phenotype resembled the ER in latA-treated cells (I:Fig.1A), *i.e.,* similar loss of sheets and induction of uneven network distribution was observed in both treatments, although the magnitude of the change varied. The slight difference between observed ER phenotypes might result from very different time dimensions that were 48h in case of myo1c depletion and 15 min in latA treatment. In general, drug treatments have a more global

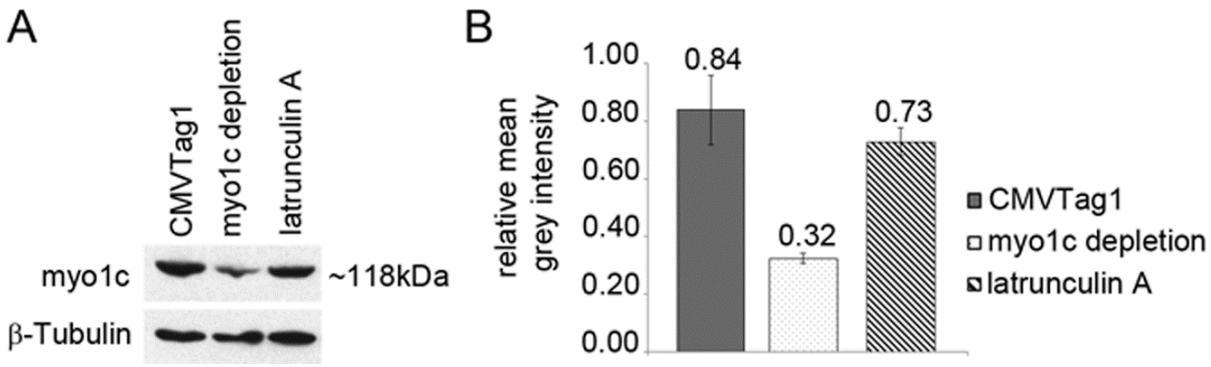

Figure 20. Myo1c depletion. Huh-7 cells were transfected with CMVTag1 (control) or pooled myo1c shRNAs (myo1c depletion), or treated with 1 µM latA for 15min. Cell lysates were analysed by (A) Western blotting with indicated antibodies and (B) the mean grey intensity of the myo1c related to β-Tubulin was measured. The quantitation results present an average of two Western blot analysis and the error bars are presented as ±SD.

effect affecting the whole cell culture uniformly in comparison to protein depletions experiments where the level of depletion changes over the time and varies from cell to cell, and in our experiments lead to an average shRNA-depletion deficiency of 60% (calculated based on 4 individual Western blot analysis) (Figure 20A and 20B). Actin depolymerization did not induce significant changes in the amount of myo1c (Figure 20A).

3.3.6.1 Myosin 1c actin- and lipid-binding domain are required for creation of actin filament arrays supporting the endoplasmic reticulum sheet persistence (I)

Our previous results had shown that the over-expression of EGFP-myo1cΔABL or myo1c-K892A-EGFP abolished the actin filament arrays and therefore, we next wanted to study the effects of dominant-negative expression of these mutant constructs on the ER morphology.

Based on confocal live cell imaging, the over-expression of EGFP-myo1cΔABL led to almost complete structural shift of ER towards reticular network as only few peripheral sheets could be observed (I: Fig.7A). Since RNA interference, *i.e.,* depletion studies with shRNAs and siRNAs, is known to cause unspecific effects, control experiments of the genes' expression reconstitution to rescue the cellular siRNA effects were needed. While the off-target effects of myo1c depletion were addressed by using scrambled siRNA sequences and multiple siRNA constructs with differing targets, we designed rescue experiments using siRNA-resistant wt myo1c (myo1c-EGFP) and mutant myo1c (EGFP-myo1cΔABL) constructs to provide further control for the experimental set-up. In the myo1c-depleted Huh-7 cells (myo1c-siRNA-Cy5), the reintroduction of the wt myo1c by over-expression of myo1c-EGFP fusion protein, led to a strong sheet-like ER phenotype (I: Fig.7B), compared to the tubular phenotype (I: Fig.7B) in the non-rescued cell. However, rather than leading to a typical ER phenotype (I: Fig.1A), the rescued phenotype resembled the sheet-like phenotype of the myo1c over-expressed cells (I: Fig.6A), revealing the sensitivity of control over myo1c level in the cells. In contrast, the expression of EGFP-myo1cΔABL did not

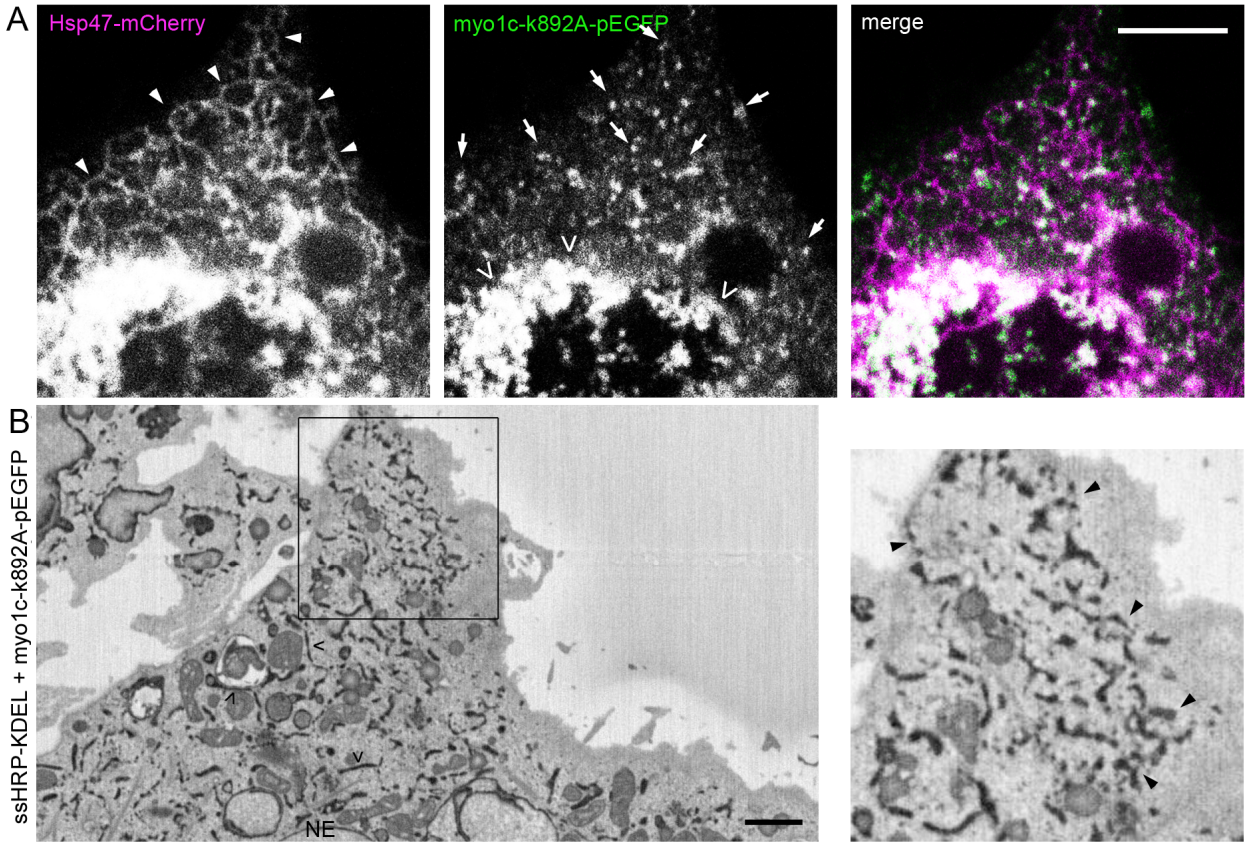

Figure 21. The effects of dominant-negative expression of myo1c lipid-binding mutant on ER. (A) Live cell confocal and (B) block-face SB-EM images of Huh-7 cells co-expressing (A) Hsp47-mCherry (magenta) and (green) or (B) myo1c-k892A-pEGFP and ssHRP-KDEL. (A) Myo1c lipid-binding mutant was observed to accumulate at the cell center (open arrowheads) and throughout the cytoplasm at distinct punctate (arrows). Resulting ER tubules are indicated with arrowheads. (B) Cytochemical staining is seen as a dark precipitate. A representative image and a magnification (on right) of the boxed region are shown. NE, uncharacteristic short ER profiles (arrowheads) and remaining slightly longer ER profiles (open arrowheads) are indicated. Bars 10 µm (A) and 1 µm (B).

rescue the myo1c-depletion induced ER-phenotype, as the ER remained tubular (I: Fig.7C).

To study the effects of dominant-negative expression of myo1c lipid-binding mutant on ER, we co-transfected Huh-7 cells with Hsp47-mCherry and myo1c-K892A-EGFP. Confocal live cell imaging revealed a structural shift of ER towards reticular network as only few peripheral sheets could be observed (Figure 21A), similarly to over-expression of EGFP-myo1cΔABL. These results were further supported by SB-EM analysis done on Huh-7 cells co-expressing ssHRP-KDEL and myo1c-K892A-EGFP, which showed that the loss of actin filament arrays resulted in ER sheets remnants and uneven ER network distribution (Figure 21B). Together these results provide further support on the role of myo1c in maintenance of ER sheet-tubule balance through actin filament arrays.

3.3.7 Synopsis of the dynamic microtubules and actin filament arrays counterbalancing the endoplasmic reticulum sheet-tubule balance

Based on our results, actin cytoskeleton and MT manipulations have opposing effects on ER morphology, indicating that there is a tug-

of-war between actin cytoskeleton and MTs on ER sheet-tubule ratio (Figure 22). MT depolymerization or stabilization by nocodazole or PAC, respectively, shifted the morphological balance towards sheets and resulted in stacked ER sheets or straight, extremely long and less fenestrated ER sheets compared to control sheets. It is noteworthy that while the nocodazole and PAC treatments shifted the ER balance towards sheets, the overall effect on ER was not similar: PAC treatment affected only the ER sheet located at central parts of the cell and the peripherally located ER sheets were not affected. These results suggested of an existence of specific subpopulations of ER sheets. Actin depolymerization or stabilization by latA or jasplakinolide treatment, respectively, shifted the balance towards tubular morphology and resulted in sheet remnants. The chosen drug treatments had opposing effects on MTs and actin - disassembling or stabilizing the filaments. Why, then, the effects of the treatments caused similar effects on the ER sheet-tubule ratio? The most likely explanation is that the

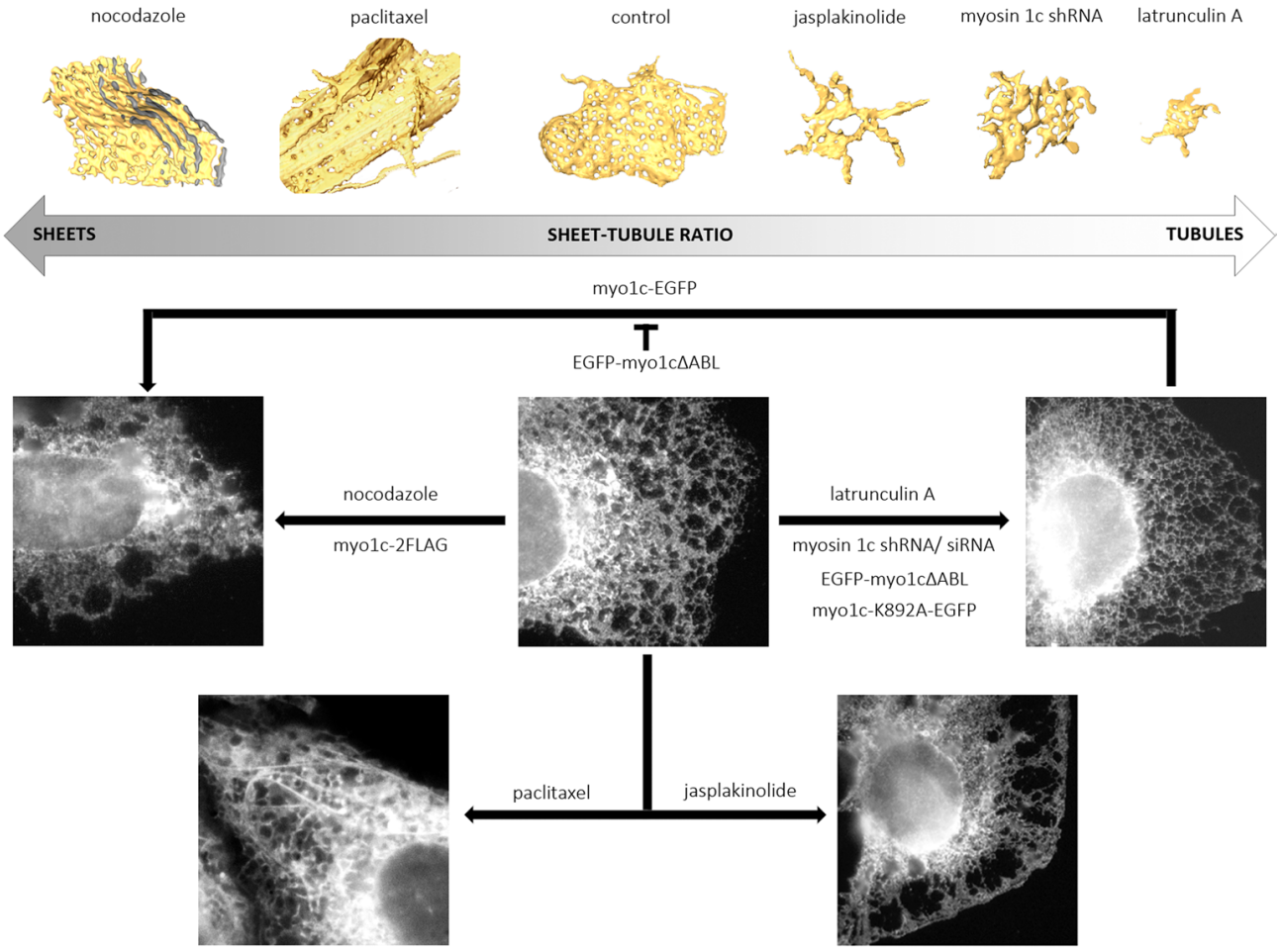

Figure 22. A synopsis of cytoskeletal factors affecting ER sheet-tubule balance. MT depolymerization (nocodazole) or stabilization (paclitaxel) shifted the ER morphology towards sheets and resulted in an induction of sheets or long and less fenestrated straight sheets, respectively (nocodazole and paclitaxel SB-EM models of representative sheets in yellow). Actin depolymerization (latrunculin A) or stabilization (jasplakinolide), or myo1c depletion, shifted the ER balance towards tubules and led to reduced sheet morphology (jasplakinolide, myosin 1c shRNA and latrunculin A SB-EM models of representative sheet in yellow).

regulation of ER sheet-tubule balance requires dynamic cytoskeletal filaments. In accordance, our results showed that myo1c regulates the dynamic actin filament arrays, which in-turn, regulate the ER sheet persistence. Myo1c depletion or dominant-negative expression of myo1c mutants, myo1c-K892A-EGFP or EGFP-myo1cΔABL, shifted the sheet-tubule balance towards tubular morphology and resulted in sheet remnants. Myo1c depletion phenotype could be rescued by over-expressing the wt myo1c (myo1c-EGFP), which shifted the ER sheet-tubule balance towards sheets -resembling the over-expression of wt myo1c (myo1c-2FLAG). The phenotype could not be rescued by over-expressing EGFP-myo1cΔABL.

As the cytoplasm is full of MT- and actin-binding proteins that provide identity to cytoskeletal filaments in response to various intra- and extracellular cues, the interplay between ER subdomains and different cytoskeletal elements provide a variety of regulatory possibilities. In addition to integral membrane proteins that support specific structural features, interaction with the cytoskeleton provides a more global and dynamic mechanism to control the ER architecture in cells. MT-driven tubular ER is suited to host dynamic ER functions and provide a mechanism to rearrange the overall network distribution within the cell. In contrast, more stationary and persistent ER sheets might be more suitable for protein synthesis and quality control or other ER functions. The functional importance of ER network transformations is an important research question for the future.

3.3.8 Towards the connection between endoplasmic reticulum form and function

Actin cytoskeleton functions in the generation and maintenance of cell morphology and polarity, in endocytosis and intracellular trafficking, in contractility, motility and cell division. The assembly and disassembly of actin filaments and their organization into functional networks is regulated by actin-binding proteins (dos Remedios *et al.*, 2003). Actin-binding proteins provide actin filaments specific identity suggesting an involvement of specific subset of actin filaments on specific functions. To study the functional importance of myo1c-regulated actin filament arrays, we studied the effect of myo1c depletion on cellular movement, to receptor and non-receptor–mediated endocytosis and to ER sheet associated functions of protein synthesis and secretion.

3.3.8.1 Actin filament arrays are not involved in cell migration (I; Unpublished)

Our findings indicate that myo1c regulates the formation and/or maintenance of short and dynamic actin filament arrays. Actin filament arrays abolishment was also obtained with latA treatment. As one of our aims was to study the ER dynamics at the cell lamella, we wanted to make sure we were not affecting the actin filaments involved in cell shape regulation or cell migration. Indeed, 15-min 1 µM latA treatment, myo1c depletion or over-expression, or dominant-negative expression of EGFP-myo1cΔABL or myo1c-K892A-pEGFP did not affect the overall shape of the cells as the cells remained flat and attached to the substratum (I: Fig.1C, 2B, 5, 6B, 6D and 7). However, a longer incubation (2 h) and/or higher concentration (5 µM) of latA eventually affected the more stable actin

filaments involved in cell shape regulation and resulted in rounding up (data not shown). Therefore, our next step was to study if the actin filament arrays were involved in cell migration.

To study the cell migration, we carried out wound healing experiments using continuous cell culturing platform with phase contrast imaging. Huh-7 cells were co-transfected with pHsp47-GFP and CMVTag1 or pooled myo1c shRNAs and incubated for 24h. The wound was created on a confluent cell monolayer with a pipette tip and then imaged in 10 min intervals until the wounds had closed (Figure 23A). Our results revealed that, unlike reported earlier in the case of over-expression of Dictyostelium myo1B (Novak and Titus, 1997) or depletion of myo1c (Brandstaetter *et al.*, 2012), myo1c depletion here did not induce changes in the wound healing duration and provided further evidence that myo1c function is limited to a specific subset of actin filaments that are not involved in cell movements (Figure 23B). The contradicting results of ours and those of Brandstaetter *et al.* (2012) might result from differences in the myo1c depletion efficiency. Based on our screen for actin-binding proteins, we observed that the depletion of myo1c in some cells was lethal. This is likely due to complete knockdown of myo1c in these cells, which probably would also cause changes in the cell migration experiments, if similar depletion efficiency was applied in our experiments. Our results indicate that myo1c is indispensable for cellular functions. Supporting our findings, we tested a number

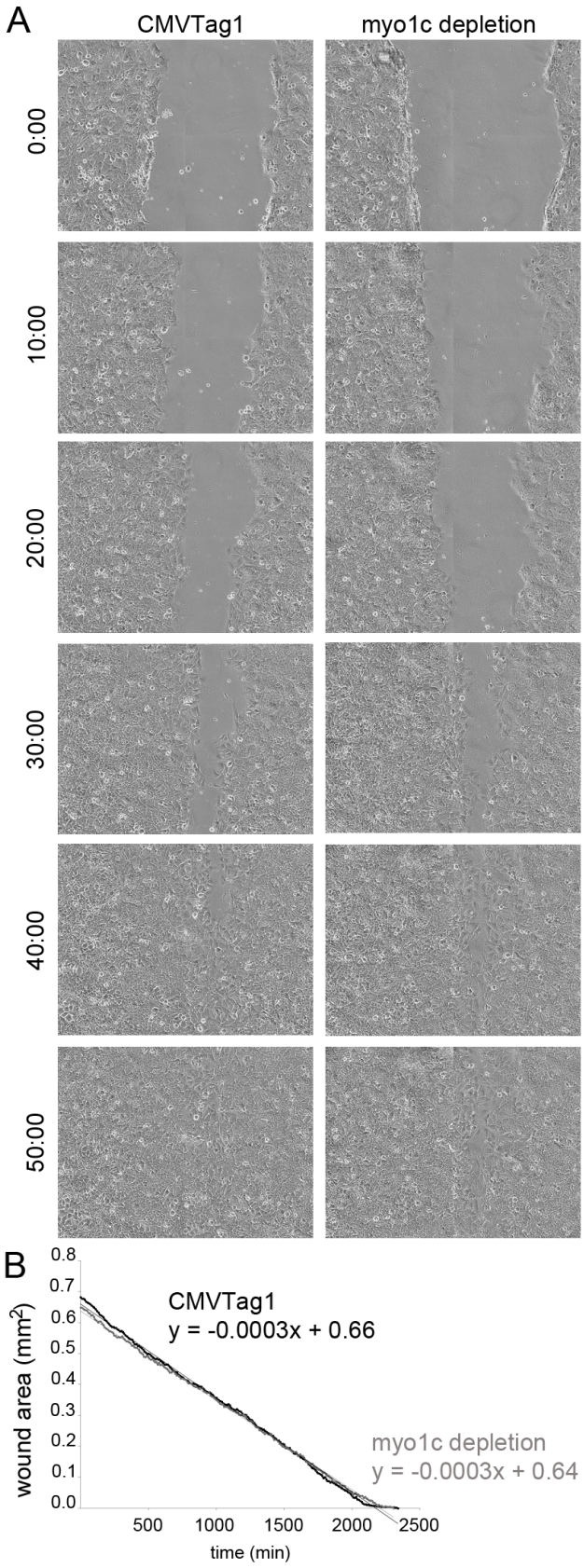

Figure 23. Myo1c depletion does not affect cell migration. (A) Wound-healing assay of Huh-7 transfected with Hsp47-GFP and either CMVTag1 (control) or pooled myo1c shRNAs (myo1c depletion). (B) The wound area (mm^2) is plotted against time (min) and the wound closing equation is shown for control and myo1c depletion. Equations present an average of four independent assays.

of actin-binding proteins known to localize to actin filaments involved in regulating the cell shape or migration. The following stress fiber-associated proteins did not show preference to actin filament arrays based on immunolabelling of the endogenous proteins (I): MHCIIA and B (Vallenius, 2013), α-actinin1 (Lazarides and Burridge, 1975) or calponin (Strasser *et al.*, 1993). Furthermore, proteins associated with actin anchorage to PM, vinculin (Hazan *et al.*, 1997) and moesin 1 (Gautreau *et al.*, 2000), did not localize to the actin filament arrays.

3.3.8.2 Myosin 1c and cortactin decorate the same actin structures but have diverging cellular roles (I)

Using immunofluorescence, we discovered that cortactin showed a clear preference to the actin filaments arrays: 94% ± 3.8 (SD) of short actin filament arrays and foci were positive for cortactin (I: Fig.S4A). In addition, immunolabelling of cortactin in respect to myo1c revealed that the proteins clearly decorate the same actin structures, but by nonidentical patterns (I: Fig.S4B). Cortactin has been shown to be involved in both receptor (Cao *et al.*, 2003) and non-receptor –mediated (Kelley and Weed, 2012) endocytosis. To compare the efficiency of receptor and non-receptor–mediated endocytosis in controls and myo1c-depleted Huh-7 cells, we measured the uptake of Transferrin Alexa Fluor 647 and Dextran Alexa Fluor 594, respectively (I: Fig.S5B-E). In contrast to recently published results in Xenopus eggs where XIMyo1c was shown to mediate compensatory endocytosis (Sokac *et al.*, 2006), our results showed that myo1c depletion and the resulting alterations in the actin filament arrays in Huh-7 cells did not induce relevant changes in receptor or non-receptor mediated endocytosis. Furthermore, immunolabelling of caveolin, involved in receptor independent endocytosis (Pelkmans and Helenius, 2002), did not show preference to the actin filament arrays. In agreement, upon dominant-negative expression of EGFP-myo1cΔABL resulting in the loss of actin filament arrays, cortactin abided localized to the remaining actin foci (I: Fig.S5A), suggesting that myo1c manipulations did not affect cortactin.

Together these results indicate that while myo1c partly localize under the PM and to structures involved in endocytosis, myo1c is most likely not involved in the endocytosis, and that the main function of myo1c is to create and/or maintain the actin filament arrays. In agreement, while the type-I myosins, Myo3 and Myo5, have been shown to be involved in the receptor-mediated endocytosis in *S. cerevisiae* (Geli and Riezman, 1996), similar role for type-I myosins in the vesicle-budding step in mammalian cells has not been demonstrated.

3.3.8.3 Structural changes in sheets induced by actin filament array manipulations do not impair protein synthesis or secretion rates (I)

Our earlier findings showed that latA treatment and myo1c depletion led to a shift towards tubular ER network and resulted in formation of ER sheet remnants. This lead to a speculation if the changes observed in the ER sheets would correlate with changes in functions assigned to sheets, *i.e.,* protein synthesis or secretion. To test this hypothesis we performed [^{35}S] methionine/cysteine metabolic labelling of proteins in control, myo1c-depleted and latA-treated Huh-7 cells.

Surprisingly, the two consecutive experiments of 20 min labelling and 1 or 4 hours chase did not show any significant difference in protein synthesis and secretion rates between control, myo1c-depleted or latA-treated cells (I: Fig.S7).

Although the metabolic labelling experiments were technically successful, the hypothesis cannot be confirmed nor excluded at this point. Few possible explanations emerge. Firstly, the time points for the chase were chosen based on the literature and along expert´s recommendations, and although significant changes on protein synthesis or secretion level were not detected, we might have simply missed the correct time frame. Secondly, although it is commonly accepted that the ribosome studded ER sheets are the main site for proteins synthesis as the ribosomes mark the on-going protein translation and the association with translocon complex and luminal protein machinery, ribosomes are also found on ER tubules. Indeed, based on our ribosome quantitation of HPF/FS thin section TEM images of Huh-7 and NRK-52E cells, the ribosomal density on ER sheets was 60% and 80% higher than the ribosomal density on tubules, respectively (II), indicating that a portion of the proteins translation occurs in ER tubules. As cells can modulate to various conditions, it is possible that the translation in the tubular ER might adapt to the loss of the sheets and rescue the protein synthesis rates. On the other hand, as we cannot observe changes in the protein synthesis or secretion rates under the chosen conditions, we can also speculate that the protein translation and secretion are not the primary tasks assigned only for ER sheets or that the ER sheet morphology and protein production are not dependent. If the changes in the ER sheet morphology after latA treatment or myo1c manipulations correlate with changes in the ribosomal density on the sheets remains to be studied.

3.3.9 Hypothetical model for endoplasmic reticulum - actin filament array interplay

Together our results indicate that both actin- and lipid-binding domain of myo1c are essential for the correct localization of myo1c and both domains are required for the creation/maintenance of the actin filament arrays, and the subsequent persistence of ER sheets. What could be the mechanism behind these observations? It has been suggested that the myo1c-PIP_2 interaction may serve to recruit and concentrate myo1c at regions of new actin polymerization driving actin-membrane interactions and/or actin/ membrane remodelling (Bose *et al.*, 2004; Diefenbach *et al.*, 2002; Holt *et al.*, 2002). In accordance, our live cell confocal imaging and immuno-EM studies suggested that myo1c localized to the ER membranes and actin filaments arrays. Consistent with this proposal: PIP_2 has been shown to facilitate actin polymerization in mammalian cells (Sechi and Wehland, 2000; Yin and Janmey, 2003); The class I myosins have been shown to contribute to actin filament nucleation in yeast (Lee *et al.*, 2000); And, myo1c binding to Neph1, which is a determinant of glomerular permeability in the visceral epithelial cells found at the Bowman's capsule in the kidneys, has been shown to be required for the proper localization of the Neph1 and subsequent activation of Arp2/3 to induce actin polymerization (Arif *et al.*, 2011; Garg *et al.*, 2007). As phosphatidyl inositols, including PIP_2, have been shown to localize to ER

(Griffiths *et al.*, 1989; Watt *et al.*, 2002; Zambrano *et al.*, 1975), it could be envisioned that PIP_2 at ER recruits myo1c to ER polygons, and that this interaction, maybe together with other factors, facilitates polymerization of the actin filament arrays. This hypothesis could explain why the incorrect association of the myo1c with PIP_2, and/or other factors, impairs the function of the motor protein on creating/maintaining the actin filament arrays, and furthermore, it explains why the saturation of myo1c mutant defective of actin binding, led to the loss of actin filament arrays. The subsequent effects of loss of actin filament arrays were observed as substantial changes in the ER sheet morphology and network organization. Similar ER phenotypes were obtained by actin depolymerization and other manipulations of myo1c. Supporting our model, myosin I has been shown to bind only dynamic actin filament population and not tropomyosin-stabilized microfilaments (Tang and Ostap, 2001), which is in agreement to the proposed role for myo1c in creating/maintaining the dynamic actin filament arrays. In accordance, based on our immunolabelling experiment, tropomyosin did not show preference to the actin filament arrays (I).

To summarize, our results indicate that ER sheet persistence in mammalian cells is coupled to actin filament arrays that localize to the polygons defined by the surrounding ER structures. These dynamic actin filament arrays are regulated by myo1c, which serves not only to create and/or maintain the actin filament arrays, but to concentrate actin polymerization to areas enriched with PIP_2, and possibly with other actin interacting proteins, providing a mechanism for recruitment of dynamic actin to ER to drive membrane-remodelling and facilitate ER sheet persistence and transformations. The actual mechanism for ER-actin interplay, however, remains open; while myo1c serves to localize actin filaments to the vicinity of ER, these filament arrays might form passive physical restriction barriers within the ER network or yet unidentified factors could be needed to mediate the interaction between ER and actin filaments.

Our model would provide a multitude of possibilities for regulation. Myo1c has 2-step working stroke defined by characteristically slow ATPase cycle compared to other myosins (Pyrpassopoulos *et al.*, 2012): fast ATP binding and the slow conformational change required for releasing the ATP hydrolysis product ADP. This ATP-cycle is linked to myo1c attachment and detachment from actin filaments: The affinity of myo1c for actin increases when ATP is hydrolysed to ADP and phosphate (P_i), and the release of P_i attach myo1c to actin filament. In the absence of free Ca^{2+} and upon tension, myo1c can stay in the ADP-bound state and associated with actin for extended periods of time (Batters *et al.*, 2004; Gillespie and Cyr, 2004; McConnell and Tyska, 2010; Ruppert *et al.*, 1995). Myo1c is therefore well adapted for maintaining and sense tension without constant dissociation and association from and with actin (Gillespie and Cyr 2004). Interestingly, prolonged ATP depletion in HeLa cells have been shown to cause a large-scale ER tubulation and lead to loss of ER sheets (Lingwood *et al.*, 2009), making it tempting to speculate if the ATP depletion impairs the myo1c function on actin filament arrays, and therefore leads to loss of ER sheets. Furthermore, myo1c binding is calmodulin- and $[Ca^{2+}]$ -dependent: Myo1c is recruited to lipid rafts in the presence of

physiological range 1-10 µM [Ca^{2+}], which releases the bound calmodulin and exposes the PIP_2-binding site (Zhu *et al.*, 1996). PIP_2, in turn, can be hydrolyzed to generate two secondary messengers: inositol 1,4,5-triphosphate (IP_3) and diacylglycerol (DAG) (Yin and Janmey, 2003). Interestingly, the IP_3 receptor (IP_3R) is highly concentrated in ER and the binding of IP_3 to its receptor causes Ca^{2+} release from ER (Nucifora *et al.*, 1996). The elevated [Ca^{2+}], on the other hand, has been shown to release the bound calmodulins from myo1c and lead to detachment of myo1c from actin filaments (Barylko *et al.*, 1992; Zhu *et al.*, 1996). Based on a recent study using correlative LM and EM, and 3D-reconstruction, DAG depletion results in failure of the NE to reform at the end of mitosis and leads to ER reorganization into multi-lamellar sheets in mammalian and echinoderm cells (Domart *et al.*, 2012), indicating that both of the secondary messengers could potentially regulate the ER structure.

VIII CONCLUDING REMARKS AND PERSPECTIVES

By using biochemical and cell biological approaches in combination with live cell imaging, EM and 3D-EM, we show that ER exhibits a great variation in its interphase organization and morphology (I; II; III) and in the mitotic progression (II; III). While the functional role of sheet fenestrations remains unclear, their suggested role as a cytosolic passage sites could be addressed with diffusion studies by computerized methods (Novak *et al.*, 2009). Another interesting aspect would be to study systematically the possible preference of MTs to fenestrations and actin filament arrays to polygons.

Our results demonstrate that the ER sheet morphology is connected to ribosome-density of the membranes (II; III) and to dynamic actin filament arrays (I), although these two phenomena have not been connected. Interestingly, free ribosomes, but not polysomes attached to ER, have been shown to associate with cytoplasmic actin (Toh *et al.*, 1980). It is tempting to speculate if actin would be involved in the delivery of ribosomes to the ER, subsequently affecting the ER structure. In accordance, actin depolymerization in mammalian cells have been shown to lead to stripping of the membrane-bound polysomes (Ramaekers *et al.*, 1983). Based on our results, both natural and drug-induced stripping of the ribosomes, as well as, natural relocation of actin filament arrays and the actin and myo1c manipulations lead to similar effects on ER sheets. Interestingly, it has been suggested that MTs play a role in segregating SER and RER (Nikonov *et al.*, 2007), and therefore ER tubules and sheets, and it could be envisioned that the niche for actin filaments on ER could involve the ribosomes. This hypothesis, however, remains to be studied, and could be firstly addressed by studying the ribosomal fate upon actin and myo1c manipulations.

Our genomic screen identified myo1c localizing to the ER associated actin filament arrays, and revealed a novel role for the motor protein in the actin filament array regulation (I). Myo1c function, thus, supports the maintenance of sheets as a stationary subdomain of the dynamic ER network. While we were not able to link the sheet structural changes to the functions assigned to the subdomain, the structure must serve a specific function. More systematic approach would be needed to study the significance of the sheet persistency to ER functions.

Collectively, our work describes the dynamic rearrangements of ER in mitosis and interphase cells and provides novel information about the role of ribosomes and actin on ER sheets and the role of myosin 1c on ER-associated actin arrays, serving as an opening for further studies on the regulation of the interplay between ER sheets and ribosomes and/or actin. To our knowledge, this work is the first systematic study on ER sheet dynamics in cultured mammalian cells. Importantly, our work also provides evidence on the significant plasticity of ER morphology and organization in different commonly used cell culture cells in interphase cells and upon inheritance of ER.

IX ACKNOWLEDGEMENTS

This work was carried out in the Institute of Biotechnology, University of Helsinki from 2008 to 2014. I would like to thank the former and present directors of the Institute of Biotechnology, Professors Mart Saarma and Tomi Mäkelä, for providing such high standard working facilities and equipment. The study was financially supported by Viikki Graduate School in Biomolecular Sciences (VGSB), Academy of Finland, Biocenter Finland Biological imaging infrastructure and the University of Helsinki dissertation completion grant. I am thankful for my supervisor Eija Jokitalo (Adjunct Professor) for introducing me to the fascinating world of cell biological science and to the finest approach a scientist can use to study it - the electron microscopy. I would also like to thank her for the encouragement and nice discussions about science and life, for setting the bar high and giving me, without me even realizing it at the time, strong professional skills and confidence to face whatever the future may bring.

I am very grateful for Adjunct Professors Varpu Marjomäki and Jussi Jäntti for reviewing my dissertation and for their helpful comments. I would like to extend my gratitude to the director of VGSB Professor Dennis Bamford and the coordinators Sanda Falck (Ph.D.), Nina Bergelin (Ph.D.) and Ulla Tuomainen (Ph.D.) for excellent courses, support on traveling and for giving me opportunity to teach at courses. I wish to express my gratitude to Ph.D. Maria K. Vartiainen and Adjunct Professor Eeva-Liisa Eskelinen from my thesis follow-up group for their understanding, support, and constructive criticism towards my work, and for their useful advice. Your input was highly appreciated! I am very thankful for my collaborators Martin Lowe, Tomasz M. Witkos, Maria K. Vartiainen and Ilya Nevzorov for their expertise on the publication I.

I would like to continue by thanking my colleagues and friends at the Electron Microscopy unit, with whom I have had the privilege to work with, and learn from, over the years. To Helena: thank you for meeting my meltdowns with a healthy level of sarcasm and the blackest humour I've ever had the pleasure to witness. I have the deepest respect for your knowledge and point of view on science and life, and I thank you for the repeated pep talks. A big thank you goes out for Ilya. If it was up to him, everything in life could be accomplished by a single press of a button. Seriously, you're a wizard! I am deeply grateful for Mervi and Arja: your technical expertise has come to my rescue countless of times (and always with a smile, or even more so, with laughter!) and I warmly thank you for over a decade of friendship. You guys are the heart of the EM-unit! To Olli: thanks for listening to my troubles, for being an excellent traveling companion, for all the lab pranks, laughs, beers, funny printouts placed not-to-subtly at inappropriate places and introducing me to the heavy metal music, which still mostly sounds like a broken lab equipment to me. Love you man! To Maija: thank you for your guidance and support especially at the beginning of my studies, for sharing the office, talks about cats, life and science, and for critical reading of my thesis, and most of all, thank you for smoothing out the path for me. I would imagine all of it would have been a lot harder without you! I wish to extend my gratitude to newest addition to the lab, Darshan: thank you for many discussions about science and life. I have learned a lot from you (true story)! I am also grateful for Antti, Chun-Mei, Maiju, Giusi, Erika, Tiina, Virpi, Pasi, Ari, Benita, Eeva-Kaisa, Tuikku and Pii who are warmly acknowledged for their valuable help, advice and discussions at the coffee table over the years.

Other past or present people of the Viikki campus: Ansku, Antti A., Maria J., Jaana V., Joseph D., K-P, Gergana G., Quillaume H., Kaisa R., Lotta H., Marion W., Satu L., Heini S., Päivi Y., Tuomas A., Giuseppe B.,

Pirjo S., Ricardo N., Ville P. and Kikka the lunch lady, a BIG thank you for being good peers and for your helpful advices, for countless borrowed antibody and reagent aliquots, for lunch and traveling company, for cheering up my day, for helpful comments at posters and for being able to talk about other stuff than mere science! Much obliged! I wish also to thank Kimmo and Mika, for all their help with LM, and Atro, Iikka and Tinde for being helpful IT-dudes.

I am so profoundly grateful for all of my friends, who have supported me by showing interest towards what I have been doing, cheering me up, making fun of my geekiness and reminding me that, at the end of the day, it's just work. I would first like to thank Milla for having always been there to support me. You are so very important to me and no matter how different paths life takes us I will always carry you in my heart. For my beloved festival animals Elli, Essi, Tuulia, Matti, Kati and Mimmi: I absolutely love you and the hunger you have for life! You guys are inspiring, true friends, full of life and love and I cannot believe how lucky I am to have you in my life! Thank you for the cheering (I did run towards it like Ryan Gosling was at the finishing line... and I still hope he is!)! I wish to thank Essi further for the very welcome support regarding my work, dragging me out from the bunker for hilarious lunches, for bringing red wine in plastic bottles to everywhere (that was true love at first sight!), spectacular sense of humour and just general awesomeness - I couldn't have done it without you! I love you to bits! Beloved Tuuli, you are one of the smartest people I have ever met and I thank you for being my shoulder and always believing in me in whatever I was doing, for the caring and love you've showed towards me and the countless moments of joy & laughter spiced up with fab music and dance-moves! You've been superb! I would also like to thank Miia for the fun years in polytechnic school, introducing me to the Uni and for her encouragement, support and true friendship. I wish to thank my scuba diving friends especially Kim, Ed, Mandy, Kate, Simon, Victoria, Caroline, Natalie, Susana, and Paul for sharing my true passion in life and reminding me that there is vibrant and colourful life out there that does not fit into curves - and don't even want to! I also would like to acknowledge Joonas: Warmest thank you for the years of support and believing in me. I literally owe you my life - how can I ever thank you enough for that?? And although I would like to acknowledge all the following people separately, I am just going to squeeze it into one big THANK YOU FOR BEING THERE: Siru, Laura T., Netta & Rob. You're support has meant the world to me -thank you for being such a good friends! I also wish to thank Esport center staff, especially Susanna, for giving me much needed Zen (and killer abs). Never underestimate the power of positive attitude and bright big smiles on people's everyday lives!!

I warmly thank my beloved family. Rakas Äiti, omistan tämän kirjan sinulle. Lämmin kiitos antamastasi tuesta ja rakkaudesta. Kiitos, että olen saanut edelleen olla lapsi silloin, kun sitä eniten olen tarvinnut. Sinua on kiittäminen sisukkuudesta, selkärangasta ja rohkeudesta tavoitella asioita, joista unelmoin - nämä ominaisuudet eivät ehkä ole tehneet elämästäni helppoa, mutta kannan niitä suurella ylpeydellä! Kiitos, että olet aina tukenut valintojani ja antanut minun löytää oman tieni. Lämmin kiitos myös Jarille, Annalle ja Ennille, että olette jaksaneet kiinnostua työstäni ja tukeneet edistymistäni. Lopuksi haluan vielä kiittää elämäni pieniä, Heikkiä, Kiaa, Lucaa ja Isabellaa, Ellaa ja Rydiä, keitä seuratessa on helppoa muistaa mikä elämässä on oikeasti tärkeää.

Helsinki, 7.4.2014 Heana

X REFERENCES

Akhmanova, A., and J.A. Hammer, 3rd. 2010. Linking molecular motors to membrane cargo. *Current opinion in cell biology*. 22:479-487.

Akhtar, A., and S.M. Gasser. 2007. The nuclear envelope and transcriptional control. *Nature reviews. Genetics*. 8:507-517.

Alber, F., S. Dokudovskaya, L.M. Veenhoff, W. Zhang, J. Kipper, D. Devos, A. Suprapto, O. Karni-Schmidt, R. Williams, B.T. Chait, A. Sali, and M.P. Rout. 2007. The molecular architecture of the nuclear pore complex. *Nature*. 450:695-701.

Almeida, C.G., A. Yamada, D. Tenza, D. Louvard, G. Raposo, and E. Coudrier. 2011. Myosin 1b promotes the formation of post-Golgi carriers by regulating actin assembly and membrane remodelling at the trans-Golgi network. *Nature cell biology*. 13:779-789.

Amarilio, R., S. Ramachandran, H. Sabanay, and S. Lev. 2005. Differential regulation of endoplasmic reticulum structure through VAP-Nir protein interaction. *The Journal of biological chemistry*. 280:5934-5944.

Anderson, D.J., and M.W. Hetzer. 2007. Nuclear envelope formation by chromatin-mediated reorganization of the endoplasmic reticulum. *Nature cell biology*. 9:1160-1166.

Anderson, D.J., and M.W. Hetzer. 2008. Reshaping of the endoplasmic reticulum limits the rate for nuclear envelope formation. *The Journal of cell biology*. 182:911-924.

Anderson, R.G., L. Orci, M.S. Brown, L.M. Garcia-Segura, and J.L. Goldstein. 1983. Ultrastructural analysis of crystalloid endoplasmic reticulum in UT-1 cells and its disappearance in response to cholesterol. *Journal of cell science*. 63:1-20.

Andrade, J., H. Zhao, B. Titus, S. Timm Pearce, and M. Barroso. 2004. The EF-hand Ca2+-binding protein p22 plays a role in microtubule and endoplasmic reticulum organization and dynamics with distinct Ca2+-binding requirements. *Molecular biology of the cell*. 15:481-496.

Area-Gomez, E., A.J. de Groof, I. Boldogh, T.D. Bird, G.E. Gibson, C.M. Koehler, W.H. Yu, K.E. Duff, M.P. Yaffe, L.A. Pon, and E.A. Schon. 2009. Presenilins are enriched in endoplasmic reticulum membranes associated with mitochondria. *The American journal of pathology*. 175:1810-1816.

Arif, E., M.C. Wagner, D.B. Johnstone, H.N. Wong, B. George, P.A. Pruthi, M.J. Lazzara, and D. Nihalani. 2011. Motor protein Myo1c is a podocyte protein that facilitates the transport of slit diaphragm protein Neph1 to the podocyte membrane. *Molecular and cellular biology*. 31:2134-2150.

Audhya, A., A. Desai, and K. Oegema. 2007. A role for Rab5 in structuring the endoplasmic reticulum. *The Journal of cell biology*. 178:43-56.

Azzam, M.E., and I.D. Algranati. 1973. Mechanism of puromycin action: fate of ribosomes after release of nascent protein chains from polysomes. *Proceedings of the National Academy of Sciences of the United States of America*. 70:3866-3869.

Babour, A., A.A. Bicknell, J. Tourtellotte, and M. Niwa. 2010. A surveillance pathway monitors the fitness of the endoplasmic reticulum to control its inheritance. *Cell*. 142:256-269.

Bannai, H., T. Inoue, T. Nakayama, M. Hattori, and K. Mikoshiba. 2004. Kinesin dependent, rapid, bi-directional transport of ER sub-compartment in dendrites of hippocampal neurons. *Journal of cell science*. 117:163-175.

Bannykh, S.I., T. Rowe, and W.E. Balch. 1996. The organization of endoplasmic reticulum export complexes. *The Journal of cell biology*. 135:19-35.

Barton, D.A., L. Cole, D.A. Collings, D.Y. Liu, P.M. Smith, D.A. Day, and R.L. Overall. 2011. Cell-to-cell transport via the lumen of the endoplasmic reticulum. *The Plant journal : for cell and molecular biology*. 66:806-817.

Barylko, B., G. Jung, and J.P. Albanesi. 2005. Structure, function, and regulation of myosin 1C. *Acta biochimica Polonica*. 52:373-380.

Barylko, B., M.C. Wagner, O. Reizes, and J.P. Albanesi. 1992. Purification and characterization of a mammalian myosin I. *Proceedings of the National Academy of Sciences of the United States of America*. 89:490-494.

Bastos, R., N. Pante, and B. Burke. 1995. Nuclear pore complex proteins. *International review of cytology*. 162B:257-302.

Batters, C., C.P. Arthur, A. Lin, J. Porter, M.A. Geeves, R.A. Milligan, J.E. Molloy, and L.M. Coluccio. 2004. Myo1c is designed for the adaptation response in the inner ear. *The EMBO journal*. 23:1433-1440.

Baughman, C., J. Morin-Leisk, and T. Lee. 2008. Nucleoside diphosphate kinase B (NDKB) scaffolds endoplasmic reticulum membranes in vitro. *Experimental cell research*. 314:2702-2714.

Baumann, O., and B. Lautenschlager. 1994. The role of actin filaments in the organization of the endoplasmic reticulum in honeybee photoreceptor cells. *Cell and tissue research*. 278:419-432.

Baumann, O., and B. Walz. 2001. Endoplasmic reticulum of animal cells and its organization into structural and functional domains. *International review of cytology*. 205:149-214.

Baur, T., K. Ramadan, A. Schlundt, J. Kartenbeck, and H.H. Meyer. 2007. NSF- and SNARE-mediated membrane fusion is required for nuclear envelope formation and completion of nuclear pore complex assembly in Xenopus laevis egg extracts. *Journal of cell science*. 120:2895-2903.

Beaudouin, J., D. Gerlich, N. Daigle, R. Eils, and J. Ellenberg. 2002. Nuclear envelope breakdown proceeds by microtubule-induced tearing of the lamina. *Cell*. 108:83-96.

Beck, M., F. Forster, M. Ecke, J.M. Plitzko, F. Melchior, G. Gerisch, W. Baumeister, and O. Medalia. 2004. Nuclear pore complex structure and dynamics revealed by cryoelectron tomography. *Science*. 306:1387-1390.

Becker, F., L. Block-Alper, G. Nakamura, J. Harada, K.D. Wittrup, and D.I. Meyer. 1999. Expression of the 180-kD ribosome receptor induces membrane proliferation and increased secretory activity in yeast. *The Journal of cell biology*. 146:273-284.

Bednarek, S.Y., M. Ravazzola, M. Hosobuchi, M. Amherdt, A. Perrelet, R. Schekman, and L. Orci. 1995. COPI- and COPII-coated vesicles bud directly from the endoplasmic reticulum in yeast. *Cell*. 83:1183-1196.

Benyamini, P., P. Webster, and D.I. Meyer. 2009. Knockdown of p180 eliminates the terminal differentiation of a secretory cell line. *Molecular biology of the cell*. 20:732-744.

Berg, J.S., B.C. Powell, and R.E. Cheney. 2001. A millennial myosin census. *Molecular biology of the cell*. 12:780-794.

Bernales, S., K.L. McDonald, and P. Walter. 2006. Autophagy counterbalances endoplasmic reticulum expansion during the unfolded protein response. *PLoS biology*. 4:e423.

Bevis, B.J., A.T. Hammond, C.A. Reinke, and B.S. Glick. 2002. De novo formation of transitional ER sites and Golgi structures in Pichia pastoris. *Nature cell biology*. 4:750-756.

Bian, X., R.W. Klemm, T.Y. Liu, M. Zhang, S. Sun, X. Sui, X. Liu, T.A. Rapoport, and J. Hu. 2011. Structures of the atlastin GTPase provide insight into homotypic fusion of endoplasmic reticulum membranes. *Proceedings of the National Academy of Sciences of the United States of America*. 108:3976-3981.

Blobel, G., and B. Dobberstein. 1975a. Transfer of proteins across membranes. I. Presence of proteolytically processed and unprocessed nascent immunoglobulin light chains on membrane-bound ribosomes of murine myeloma. *The Journal of cell biology*. 67:835-851.

Blobel, G., and B. Dobberstein. 1975b. Transfer of proteins across membranes. II. Reconstitution of functional rough microsomes from heterologous components. *The Journal of cell biology*. 67:852-862.

Bobinnec, Y., C. Marcaillou, X. Morin, and A. Debec. 2003. Dynamics of the endoplasmic reticulum during early development of Drosophila melanogaster. *Cell motility and the cytoskeleton*. 54:217-225.

Bond, L.M., H. Brandstaetter, J. Kendrick-Jones, and F. Buss. 2013. Functional roles for myosin 1c in cellular signaling pathways. *Cellular signalling*. 25:229-235.

Bose, A., A. Guilherme, S.I. Robida, S.M. Nicoloro, Q.L. Zhou, Z.Y. Jiang, D.P. Pomerleau, and M.P. Czech. 2002. Glucose transporter recycling in response to insulin is facilitated by myosin Myo1c. *Nature*. 420:821-824.

Bose, A., S. Robida, P.S. Furcinitti, A. Chawla, K. Fogarty, S. Corvera, and M.P. Czech. 2004. Unconventional myosin Myo1c promotes membrane fusion in a regulated exocytic pathway. *Molecular and cellular biology*. 24:5447-5458.

Brandizzi, F., and C. Barlowe. 2013. Organization of the ER-Golgi interface for membrane traffic control. *Nature reviews. Molecular cell biology*. 14:382-392.

Brandstaetter, H., J. Kendrick-Jones, and F. Buss. 2012. Molecular roles of Myo1c function in lipid raft exocytosis. *Communicative & integrative biology*. 5:508-510.

Bridgman, P.C. 1999. Myosin Va movements in normal and dilute-lethal axons provide support for a dual filament motor complex. *The Journal of cell biology*. 146:1045-1060.

Brown, D. 1978. Fenestrae in the rough endoplasmic reticulum of Xenopus laevis hepatocytes. *The Anatomical record*. 191:103-110.

Bubb, M.R., A.M. Senderowicz, E.A. Sausville, K.L. Duncan, and E.D. Korn. 1994. Jasplakinolide, a cytotoxic natural product, induces actin polymerization and competitively inhibits the binding of phalloidin to F-actin. *The Journal of biological chemistry*. 269:14869-14871.

Burke, B., and J. Ellenberg. 2002. Remodelling the walls of the nucleus. *Nature reviews. Molecular cell biology*. 3:487-497.

Canagarajah, B.J., G. Hummer, W.A. Prinz, and J.H. Hurley. 2008. Dynamics of cholesterol exchange in the oxysterol binding protein family. *Journal of molecular biology*. 378:737-748.

Cao, H., J.D. Orth, J. Chen, S.G. Weller, J.E. Heuser, and M.A. McNiven. 2003. Cortactin is a component of clathrin-coated pits and participates in receptor-mediated endocytosis. *Molecular and cellular biology*. 23:2162-2170.

Cao, T.T., W. Chang, S.E. Masters, and M.S. Mooseker. 2004. Myosin-Va binds to and mechanochemically couples microtubules to actin filaments. *Molecular biology of the cell*. 15:151-161.

Caputo, A., E. Caci, L. Ferrera, N. Pedemonte, C. Barsanti, E. Sondo, U. Pfeffer, R. Ravazzolo, O. Zegarra-Moran, and L.J. Galietta. 2008. TMEM16A, a membrane protein associated with calcium-dependent chloride channel activity. *Science*. 322:590-594.

Casey, J.R., S. Grinstein, and J. Orlowski. 2010. Sensors and regulators of intracellular pH. *Nature reviews. Molecular cell biology*. 11:50-61.

Chang, J., S. Lee, and C. Blackstone. 2013. Protrudin binds atlastins and endoplasmic reticulum-shaping proteins and regulates network formation. *Proceedings of the National Academy of Sciences of the United States of America*. 110:14954-14959.

Chang, L., and R.D. Goldman. 2004. Intermediate filaments mediate cytoskeletal crosstalk. *Nature reviews. Molecular cell biology*. 5:601-613.

Chen, S., P. Novick, and S. Ferro-Novick. 2012. ER network formation requires a balance of the dynamin-like GTPase Sey1p and the Lunapark family member Lnp1p. *Nature cell biology*. 14:707-716.

Chernomordik, L.V., and M.M. Kozlov. 2005. Membrane hemifusion: crossing a chasm in two leaps. *Cell*. 123:375-382.

Chernomordik, L.V., and M.M. Kozlov. 2008. Mechanics of membrane fusion. *Nature structural & molecular biology*. 15:675-683.

Chhabra, E.S., V. Ramabhadran, S.A. Gerber, and H.N. Higgs. 2009. INF2 is an endoplasmic reticulum-associated formin protein. *Journal of cell science*. 122:1430-1440.

Chi, Y.H., K. Haller, J.M. Peloponese, Jr., and K.T. Jeang. 2007. Histone acetyltransferase hALP and nuclear membrane protein hsSUN1 function in de-condensation of mitotic chromosomes. *The Journal of biological chemistry*. 282:27447-27458.

Chin, D.J., K.L. Luskey, R.G. Anderson, J.R. Faust, J.L. Goldstein, and M.S. Brown. 1982. Appearance of crystalloid endoplasmic reticulum in compactin-resistant Chinese hamster cells with a 500-fold increase in 3-hydroxy-3-methylglutaryl-coenzyme A reductase. *Proceedings of the National Academy of Sciences of the United States of America*. 79:1185-1189.

Chuang, C.H., A.E. Carpenter, B. Fuchsova, T. Johnson, P. de Lanerolle, and A.S. Belmont. 2006. Long-range directional movement of an interphase chromosome site. *Current biology : CB*. 16:825-831.

Cohen, T.V., L. Hernandez, and C.L. Stewart. 2008. Functions of the nuclear envelope and lamina in development and disease. *Biochemical Society transactions*. 36:1329-1334.

Collas, P., and J.C. Courvalin. 2000. Sorting nuclear membrane proteins at mitosis. *Trends in cell biology*. 10:5-8.

Coluccio, L.M., and M.A. Geeves. 1999. Transient kinetic analysis of the 130-kDa myosin I (MYR-1 gene product) from rat liver. A myosin I designed for maintenance of tension? *The Journal of biological chemistry*. 274:21575-21580.

Conibear, P.B. 1999. Kinetic studies on the effects of ADP and ionic strength on the interaction between myosin subfragment-1 and actin: implications for load-sensitivity and regulation of the crossbridge cycle. *Journal of muscle research and cell motility*. 20:727-742.

Connolly, C.N., C.E. Futter, A. Gibson, C.R. Hopkins, and D.F. Cutler. 1994. Transport into and out of the Golgi complex studied by transfecting cells with cDNAs encoding horseradish peroxidase. *The Journal of cell biology*. 127:641-652.

Crisp, M., Q. Liu, K. Roux, J.B. Rattner, C. Shanahan, B. Burke, P.D. Stahl, and D. Hodzic. 2006. Coupling of the nucleus and cytoplasm: role of the LINC complex. *The Journal of cell biology*. 172:41-53.

Csordas, G., C. Renken, P. Varnai, L. Walter, D. Weaver, K.F. Buttle, T. Balla, C.A. Mannella, and G. Hajnoczky. 2006. Structural and functional features and significance of the physical linkage between ER and mitochondria. *The Journal of cell biology*. 174:915-921.

Czichi, U., and W.J. Lennarz. 1977. Localization of the enzyme system for glycosylation of proteins via the lipid-linked pathway in rough endoplasmic reticulum. *The Journal of biological chemistry*. 252:7901-7904.

D'Angelo, M.A., D.J. Anderson, E. Richard, and M.W. Hetzer. 2006. Nuclear pores form de novo from both sides of the nuclear envelope. *Science*. 312:440-443.

D'Angelo, M.A., and M.W. Hetzer. 2006. The role of the nuclear envelope in cellular organization. *Cellular and molecular life sciences : CMLS*. 63:316-332.

D'Angelo, M.A., and M.W. Hetzer. 2008. Structure, dynamics and function of nuclear pore complexes. *Trends in cell biology*. 18:456-466.

Daigle, N., J. Beaudouin, L. Hartnell, G. Imreh, E. Hallberg, J. Lippincott-Schwartz, and J. Ellenberg. 2001. Nuclear pore complexes form immobile networks and have a very low turnover in live mammalian cells. *The Journal of cell biology*. 154:71-84.

Darzacq, X., E. Powrie, W. Gu, R.H. Singer, and D. Zenklusen. 2003. RNA asymmetric distribution and daughter/mother differentiation in yeast. *Current opinion in microbiology*. 6:614-620.

Dawson, T.R., M.D. Lazarus, M.W. Hetzer, and S.R. Wente. 2009. ER membrane-bending proteins are necessary for de novo nuclear pore formation. *The Journal of cell biology*. 184:659-675.

Dayel, M.J., E.F. Hom, and A.S. Verkman. 1999. Diffusion of green fluorescent protein in the aqueous-phase lumen of endoplasmic reticulum. *Biophysical journal*. 76:2843-2851.

de Brito, O.M., and L. Scorrano. 2008. Mitofusin 2: a mitochondria-shaping protein with signaling roles beyond fusion. *Antioxidants & redox signaling*. 10:621-633.

de Brito, O.M., and L. Scorrano. 2010. An intimate liaison: spatial organization of the endoplasmic reticulum-mitochondria relationship. *The EMBO journal*. 29:2715-2723.

De La Cruz, E.M., and E.M. Ostap. 2004. Relating biochemistry and function in the myosin superfamily. *Current opinion in cell biology*. 16:61-67.

Di Paolo, G., and P. De Camilli. 2006. Phosphoinositides in cell regulation and membrane dynamics. *Nature*. 443:651-657.

Diefenbach, T.J., V.M. Latham, D. Yimlamai, C.A. Liu, I.M. Herman, and D.G. Jay. 2002. Myosin 1c and myosin IIB serve opposing roles in lamellipodial dynamics of the neuronal growth cone. *The Journal of cell biology*. 158:1207-1217.

Domart, M.C., T.M. Hobday, C.J. Peddie, G.H. Chung, A. Wang, K. Yeh, N. Jethwa, Q. Zhang, M.J. Wakelam, R. Woscholski, R.D. Byrne, L.M. Collinson, D.L. Poccia, and B. Larijani. 2012. Acute manipulation of diacylglycerol reveals roles in nuclear envelope assembly & endoplasmic reticulum morphology. *PloS one*. 7:e51150.

Dorner, D., J. Gotzmann, and R. Foisner. 2007. Nucleoplasmic lamins and their interaction partners, LAP2alpha, Rb, and BAF, in transcriptional regulation. *The FEBS journal*. 274:1362-1373.

dos Remedios, C.G., D. Chhabra, M. Kekic, I.V. Dedova, M. Tsubakihara, D.A. Berry, and N.J. Nosworthy. 2003. Actin binding proteins: regulation of cytoskeletal microfilaments. *Physiological reviews*. 83:433-473.

Dreier, L., and T.A. Rapoport. 2000. In vitro formation of the endoplasmic reticulum occurs independently of microtubules by a controlled fusion reaction. *The Journal of cell biology*. 148:883-898.

Du, Y., S. Ferro-Novick, and P. Novick. 2004. Dynamics and inheritance of the endoplasmic reticulum. *Journal of cell science*. 117:2871-2878.

Dumont, R.A., Y.D. Zhao, J.R. Holt, M. Bahler, and P.G. Gillespie. 2002. Myosin-I isozymes in neonatal rodent auditory and vestibular epithelia. *Journal of the Association for Research in Otolaryngology : JARO*. 3:375-389.

Dykstra, K.M., J.E. Pokusa, J. Suhan, and T.H. Lee. 2010. Yip1A structures the mammalian endoplasmic reticulum. *Molecular biology of the cell*. 21:1556-1568.

Dzijak, R., S. Yildirim, M. Kahle, P. Novak, J. Hnilicova, T. Venit, and P. Hozak. 2012. Specific nuclear localizing sequence directs two myosin isoforms to the cell nucleus in calmodulin-sensitive manner. *PloS one*. 7:e30529.

El Mezgueldi, M., N. Tang, S.S. Rosenfeld, and E.M. Ostap. 2002. The kinetic mechanism of Myo1e (human myosin-IC). *The Journal of biological chemistry*. 277:21514-21521.

Ellenberg, J., E.D. Siggia, J.E. Moreira, C.L. Smith, J.F. Presley, H.J. Worman, and J. Lippincott-Schwartz. 1997. Nuclear membrane dynamics and reassembly in living cells: targeting of an inner nuclear membrane protein in interphase and mitosis. *The Journal of cell biology*. 138:1193-1206.

English, A.R., and G.K. Voeltz. 2013. Rab10 GTPase regulates ER dynamics and morphology. *Nature cell biology*. 15:169-178.

English, A.R., N. Zurek, and G.K. Voeltz. 2009. Peripheral ER structure and function. *Current opinion in cell biology*. 21:596-602.

Estrada, P., J. Kim, J. Coleman, L. Walker, B. Dunn, P. Takizawa, P. Novick, and S. Ferro-Novick. 2003. Myo4p and She3p are required for cortical ER inheritance in Saccharomyces cerevisiae. *The Journal of cell biology*. 163:1255-1266.

Fan, Y., S.M. Eswarappa, M. Hitomi, and P.L. Fox. 2012. Myo1c facilitates G-actin transport to the leading edge of migrating endothelial cells. *The Journal of cell biology*. 198:47-55.

Fehrenbacher, K.L., D. Davis, M. Wu, I. Boldogh, and L.A. Pon. 2002. Endoplasmic reticulum dynamics, inheritance, and cytoskeletal interactions in budding yeast. *Molecular biology of the cell*. 13:854-865.

Feiguin, F., A. Ferreira, K.S. Kosik, and A. Caceres. 1994. Kinesin-mediated organelle translocation revealed by specific cellular manipulations. *The Journal of cell biology*. 127:1021-1039.

Feldman, D., R.L. Swarm, and J. Becker. 1981. Ultrastructural study of rat liver and liver neoplasms after long-term treatment with phenobarbital. *Cancer research*. 41:2151-2162.

Field, C.M., and P. Lenart. 2011. Bulk cytoplasmic actin and its functions in meiosis and mitosis. *Current biology : CB*. 21:R825-830.

Foisner, R. 2003. Cell cycle dynamics of the nuclear envelope. *TheScientificWorldJournal*. 3:1-20.

Friedman, J.R., J.R. Dibenedetto, M. West, A.A. Rowland, and G.K. Voeltz. 2013. Endoplasmic reticulum-endosome contact increases as endosomes traffic and mature. *Molecular biology of the cell*. 24:1030-1040.

Friedman, J.R., B.M. Webster, D.N. Mastronarde, K.J. Verhey, and G.K. Voeltz. 2010. ER sliding dynamics and ER-mitochondrial contacts occur on acetylated microtubules. *The Journal of cell biology*. 190:363-375.

Friedman, J.R., and G.K. Voeltz. 2011. The ER in 3D: a multifunctional dynamic membrane network. *Trends in cell biology*. 21:709-717.

Fuchs, E., and I. Karakesisoglou. 2001. Bridging cytoskeletal intersections. *Genes & development*. 15:1-14.

Funato, K., and H. Riezman. 2001. Vesicular and nonvesicular transport of ceramide from ER to the Golgi apparatus in yeast. *The Journal of cell biology*. 155:949-959.

Galteau, M.M., B. Antoine, and H. Reggio. 1985. Epoxide hydrolase is a marker for the smooth endoplasmic reticulum in rat liver. *The EMBO journal*. 4:2793-2800.

Garg, P., R. Verma, D. Nihalani, D.B. Johnstone, and L.B. Holzman. 2007. Neph1 cooperates with nephrin to transduce a signal that induces actin polymerization. *Molecular and cellular biology*. 27:8698-8712.

Gautreau, A., D. Louvard, and M. Arpin. 2000. Morphogenic effects of ezrin require a phosphorylation-induced transition from oligomers to monomers at the plasma membrane. *The Journal of cell biology*. 150:193-203.

Geli, M.I., and H. Riezman. 1996. Role of type I myosins in receptor-mediated endocytosis in yeast. *Science*. 272:533-535.

Geng, J., U. Nair, K. Yasumura-Yorimitsu, and D.J. Klionsky. 2010. Post-Golgi Sec proteins are required for autophagy in Saccharomyces cerevisiae. *Molecular biology of the cell*. 21:2257-2269.

Gillespie, P.G., J.P. Albanesi, M. Bahler, W.M. Bement, J.S. Berg, D.R. Burgess, B. Burnside, R.E. Cheney, D.P. Corey, E. Coudrier, P. de Lanerolle, J.A. Hammer, T. Hasson, J.R. Holt, A.J. Hudspeth, M. Ikebe, J. Kendrick-Jones, E.D. Korn, R. Li, J.A. Mercer, R.A. Milligan, M.S. Mooseker, E.M. Ostap, C. Petit, T.D. Pollard, J.R. Sellers, T. Soldati, and M.A. Titus. 2001. Myosin-I nomenclature. *The Journal of cell biology*. 155:703-704.

Gillespie, P.G., and J.L. Cyr. 2004. Myosin-1c, the hair cell's adaptation motor. *Annual review of physiology*. 66:521-545.

Giordano, F., Y. Saheki, O. Idevall-Hagren, S.F. Colombo, M. Pirruccello, I. Milosevic, E.O. Gracheva, S.N. Bagriantsev, N. Borgese, and P. De Camilli. 2013. PI(4,5)P(2)-dependent and Ca(2+)-regulated ER-PM interactions mediated by the extended synaptotagmins. *Cell*. 153:1494-1509.

Goda, Y., and S.R. Pfeffer. 1989. Cell-free systems to study vesicular transport along the secretory and endocytic pathways. *FASEB journal : official publication of the Federation of American Societies for Experimental Biology*. 3:2488-2495.

Godi, A., I. Santone, P. Pertile, P. Devarajan, P.R. Stabach, J.S. Morrow, G. Di Tullio, R. Polishchuk, T.C. Petrucci, A. Luini, and M.A. De Matteis. 1998. ADP ribosylation factor regulates spectrin binding to the Golgi complex. *Proceedings of the National Academy of Sciences of the United States of America*. 95:8607-8612.

Goffeau, A., B.G. Barrell, H. Bussey, R.W. Davis, B. Dujon, H. Feldmann, F. Galibert, J.D. Hoheisel, C. Jacq, M. Johnston, E.J. Louis, H.W. Mewes, Y. Murakami, P. Philippsen, H. Tettelin, and S.G. Oliver. 1996. Life with 6000 genes. *Science*. 274:546, 563-547.

Goode, B.L., D.G. Drubin, and G. Barnes. 2000. Functional cooperation between the microtubule and actin cytoskeletons. *Current opinion in cell biology*. 12:63-71.

Goss, V.L., B.A. Hocevar, L.J. Thompson, C.A. Stratton, D.J. Burns, and A.P. Fields. 1994. Identification of nuclear beta II protein kinase C as a mitotic lamin kinase. *The Journal of biological chemistry*. 269:19074-19080.

Goyal, U., and C. Blackstone. 2013. Untangling the web: mechanisms underlying ER network formation. *Biochimica et biophysica acta*. 1833:2492-2498.

Griffing, L.R. 2010. Networking in the endoplasmic reticulum. *Biochemical Society transactions*. 38:747-753.

Griffiths, G., R. Back, and M. Marsh. 1989. A quantitative analysis of the endocytic pathway in baby hamster kidney cells. *The Journal of cell biology*. 109:2703-2720.

Grigoriev, I., S.M. Gouveia, B. van der Vaart, J. Demmers, J.T. Smyth, S. Honnappa, D. Splinter, M.O. Steinmetz, J.W. Putney, Jr., C.C. Hoogenraad, and A. Akhmanova. 2008. STIM1 is a MT-plus-end-tracking protein involved in remodeling of the ER. *Current biology : CB*. 18:177-182.

Gruenbaum, Y., A. Margalit, R.D. Goldman, D.K. Shumaker, and K.L. Wilson. 2005. The nuclear lamina comes of age. *Nature reviews. Molecular cell biology*. 6:21-31.

Gruenbaum, Y., K.L. Wilson, A. Harel, M. Goldberg, and M. Cohen. 2000. Review: nuclear lamins--structural proteins with fundamental functions. *Journal of structural biology*. 129:313-323.

Gupta, V., K.J. Palmer, P. Spence, A. Hudson, and D.J. Stephens. 2008. Kinesin-1 (uKHC/KIF5B) is required for bidirectional motility of ER exit sites and efficient ER-to-Golgi transport. *Traffic*. 9:1850-1866.

Gupton, S.L., D.A. Collings, and N.S. Allen. 2006. Endoplasmic reticulum targeted GFP reveals ER organization in tobacco NT-1 cells during cell division. *Plant physiology and biochemistry : PPB / Societe francaise de physiologie vegetale*. 44:95-105.

Hagan, G.N., Y. Lin, M.A. Magnuson, J. Avruch, and M.P. Czech. 2008. A Rictor-Myo1c complex participates in dynamic cortical actin events in 3T3-L1 adipocytes. *Molecular and cellular biology*. 28:4215-4226.

Hailey, D.W., A.S. Rambold, P. Satpute-Krishnan, K. Mitra, R. Sougrat, P.K. Kim, and J. Lippincott-Schwartz. 2010. Mitochondria supply membranes for autophagosome biogenesis during starvation. *Cell*. 141:656-667.

Hajnoczky, G., G. Csordas, S. Das, C. Garcia-Perez, M. Saotome, S. Sinha Roy, and M. Yi. 2006. Mitochondrial calcium signalling and cell death: approaches for assessing the role of mitochondrial Ca2+ uptake in apoptosis. *Cell calcium*. 40:553-560.

Hales, C.N., J.P. Luzio, J.A. Chandler, and L. Herman. 1974. Localization of calcium in the smooth endoplasmic reticulum of rat isolated fat cells. *Journal of cell science*. 15:1-15.

Harada, T., J. Swift, J. Irianto, J.W. Shin, K.R. Spinler, A. Athirasala, R. Diegmiller, P.C. Dingal, I.L. Ivanovska, and D.E. Discher. 2014. Nuclear lamin stiffness is a barrier to 3D migration, but softness can limit survival. *The Journal of cell biology*.

Hawes, C.R., B.E. Juniper, and J.C. Horne. 1981. Low and high voltage electron microscopy of mitosis and cytokinesis in maize roots. *Planta*. 152:397-407.

Hayashi-Nishino, M., N. Fujita, T. Noda, A. Yamaguchi, T. Yoshimori, and A. Yamamoto. 2009. A subdomain of the endoplasmic reticulum forms a cradle for autophagosome formation. *Nature cell biology*. 11:1433-1437.

Hazan, R.B., L. Kang, S. Roe, P.I. Borgen, and D.L. Rimm. 1997. Vinculin is associated with the E-cadherin adhesion complex. *The Journal of biological chemistry*. 272:32448-32453.

Heidtman, M., C.Z. Chen, R.N. Collins, and C. Barlowe. 2003. A role for Yip1p in COPII vesicle biogenesis. *The Journal of cell biology*. 163:57-69.

Helfrich, P., and E. Jakobsson. 1990. Calculation of deformation energies and conformations in lipid membranes containing gramicidin channels. *Biophysical journal*. 57:1075-1084.

Helms, J.B., K.J. de Vries, and K.W. Wirtz. 1991. Synthesis of phosphatidylinositol 4,5-bisphosphate in the endoplasmic reticulum of Chinese hamster ovary cells. *The Journal of biological chemistry*. 266:21368-21374.

Hepler, P.K. 1980. Membranes in the mitotic apparatus of barley cells. *The Journal of cell biology*. 86:490-499.

Hepler, P.K. 1981. The structure of the endoplasmic reticulum revealed by osmium tetroxide-potassium ferricyanide staining. *European journal of cell biology*. 26:102-111.

Herrmann, H., M. Hesse, M. Reichenzeller, U. Aebi, and T.M. Magin. 2003. Functional complexity of intermediate filament cytoskeletons: from structure to assembly to gene ablation. *International review of cytology*. 223:83-175.

Hetzer, M., H.H. Meyer, T.C. Walther, D. Bilbao-Cortes, G. Warren, and I.W. Mattaj. 2001. Distinct AAA-ATPase p97 complexes function in discrete steps of nuclear assembly. *Nature cell biology*. 3:1086-1091.

Hetzer, M.W. 2010. The nuclear envelope. *Cold Spring Harbor perspectives in biology*. 2:a000539.

Hetzer, M.W., T.C. Walther, and I.W. Mattaj. 2005. Pushing the envelope: structure, function, and dynamics of the nuclear periphery. *Annual review of cell and developmental biology*. 21:347-380.

Hinman, N.D., and A.H. Phillips. 1970. Similarity and limited multiplicity of membrane proteins from rough and smooth endoplasmic reticulum. *Science*. 170:1222-1223.

Hirono, M., C.S. Denis, G.P. Richardson, and P.G. Gillespie. 2004. Hair cells require phosphatidylinositol 4,5-bisphosphate for mechanical transduction and adaptation. *Neuron*. 44:309-320.

Hoepfner, D., D. Schildknegt, I. Braakman, P. Philippsen, and H.F. Tabak. 2005. Contribution of the endoplasmic reticulum to peroxisome formation. *Cell*. 122:85-95.

Hoffmann, K., K. Sperling, A.L. Olins, and D.E. Olins. 2007. The granulocyte nucleus and lamin B receptor: avoiding the ovoid. *Chromosoma*. 116:227-235.

Hokanson, D.E., J.M. Laakso, T. Lin, D. Sept, and E.M. Ostap. 2006. Myo1c binds phosphoinositides through a putative pleckstrin homology domain. *Molecular biology of the cell*. 17:4856-4865.

Hokanson, D.E., and E.M. Ostap. 2006. Myo1c binds tightly and specifically to phosphatidylinositol 4,5-bisphosphate and inositol 1,4,5-trisphosphate. *Proceedings of the National Academy of Sciences of the United States of America*. 103:3118-3123.

Holt, J.R., S.K. Gillespie, D.W. Provance, K. Shah, K.M. Shokat, D.P. Corey, J.A. Mercer, and P.G. Gillespie. 2002. A chemical-genetic strategy implicates myosin-1c in adaptation by hair cells. *Cell*. 108:371-381.

Holzinger, A. 2009. Jasplakinolide: an actin-specific reagent that promotes actin polymerization. *Methods Mol Biol*. 586:71-87.

Hong, W. 1998. Protein transport from the endoplasmic reticulum to the Golgi apparatus. *Journal of cell science*. 111 (Pt 19):2831-2839.

Hoshikawa, Y., H.J. Kwon, M. Yoshida, S. Horinouchi, and T. Beppu. 1994. Trichostatin A induces morphological changes and gelsolin expression by inhibiting histone deacetylase in human carcinoma cell lines. *Experimental cell research*. 214:189-197.

Hosoi, T., and K. Ozawa. 2010. Endoplasmic reticulum stress in disease: mechanisms and therapeutic opportunities. *Clinical science*. 118:19-29.

Hotulainen, P., E. Paunola, M.K. Vartiainen, and P. Lappalainen. 2005. Actin-depolymerizing factor and cofilin-1 play overlapping roles in promoting rapid F-actin depolymerization in mammalian nonmuscle cells. *Molecular biology of the cell*. 16:649-664.

Hu, J., Y. Shibata, C. Voss, T. Shemesh, Z. Li, M. Coughlin, M.M. Kozlov, T.A. Rapoport, and W.A. Prinz. 2008. Membrane proteins of the endoplasmic reticulum induce high-curvature tubules. *Science*. 319:1247-1250.

Hu, J., Y. Shibata, P.P. Zhu, C. Voss, N. Rismanchi, W.A. Prinz, T.A. Rapoport, and C. Blackstone. 2009. A class of dynamin-like GTPases involved in the generation of the tubular ER network. *Cell*. 138:549-561.

Iseri, O.A., C.S. Lieber, and L.S. Gottlieb. 1966. The ultrastructure of fatty liver induced by prolonged ethanol ingestion. *The American journal of pathology*. 48:535-555.

Iwasawa, R., A.L. Mahul-Mellier, C. Datler, E. Pazarentzos, and S. Grimm. 2011. Fis1 and Bap31 bridge the mitochondria-ER interface to establish a platform for apoptosis induction. *The EMBO journal*. 30:556-568.

Jaalouk, D.E., and J. Lammerding. 2009. Mechanotransduction gone awry. *Nature reviews. Molecular cell biology*. 10:63-73.

Jacquier, N., V. Choudhary, M. Mari, A. Toulmay, F. Reggiori, and R. Schneiter. 2011. Lipid droplets are functionally connected to the endoplasmic reticulum in Saccharomyces cerevisiae. *Journal of cell science*. 124:2424-2437.

Jamieson, J.D., and G.E. Palade. 1968. Intracellular transport of secretory proteins in the pancreatic exocrine cell. 3. Dissociation of intracellular transport from protein synthesis. *The Journal of cell biology*. 39:580-588.

Jokitalo, E., N. Cabrera-Poch, G. Warren, and D.T. Shima. 2001. Golgi clusters and vesicles mediate mitotic inheritance independently of the endoplasmic reticulum. *The Journal of cell biology*. 154:317-330.

Jozsef, L., K. Tashiro, A. Kuo, E. Park, A. Skoura, S. Albinsson, F. Rivera-Molina, K.D. Harrison, Y. Iwakiri, D. Toomre, and W.C. Sessa. 2014. Reticluon 4 is necessary for ER tubulation, STIM1-Orai1 coupling and store-operated calcium entry. *The Journal of biological chemistry*.

Kaksonen, M., C.P. Toret, and D.G. Drubin. 2006. Harnessing actin dynamics for clathrin-mediated endocytosis. *Nature reviews. Molecular cell biology*. 7:404-414.

Kano, F., H. Kondo, A. Yamamoto, Y. Kaneko, K. Uchiyama, N. Hosokawa, K. Nagata, and M. Murata. 2005. NSF/SNAPs and p97/p47/VCIP135 are sequentially required for cell cycle-dependent reformation of the ER network. *Genes to cells : devoted to molecular & cellular mechanisms*. 10:989-999.

Kao, F.T., and T.T. Puck. 1968. Genetics of somatic mammalian cells, VII. Induction and isolation of nutritional mutants in Chinese hamster cells. *Proceedings of the National Academy of Sciences of the United States of America*. 60:1275-1281.

Kawano, M., K. Kumagai, M. Nishijima, and K. Hanada. 2006. Efficient trafficking of ceramide from the endoplasmic reticulum to the Golgi apparatus requires a VAMP-associated protein-interacting FFAT motif of CERT. *The Journal of biological chemistry*. 281:30279-30288.

Kelley, L.C., and S.A. Weed. 2012. Cortactin is a substrate of activated Cdc42-associated kinase 1 (ACK1) during ligand-induced epidermal growth factor receptor downregulation. *PloS one*. 7:e44363.

Keppler, A., C. Arrivoli, L. Sironi, and J. Ellenberg. 2006. Fluorophores for live cell imaging of AGT fusion proteins across the visible spectrum. *BioTechniques*. 41:167-170, 172, 174-165.

Kim, P.K., R.T. Mullen, U. Schumann, and J. Lippincott-Schwartz. 2006. The origin and maintenance of mammalian peroxisomes involves a de novo PEX16-dependent pathway from the ER. *The Journal of cell biology*. 173:521-532.

Kiseleva, E., K.N. Morozova, G.K. Voeltz, T.D. Allen, and M.W. Goldberg. 2007. Reticulon 4a/NogoA locates to regions of high membrane curvature and may have a role in nuclear envelope growth. *Journal of structural biology*. 160:224-235.

Klemm, E.J., E. Spooner, and H.L. Ploegh. 2011. Dual role of ancient ubiquitous protein 1 (AUP1) in lipid droplet accumulation and endoplasmic reticulum (ER) protein quality control. *The Journal of biological chemistry*. 286:37602-37614.

Klopfenstein, D.R., F. Kappeler, and H.P. Hauri. 1998. A novel direct interaction of endoplasmic reticulum with microtubules. *The EMBO journal*. 17:6168-6177.

Klopfenstein, D.R., J. Klumperman, A. Lustig, R.A. Kammerer, V. Oorschot, and H.P. Hauri. 2001. Subdomain-specific localization of CLIMP-63 (p63) in the endoplasmic reticulum is mediated by its luminal alpha-helical segment. *The Journal of cell biology*. 153:1287-1300.

Knebel, W., H. Quader, and E. Schnepf. 1990. Mobile and immobile endoplasmic reticulum in onion bulb epidermis cells: short- and long-term observations with a confocal laser scanning microscope. *European journal of cell biology*. 52:328-340.

Koning, A.J., C.J. Roberts, and R.L. Wright. 1996. Different subcellular localization of Saccharomyces cerevisiae HMG-CoA reductase isozymes at elevated levels corresponds to distinct endoplasmic reticulum membrane proliferations. *Molecular biology of the cell*. 7:769-789.

Korkhov, V.M., and B. Zuber. 2009. Direct observation of molecular arrays in the organized smooth endoplasmic reticulum. *BMC cell biology*. 10:59.

Kornmann, B., E. Currie, S.R. Collins, M. Schuldiner, J. Nunnari, J.S. Weissman, and P. Walter. 2009. An ER-mitochondria tethering complex revealed by a synthetic biology screen. *Science*. 325:477-481.

Kornmann, B., and P. Walter. 2010. ERMES-mediated ER-mitochondria contacts: molecular hubs for the regulation of mitochondrial biology. *Journal of cell science*. 123:1389-1393.

Korobova, F., V. Ramabhadran, and H.N. Higgs. 2013. An actin-dependent step in mitochondrial fission mediated by the ER-associated formin INF2. *Science*. 339:464-467.

Kozlov, M.M., and L.V. Chernomordik. 2002. The protein coat in membrane fusion: lessons from fission. *Traffic*. 3:256-267.

Kreibich, G., M. Czako-Graham, R. Grebenau, W. Mok, E. Rodriguez-Boulan, and D.D. Sabatini. 1978. Characterization of the ribosomal binding site in rat liver rough microsomes: ribophorins I and II, two integral membrane proteins related to ribosome binding. *Journal of supramolecular structure*. 8:279-302.

Krendel, M., E.K. Osterweil, and M.S. Mooseker. 2007. Myosin 1E interacts with synaptojanin-1 and dynamin and is involved in endocytosis. *FEBS letters*. 581:644-650.

Kucharz, K., T. Wieloch, and H. Toresson. 2013. Fission and fusion of the neuronal endoplasmic reticulum. *Translational stroke research*. 4:652-662.

Kumar, J., H. Yu, and M.P. Sheetz. 1995. Kinectin, an essential anchor for kinesin-driven vesicle motility. *Science*. 267:1834-1837.

Kuokkanen, E., W. Smith, M. Mäkinen, H. Tuominen, M. Puhka, E. Jokitalo, S. Duvet, T. Berg, and P. Heikinheimo. 2007. Characterization and subcellular localization of human neutral class II alpha-mannosidase [corrected]. *Glycobiology*. 17:1084-1093.

Kuznetsov, S.A., D.T. Rivera, F.F. Severin, D.G. Weiss, and G.M. Langford. 1994. Movement of axoplasmic organelles on actin filaments from skeletal muscle. *Cell motility and the cytoskeleton*. 28:231-242.

Lamb, C.A., T. Yoshimori, and S.A. Tooze. 2013. The autophagosome: origins unknown, biogenesis complex. *Nature reviews. Molecular cell biology*. 14:759-774.

Langley, R., E. Leung, C. Morris, R. Berg, M. McDonald, A. Weaver, D.A. Parry, J. Ni, J. Su, R. Gentz, N. Spurr, and G.W. Krissansen. 1998. Identification of multiple forms of 180-kDa ribosome receptor in human cells. *DNA and cell biology*. 17:449-460.

Lantz, V.A., and K.G. Miller. 1998. A class VI unconventional myosin is associated with a homologue of a microtubule-binding protein, cytoplasmic linker protein-170, in neurons and at the posterior pole of Drosophila embryos. *The Journal of cell biology*. 140:897-910.

Lavoie, C., J. Lanoix, F.W. Kan, and J. Paiement. 1996. Cell-free assembly of rough and smooth endoplasmic reticulum. *Journal of cell science*. 109 (Pt 6):1415-1425.

Lazarides, E., and K. Burridge. 1975. Alpha-actinin: immunofluorescent localization of a muscle structural protein in nonmuscle cells. *Cell*. 6:289-298.

Le Breton, M., P. Cormier, R. Belle, O. Mulner-Lorillon, and J. Morales. 2005. Translational control during mitosis. *Biochimie*. 87:805-811.

Lederkremer, G.Z. 2009. Glycoprotein folding, quality control and ER-associated degradation. *Current opinion in structural biology*. 19:515-523.

Lee, C., and L.B. Chen. 1988. Dynamic behavior of endoplasmic reticulum in living cells. *Cell*. 54:37-46.

Lee, C., M. Ferguson, and L.B. Chen. 1989. Construction of the endoplasmic reticulum. *The Journal of cell biology*. 109:2045-2055.

Lee, W.L., M. Bezanilla, and T.D. Pollard. 2000. Fission yeast myosin-I, Myo1p, stimulates actin assembly by Arp2/3 complex and shares functions with WASp. *The Journal of cell biology*. 151:789-800.

Lenart, P., G. Rabut, N. Daigle, A.R. Hand, M. Terasaki, and J. Ellenberg. 2003. Nuclear envelope breakdown in starfish oocytes proceeds by partial NPC disassembly followed by a rapidly spreading fenestration of nuclear membranes. *The Journal of cell biology*. 160:1055-1068.

Lerich, A., S. Hillmer, M. Langhans, D. Scheuring, P. van Bentum, and D.G. Robinson. 2012. ER Import Sites and Their Relationship to ER Exit Sites: A New Model for Bidirectional ER-Golgi Transport in Higher Plants. *Frontiers in plant science*. 3:143.

Levental, I., D.A. Christian, Y.H. Wang, J.J. Madara, D.E. Discher, and P.A. Janmey. 2009. Calcium-dependent lateral organization in phosphatidylinositol 4,5-bisphosphate (PIP2)- and cholesterol-containing monolayers. *Biochemistry*. 48:8241-8248.

Levine, T., and C. Loewen. 2006. Inter-organelle membrane contact sites: through a glass, darkly. *Current opinion in cell biology*. 18:371-378.

Lewis, N.E., X. Liu, Y. Li, H. Nagarajan, G. Yerganian, E. O'Brien, A. Bordbar, A.M. Roth, J. Rosenbloom, C. Bian, M. Xie, W. Chen, N. Li, D. Baycin-Hizal, H. Latif, J. Forster, M.J. Betenbaugh, I. Famili, X. Xu, J. Wang, and B.O. Palsson. 2013. Genomic landscapes of Chinese hamster ovary cell lines as revealed by the Cricetulus griseus draft genome. *Nature biotechnology*. 31:759-765.

Lieber, C.S. 2004. The discovery of the microsomal ethanol oxidizing system and its physiologic and pathologic role. *Drug metabolism reviews*. 36:511-529.

Lieberman, A.R. 1971. Microtubule-associated smooth endoplasmic reticulum in the frog's brain. *Zeitschrift fur Zellforschung und mikroskopische Anatomie*. 116:564-577.

Lingwood, D., S. Schuck, C. Ferguson, M.J. Gerl, and K. Simons. 2009. Generation of cubic membranes by controlled homotypic interaction of membrane proteins in the endoplasmic reticulum. *The Journal of biological chemistry*. 284:12041-12048.

Liou, J., M. Fivaz, T. Inoue, and T. Meyer. 2007. Live-cell imaging reveals sequential oligomerization and local plasma membrane targeting of stromal interaction molecule 1 after Ca2+ store depletion. *Proceedings of the National Academy of Sciences of the United States of America*. 104:9301-9306.

Liu, R., S. Woolner, J.E. Johndrow, D. Metzger, A. Flores, and S.M. Parkhurst. 2008. Sisyphus, the Drosophila myosin XV homolog, traffics within filopodia transporting key sensory and adhesion cargos. *Development*. 135:53-63.

Loewen, C.J., B.P. Young, S. Tavassoli, and T.P. Levine. 2007. Inheritance of cortical ER in yeast is required for normal septin organization. *The Journal of cell biology*. 179:467-483.

Lombardi, M.L., D.E. Jaalouk, C.M. Shanahan, B. Burke, K.J. Roux, and J. Lammerding. 2011. The interaction between nesprins and sun proteins at the nuclear envelope is critical for force transmission between the nucleus and cytoskeleton. *The Journal of biological chemistry*. 286:26743-26753.

Lowe, M., and F.A. Barr. 2007. Inheritance and biogenesis of organelles in the secretory pathway. *Nature reviews. Molecular cell biology*. 8:429-439.

Lu, L., M.S. Ladinsky, and T. Kirchhausen. 2009. Cisternal organization of the endoplasmic reticulum during mitosis. *Molecular biology of the cell*. 20:3471-3480.

Lu, L., M.S. Ladinsky, and T. Kirchhausen. 2011. Formation of the postmitotic nuclear envelope from extended ER cisternae precedes nuclear pore assembly. *The Journal of cell biology*. 194:425-440.

Lu, X., Y. Shi, Q. Lu, Y. Ma, J. Luo, Q. Wang, J. Ji, Q. Jiang, and C. Zhang. 2010. Requirement for lamin B receptor and its regulation by importin {beta} and phosphorylation in nuclear envelope assembly during mitotic exit. *The Journal of biological chemistry*. 285:33281-33293.

Lynch, C.D., N.C. Gauthier, N. Biais, A.M. Lazar, P. Roca-Cusachs, C.H. Yu, and M.P. Sheetz. 2011. Filamin depletion blocks endoplasmic spreading and destabilizes force-bearing adhesions. *Molecular biology of the cell*. 22:1263-1273.

Ma, Y., S. Cai, Q. Lv, Q. Jiang, Q. Zhang, Sodmergen, Z. Zhai, and C. Zhang. 2007. Lamin B receptor plays a role in stimulating nuclear envelope production and targeting membrane vesicles to chromatin during nuclear envelope assembly through direct interaction with importin beta. *Journal of cell science*. 120:520-530.

Maison, C., H. Horstmann, and S.D. Georgatos. 1993. Regulated docking of nuclear membrane vesicles to vimentin filaments during mitosis. *The Journal of cell biology*. 123:1491-1505.

Malhotra, V. 2013. Unconventional protein secretion: an evolving mechanism. *The EMBO journal*. 32:1660-1664.

Mancini, M.A., D. He, Ouspenski, II, and B.R. Brinkley. 1996. Dynamic continuity of nuclear and mitotic matrix proteins in the cell cycle. *Journal of cellular biochemistry*. 62:158-164.

Manford, A.G., C.J. Stefan, H.L. Yuan, J.A. Macgurn, and S.D. Emr. 2012. ER-to-plasma membrane tethering proteins regulate cell signaling and ER morphology. *Developmental cell*. 23:1129-1140.

Mannan, A.U., J. Boehm, S.M. Sauter, A. Rauber, P.C. Byrne, J. Neesen, and W. Engel. 2006. Spastin, the most commonly mutated protein in hereditary spastic paraplegia interacts with Reticulon 1 an endoplasmic reticulum protein. *Neurogenetics*. 7:93-103.

Mannherz, H.G., R.S. Goody, M. Konrad, and E. Nowak. 1980. The interaction of bovine pancreatic deoxyribonuclease I and skeletal muscle actin. *European journal of biochemistry / FEBS*. 104:367-379.

Mansfeld, J., S. Guttinger, L.A. Hawryluk-Gara, N. Pante, M. Mall, V. Galy, U. Haselmann, P. Muhlhausser, R.W. Wozniak, I.W. Mattaj, U. Kutay, and W. Antonin. 2006. The conserved transmembrane nucleoporin NDC1 is required for nuclear pore complex assembly in vertebrate cells. *Molecular cell*. 22:93-103.

Maravillas-Montero, J.L., P.G. Gillespie, G. Patino-Lopez, S. Shaw, and L. Santos-Argumedo. 2011. Myosin 1c participates in B cell cytoskeleton rearrangements, is recruited to the immunologic synapse, and contributes to antigen presentation. *J Immunol*. 187:3053-3063.

Marquardt, T., D.N. Hebert, and A. Helenius. 1993. Posttranslational Folding of Influenza Hemagglutinin in Isolated Endoplasmic Reticulum-Derived Microsomes. *Journal of Biological Chemistry*. 268:19618-19625.

Marsh, B.J., D.N. Mastronarde, K.F. Buttle, K.E. Howell, and J.R. McIntosh. 2001a. Organellar relationships in the Golgi region of the pancreatic beta cell line, HIT-T15, visualized by high resolution electron tomography. *Proceedings of the National Academy of Sciences of the United States of America*. 98:2399-2406.

Marsh, B.J., D.N. Mastronarde, J.R. McIntosh, and K.E. Howell. 2001b. Structural evidence for multiple transport mechanisms through the Golgi in the pancreatic beta-cell line, HIT-T15. *Biochemical Society transactions*. 29:461-467.

Mattaj, I.W. 2004. Sorting out the nuclear envelope from the endoplasmic reticulum. *Nature reviews. Molecular cell biology*. 5:65-69.

Mattaj, I.W., and L. Englmeier. 1998. Nucleocytoplasmic transport: the soluble phase. *Annual review of biochemistry*. 67:265-306.

McConnell, R.E., and M.J. Tyska. 2007. Myosin-1a powers the sliding of apical membrane along microvillar actin bundles. *The Journal of cell biology*. 177:671-681.

McConnell, R.E., and M.J. Tyska. 2010. Leveraging the membrane - cytoskeleton interface with myosin-1. *Trends in cell biology*. 20:418-426.

McCullough, S., and J. Lucocq. 2005. Endoplasmic reticulum positioning and partitioning in mitotic HeLa cells. *Journal of anatomy*. 206:415-425.

McGraw, C.F., A.V. Somlyo, and M.P. Blaustein. 1980. Localization of calcium in presynaptic nerve terminals. An ultrastructural and electron microprobe analysis. *The Journal of cell biology*. 85:228-241.

McMahon, H.T., and J.L. Gallop. 2005. Membrane curvature and mechanisms of dynamic cell membrane remodelling. *Nature*. 438:590-596.

Mogelsvang, S., B.J. Marsh, M.S. Ladinsky, and K.E. Howell. 2004. Predicting function from structure: 3D structure studies of the mammalian Golgi complex. *Traffic*. 5:338-345.

Moseley, J.B., and B.L. Goode. 2006. The yeast actin cytoskeleton: from cellular function to biochemical mechanism. *Microbiology and molecular biology reviews : MMBR*. 70:605-645.

Mullins, J.M. 1984. Spindle-membrane associations in freeze fractured HeLa cells. *Cell biology international reports*. 8:107-115.

Nagata, K. 1998. Expression and function of heat shock protein 47: a collagen-specific molecular chaperone in the endoplasmic reticulum. *Matrix biology : journal of the International Society for Matrix Biology*. 16:379-386.

Nebl, T., K.N. Pestonjamasp, J.D. Leszyk, J.L. Crowley, S.W. Oh, and E.J. Luna. 2002. Proteomic analysis of a detergent-resistant membrane skeleton from neutrophil plasma membranes. *The Journal of biological chemistry*. 277:43399-43409.

Niclas, J., V.J. Allan, and R.D. Vale. 1996. Cell cycle regulation of dynein association with membranes modulates microtubule-based organelle transport. *The Journal of cell biology*. 133:585-593.

Nikonov, A.V., H.P. Hauri, B. Lauring, and G. Kreibich. 2007. Climp-63-mediated binding of microtubules to the ER affects the lateral mobility of translocon complexes. *Journal of cell science*. 120:2248-2258.

Nowak, G., L. Pestic-Dragovich, P. Hozak, A. Philimonenko, C. Simerly, G. Schatten, and P. de Lanerolle. 1997. Evidence for the presence of myosin I in the nucleus. *The Journal of biological chemistry*. 272:17176-17181.

Novak, I.L., P. Kraikivski, and B.M. Slepchenko. 2009. Diffusion in cytoplasm: effects of excluded volume due to internal membranes and cytoskeletal structures. *Biophysical journal*. 97:758-767.

Novak, K.D., M.D. Peterson, M.C. Reedy, and M.A. Titus. 1995. Dictyostelium myosin I double mutants exhibit conditional defects in pinocytosis. *The Journal of cell biology*. 131:1205-1221.

Novak, K.D., and M.A. Titus. 1997. Myosin I overexpression impairs cell migration. *The Journal of cell biology*. 136:633-647.

Nucifora, F.C., Jr., A.H. Sharp, S.L. Milgram, and C.A. Ross. 1996. Inositol 1,4,5-trisphosphate receptors in endocrine cells: localization and association in hetero- and homotetramers. *Molecular biology of the cell*. 7:949-960.

Oertle, T., and M.E. Schwab. 2003. Nogo and its paRTNers. *Trends in cell biology*. 13:187-194.

Ogawa-Goto, K., K. Tanaka, T. Ueno, K. Tanaka, T. Kurata, T. Sata, and S. Irie. 2007. p180 is involved in the interaction between the endoplasmic reticulum and microtubules through a novel microtubule-binding and bundling domain. *Molecular biology of the cell*. 18:3741-3751.

Olety, B., M. Walte, U. Honnert, H. Schillers, and M. Bahler. 2010. Myosin 1G (Myo1G) is a haematopoietic specific myosin that localises to the plasma membrane and regulates cell elasticity. *FEBS letters*. 584:493-499.

Orci, L., M. Ravazzola, M. Le Coadic, W.W. Shen, N. Demaurex, and P. Cosson. 2009. From the Cover: STIM1-induced precortical and cortical subdomains of the endoplasmic reticulum. *Proceedings of the National Academy of Sciences of the United States of America*. 106:19358-19362.

Orci, L., M. Ravazzola, P. Meda, C. Holcomb, H.P. Moore, L. Hicke, and R. Schekman. 1991. Mammalian Sec23p homologue is restricted to the endoplasmic reticulum transitional cytoplasm. *Proceedings of the National Academy of Sciences of the United States of America*. 88:8611-8615.

Orrenius, S., J.L. Ericsson, and L. Ernster. 1965. Phenobarbital-induced synthesis of the microsomal drug-metabolizing enzyme system and its relationship to the proliferation of endoplasmic membranes. A morphological and biochemical study. *The Journal of cell biology*. 25:627-639.

Orso, G., D. Pendin, S. Liu, J. Tosetto, T.J. Moss, J.E. Faust, M. Micaroni, A. Egorova, A. Martinuzzi, J.A. McNew, and A. Daga. 2009. Homotypic fusion of ER membranes requires the dynamin-like GTPase atlastin. *Nature*. 460:978-983.

Owen, D.M., A. Magenau, D. Williamson, and K. Gaus. 2012. The lipid raft hypothesis revisited--new insights on raft composition and function from super-resolution fluorescence microscopy. *BioEssays : news and reviews in molecular, cellular and developmental biology*. 34:739-747.

Ozato-Sakurai, N., A. Fujita, and T. Fujimoto. 2011. The distribution of phosphatidylinositol 4,5-bisphosphate in acinar cells of rat pancreas revealed with the freeze-fracture replica labeling method. *PloS one*. 6:e23567.

Padmakumar, V.C., T. Libotte, W. Lu, H. Zaim, S. Abraham, A.A. Noegel, J. Gotzmann, R. Foisner, and I. Karakesisoglou. 2005. The inner nuclear membrane protein Sun1 mediates the anchorage of Nesprin-2 to the nuclear envelope. *Journal of cell science*. 118:3419-3430.

Palade, G.E. 1956. The endoplasmic reticulum. *The Journal of biophysical and biochemical cytology*. 2:85-98.

Palade, G.E., and P. Siekevitz. 1956. Liver microsomes; an integrated morphological and biochemical study. *The Journal of biophysical and biochemical cytology*. 2:171-200.

Park, C.Y., P.J. Hoover, F.M. Mullins, P. Bachhawat, E.D. Covington, S. Raunser, T. Walz, K.C. Garcia, R.E. Dolmetsch, and R.S. Lewis. 2009. STIM1 clusters and activates CRAC channels via direct binding of a cytosolic domain to Orai1. *Cell*. 136:876-890.

Park, S.H., and C. Blackstone. 2010. Further assembly required: construction and dynamics of the endoplasmic reticulum network. *EMBO reports*. 11:515-521.

Park, S.H., P.P. Zhu, R.L. Parker, and C. Blackstone. 2010. Hereditary spastic paraplegia proteins REEP1, spastin, and atlastin-1 coordinate microtubule interactions with the tubular ER network. *The Journal of clinical investigation*. 120:1097-1110.

Parry, H., A. McDougall, and M. Whitaker. 2005. Microdomains bounded by endoplasmic reticulum segregate cell cycle calcium transients in syncytial Drosophila embryos. *The Journal of cell biology*. 171:47-59.

Pelkmans, L., and A. Helenius. 2002. Endocytosis via caveolae. *Traffic*. 3:311-320.

Pendin, D., J.A. McNew, and A. Daga. 2011. Balancing ER dynamics: shaping, bending, severing, and mending membranes. *Current opinion in cell biology*. 23:435-442.

Peretti, D., N. Dahan, E. Shimoni, K. Hirschberg, and S. Lev. 2008. Coordinated lipid transfer between the endoplasmic reticulum and the Golgi complex requires the VAP proteins and is essential for Golgi-mediated transport. *Molecular biology of the cell*. 19:3871-3884.

Pezzati, R., M. Bossi, P. Podini, J. Meldolesi, and F. Grohovaz. 1997. High-resolution calcium mapping of the endoplasmic reticulum-Golgi-exocytic membrane system. Electron energy loss imaging analysis of quick frozen-freeze dried PC12 cells. *Molecular biology of the cell*. 8:1501-1512.

Philimonenko, V.V., J. Zhao, S. Iben, H. Dingova, K. Kysela, M. Kahle, H. Zentgraf, W.A. Hofmann, P. de Lanerolle, P. Hozak, and I. Grummt. 2004. Nuclear actin and myosin I are required for RNA polymerase I transcription. *Nature cell biology*. 6:1165-1172.

Pichler, H., B. Gaigg, C. Hrastnik, G. Achleitner, S.D. Kohlwein, G. Zellnig, A. Perktold, and G. Daum. 2001. A subfraction of the yeast endoplasmic reticulum associates with the plasma membrane and has a high capacity to synthesize lipids. *European journal of biochemistry / FEBS*. 268:2351-2361.

Pollard, T.D., L. Blanchoin, and R.D. Mullins. 2000. Molecular mechanisms controlling actin filament dynamics in nonmuscle cells. *Annual review of biophysics and biomolecular structure*. 29:545-576.

Pollard, T.D., S.K. Doberstein, and H.G. Zot. 1991. Myosin-I. *Annual review of physiology*. 53:653-681.

Poteryaev, D., J.M. Squirrell, J.M. Campbell, J.G. White, and A. Spang. 2005. Involvement of the actin cytoskeleton and homotypic membrane fusion in ER dynamics in Caenorhabditis elegans. *Molecular biology of the cell*. 16:2139-2153.

Prinz, W.A., L. Grzyb, M. Veenhuis, J.A. Kahana, P.A. Silver, and T.A. Rapoport. 2000. Mutants affecting the structure of the cortical endoplasmic reticulum in Saccharomyces cerevisiae. *The Journal of cell biology*. 150:461-474.

Prunuske, A.J., and K.S. Ullman. 2006. The nuclear envelope: form and reformation. *Current opinion in cell biology*. 18:108-116.

Pruyne, D., A. Legesse-Miller, L. Gao, Y. Dong, and A. Bretscher. 2004. Mechanisms of polarized growth and organelle segregation in yeast. *Annual review of cell and developmental biology*. 20:559-591.

Pyrpasopoulou, A., J. Meier, C. Maison, G. Simos, and S.D. Georgatos. 1996. The lamin B receptor (LBR) provides essential chromatin docking sites at the nuclear envelope. *The EMBO journal*. 15:7108-7119.

Pyrpassopoulos, S., E.A. Feeser, J.N. Mazerik, M.J. Tyska, and E.M. Ostap. 2012. Membrane-bound myo1c powers asymmetric motility of actin filaments. *Current biology : CB*. 22:1688-1692.

Quader, H., A. Hofmann, and E. Schnepf. 1989. Reorganization of the endoplasmic reticulum in epidermal cells of onion bulb scales after cold stress: Involvement of cytoskeletal elements. *Planta*. 177:273-280.

Rabouille, C., V. Malhotra, and W. Nickel. 2012. Diversity in unconventional protein secretion. *Journal of cell science*. 125:5251-5255.

Rabut, G., V. Doye, and J. Ellenberg. 2004. Mapping the dynamic organization of the nuclear pore complex inside single living cells. *Nature cell biology*. 6:1114-1121.

Rajasekaran, A.K., T. Morimoto, D.K. Hanzel, E. Rodriguez-Boulan, and G. Kreibich. 1993. Structural reorganization of the rough endoplasmic reticulum without size expansion accounts for dexamethasone-induced secretory activity in AR42J cells. *Journal of cell science*. 105 (Pt 2):333-345.

Ralston, E., Z. Lu, N. Biscocho, E. Soumaka, M. Mavroidis, C. Prats, T. Lomo, Y. Capetanaki, and T. Ploug. 2006. Blood vessels and desmin control the positioning of nuclei in skeletal muscle fibers. *Journal of cellular physiology*. 209:874-882.

Ramaekers, F.C., E.L. Benedetti, I. Dunia, P. Vorstenbosch, and H. Bloemendal. 1983. Polyribosomes associated with microfilaments in cultured lens cells. *Biochimica et biophysica acta*. 740:441-448.

Rambourg, A., C.L. Jackson, and Y. Clermont. 2001. Three dimensional configuration of the secretory pathway and segregation of secretion granules in the yeast Saccharomyces cerevisiae. *Journal of cell science*. 114:2231-2239.

Raposo, G., M.N. Cordonnier, D. Tenza, B. Menichi, A. Durrbach, D. Louvard, and E. Coudrier. 1999. Association of myosin I alpha with endosomes and lysosomes in mammalian cells. *Molecular biology of the cell*. 10:1477-1494.

Ravikumar, B., K. Moreau, L. Jahreiss, C. Puri, and D.C. Rubinsztein. 2010. Plasma membrane contributes to the formation of pre-autophagosomal structures. *Nature cell biology*. 12:747-757.

Raychaudhuri, S., and W.A. Prinz. 2008. Nonvesicular phospholipid transfer between peroxisomes and the endoplasmic reticulum. *Proceedings of the National Academy of Sciences of the United States of America*. 105:15785-15790.

Reizes, O., B. Barylko, C. Li, T.C. Sudhof, and J.P. Albanesi. 1994. Domain structure of a mammalian myosin I beta. *Proceedings of the National Academy of Sciences of the United States of America*. 91:6349-6353.

Riedl, J., A.H. Crevenna, K. Kessenbrock, J.H. Yu, D. Neukirchen, M. Bista, F. Bradke, D. Jenne, T.A. Holak, Z. Werb, M. Sixt, and R. Wedlich-Soldner. 2008. Lifeact: a versatile marker to visualize F-actin. *Nature methods*. 5:605-607.

Rismanchi, N., C. Soderblom, J. Stadler, P.P. Zhu, and C. Blackstone. 2008. Atlastin GTPases are required for Golgi apparatus and ER morphogenesis. *Human molecular genetics*. 17:1591-1604.

Rizzo, R., S. Parashuraman, P. Mirabelli, C. Puri, J. Lucocq, and A. Luini. 2013. The dynamics of engineered resident proteins in the mammalian Golgi complex relies on cisternal maturation. *The Journal of cell biology*. 201:1027-1036.

Rizzuto, R., P. Pinton, W. Carrington, F.S. Fay, K.E. Fogarty, L.M. Lifshitz, R.A. Tuft, and T. Pozzan. 1998. Close contacts with the endoplasmic reticulum as determinants of mitochondrial Ca2+ responses. *Science*. 280:1763-1766.

Rocha, N., C. Kuijl, R. van der Kant, L. Janssen, D. Houben, H. Janssen, W. Zwart, and J. Neefjes. 2009. Cholesterol sensor ORP1L contacts the ER protein VAP to control Rab7-RILP-p150 Glued and late endosome positioning. *The Journal of cell biology*. 185:1209-1225.

Rossanese, O.W., J. Soderholm, B.J. Bevis, I.B. Sears, J. O'Connor, E.K. Williamson, and B.S. Glick. 1999. Golgi structure correlates with transitional endoplasmic reticulum organization in Pichia pastoris and Saccharomyces cerevisiae. *The Journal of cell biology*. 145:69-81.

Rossi, D., V. Barone, E. Giacomello, V. Cusimano, and V. Sorrentino. 2008. The sarcoplasmic reticulum: an organized patchwork of specialized domains. *Traffic*. 9:1044-1049.

Roy, A., and W.F. Wonderlin. 2003. The permeability of the endoplasmic reticulum is dynamically coupled to protein synthesis. *The Journal of biological chemistry*. 278:4397-4403.

Ruppert, C., J. Godel, R.T. Muller, R. Kroschewski, J. Reinhard, and M. Bahler. 1995. Localization of the rat myosin I molecules myr 1 and myr 2 and in vivo targeting of their tail domains. *Journal of cell science*. 108 (Pt 12):3775-3786.

Rutishauser, J., and M. Spiess. 2002. Endoplasmic reticulum storage diseases. *Swiss medical weekly*. 132:211-222.

Saarikangas, J., H. Zhao, and P. Lappalainen. 2010. Regulation of the actin cytoskeleton-plasma membrane interplay by phosphoinositides. *Physiological reviews*. 90:259-289.

Salas-Cortes, L., F. Ye, D. Tenza, C. Wilhelm, A. Theos, D. Louvard, G. Raposo, and E. Coudrier. 2005. Myosin Ib modulates the morphology and the protein transport within multi-vesicular sorting endosomes. *Journal of cell science*. 118:4823-4832.

Salinas, S., C. Proukakis, A. Crosby, and T.T. Warner. 2008. Hereditary spastic paraplegia: clinical features and pathogenetic mechanisms. *Lancet neurology*. 7:1127-1138.

Salonen, A., L. Vasiljeva, A. Merits, J. Magden, E. Jokitalo, and L. Kääriäinen. 2003. Properly folded nonstructural polyprotein directs the semliki forest virus replication complex to the endosomal compartment. *Journal of virology*. 77:1691-1702.

Sanderfoot, A.A., F.F. Assaad, and N.V. Raikhel. 2000. The Arabidopsis genome. An abundance of soluble N-ethylmaleimide-sensitive factor adaptor protein receptors. *Plant physiology*. 124:1558-1569.

Sanderson, C.M., J.W. Connell, T.L. Edwards, N.A. Bright, S. Duley, A. Thompson, J.P. Luzio, and E. Reid. 2006. Spastin and atlastin, two proteins mutated in autosomal-dominant hereditary spastic paraplegia, are binding partners. *Human molecular genetics*. 15:307-318.

Sanger, J.M., J.S. Dome, B. Mittal, A.V. Somlyo, and J.W. Sanger. 1989. Dynamics of the endoplasmic reticulum in living non-muscle and muscle cells. *Cell motility and the cytoskeleton*. 13:301-319.

Santama, N., C.P. Er, L.L. Ong, and H. Yu. 2004. Distribution and functions of kinectin isoforms. *Journal of cell science*. 117:4537-4549.

Saraste, J., and E. Kuismanen. 1984. Pre- and post-Golgi vacuoles operate in the transport of Semliki Forest virus membrane glycoproteins to the cell surface. *Cell*. 38:535-549.

Saraste, J., and E. Kuismanen. 1992. Pathways of protein sorting and membrane traffic between the rough endoplasmic reticulum and the Golgi complex. *Seminars in cell biology*. 3:343-355.

Sasaki, N., H. Asukagawa, R. Yasuda, T. Hiratsuka, and K. Sutoh. 1999. Deletion of the myopathy loop of Dictyostelium myosin II and its impact on motor functions. *The Journal of biological chemistry*. 274:37840-37844.

Satoh, T., C.A. Ross, A. Villa, S. Supattapone, T. Pozzan, S.H. Snyder, and J. Meldolesi. 1990. The inositol 1,4,5,-trisphosphate receptor in cerebellar Purkinje cells: quantitative immunogold labeling reveals concentration in an ER subcompartment. *The Journal of cell biology*. 111:615-624.

Scharff, M.D., and E. Robbins. 1966. Polyribosome disaggregation during metaphase. *Science*. 151:992-995.

Schietroma, C., H.Y. Yu, M.C. Wagner, J.A. Umbach, W.M. Bement, and C.B. Gundersen. 2007. A role for myosin 1e in cortical granule exocytosis in Xenopus oocytes. *The Journal of biological chemistry*. 282:29504-29513.

Schirmer, E.C., and R. Foisner. 2007. Proteins that associate with lamins: many faces, many functions. *Experimental cell research*. 313:2167-2179.

Schuck, S., W.A. Prinz, K.S. Thorn, C. Voss, and P. Walter. 2009. Membrane expansion alleviates endoplasmic reticulum stress independently of the unfolded protein response. *The Journal of cell biology*. 187:525-536.

Schulz, T.A., and W.A. Prinz. 2007. Sterol transport in yeast and the oxysterol binding protein homologue (OSH) family. *Biochimica et biophysica acta*. 1771:769-780.

Sechi, A.S., and J. Wehland. 2000. The actin cytoskeleton and plasma membrane connection: PtdIns(4,5)P(2) influences cytoskeletal protein activity at the plasma membrane. *Journal of cell science*. 113 Pt 21:3685-3695.

Seiser, R.M., and C.V. Nicchitta. 2000. The fate of membrane-bound ribosomes following the termination of protein synthesis. *The Journal of biological chemistry*. 275:33820-33827.

Semenova, I., A. Burakov, N. Berardone, I. Zaliapin, B. Slepchenko, T. Svitkina, A. Kashina, and V. Rodionov. 2008. Actin dynamics is essential for myosin-based transport of membrane organelles. *Current biology : CB*. 18:1581-1586.

Senda, T., and T. Yoshinaga-Hirabayashi. 1998. Intermembrane bridges within membrane organelles revealed by quick-freeze deep-etch electron microscopy. *The Anatomical record*. 251:339-345.

Sesso, A., F.P. de Faria, E.S. Iwamura, and H. Correa. 1994. A three-dimensional reconstruction study of the rough ER-Golgi interface in serial thin sections of the pancreatic acinar cell of the rat. *Journal of cell science*. 107 (Pt 3):517-528.

Sevier, C.S., H. Qu, N. Heldman, E. Gross, D. Fass, and C.A. Kaiser. 2007. Modulation of cellular disulfide-bond formation and the ER redox environment by feedback regulation of Ero1. *Cell*. 129:333-344.

Shibata, Y., J. Hu, M.M. Kozlov, and T.A. Rapoport. 2009. Mechanisms shaping the membranes of cellular organelles. *Annual review of cell and developmental biology*. 25:329-354.

Shibata, Y., T. Shemesh, W.A. Prinz, A.F. Palazzo, M.M. Kozlov, and T.A. Rapoport. 2010. Mechanisms determining the morphology of the peripheral ER. *Cell*. 143:774-788.

Shibata, Y., G.K. Voeltz, and T.A. Rapoport. 2006. Rough sheets and smooth tubules. *Cell*. 126:435-439.

Shibata, Y., C. Voss, J.M. Rist, J. Hu, T.A. Rapoport, W.A. Prinz, and G.K. Voeltz. 2008. The reticulon and DP1/Yop1p proteins form immobile oligomers in the tubular endoplasmic reticulum. *The Journal of biological chemistry*. 283:18892-18904.

Silberstein, S., P.G. Collins, D.J. Kelleher, P.J. Rapiejko, and R. Gilmore. 1995. The alpha subunit of the Saccharomyces cerevisiae oligosaccharyltransferase complex is essential for vegetative growth of yeast and is homologous to mammalian ribophorin I. *The Journal of cell biology*. 128:525-536.

Simone, L.C., S. Caplan, and N. Naslavsky. 2013. Role of phosphatidylinositol 4,5-bisphosphate in regulating EHD2 plasma membrane localization. *PloS one*. 8:e74519.

Simons, K., and E. Ikonen. 1997. Functional rafts in cell membranes. *Nature*. 387:569-572.

Simons, K., and J.L. Sampaio. 2011. Membrane organization and lipid rafts. *Cold Spring Harbor perspectives in biology*. 3:a004697.

Sivan, G., N. Kedersha, and O. Elroy-Stein. 2007. Ribosomal slowdown mediates translational arrest during cellular division. *Molecular and cellular biology*. 27:6639-6646.

Sleight, R.G., and R.E. Pagano. 1983. Rapid appearance of newly synthesized phosphatidylethanolamine at the plasma membrane. *The Journal of biological chemistry*. 258:9050-9058.

Slomiany, A., M. Grabska, and B.L. Slomiany. 2006. Homeostatic restitution of cell membranes. Nuclear membrane lipid biogenesis and transport of protein from cytosol to intranuclear spaces. *International journal of biological sciences*. 2:216-226.

Smyth, J.T., J.G. Petranka, R.R. Boyles, W.I. DeHaven, M. Fukushima, K.L. Johnson, J.G. Williams, and J.W. Putney, Jr. 2009. Phosphorylation of STIM1 underlies suppression of store-operated calcium entry during mitosis. *Nature cell biology*. 11:1465-1472.

Snapp, E.L., R.S. Hegde, M. Francolini, F. Lombardo, S. Colombo, E. Pedrazzini, N. Borgese, and J. Lippincott-Schwartz. 2003. Formation of stacked ER cisternae by low affinity protein interactions. *The Journal of cell biology*. 163:257-269.

Sokac, A.M., C. Schietroma, C.B. Gundersen, and W.M. Bement. 2006. Myosin-1c couples assembling actin to membranes to drive compensatory endocytosis. *Developmental cell*. 11:629-640.

Sollner, T., M.K. Bennett, S.W. Whiteheart, R.H. Scheller, and J.E. Rothman. 1993. A protein assembly-disassembly pathway in vitro that may correspond to sequential steps of synaptic vesicle docking, activation, and fusion. *Cell*. 75:409-418.

Sparkes, I., J. Runions, C. Hawes, and L. Griffing. 2009. Movement and remodeling of the endoplasmic reticulum in nondividing cells of tobacco leaves. *The Plant cell*. 21:3937-3949.

Staehelin, L.A. 1997. The plant ER: a dynamic organelle composed of a large number of discrete functional domains. *The Plant journal : for cell and molecular biology*. 11:1151-1165.

Starr, D.A. 2007. Communication between the cytoskeleton and the nuclear envelope to position the nucleus. *Molecular bioSystems*. 3:583-589.

Starr, D.A., and H.N. Fridolfsson. 2010. Interactions between nuclei and the cytoskeleton are mediated by SUN-KASH nuclear-envelope bridges. *Annual review of cell and developmental biology*. 26:421-444.

Starr, D.A., and M. Han. 2002. Role of ANC-1 in tethering nuclei to the actin cytoskeleton. *Science*. 298:406-409.

Stavru, F., B.B. Hulsmann, A. Spang, E. Hartmann, V.C. Cordes, and D. Gorlich. 2006. NDC1: a crucial membrane-integral nucleoporin of metazoan nuclear pore complexes. *The Journal of cell biology*. 173:509-519.

Stephens, D.J. 2003. De novo formation, fusion and fission of mammalian COPII-coated endoplasmic reticulum exit sites. *EMBO reports*. 4:210-217.

Steward, D.L., J.R. Shaeffer, and R.M. Humphrey. 1968. Breakdown and assembly of polyribosomes in synchronized Chinese hamster cells. *Science*. 161:791-793.

Strasser, P., M. Gimona, H. Moessler, M. Herzog, and J.V. Small. 1993. Mammalian calponin. Identification and expression of genetic variants. *FEBS letters*. 330:13-18.

Strating, J.R., and G.J. Martens. 2009. The p24 family and selective transport processes at the ER-Golgi interface. *Biology of the cell / under the auspices of the European Cell Biology Organization*. 101:495-509.

Sturmer, K., O. Baumann, and B. Walz. 1995. Actin-dependent light-induced translocation of mitochondria and ER cisternae in the photoreceptor cells of the locust Schistocerca gregaria. *Journal of cell science*. 108 (Pt 6):2273-2283.

Stuurman, N., S. Heins, and U. Aebi. 1998. Nuclear lamins: their structure, assembly, and interactions. *Journal of structural biology*. 122:42-66.

Sullivan, D.P., H. Ohvo-Rekila, N.A. Baumann, C.T. Beh, and A.K. Menon. 2006. Sterol trafficking between the endoplasmic reticulum and plasma membrane in yeast. *Biochemical Society transactions*. 34:356-358.

Svitkina, T. 2009. Imaging cytoskeleton components by electron microscopy. *Methods Mol Biol*. 586:187-206.

Szabadkai, G., K. Bianchi, P. Varnai, D. De Stefani, M.R. Wieckowski, D. Cavagna, A.I. Nagy, T. Balla, and R. Rizzuto. 2006. Chaperone-mediated coupling of endoplasmic reticulum and mitochondrial Ca2+ channels. *The Journal of cell biology*. 175:901-911.

Tabb, J.S., B.J. Molyneaux, D.L. Cohen, S.A. Kuznetsov, and G.M. Langford. 1998. Transport of ER vesicles on actin filaments in neurons by myosin V. *Journal of cell science*. 111 (Pt 21):3221-3234.

Takagishi, Y., S. Oda, S. Hayasaka, K. Dekker-Ohno, T. Shikata, M. Inouye, and H. Yamamura. 1996. The dilute-lethal (dl) gene attacks a Ca2+ store in the dendritic spine of Purkinje cells in mice. *Neuroscience letters*. 215:169-172.

Takahashi, T., J.M. Lasker, A.S. Rosman, and C.S. Lieber. 1993. Induction of cytochrome P-4502E1 in the human liver by ethanol is caused by a corresponding increase in encoding messenger RNA. *Hepatology*. 17:236-245.

Takei, K., G.A. Mignery, E. Mugnaini, T.C. Sudhof, and P. De Camilli. 1994. Inositol 1,4,5-trisphosphate receptor causes formation of ER cisternal stacks in transfected fibroblasts and in cerebellar Purkinje cells. *Neuron*. 12:327-342.

Takei, K., H. Stukenbrok, A. Metcalf, G.A. Mignery, T.C. Sudhof, P. Volpe, and P. De Camilli. 1992. Ca2+ stores in Purkinje neurons: endoplasmic reticulum subcompartments demonstrated by the heterogeneous distribution of the InsP3 receptor, Ca(2+)-ATPase, and calsequestrin. *The Journal of neuroscience : the official journal of the Society for Neuroscience*. 12:489-505.

Talcott, B., and M.S. Moore. 1999. Getting across the nuclear pore complex. *Trends in cell biology*. 9:312-318.

Tamaki, H., and S. Yamashina. 1991. Changes in cell polarity during mitosis in rat parotid acinar cells. *The journal of histochemistry and cytochemistry : official journal of the Histochemistry Society*. 39:1077-1087.

Tanaka, Y., Y. Kanai, Y. Okada, S. Nonaka, S. Takeda, A. Harada, and N. Hirokawa. 1998. Targeted disruption of mouse conventional kinesin heavy chain, kif5B, results in abnormal perinuclear clustering of mitochondria. *Cell*. 93:1147-1158.

Tang, N., and E.M. Ostap. 2001. Motor domain-dependent localization of myo1b (myr-1). *Current biology : CB*. 11:1131-1135.

Terasaki, M. 2000. Dynamics of the endoplasmic reticulum and golgi apparatus during early sea urchin development. *Molecular biology of the cell*. 11:897-914.

Terasaki, M., L.B. Chen, and K. Fujiwara. 1986. Microtubules and the endoplasmic reticulum are highly interdependent structures. *The Journal of cell biology*. 103:1557-1568.

Terasaki, M., and T.S. Reese. 1994. Interactions among endoplasmic reticulum, microtubules, and retrograde movements of the cell surface. *Cell motility and the cytoskeleton*. 29:291-300.

Terasaki, M., L.L. Runft, and A.R. Hand. 2001. Changes in organization of the endoplasmic reticulum during Xenopus oocyte maturation and activation. *Molecular biology of the cell*. 12:1103-1116.

Terry, L.J., E.B. Shows, and S.R. Wente. 2007. Crossing the nuclear envelope: hierarchical regulation of nucleocytoplasmic transport. *Science*. 318:1412-1416.

Todorov, P.T., R.E. Hardisty, and S.D. Brown. 2001. Myosin VIIA is specifically associated with calmodulin and microtubule-associated protein-2B (MAP-2B). *The Biochemical journal*. 354:267-274.

Toh, B.H., S.J. Lolait, J.P. Mathy, and R. Baum. 1980. Association of mitochondria with intermediate filaments and of polyribosomes with cytoplasmic actin. *Cell and tissue research*. 211:163-169.

Toivola, D.M., G.Z. Tao, A. Habtezion, J. Liao, and M.B. Omary. 2005. Cellular integrity plus: organelle-related and protein-targeting functions of intermediate filaments. *Trends in cell biology*. 15:608-617.

Tran, E.J., and S.R. Wente. 2006. Dynamic nuclear pore complexes: life on the edge. *Cell*. 125:1041-1053.

Trapnell, C., A. Roberts, L. Goff, G. Pertea, D. Kim, D.R. Kelley, H. Pimentel, S.L. Salzberg, J.L. Rinn, and L. Pachter. 2012. Differential gene and transcript expression analysis of RNA-seq experiments with TopHat and Cufflinks. *Nature protocols*. 7:562-578.

Turner, M.D., H. Plutner, and W.E. Balch. 1997. A Rab GTPase is required for homotypic assembly of the endoplasmic reticulum. *The Journal of biological chemistry*. 272:13479-13483.

Uchiyama, K., E. Jokitalo, F. Kano, M. Murata, X. Zhang, B. Canas, R. Newman, C. Rabouille, D. Pappin, P. Freemont, and H. Kondo. 2002. VCIP135, a novel essential factor for p97/p47-mediated membrane fusion, is required for Golgi and ER assembly in vivo. *The Journal of cell biology*. 159:855-866.

Ueno, T., K. Kaneko, H. Katano, Y. Sato, R. Mazitschek, K. Tanaka, S. Hattori, S. Irie, T. Sata, and K. Ogawa-Goto. 2010. Expansion of the trans-Golgi network following activated collagen secretion is supported by a coiled-coil microtubule-bundling protein, p180, on the ER. *Experimental cell research*. 316:329-340.

Ueno, T., K. Kaneko, T. Sata, S. Hattori, and K. Ogawa-Goto. 2012. Regulation of polysome assembly on the endoplasmic reticulum by a coiled-coil protein, p180. *Nucleic acids research*. 40:3006-3017.

Urbani, L., and R.D. Simoni. 1990. Cholesterol and vesicular stomatitis virus G protein take separate routes from the endoplasmic reticulum to the plasma membrane. *The Journal of biological chemistry*. 265:1919-1923.

Wagner, M.C., B. Barylko, and J.P. Albanesi. 1992. Tissue distribution and subcellular localization of mammalian myosin I. *The Journal of cell biology*. 119:163-170.

Wagner, M.C., and B.A. Molitoris. 1997. ATP depletion alters myosin I beta cellular location in LLC-PK1 cells. *The American journal of physiology*. 272:C1680-1690.

Wagner, W., S.D. Brenowitz, and J.A. Hammer, 3rd. 2011. Myosin-Va transports the endoplasmic reticulum into the dendritic spines of Purkinje neurons. *Nature cell biology*. 13:40-48.

Vallenius, T. 2013. Actin stress fibre subtypes in mesenchymal-migrating cells. *Open biology*. 3:130001.

Walter, P., and V.R. Lingappa. 1986. Mechanism of protein translocation across the endoplasmic reticulum membrane. *Annual review of cell biology*. 2:499-516.

van Anken, E., E.P. Romijn, C. Maggioni, A. Mezghrani, R. Sitia, I. Braakman, and A.J. Heck. 2003. Sequential waves of functionally related proteins are expressed when B cells prepare for antibody secretion. *Immunity*. 18:243-253.

Van Coppenolle, F., F. Vanden Abeele, C. Slomianny, M. Flourakis, J. Hesketh, E. Dewailly, and N. Prevarskaya. 2004. Ribosome-translocon complex mediates calcium leakage from endoplasmic reticulum stores. *Journal of cell science*. 117:4135-4142.

van Meer, G., and A.I. de Kroon. 2011. Lipid map of the mammalian cell. *Journal of cell science*. 124:5-8.

van Meer, G., D.R. Voelker, and G.W. Feigenson. 2008. Membrane lipids: where they are and how they behave. *Nature reviews. Molecular cell biology*. 9:112-124.

Vance, J.E. 1990. Phospholipid synthesis in a membrane fraction associated with mitochondria. *The Journal of biological chemistry*. 265:7248-7256.

Vance, J.E. 2003. Molecular and cell biology of phosphatidylserine and phosphatidylethanolamine metabolism. *Progress in nucleic acid research and molecular biology*. 75:69-111.

Wang, H.J., G. Guay, L. Pogan, R. Sauve, and I.R. Nabi. 2000. Calcium regulates the association between mitochondria and a smooth subdomain of the endoplasmic reticulum. *The Journal of cell biology*. 150:1489-1498.

Wang, Y.J., R.B. Gregory, and G.J. Barritt. 2002. Maintenance of the filamentous actin cytoskeleton is necessary for the activation of store-operated Ca2+ channels, but not other types of plasma-membrane Ca2+ channels, in rat hepatocytes. *The Biochemical journal*. 363:117-126.

Wanker, E.E., Y. Sun, A.J. Savitz, and D.I. Meyer. 1995. Functional characterization of the 180-kD ribosome receptor in vivo. *The Journal of cell biology*. 130:29-39.

Warren, G. 1993. Membrane partitioning during cell division. *Annual review of biochemistry*. 62:323-348.

Warren, G., and W. Wickner. 1996. Organelle inheritance. *Cell*. 84:395-400.

Vartiainen, M.K., S. Guettler, B. Larijani, and R. Treisman. 2007. Nuclear actin regulates dynamic subcellular localization and activity of the SRF cofactor MAL. *Science*. 316:1749-1752.

Waterman-Storer, C.M., and E.D. Salmon. 1998. Endoplasmic reticulum membrane tubules are distributed by microtubules in living cells using three distinct mechanisms. *Current biology : CB*. 8:798-806.

Watt, S.A., G. Kular, I.N. Fleming, C.P. Downes, and J.M. Lucocq. 2002. Subcellular localization of phosphatidylinositol 4,5-bisphosphate using the pleckstrin homology domain of phospholipase C delta1. *The Biochemical journal*. 363:657-666.

Vazquez-Martinez, R., A. Diaz-Ruiz, F. Almabouada, Y. Rabanal-Ruiz, F. Gracia-Navarro, and M.M. Malagon. 2012. Revisiting the regulated secretory pathway: from frogs to human. *General and comparative endocrinology*. 175:1-9.

Weber, K.L., A.M. Sokac, J.S. Berg, R.E. Cheney, and W.M. Bement. 2004. A microtubule-binding myosin required for nuclear anchoring and spindle assembly. *Nature*. 431:325-329.

Vedrenne, C., D.R. Klopfenstein, and H.P. Hauri. 2005. Phosphorylation controls CLIMP-63-mediated anchoring of the endoplasmic reticulum to microtubules. *Molecular biology of the cell*. 16:1928-1937.

West, M., N. Zurek, A. Hoenger, and G.K. Voeltz. 2011. A 3D analysis of yeast ER structure reveals how ER domains are organized by membrane curvature. *The Journal of cell biology*. 193:333-346.

Wiest, D.L., J.K. Burkhardt, S. Hester, M. Hortsch, D.I. Meyer, and Y. Argon. 1990. Membrane biogenesis during B cell differentiation: most endoplasmic reticulum proteins are expressed coordinately. *The Journal of cell biology*. 110:1501-1511.

Wilhelmsen, K., M. Ketema, H. Truong, and A. Sonnenberg. 2006. KASH-domain proteins in nuclear migration, anchorage and other processes. *Journal of cell science*. 119:5021-5029.

Wilhelmsen, K., S.H. Litjens, I. Kuikman, N. Tshimbalanga, H. Janssen, I. van den Bout, K. Raymond, and A. Sonnenberg. 2005. Nesprin-3, a novel outer nuclear membrane protein, associates with the cytoskeletal linker protein plectin. *The Journal of cell biology*. 171:799-810.

Vlcek, S., and R. Foisner. 2007. A-type lamin networks in light of laminopathic diseases. *Biochimica et biophysica acta*. 1773:661-674.

Voeltz, G.K., and W.A. Prinz. 2007. Sheets, ribbons and tubules - how organelles get their shape. *Nature reviews. Molecular cell biology*. 8:258-264.

Voeltz, G.K., W.A. Prinz, Y. Shibata, J.M. Rist, and T.A. Rapoport. 2006. A class of membrane proteins shaping the tubular endoplasmic reticulum. *Cell*. 124:573-586.

Voeltz, G.K., M.M. Rolls, and T.A. Rapoport. 2002. Structural organization of the endoplasmic reticulum. *EMBO reports*. 3:944-950.

Vogel, J.P., L.M. Misra, and M.D. Rose. 1990. Loss of BiP/GRP78 function blocks translocation of secretory proteins in yeast. *The Journal of cell biology*. 110:1885-1895.

Wolf, W., A. Kilic, B. Schrul, H. Lorenz, B. Schwappach, and M. Seedorf. 2012. Yeast Ist2 recruits the endoplasmic reticulum to the plasma membrane and creates a ribosome-free membrane microcompartment. *PloS one*. 7:e39703.

Wollert, T., D.G. Weiss, H.H. Gerdes, and S.A. Kuznetsov. 2002. Activation of myosin V-based motility and F-actin-dependent network formation of endoplasmic reticulum during mitosis. *The Journal of cell biology*. 159:571-577.

Worman, H.J., and G. Bonne. 2007. "Laminopathies": a wide spectrum of human diseases. *Experimental cell research*. 313:2121-2133.

Worman, H.J., C. Ostlund, and Y. Wang. 2010. Diseases of the nuclear envelope. *Cold Spring Harbor perspectives in biology*. 2:a000760.

Wozniak, M.J., B. Bola, K. Brownhill, Y.C. Yang, V. Levakova, and V.J. Allan. 2009. Role of kinesin-1 and cytoplasmic dynein in endoplasmic reticulum movement in VERO cells. *Journal of cell science*. 122:1979-1989.

Wright, R., M. Basson, L. D'Ari, and J. Rine. 1988. Increased amounts of HMG-CoA reductase induce "karmellae": a proliferation of stacked membrane pairs surrounding the yeast nucleus. *The Journal of cell biology*. 107:101-114.

Wyles, J.P., C.R. McMaster, and N.D. Ridgway. 2002. Vesicle-associated membrane protein-associated protein-A (VAP-A) interacts with the oxysterol-binding protein to modify export from the endoplasmic reticulum. *The Journal of biological chemistry*. 277:29908-29918.

Yamamoto, A., R. Masaki, and Y. Tashiro. 1990. Characterization of the isolation membranes and the limiting membranes of autophagosomes in rat hepatocytes by lectin cytochemistry. *The journal of histochemistry and cytochemistry : official journal of the Histochemistry Society*. 38:573-580.

Yamamoto, K., R. Fujii, Y. Toyofuku, T. Saito, H. Koseki, V.W. Hsu, and T. Aoe. 2001. The KDEL receptor mediates a retrieval mechanism that contributes to quality control at the endoplasmic reticulum. *The EMBO journal*. 20:3082-3091.

Yang, L., T. Guan, and L. Gerace. 1997a. Integral membrane proteins of the nuclear envelope are dispersed throughout the endoplasmic reticulum during mitosis. *The Journal of cell biology*. 137:1199-1210.

Yang, L., T. Guan, and L. Gerace. 1997b. Lamin-binding fragment of LAP2 inhibits increase in nuclear volume during the cell cycle and progression into S phase. *The Journal of cell biology*. 139:1077-1087.

Ye, J., J.Z. Li, Y. Liu, X. Li, T. Yang, X. Ma, Q. Li, Z. Yao, and P. Li. 2009. Cideb, an ER- and lipid droplet-associated protein, mediates VLDL lipidation and maturation by interacting with apolipoprotein B. *Cell metabolism*. 9:177-190.

Ye, Q., and H.J. Worman. 1994. Primary structure analysis and lamin B and DNA binding of human LBR, an integral protein of the nuclear envelope inner membrane. *The Journal of biological chemistry*. 269:11306-11311.

Yin, H.L., and P.A. Janmey. 2003. Phosphoinositide regulation of the actin cytoskeleton. *Annual review of physiology*. 65:761-789.

Yla-Anttila, P., H. Vihinen, E. Jokitalo, and E.L. Eskelinen. 2009. 3D tomography reveals connections between the phagophore and endoplasmic reticulum. *Autophagy*. 5:1180-1185.

Yvon, A.M., P. Wadsworth, and M.A. Jordan. 1999. Taxol suppresses dynamics of individual microtubules in living human tumor cells. *Molecular biology of the cell*. 10:947-959.

Zambrano, F., S. Fleischer, and B. Fleischer. 1975. Lipid composition of the Golgi apparatus of rat kidney and liver in comparison with other subcellular organelles. *Biochimica et biophysica acta*. 380:357-369.

Zeligs, J.D., and S.H. Wollman. 1979. Mitosis in rat thyroid epithelial cells in vivo. IV. Cell surface changes. *Journal of ultrastructure research*. 67:297-308.

Zhang, X., Y.H. Tee, J.K. Heng, Y. Zhu, X. Hu, F. Margadant, C. Ballestrem, A. Bershadsky, G. Griffiths, and H. Yu. 2010. Kinectin-mediated endoplasmic reticulum dynamics supports focal adhesion growth in the cellular lamella. *Journal of cell science*. 123:3901-3912.

Zhu, T., M. Sata, and M. Ikebe. 1996. Functional expression of mammalian myosin I beta: analysis of its motor activity. *Biochemistry*. 35:513-522.

Zimmerberg, J., and M.M. Kozlov. 2006. How proteins produce cellular membrane curvature. *Nature reviews. Molecular cell biology*. 7:9-19.

Zuchner, S., I.V. Mersiyanova, M. Muglia, N. Bissar-Tadmouri, J. Rochelle, E.L. Dadali, M. Zappia, E. Nelis, A. Patitucci, J. Senderek, Y. Parman, O. Evgrafov, P.D. Jonghe, Y. Takahashi, S. Tsuji, M.A. Pericak-Vance, A. Quattrone, E. Battaloglu, A.V. Polyakov, V. Timmerman, J.M. Schroder, and J.M. Vance. 2004. Mutations in the mitochondrial GTPase mitofusin 2 cause Charcot-Marie-Tooth neuropathy type 2A. *Nature genetics*. 36:449-451.